SHERIDAN TECHNICAL ASSOCIATES INC.

Consulting Research Laboratory Services

FINAL REPORT

DEASPHALTING OF NON-CONVENTIONAL RESIDUES AND CATALYTIC CRACKING OF DE-ASPHALTED OILS BY METAL-TOLERANT CATALYST

DECEMBER, 1988

S.C.C. FILE NUMBER	:	07SQ.23440-7-9126
CONTRACT SERIAL NUMBER	:	23440-7-9126/01SQ
SCIENTIFIC AUTHORITY	:	DR. S. H. NG
STA FILE NUMBER	:	167-87-30

SHERIDAN TECHNICAL ASSOCIATES INC.
333 WYECROFT ROAD, UNITS 6 & 7
OAKVILLE, ONTARIO
L6K 2H2

127 pp

DECEMBER, 1988

MICROMEDIA

EXECUTIVE SUMMARY

This contract was undertaken to study the deasphalting characteristics of non-conventional residuums and to assess the quality of the resulting deasphalted oils as catalytic cracking feedstock. The objective was to provide a good experimental data base for assessing the applicability of deasphalting and catalytic cracking technology to non-conventional residuum upgrading.

Two typical non-conventional residuums from Athabasca and Lloydminster were selected for the study. These materials were deasphalted using four solvents (propane, n-butane, n-pentane, and n-heptane) over a range of solvent/oil ratios and temperatures. Sufficient deasphalting experimentation with feed and product testing was carried out to:

1. Develop ternary phase envelopes for the eight solvent/residuum systems

2. Define the effect of solvent and conditions on DA oil yield and quality

Selected DA oils were also catalytically cracked over a range of severities using a modified MAT reactor and commercial equilibrium catalyst. The resulting yield profiles were used to further assess the cracking characteristics of non-conventional DA oils.

The overall results from this study showed similar trends to literature data reported for conventional residuums. DA oil yield and quality can be correlated with feedstock quality, solvent selection and operating conditions. Furthermore, DA oil composition can be used to estimate catalytic cracking yields and evaluate the suitability of the material as a feedstock to an FCCU.

In conclusion the report provides an excellent source of information about the deasphalting characteristics of non-conventional residuums and the effect of DA oil quality on catalytic cracking yield profiles. This should form the basis for evaluating the applicability of this technology to future non-conventional oil developments.

SOMMAIRE EXECUTIF

Ce contrat a été entrepris pour étudier les caractéristiques de désasphaltage des résidus non classiques et évaluer la qualité des huiles désasphaltées qui en découlent comme stocks d'alimentation du catalyseur de craquage. L'objectif était de fournir une bonne base de données expérimentales pour évaluer l'application de la technologie du désasphaltage et du craquage catalytique à l'amélioration des résidus non classiques.

Deux échantillons de résidus non classiques typiques d'Athabasca et de Lloydminster ont été choisis pour cette étude. Ces matériaux ont été désasphaltés en utilisant quatre solvants (propane, n-butane, n-pentane et n-heptane) à différentes températures et à différents rapports de solvant/huile. Des essais suffisants de désasphaltage avec les charges d'alimentation et les produits ont été effectués pour:

1. Développer des enveloppes de phase ternaire pour les huit combinaisons de solvants/résidus

2. Déterminer l'action des solvants et des conditions sur le rendement et la qualité des huiles désasphaltées (DA).

Des huiles DA sélectionnées ont aussi été craquées catalytiquement sur une plage de conditions expérimentales utilisant un réacteur de micro-activité modifié et un catalyseur à l'équilibre commercial. Les profils de rendement qui en ont résulté ont été utilisés pour évaluer en plus les caractéristiques de craquage des huiles DA non classiques.

Les résultats d'ensemble de cette étude font ressortir des tendances semblables aux résultats publiés dans la documentation sur les résidus classiques. Le rendement et la qualité des huiles DA peuvent être corrélés avec la qualité du stock d'alimentation, la sélection des solvants et les conditions de fonctionnement. De plus, la composition des huiles DA peut être utilisée pour estimer le rendement du craquage catalytique et évaluer la convenance du matériel comme stock d'alimentation pour un craquage catalytique en lit fluidisé (CCF).

En conclusion le rapport fournit une excellente source d'information concernant les caractéristiques de désasphaltage des résidus non classiques et l'effet de la qualité des huiles DA sur les profils de rendement du craquage catalytique. Cette étude devrait constituer un outil pour évaluer l'applicabilité de cette technologie aux développements futurs des huiles non classiques.

RECOMMENDATIONS

This technology offers the potential of a relatively inexpensive route for upgrading heavy oils to saleable gasoline and diesel products. It is recommended that the information in this report be used as a basis for developing processing concepts and first pass economics to better define the value of this technology.

Specific recommendations include:

1. Formulate potential processing schemes which utilize deasphalting, catalytic cracking and perhaps hydrotreating technology.

2. Develop a model for bitumen deasphalting to allow the optimization of the yield and quality constraints for a multi-contacting deasphalting process.

3. Develop correlations relating DA oil and gas oil quality to FCC yields and use this data to predict a commercial, heat-balanced, FCC operation.

4. Review methods for economically ultilizing the asphaltic residuum fraction

5. Utilizing the above information, select the more promising processing schemes and assess process economics.

TABLE OF CONTENTS

PAGE NO.

EXECUTIVE SUMMARY
SOMMAIRE EXECUTIF

RECOMMENDATIONS

INTRODUCTION 1

BACKGROUND
1. Solvent Deasphalting 2
2. Catalytic Cracking 3
3. VTB Composition 4
4. Phase Separation of the Heavy Fractions 6

EXPERIMENTAL
1. Fractionation 8
2. Feedstock Characterization 8
3. Catalyst Characterization 10
4. Solvent Deasphalting - Experiments and Phase Behaviour Measurements 13
5. Characterization of the Oil from the Deasphalting Experiments 14
6. The Microactivity Test (MAT) 14

DISCUSSION
1. Athabasca Sample Fractionation - Result 19
2. Lloydminster Sample Blending 19
3. Feedstock Characterization Results 19
4. Catalyst Characterization 21
5. Deasphalting Experiments - Results and Discussion 32
6. Generation of Phase Envelopes 32
7. Effects of Phase Behaviour on DAO 35
8. Deasphalted Oil Quality and Composition 39
9. Results from the Microactivity Testing Program 66
10. General Relationships Between MAT Yields and DA Oil Quality 67
11. Cracking Characteristics of the Propane DA Oils and Associated VGOs 73
12. Cracking Characteristics of the Butane DA Oils 80
13. Cracking Characteristics of the Pentane DA Oils 90
14. Cracking Characteristics of the Heptane DA Oils 99
15. Solvent Effects 108

REFERENCES 112

APPENDIX

INTRODUCTION

The work was carried out to fulfill a contract awarded in October 1987 to study the Deasphalting Characteristics of Two Non-Conventional Residues and the suitability of the produced DA Oils as FCC feedstocks.

Sheridan Technical Associates provided the following samples for this study:-

1. Syncrude Coker Feed 305°C plus material. This sample, which is typical of the ATB cut of Athabasca bitumen, was further fractionated to yield a heavy distillate, a vacuum gas oil and a vacuum tower bottoms.
2. Lloydminster vacuum gas oils and vacuum tower bottoms samples were obtained from an Ontario Refinery processing pipeline quality Lloydminster crude oil.
3. DA-440 equilibrium FCC catalyst was obtained from a Canadian Refinery.

In February, 1988 the contract was modified to include the extraction and evaluation of a number of other non-conventional feedstocks. The final report on this work, entitled "Task 6: Special Deasphalting/MAT Runs", was issued in July, 1988.

BACKGROUND

Canada will in the future have to rely more on non-conventional oils and bitumens to produce transportation fuels as Western Canadian light crude oil production declines. Refineries are presently limited to the amount of heavy oil that they can accept for processing and tar sands bitumens have to be upgraded before shipment to refineries. Athabasca bitumen is presently upgraded commercially by coking the raw bitumen and hydrotreating the liquid products.

A number of other processes involving hydrogen addition rather than carbon rejection, have been evaluated on a semi-commercial scale for both bitumen and heavy oil upgrading. High pressure catalytic hydrocracking technology has recently been installed in one plant and is presently the process of choice for future development. Although these processes yield refinery quality feedstocks, they are expensive both in terms of operating and capital costs. Thus, there is still the incentive to develop upgrading technology which will increase processing flexibility and reduce processing costs.

1. Solvent Deasphalting

Solvent deasphalting is a relatively inexpensive process that has been used for a number of years to upgrade vacuum tower bottoms (VTB) for either Lube Processing or FCC feedstock production. The solvent extracts the oil fraction from the VTB leaving the asphaltenes in the residue. The resins are partitioned between the oil and the residue with their distribution controlled by solvent selection and operating conditions. Light solvents such as propane produce high quality DA oil with a low Conradson Carbon Residue (CCR) and a low metals content. As the solvent molecular weight increases, the DA oil quality decreases but the DA oil yield increases. Extraction temperature can also be used within limits to control DA oil quality, with the higher temperature producing a lower yield of superior quality DA oil. In addition, increasing the solvent to oil ratio increases both the oil yield and quality at the expense of increased operating cost. Thus in any deasphalting operation there is a trade off between yield and quality of the DA oil and the operating expense.

Newer units use supercritical solvent recovery techniques (1) to improve process economics by minimizing energy consumption. The oil and solvent are separated under supercritical condition saving solvent evaporation, condensation and recompression costs.

Although there is a significant body of information available on deasphalting conventional VTB streams there is not to our knowledge any detailed information published in the open literature on the deasphalting of VTBs derived from Canadian Heavy Oils and Bitumens. The objectives of this contract are to develop a data base for the solvent deasphalting of typical VTBs derived from tar sands bitumen and heavy oil and to evaluate the resulting DA oils as FCC feedstocks.

2. Catalytic Cracking

Data in the literature on the crackability of DA oils in an FCC unit is again limited to materials derived from conventional crude oils (2). It has been reported that propane DA oils are excellent feedstocks for conventional FCC units, butane DA oils can be processed neat but throughput may be limited by the unit's coke burning capacity, while pentane DA oils require dilution with gas oils or hydrotreating prior to cracking.

For DA oils derived from unconventional oils, it may be more appropriate to consider cracking in a residual oil FCC (3). These units are designed to handle the high coke and gas make generated by cracking residual oils. The DA oil quality in terms of Conradson Carbon Residue and metals (Ni and V) content would not be so critical for these units and thus greater quantities of DA oil can be produced and utilized. In this scenario it is expected that the DA oil would be blended with gas oils to produce a standard feed for the FCC unit.

Even with a residual oil FCC unit there are both process and economic limits on the quality of oil which can be processed. A major process limitation is the coke burning capacity of the unit. As this is approached either the feedrate or the conversion has to be decreased. This in turn is related to feedstock CCR and metals. The effect of Ni and V can be mitigated by increasing catalyst addition rate, using metals resistant catalyst, or using passivators. However, each of these methods of controlling the deleterious effects of metals has an associated cost which reduces the economic incentive to process residual feeds in the FCC unit. It has been estimated that at present price levels, the economic limit for Ni + V content of a residual feed to an FCC unit is 35 - 45 ppm based on catalyst addition cost of $1/bbl (3).

The new designs of residual oil FCC units claim to be able to handle feedstocks containing up to nearly 50 ppm of metals and 8-10 wt% Conradson Carbon Residue (4). It is anticipated that if there is a continuing economic incentive to crack residual oils then these limits will be increased.

The crackability of heavy fractions is the subject of some controversy. One opinion is that 100% of the Conradson Carbon

Residue in the feed is yielded as coke in the FCC reactor (5) for all commercial FCC units. Another opinion is that with proper feed/catalyst contacting there is no casual relationship between coke and carbon residue (3). This author recommends the following to minimize coke formation:

- High temperatures to promote rapid vaporization and "shattering" of asphaltenes
- Atomized oil injection to maximize the rate of heat transfer and cracking
- Minimum of backmixing
- A short contact time

Under these conditions it is postulated that there will be a minimum thermal degradation in the liquid phase thus minimizing coke formation in the reactor.

From a chemical viewpoint the crackability of asphaltenes is central to any economic assessment of the catalytic cracking of asphaltic residual oils. Can these materials be cracked to yield valuable liquid products or must they, because of their structure, yield coke. Although the MAT reactor does not provide the type of oil/catalyst contact recommended for cracking residual oils, it should provide a minimum yield estimate which may be improved upon in a short contact high temperature riser.

3. VTB Composition

The structural complexity of materials in the residual oil fraction is gradually being understood as a range of analytical techniques are being used to separate and identify the types of components present. Residual oils are normally separated into asphaltenes, resins, and oil fractions prior to more detailed investigation.

Asphaltenes comprise the highest molecular weight material and are classified as the portion of the fluid soluble in benzene but insoluble in a non-polar solvent such as n-pentane or n-heptane. The deasphalted material is further separated into oils and resins by adsorption (clay) chromatography: the resins contain the remaining polar components while the saturate and aromatic material constitutes the oils. The combined oils and resins fractions are commonly referred to as the maltene fraction, the resins and asphaltenes together are termed asphalt. Although these classifications tend to be arbitrary and subject to some variability depending on the specific separation techniques used, they do seem to be consistent with the major chemical and physical characteristics of the fractions.

The asphaltenes has been studied extensively by many researchers (6-9) and some of the findings are summarized here:-

- Asphaltenes are rich in heteroatoms and deficient in hydrogen. A typical analysis of Athabasca asphaltene is C 79.9, H 8.3, N 1.2, S 7.6, O 3.2 wt% (6)
- Asphaltenes contain the major portion of porphyrins and other organometallic compounds of nickel and vanadium found in crude oil
- They contain a fair quantity of stable free radicals (10)
- Many components in the asphaltene fraction can be separated by column chromatograph as acids and bases (8). Possible basic and acidic functional groups include carboxylic acids, phenols, indoles, amides, pyrazine, sulphoxides, pyridine type structures (7)
- Recent NMR studies indicate that there are approximately 40 aromatic carbon atoms per 100 carbon atoms in an Athabasca asphaltene (6). UV studies and thermal techniques (9) suggest the presence of relatively small (1-4 ring) polynuclear aromatic systems rather than large (>10 ring) systems (9)
- Typical reported average molecular weight of asphaltenes are 2000 to 3600 Daltons (6, 8). It has been suggested (6, 8) that the more aromatic structures are relatively low molecular weight (800-1200 Daltons).
- Asphaltenes strongly associate in solution. In crude oil they are associated with the resins which maintain them in solution.

The resins can be considered as somewhat similar to asphaltenes in that they are polar materials but with lower molecular weight. As such they are generally lower in metals and sulphur and less hydrogen deficient than asphaltenes (1). They contain a similar range of functional groups to asphaltenes and can be separated into a number of acidic, basic and neutral fractions (11). According to S.R. Nelson (1) resins can be hydrotreated and hydrocracked to yield more valuable products. One aim of the present study is to determine if resins can be catalytically cracked to yield liquid products rather than gas and coke.

The oil fraction recovered from a VTB can be considered as a high molecular weight "gas oil". It contains similar saturate, and aromatic, materials that can be determined by high resolution mass spectrometry, the major difference being in the higher concentration of polycondensed structures.

4. Phase Separation of the Heavy Fractions

In determining the solubility features of crude oils and residual fractions, the resins play a key role. Asphaltenes are not soluble in the oil fraction unless there are resins present. The solubilization, or dispersion properties of the resins is a function of their degree of aromaticity and the proportion of hetero elements in the fraction; with high values of these parameters enhancing solubility.

Addition of light hydrocarbon solvents such as n-alkanes to the complex, but balanced, system represented by a petroleum fluid, will destabilize it thermodynamically leading, ultimately, to phase separation. Increasing the level of saturates in the system emphasizes the contrast between the different chemical species - aromatics and non-aromatics, saturates and polars etc., until they physically separate. One phase will be predominantly non-polar (solvent and oils) while the other will contain most of the polars (resins and asphaltenes).

To summarize, the separation of the heavy fractions from a petroleum fluid is a liquid-liquid phase phenomenon in which the principal components are defined as solubility classes, and at least one of these classes, the asphaltenes, has polymer-like properties. This description suggests that polymer solution models, possibly combined with elements of regular solution theory to accomodate the classification of components by solubility, would simulate the phase behaviour.

Correlation of the mass of asphaltene precipitated from Athabasca bitumen with the solubility parameter of the precipitating solvent was noted by Mitchell and Speight (14). More recently, Hirschberg (15) and coworkers at Shell's E&P Laboratory used a modified Flory-Huggins equation to calculate asphaltene flocculation from light crudes under gas injection. A similar approach was followed by Mansoori, Jiang and Kawanaka (16) in their model for predicting the onset of asphaltene deposition, with modifications to account for the heterogeneity of both the polymer and the solvent constituents of the solution.

Qualitatively, the principal features of a Flory-Huggins type solution may be used as a guide to the type of behaviour that may be anticipated in the deasphalting of petroleum fluids with light paraffin solvents.

In a Flory-Huggins liquid system, the phase behaviour is determined by the similarity, or dissimilarity, between the species designated as solvent and solute (polymer) as regards to molecular type and size. In general, for species which are relatively similar, the two phase liquid-liquid region, or region of immiscibility, will be small or non-existent. As the disparity between the type and size of the solvent and solute molecules increases, so will the extent of the region of immiscibility. Miscibility of solvent and solute will be possible only at high polymer (solute) concentrations on the one hand, or at very high solvent concentrations (almost infinite dilution) at the other extreme. Temperature-pressure effects are manifested by the relative changes in molar volume and solubility parameter between solvent and solute. Over the regions of temperature and pressure in this study, the solvents showed greater parameter variability than the VTBs (solutes). Increasing temperature-pressure emphasizes the disparity between solvent and solute leading to a broadening of the two phase region.

EXPERIMENTAL

The experimental work carried out under this contract included:-

1. Fractionation of Athabasca reduced crude sample
2. Characterization of reduced crudes (ATB), the vacuum gas oils and the vacuum tower bottoms samples
3. Catalyst characterization
4. Deasphalting experiments and phase behaviour measurements
5. Characterization of DA oils and residues from DA extraction
6. Microactivity Testing (MAT) of deasphalted oils and vacuum gas oils

1. Fractionation

The Athabasca sample (Syncrude Coker Distillate feed 305°C plus material) was distilled according to a modified ASTM method D1160 procedure. A vacuum of 1 mm was used to distill the heavy distillate then the vacuum was increased to 200 microns to remove the vacuum gas oil and leave the vacuum residue.

2. Feedstock Characterization

The Athabasca and Lloydminster VTB and gas oil samples were characterized by a number of physical and compositional properties determined by ASTM and other generally accepted methods. The standard properties determined include: density, aniline point, viscosity, Conradson Carbon content, as well as nitrogen, sulphur and metals concentrations, normal boiling range and composition by high resolution mass spectrometry. In addition, the softening point, penetration at 25°C and the oils, resins and asphaltenes content of the two VTB samples were determined.

Densities for the gas oils were determined in a Paar Densitometer at specific temperatures such that the material was a liquid. The density was then corrected to 15°C by standard correlation tables. The densitometer measures density on the basis of an oscillating tube filled with liquid. Specific methodology is outlined in ASTM Method D4052. The relative densities for the VTB samples were determined according to Gulf Canada Method GCM 243-5. This method is used to determine the relative density of asphaltic materials that are solid at room temperature. A molten sample is poured into a 1 cc mold and allowed to solidify. The resultant cube is placed in a glycerol-methanol-water solution and the composition adjusted until the cube and the solution have the same apparent density. The relative density of the solution is determined by means of a hydrometer and recorded as the relative density of the sample. The density at 15°C is converted to the specific gravity, which in turn is converted to the API gravity by the following relationship:-

$$API = (141.5/s.g. @ 60°F) - 131.5$$

Aniline point (D611) is the temperature at which aniline and an equal volume of liquid hydrocarbon sample are miscible. The aniline point decreases as the aromaticity of the sample increases, assuming all factors such as molecular weight and boiling range are equal. The two VTB samples and the Athabasca gas oil were too dark to allow an aniline point determination.

All gas oil and VTB samples were analyzed for normal boiling range by a gas chromatographic simulated distillation, as described in ASTM D2887. The method consists of injecting a liquid sample into a temperature programmable gas chromatograph equipped with an 2' x 1/4" dia. 10% OV-101/Chromasorb P column and an FID detector. The instrument is calibrated for retention time against true boiling point with a blend of n-paraffins which cover the boiling range of the sample to be determined. The instrument produces a chromatogram whose area slices are summed and normalized with respect to the total area to report a true boiling point curve for distillates on a mass % basis. Toluene was used as an internal standard in order to determine the percent recovered for the VTB samples.

ASTM D2170-85 describes the procedures for the determination of kinematic viscosity of liquid asphalts (bitumens), and distillation residues of liquid asphalts (bitumens) between 60°C and 150°C and in the range of 6 to 100,000 cSt. Viscosity is determined by measuring the time for a fixed volume of liquid to flow through the capillary of a calibrated glass viscometer under a reproducible head and at a closely controlled temperature. The kinematic viscosity can then be calculated from the efflux time and the viscometer calibration factor.

The Conradson Carbon determination is used to measure a material's propensity for forming coke. The experimental procedure employed was a modification of ASTM D189 in that an Alcor Mini Conradson Carbon analyzer was used. This instrument produces superior results because it employs both a nitrogen gas blanket and an automatic programmed temperature profile. As a result, analytical data is both more precise and reproducible.

The softening points of the VTB samples were measured in accordance with ASTM test D-36. This test method covers the determination of the softening point of bitumen in the range from 30 to 157°C. The apparatus consists of a ball and ring immersed in a heated medium. The softening point is reported as the mean of the temperatures at which two disks soften enough to allow each ball, enveloped in the bitumen, to fall a distance of 25 mm.

Metals analyses, particularly nickel and vanadium and sodium are another very important factor in assessing gas oils and residuum.

Metals analyses are carried out using a sequential, inductively coupled plasma instrument (ICP). DAO and residue samples, ranging in weight from 0.5 to 2.0 g are dissolved in 50 mL of xylene. This mixture is introduced into the ICP and the nickel and vanadium concentrations determined by comparison with a 3 point calibration curve.

Penetration of the VTB samples was carried out using ASTM Method D-5. This method is used in the determination of the penetration of semi-solid and solid bituminous materials. The sample is melted and cooled under controlled conditions. The penetration is measured with a penetrometer, and is expressed in tenths of a millimeter that a standard needle vertically penetrates a sample of the material under known conditions of loading, time and temperature.

The total sulphur content was determined by X-ray fluorescence according to ASTM D4292. The VTB samples were dissolved in toluene prior to testing. The total nitrogen content was determined by the ASTM Kjeldahl Method, D-3228-83. This method is applicable for determination of nitrogen in the concentration range from 0.03 to 2.0 weight %. The sample is digested in a mixture of concentrated sulfuric acid, potassium sulfate, mercuric oxide, and copper sulfate. After digestion, sodium sulfide is added to precipitate the mercury and the mixture made alkaline with the addition of caustic. Nitrogen in the form of ammonia is distilled into a boric acid solution and the ammonia titrated with standard sulfuric acid using methyl purple indicator. The basic nitrogen was determined by titration using GCM Method 212. Basic nitrogen content is determined by dissolving a weighed sample in an acetic acid-chloroform solvent and then titrating with a standard perchloric acid solution, using crystal violet indicator.

The two VTB samples were separated into asphaltenes, resins and oils fractions. The asphaltenes were determined as n-heptane insolubles according to ASTM Method D3279. The resulting maltene fraction from the deasphalting was further separated into a resins and oils fraction using an Attapulgus clay column as described by GCM 302.

The compositions of the gas oils and the oil fractions from the VTB separations were determined by high resolution mass spectrometry according to GCR 35.

The feedstock characterization and distillation data are given in Table 1, and the mass spectrometric analysis in Table 2.

3. Catalyst Characterization

The equilibrium catalyst sample (DA-440) was dried and decoked in accordance with ASTM D3907 prior to characterization. The following properties of the catalyst were determined:-

1. Surface area, pore size distribution and zeolite area by N_2 adsorption-desorption.
2. Surface area, pore volume and pore size distribution by mercury porosimetry.
3. Elemental analysis: V, Ni, Fe, Cu, Na and Al.
4. Zeolite unit cell dimension.

In addition, microactivity data and physical properties were obtained from Davison Chemical.

a. Nitrogen Sorption Measurements

The gas adsorption-desorption isotherm was obtained using the Micromeritics Orr SAPV Analyzer Model 2100. The sample was outgassed at 100°C for 24 hours to remove any residual species. Nitrogen was used as the adsorbing gas. Relative pressure vs. volume adsorption measurements were made over a range of relative pressures.

$$P2/P0 = 0.1 - 0.99 \text{ for DA-440}$$

The BET surface area was determined by ASTM D3663. The slope and intercept of the BET diagram were used to calculate the volume of adsorbate required to complete a statistical monolayer of nitrogen and this value was converted into $(nm)^2$ surface area by assuming a 0.162 $(nm)^2$ cross sectional area for the nitrogen molecule.

The zeolite surface area was determined according to ASTM D4365 following the procedures described by Johnson (12). The thickness of the adsorbed nitrogen layer (t) calculated according to the equation:-

$$t = \left(\frac{13.99}{0.034 - \log P2/P0} \right)^{1/2}$$

was plotted against the volume of nitrogen adsorbed. The surface area obtained from the slope of this plot is the mesopore area. This is subtracted from the BET surface area to give the zeolite surface area. The micropore (zeolite) volume is obtained from the intercept of the t plot. The zeolite surface area has been correlated with the micropore volume and the percentage zeolite by Johnson (12). The nitrogen sorption measurements were also used to calculate a pore size distribution.

b. **Mercury Porosimetry**

Samples of the catalyst were subjected to high pressure mercury intrusion using the Micromeritics Autopore 9200 porosimeter. The instrument operates on the principle that when mercury, a non-wetting liquid, is forced into a solid material the pressure required to completely fill the pores is in inverse proportion to the size of the pore. The exact relationship is given by the Washburn equation.

$$d = \frac{-4\sigma\cos\theta}{p}$$

where d is the pore diameter, σ the surface tension of mercury, θ the contact angle mercury makes with the solid and p is the pressure.

The following conditions were employed:-

Mercury Contact Angle θ	:	130°
Mercury Surface Tension σ	:	485 dynes/cm
Pressure Range p	:	0.5 - 60000 psia

Since θ and σ remain constant, application of a known pressure yields the corresponding dimension.

The raw data were corrected for intrusion into the interparticle voids prior to calculating the intraparticle pore volume, the surface area and the average pore diameter. Mercury at 60000 psia will fill 30A° pores limiting the pore volume distribution obtained by this method. Thus, this method considers only the matrix mesopores ranging from 2400A° to 30A° while nitrogen adsorption ranges from the zeolite micropores to pores of 1000A°.

c. **Zeolite Unit Cell Dimension**

The unit cell size can be correlated with both the activity and selectivity of a gas oil cracking catalyst.

The unit cell size was determined for the catalyst by X-ray diffraction according to ASTM D3942. The sample was mixed with powdered silicon, and the unit cell size calculated from the X-ray diffraction pattern of the mixture, using silicon reflections as a reference.

d. **Elemental Analysis**

Nickel, vanadium, iron and aluminum were determined by X-ray spectroscopy. In summary, a dried sample was mixed with lithium tetraborate-lithium carbonate flux and fused at 954-982°C. The fusion bead was crushed, briquetted on a boric acid backing and counted in an X-ray vacuum spectrometer.

Aluminum was reported as wt% alumina (Al_2O_3).

Sodium and copper were determined by atomic absorption spectroscopy and carbon using a Leco carbon analyzer.

The data obtained from the catalyst characterization is summarized in Table 4.

4. Solvent Deasphalting - Experiments and Phase Behaviour Measurements

The equipment used to carry out the deasphalting experiments is shown in Figure 1. A known weight of VTB is dissolved into a known weight of toluene (approximately 1 mL toluene/0.3 mL VTB). The blend is transferred into a double-ended sample cylinder (transfer vessel) capable of withstanding pressure to approximately 500 psi and compressed with mercury.

The required amount of the blend is transferred by mercury displacement to the PVT cell which is held at 75°C. The volume displaced from the sample cylinder and the volume added to the cell are measured before an additional 100 mL of mercury is removed from the cell. The top valve of the cell is shut and the inlet line is attached from the top valve to a vacuum system. Toluene is evaporated from the blend by opening the top valve and evacuating the cell and its contents overnight.

The volume of solvent required to give the desired VTB/solvent ratio is determined using Starling's tabulations (17). This volume is added to the PVT cell, again using the mercury displacement technique. The cell is then brought to the operating temperature and pressure, and the mixture is equilibrated by shaking for one hour.

The phases are allowed to separate for 3 hours, at equilibrium temperature and pressure, before the solvent rich phase is removed at the equilibrium pressure from the cell by mercury displacement. The solvent rich phase is collected in a tared flask, sufficiently chilled to prevent solvent losses (propane requires a dry ice - acetone slurry, butane and pentane require dry ice, while an ice bath is sufficient for n-heptane). When all the solvent rich phase is removed from the cell, there is a sudden increase in the resistance of the mercury pump (due to the difference in viscosities between the solvent rich and solvent lean phases). The volume of mercury added to the cell is recorded. The cell temperature is set at 75°C, and toluene (50 mL) is added to the cell. After shaking for 20 minutes, the toluene fraction is displaced from the cell using the mercury pump. This washing procedure is repeated four times.

The weight of the solvent rich phase is determined before the solvent is evaporated off and the weight of deasphalted oil determined. Toluene is evaporated from the solvent lean phase in order to determine the weight of residue. The weight of solvent in the solvent lean phase is obtained by subtracting the weight of solvent in solvent rich phases from the total weight of solvent added to the cell. This value can be verified by analyzing the first 50 mL toluene extract for solvent content by gas chromatography.

To complete the phase behaviour measurements, the concentrations of the oils, resins and asphaltenes in the solvent rich and solvent lean phases are required. The DA oil and the residue are deasphalted using ASTM Method D3279 and the recovered maltene fractions are then separated into oils and resins on an Attapulgus clay column according to GCM 302. For this study, 33 g of clay was used to separate 1 g of maltenes dissolved in 10 mL of n-heptane. The oils were eluted from the column with 200 mL of n-heptane. Resins were then eluted from the column using 70 mL of methylene chloride followed by 70 mL of a 80% methylene chloride, 20% diethylether mixture. The data obtained from the Deasphalting experiments are presented in Tables 6 to 11.

5. Characterization of the Oil from the Deasphalting Experiments

When DA oils were to be used in the MAT program they were initially characterized by standard testing methods to determine density, aniline point, Conradson Carbon residue, sulphur content, total nitrogen content, and basic nitrogen content. In addition, the nickel and vanadium concentrations in the oil and the residue samples were also determined. The methods used were those reported for the feeds in Section 2 above. The properties of the DA oils are reported in Tables 12 to 19.

6. The Microactivity Test (MAT)

A schematic drawing of the MAT unit is shown in Figure 2. The reactor is loaded with 4.0 g of catalyst and the unit is purged with nitrogen, at temperature, for at least 30 minutes before performing a test. The feed (which is preheated to 40-130°C) is delivered at 1.28 g/min. by a constant drive syringe pump through a syringe needle. On entering the reactor, the feed is injected approximately 1 cm above the bed and the liquid vapour mix cracks in the catalyst bed. The nitrogen purge (20 mL/min) continues during and after feed injection and the run is terminated 15 minutes after start of feed injection. The weight of feed injected is determined by weighing the syringe before and after the run. All thermocouples are attached to the wall of the reactor and the thermocouple at the middle of the catalyst bed is used as the sensor for the furnace temperature controller.

The cracked products and nitrogen purge gas pass down into an ice bath cooled receiver, where the liquid products condense. The gaseous products and nitrogen purge gas pass out of the side arm of the receiver and are collected in a Ruska volumeter. The weight of liquid product is obtained by weighing the receiver before and after the run. The volume of gaseous product plus nitrogen is determined as a direct reading from the volumeter. After weighing the total liquid product, a portion is immediately pipetted into a cooled vial and the vial is then "capped" and the sample is analyzed by gas chromatographic distillation. The gas sample is discharged into an evacuated gas sample bag and the sample immediately analyzed by G.C. for (a) hydrogen and (b) all other components. After cooling, the catalyst is removed from the reactor into a sample vial, homogenized, and submitted for a "Leco" carbon determination.

A Hewlett-Packard 5500 gas chromatograph fitted with a 2 ft. x 1/4" 10% OV-101 column and a flame ionization detector is used to determine the gas chromatographic distillation (GCD). The instrument is temperature programmed from -50°C to 350°C and the percent distilled vs. normal boiling point is automatically calculated. Calibration of elution temperature vs. boiling point is done using a standard n-paraffin blend. It is most important that the elution time/b.p. calibration be maintained to ensure correct gasoline, LCO and decant oil yields. Visual inspection of the reactor effluent liquid chromatograms are used to confirm that the calibration is correct. When a small deviation is noted, the instrument is immediately recalibrated. Since there are small amounts of C_4 hydrocarbon and significant amounts of C_5 hydrocarbon in the liquid product, the GCD procedure is modified to calculate these components as well as a C_6+ gasoline concentration. Temperatures of 216°C and 343°C are used as the end points for the gasoline and LCO fractions respectively. It is assumed that the weight response factor for the flame ionization detector is unity.

The major gas analysis is carried out using a Varian gas chromatograph fitted with a thermal conductivity detector and using helium as a carrier gas. The valving/column arrangement separates all the C_1-C_5 paraffins and olefins, H_2, N_2, O_2, CO, CO_2 and H_2S and provides an analysis of the C_6+ components as a single peak.

Since the gas always contains a high concentration of nitrogen (from the purge) the chromatograph is calibrated for nitrogen on an absolute basis (known partial pressure of nitrogen at a known temperature) and the concentration of nitrogen in a gas sample is calculated directly from this calibration. This analysis is then used along with the total volume of gas collected to calculate the volume of nitrogen purge gas. This volume is then compared to the volume of nitrogen computed from the nitrogen flow rate and purge time (analytical material balance and flow material balance). With the exception of hydrogen (see below) all other component concentrations are determined using relative response factors. The response factors for this instrument are established and if necessary updated using a certified primary calibration blend from Matheson which contains nineteen hydrocarbons of interest. Separate calibration is carried out for H_2S because of the reactive nature of this species. Hydrogen is determined on an absolute basis with a chromatograph that uses a TC detector and nitrogen as the carried gas. Hydrogen is separated from other permanent gases on a molecular sieve column while all other components are stripped to vent.

a. **Yield Calculations**

Yields are automatically computed using an IBM PC to generate the two page report shown as Tables 5 & 6. The first page contains all the input data while the second page gives component yields as weight percent (and volume percent) of feed.

The material balance is computed as follows:-

- The feed and liquid product are directly weighed.
- The weight of reactor effluent gas is calculated from the gas volume and analysis.

The weight of coke is calculated as:-

$$\text{wt\% Coke on Catalyst} \times \text{wt. Catalyst} \times 1.1 \times 0.01$$

The 1.1 factor assumes catalytic coke is 91% carbon.

For reasonable quality feedstocks the material balance ranges between 97 and 102%. Under these circumstances, the yields are normalized by adjusting the weight of gas to give a correct material balance.

This procedure gave good material balances for the initial DA oils evaluated in the MAT program. However, for the more asphaltic DA oils evaluated later in the program the MAT material balance was no longer acceptable. The reason was that the coke make was an underestimate because:-

1. The simple coke yield calculation used above overestimates the amount of carbon in additive coke and underestimates the coke yield.

2. The significant coke build-up in the reactor internals which occurs when cracking asphaltic DA oils is not accounted for in the material balance.

A revised calculation procedure was developed to account for the higher additive coke values but this did not account for reactor coke deposits. After consulting with the Scientific Authority it was decided to determine the coke make for asphaltic DA oils as the difference in the material balance.

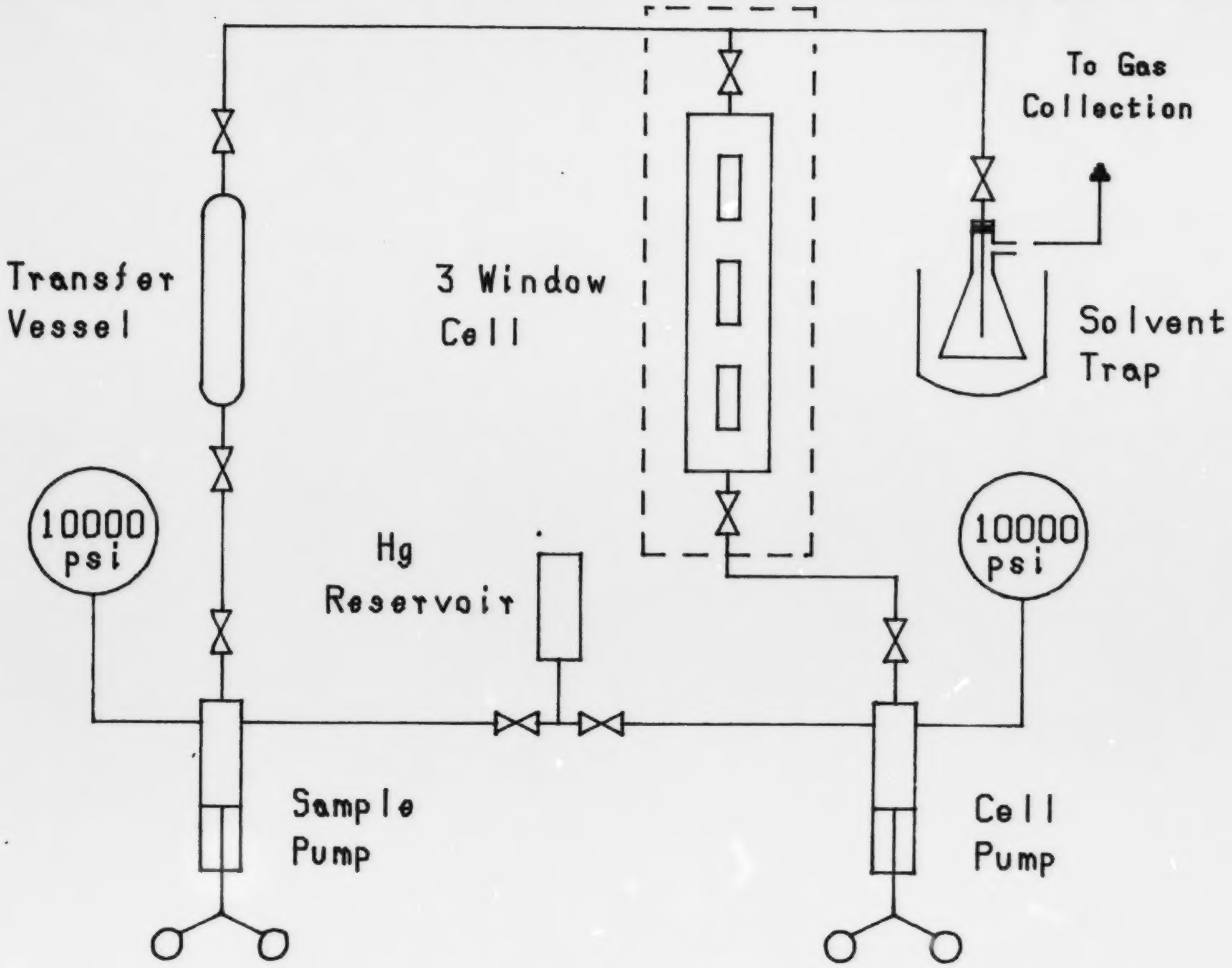
Transfer
Vessel
3 Window
Cell
To Gas
Collection
Solvent
Trap
10000
psi
Hg
Reservoir
10000
psi
Sample
Pump
Cell
Pump

Figure 1: SOLVENT DEASPHALTING EQUIPMENT

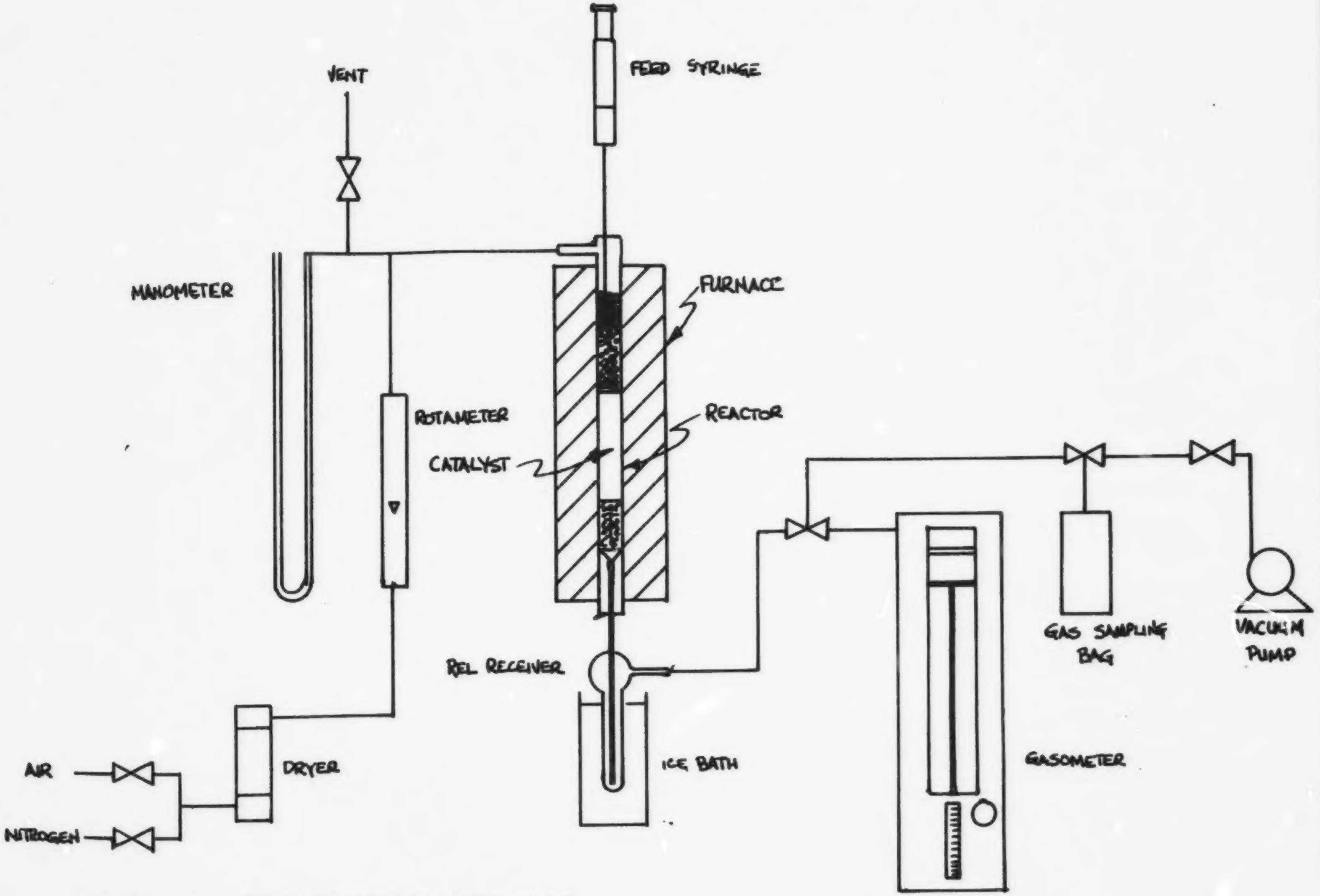
VENT
FEED SYRINGE
MANOMETER
FURNACE
ROTAMETER
REACTOR
CATALYST
REL RECEIVER
GAS SAMPLING BAG
VACUUM PUMP
AIR
NITROGEN
DRYER
ICE BATH
GASOMETER

Figure 2: MICROACTIVITY TEST UNIT

DISCUSSION

1. Athabasca Sample Fractionation - Result

A sample of Syncrude Coker Feed 305°C plus material was distilled using a modified D1160 procedure to yield a heavy distillate, a vacuum gas oil and a vacuum tower bottom.

Heavy Distillate	IBP - 360°C	12.4 wt%
Vacuum Gas Oil	360 - 544°C	24.1 wt%
Vacuum Tower Bottoms	544C°+ material	63.5 wt%

The VGO and VTB were further characterized while density and GCD data were obtained on the Syncrude Coker Feed.

2. Lloydminster Sample Blending

These samples were obtained from an Ontario refinery processing Lloydminster crude oil. In this operation, both light and heavy vacuum gas oil samples are drawn from the vacuum tower. These were backblended based on refinery yield data to produce a composite VGO sample (41.7 vol% LVGO to 58.3 vol% HVGO). The vacuum tower bottoms was of course a composite sample.

3. Feedstock Characterization Results

Table 1 contains the characterization of the two VGO and VTB samples along with density and GCD data for the two ATB samples.

The high resolution mass spectrometric analysis of the two VGO samples and the oil fractions from the two VTB samples are given in Table 2.

To verify that the VTB samples used in this study were typical of Athbasca and Lloydminster VTBs the results were compared with previous data. In the case of the Athabasca VTB we report the results of three separate laboratories (A, B and C) analyzing an Athabasca VTB sample. Considering that the present work was based on a different sample, the comparison in Table 3 shows that there is excellent agreement between the present data and the other sets of analyses.

The quality of the Lloydminster VTB is somewhat more variable which is to be expected. The results of the present study are compared in Table 3 with:-

1. Another VTB sample from an Ontario Refinery.
2. A residuum sample obtained from the crude oil assay of primary (field produced) Lloydminster heavy oil.

As can be seen, the dilution of the primary produced heavy oil with condensate and the pipelining to Ontario changes the characteristics of the Lloydminster VTB. The residuum from the primary produced heavy oil show a greater density, viscosity, sulphur content and nitrogen content than the refinery material used in the present study (Table 3).

The feedstock characterization results from Table 1, show that the Athabasca VTB is a significantly heavier feedstock than the Lloydminster VTB. It contains approximately a third more sulphur, nitrogen and asphaltic material (asphaltenes + resins) and 2 1/2 times the Ni + V content. In addition, the Conradson Carbon residue for the Athabasca VTB is one third higher than for the Lloydminster VTB. The GCD data indicate that the Athabasca sample has been cut a little heavier than the Lloydminster sample.

The high resolution mass spectrometric analysis of the oil fractions obtained from the two VTB samples again shows that the Athabasca sample is much more aromatic than the Lloyd sample and would make a poorer FCC feedstock. Using standard gas oil correlations that assume the crackable components are limited principally to the saturates and monoaromatics, it can be seen that the Lloyd oil sample contains approximately twice the amount of crackable components than the Athabasca sample (42.5 wt% vs. 22.9 wt%). However, for these residual oils there has to be significant cracking and dealkylation of the more condensed aromatics and naphthenoaromatics to yield further gasoline and light liquid products. This should reduce the expected difference in catalytic cracking yields between the two residual oils.

It is interesting to compare the properties of Lloyd and Athabasca VTB with other VTBs which have been considered for upgrading to FCC feed by solvent deasphalting. The data below compares the VTB properties of two other major crude oils with the present samples (13).

Comparison of VTB Properties

	Light Arabian*	Maya*	Lloyd	Athabasca
° API	6.9	0.99	6.3	-0.7
Sulphur, wt%	4.0	5.4	4.53	5.93
Nitrogen, wt%	0.31	0.27	0.50	0.64
Conradson Carbon, wt%	20.8	25.2	18.3	24.3
Asphaltenes, wt%	10.0	12.6	13.7	17.3
V + Ni, wt, ppm	98	511	173	440

* R.T. Penning, A.G. Vickers and B.R. Shah, H.P., May, 1982, p. 145

The Lloyd VTB has similar properties to the Light Arabian VTB, while the Athabasca VTB is closer to the Maya VTB. The two properties which do not fall into line are the nitrogen content and asphaltenes which are higher for the Lloyd and Athabasca samples which may be expected since these are classified as more asphaltic materials.

The two vacuum gas oils are quite different character. The Lloyd gas oil has an API gravity of 21.1, an aniline point of 65°C and a total nitrogen of 606 ppm and is considered a reasonable quality asphaltic FCC feedstock. The Athabasca vacuum gas oil has an API gravity of 13, a total nitrogen content of 1635 ppm, is too dark for aniline point determination and is considered a poor quality FCC feedstock. These conclusions are supported by the high resolution mass spectrometric analysis of the two gas oils (Table 2) which are summarized below.

	Lloyd VGO	Athabasca VGO
Crackable Components	69.7	60.1
Refractory Components	30.3	39.9
Compositional Conversion Constraint	69.7	60.1

These results suggest for a given severity, there would be 9-10 numbers difference in conversion between the two gas oils.

4. Catalyst Characterization

Table 4 summarizes the data obtained for the catalyst. The microactivity and particle size distributions were obtained from Davison, while the remaining information was obtained by Sheridan Technical Associates.

The microactivity data shows the DA-440 catalyst is typical equilibrium catalyst.

Microactivity Data

	DA-440
% Conversion	70
Coke Factor	1.0
Gas Factor	1.1

The conditions specified by Davison Chemical to determine the % conversion are:-

West Texas Gas Oil	260 - 482°C
C/O Ratio	2.9
WHSV	16 h^{-1}
Injection Time	75 s
Reactor Temperature	482°C

The surface area and pore volumes reported by Davison are in good agreement with the values determined for Sheridan Technical Associates.

		DA-440
BET Surface Area - Davison	m^2/g	76
BET Surface Area - This Study	m^2/g	75.5
Pore Volume - Davison	cc/c	0.26
Pore Volume - This Study	cc/g	0.245

Based on the microactivity data, the metals loading, and the physical properties, the sample is considered a typical example of equilibrium gas oil cracking catalyst.

The measured unit cell dimension for the DA-440 catalyst was 24.42 A°, which is considered typical for a conventional REY catalyst.

The zeolite content of the DA-440 catalyst was estimated at 7.6%, based on nitrogen adsorption measurements. The volume of nitrogen adsorbed plotted against the thickness of the adsorbed layer (t plot) is shown in Figure 3. The slope of the t plot is used to estimate the mesopore surface area which when subtracted from the BET surface area, gives the zeolite surface area. The zeolite content was then estimated for the zeolite surface area using data presented by Johnson (12).

N_2 Adsorption Data

		DA-440
BET Surface Area	m^2/g	75.5
Mesopore Surface Area	m^2/g	26.7
Zeolite Surface Area	m^2/g	48.8
Zeolite Content	%	7.6

The nitrogen adsorption method provides data on surfaces for pore diameters of approximately 1000 A° and less. The pore size distribution within this range is given in Figure 4.

The pore volume, surface area and pore size distribution were also determined by mercury intrusion porosimetry. This method investigates pores down to 30 A°, effectively limiting its range to the mesopore or matrix surface properties. As is shown by the alumina content, see Table 4, the catalyst is designed with an active matrix to encourage bottoms cracking. Based on the porosimetry data, the average matrix pore diameter for the DA-440 catalyst is 280 A°.

Figure 5 shows the plot of pore volume vs. pore diameter for the DA-440 catalyst.

TABLE 1

CHARACTERIZATION OF FEEDSTOCKS
FEEDSTOCK INSPECTION DATA

	ASTM METHOD	LLOYD VTB	LLOYD VGO	LLOYD ATB	ATHABASCA VTB	ATHABASCA VGO	ATHABASCA ATB
API		6.3	21.1	10.8	-0.7	13.0	6.8
Density at 15°C	D4052, D1250	1.0262	0.9265	0.9938	1.0818	0.9785	1.0225
Softening Point, °C	D36	36	-	-	66	-	-
Pen at 25°C, 0.1 mm	D5	192	-	-	11	-	-
Viscosity at 135°C, cSt	D2170	205	-	-	2002	-	-
Viscosity at 150°C, cSt	D2170	113	-	-	959	-	-
Aniline Point, °C	D611	-	65	-	-	Too Dark	-
Conradson Carbon, wt%	D189	18.34	0.07	-	24.33	0.92	-
Total Nitrogen, ppm	D3228	4964	606	-	6390	1635	-
Basic Nitrogen, ppm	UOP-269-59	1352	195	-	1820	551	-
Total Sulfur, wt%	D4294	4.53	2.10	-	5.93	3.73	-
Ni, ppm	Zenon/ICP	84	0.10	-	130	0.55	-
V, ppm	Zenon/ICP	189	0.14	-	310	3.5	-
Fe, ppm	Zenon/ICP	0.51	0.77	-	470	11	-
Cu, ppm	Zenon/ICP	0.1	<0.02	-	0.8	0.06	-
Na, ppm	Zenon/ICP	<1	<2	-	64	<3	-
Oil Fraction, wt%	GCM 302-3	59.0	-	-	46.0	-	-
Resin Fraction, wt%	GCM 302-3	27.3	-	-	36.7	-	-
Asphaltenes, wt%	D3279	13.7	-	-	17.3	-	-
Boiling Range by GCD, °C							
IBP		316	238	232	331	313	246
5%		429	291	337	507	364	305
10%		465	319	370	535	379	346
30%		554	367	460	-	417	462
50%		-	398	554	-	448	568
70%		-	431	-	-	475	-
90%		-	480	-	-	515	-
95%		-	510	-	-	544	-
FBP		-	554	-	-	583	-

TABLE 2

FEEDSTOCK COMPOSITION BY HIGH RESOLUTION MASS SPECTROMETRY
(MASS %)

	LLOYD VTB (Oil Fraction)	LLOYD VGO	ATHABASCA VTB (Oil Fraction)	ATHABASCA VGO
Paraffins	3.1	8.0	0.7	2.6
Monocycloparaffins	8.3	14.0	3.6	9.2
Condensed Cycloparaffins	18.4	26.6	10.7	27.3
Alkylbenzenes	5.2	6.6	2.8	6.1
Benzocycloparaffins	3.4	5.9	1.9	4.5
Benzodicycloparaffins	4.1	5.7	3.2	5.5
Diaromatics	11.7	15.6	10.2	15.7
Triaromatics	7.9	6.7	10.7	10.1
Tetraaromatics	7.0	1.2	9.1	4.1
Pentaaromatics	7.0	0.0	15.4	0.8
Polyaromatics	5.3	0.0	11.5	0.2
Thiophenes	4.1	2.1	2.5	4.5
Benzothiophenes	5.5	3.6	3.7	3.0
Dibenzo/Naphtho-thiophenes	5.1	3.2	3.7	5.5
Benzonaphthothiophenes	3.6	0.0	10.3	0.5
Furans	0.3	0.8	0.0	0.4
	100.0	100.0	100.0	100.0

TABLE 3

COMPARATIVE DATA: ATHABASCA AND LLOYDMINSTER VTBs

	ATHABASCA VTB				LLOYDMINSTER VTB		
	Lab A	Lab B	Lab C	Present Study	Refinery Material	Assay of Primary 507+ Resid	Present Study
API				-0.7	8.6	3.5	6.3
Density at 15°C	1.0607	1.0589	1.0664	1.0818	1.0093	1.0475	1.0262
Softening Point, °C	70	67	66.5	66			36
Pen at 25°C, 0.1 mm	8			11			192
Viscosity at 135°C, cSt	2214	1702	1938	2002		1652	205
Viscosity at 150°C, cSt	921	756	832	959		696	113
Aniline Point, °C				-			-
Conradson Carbon, wt%	23.2	23.25	22.76	24.33	17.3		18.34
Total Nitrogen, ppm	6550			6390	3490	5835	4964
Basic Nitrogen, ppm				1820			1352
Total Sulfur, wt%	6.90	5.68	6.42	5.93	5.27	6.29	4.53
Ni, ppm	111	120	129	130	63.1		84
V, ppm	370	365	341	310	136		189
Fe, ppm	72			470	35		0.51
Cu, ppm	2.49			0.8	0.57		0.1
Na, ppm				64			<1
Oil Fraction, wt%				46.0			59.0
Resin Fraction, wt%				36.7			27.3
Asphaltenes, wt%				17.3	14.2		13.7
Boiling Range by GCD, °C							
IBP				331	337		316
5%				507	376		429
10%				535	401		465
30%				-	500		554
50%				-			-
70%				-			-
90%				-			-
95%				-			-
FBP				-			-

TABLE 4

EQUILIBRIUM CATALYST PROPERTIES

Catalyst Source	DA 440 Canadian Refinery
N_2 Adsorption Measurements	
BET Surface Area, m^2g	75.5
t Plot Surface Area, m^2/g	26.7
Zeolite Surface Area, m^2/g	48.8
Micropore Volume, cc/g	0.025
Zeolite Content, wt%	7.6
Hg Intrusion Porosimetry to 30A°	
Surface Area, m^2/g	35.0
Intraparticle Pore Volume, cc/g	0.2453
Average Pore Diameter, A°	280
Elemental Analysis	
V, ppm w/w	141
Ni, ppm w/w	374
Ni + V/5, ppm w/w	402
Cu, ppm w/w	20
Fe, wt%	0.72
Na, wt%	0.34
C, wt%	0.26
Al_2O_3, wt%	42.1
Unit Cell Dimension, A°	24.42
Physical Properties*	
Surface Area, m^2/g	76
Pore Volume, cc/g	0.26
Apparent Bulk Density, g/cc	0.93
Particle Size Distribution, wt%*	
0 - 20 microns	1
0 - 40 microns	8
0 - 80 microns	58
APS microns	75
Microactivity Data*	
% Conversion	70
Coke Factor	1.0
Gas Factor	1.1

* Davison Values

TABLE 5

MICROACTIVITY TEST: INPUT PARAMETERS

FILE NAME : MAT7

Date of Run	88-02-12
Catalyst Type	DA-440
Fresh Feed	DAO 20A-10
Comments	

GAS CHROMATOGRAPHIC ANALYSIS
REACTOR EFFLUENT GAS

Compound	Moles	Mole %	Compound	Moles	Mole %
Hydrogen	1.31	3.833	1-Butene	3.59	3.452
Carbon Monoxide	0.00	0.000	2-Methylpropene	0.59	0.567
Nitrogen	65.82	0.000	trans-2-Butene	2.85	2.741
Hydrogen Sulphide	17.38	16.714	cis-2-Butene	2.11	2.029
Carbon Dioxide	0.00	0.000	i-Pentane	6.55	6.299
Methane	14.86	14.290	n-Pentane	1.01	0.971
Ethane	6.97	6.703	1-Pentene	0.22	0.212
Ethylene	5.17	4.972	2-Methyl-1-Butene	0.33	0.317
Propane	6.76	6.501	trans-2-Pentene	0.56	0.539
Propene	13.97	13.435	cis-2-Pentene	0.65	0.625
i-Butane	9.26	8.905	2-Methyl-2-Butene	0.83	0.798
n-Butane	3.38	3.250	C6+	2.96	2.847

Total Moles :167.13

Molar Mass : 32.67
Hydrocarbon : 41.63

RUN CONDITIONS

Room Temperature :	24.0	Catalyst Charge g:	4.0081
Atm. Press. mmHg:	741.5	Fresh Feed g:	1.0428
Gas Volume mL:	460.0	Reactor Liquid g:	0.6628
Cat. Bed Temp. :	510.0	Injection Time s:	46.0500
Carbon on Cat. :	2.67	Feed Density g/mL:	0.9937
N2 Flow ml/min:	20.8		

REACTOR EFFLUENT LIQUID

C4 i-Paraffin :	0.020	C5 n-Paraffin :	0.210
C4 n-Paraffin :	0.030	C5 Olefin :	0.860
C4 Olefin :	0.080	IBP-216 EP :	51.700
C5 i-Paraffin :	1.160	IBP-343 EP :	82.200

TABLE 6

```
MICROACTIVITY TEST: PRODUCT YIELD STRUCTURE

                                       FILE NAME : MAT7

        Date of Run      88-02-12
        Catalyst Type    DA-440
        Fresh Feed       DAO 20A-10
        Comments

   ----------------------------------------------------------

               PRODUCT YIELD STRUCTURE
                              (% Fresh Feed)

                              ---- YIELD ----    YIELD/CONVERSION
                              Mass %   Vol. %      m/m     V/V
 -----------------------------------------------------------------
    Hydrogen                :   0.05     0.00     0.001   0.000
    Hydrogen Sulphide       :   3.44     0.00     0.050   0.000
    Methane                 :   1.38     0.00     0.020   0.000
    Ethane                  :   1.22     0.00     0.018   0.000
    Ethylene                :   0.84     0.00     0.012   0.000
    Propane                 :   1.73     3.39     0.025   0.050
    Propylene               :   3.42     6.50     0.049   0.095
    i-Butane                :   3.14     5.54     0.045   0.081
    n-Butane                :   1.16     1.97     0.017   0.029
    C4 Olefins              :   3.03     4.94     0.044   0.072
    i-Pentane               :   3.48     5.54     0.050   0.081
    n-Pentane               :   0.56     0.88     0.008   0.013
    C5 Olefins              :   1.60     2.42     0.023   0.035
    C6+ Gasoline  (216C EP) :  32.96    41.99     0.476   0.614
    LCO     (216C-343C Cut) :  19.39    20.71     0.280   0.303
    Decant      (343C+ Cut) :  11.31    10.91     0.163   0.160
    Coke Make               :  11.29              0.163
 REL & REG OVERALL YIELDS
   Effluent Liquid          :  63.56
   Effluent Gas    (meas.)  :  25.12
   Effluent Gas    (calc.)  :  25.15
 ----------
   Conversion               :  69.30    68.37
 =================================================================

 Catalyst Charge g : 4.008         Liquid SV, W/(W.hr) : 20.3
 Fresh Feed      g : 1.043         Gas SV, V/(V.sec)   :  0.95
 Catalyst to Oil   : 3.844
 Coke on Catalyst  : 2.937

            MASS BALANCE (mass% FF)  : 99.97  Analytical
                                       98.61  Flow


 SHERIDAN TECHNICAL ASSOCIATES INC                  02-25-1988
```

Figure 3

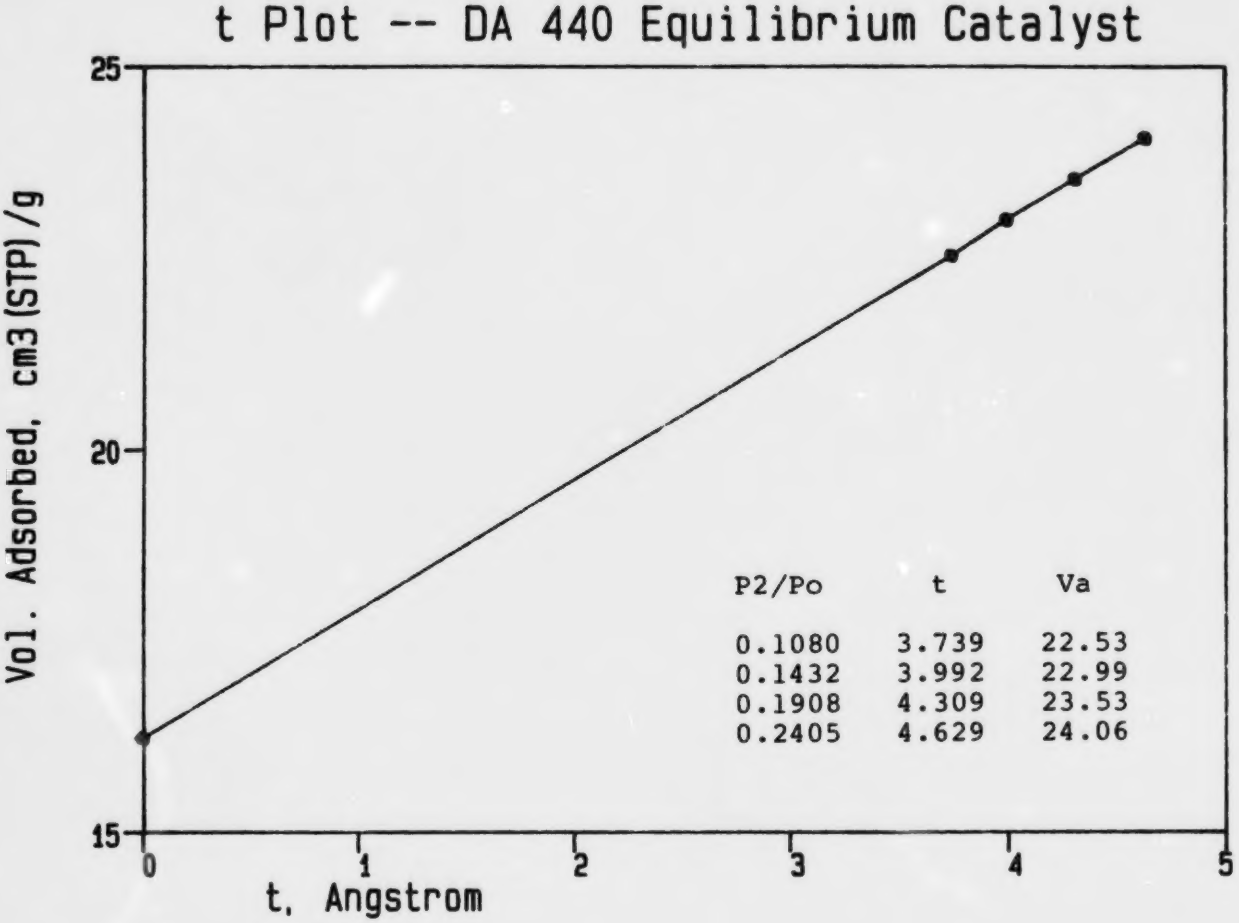
t Plot -- DA 440 Equilibrium Catalyst

P2/Po	t	Va
0.1080	3.739	22.53
0.1432	3.992	22.99
0.1908	4.309	23.53
0.2405	4.629	24.06

$$S = \frac{24.63 - 16.23}{5} = 1.68$$

$$t(\text{area}) = \frac{S \times 15.47}{0.975} = 26.66 \text{ m2/g}$$

BET area = 75.5 m2/g

Micropore area = 48.8 m2/g

$$\text{Micropore volume} = 16.23 \times 15.47 \times 10^{-4} = 0.025 \text{ cc/g}$$

From M.L.F. Johnson's plots, this micropore volume corresponds to a zeolite area of 50 m2/g and a micropore area of 48.8 m2/g corresponds to approx. 7.6% zeolite.

Figure 4

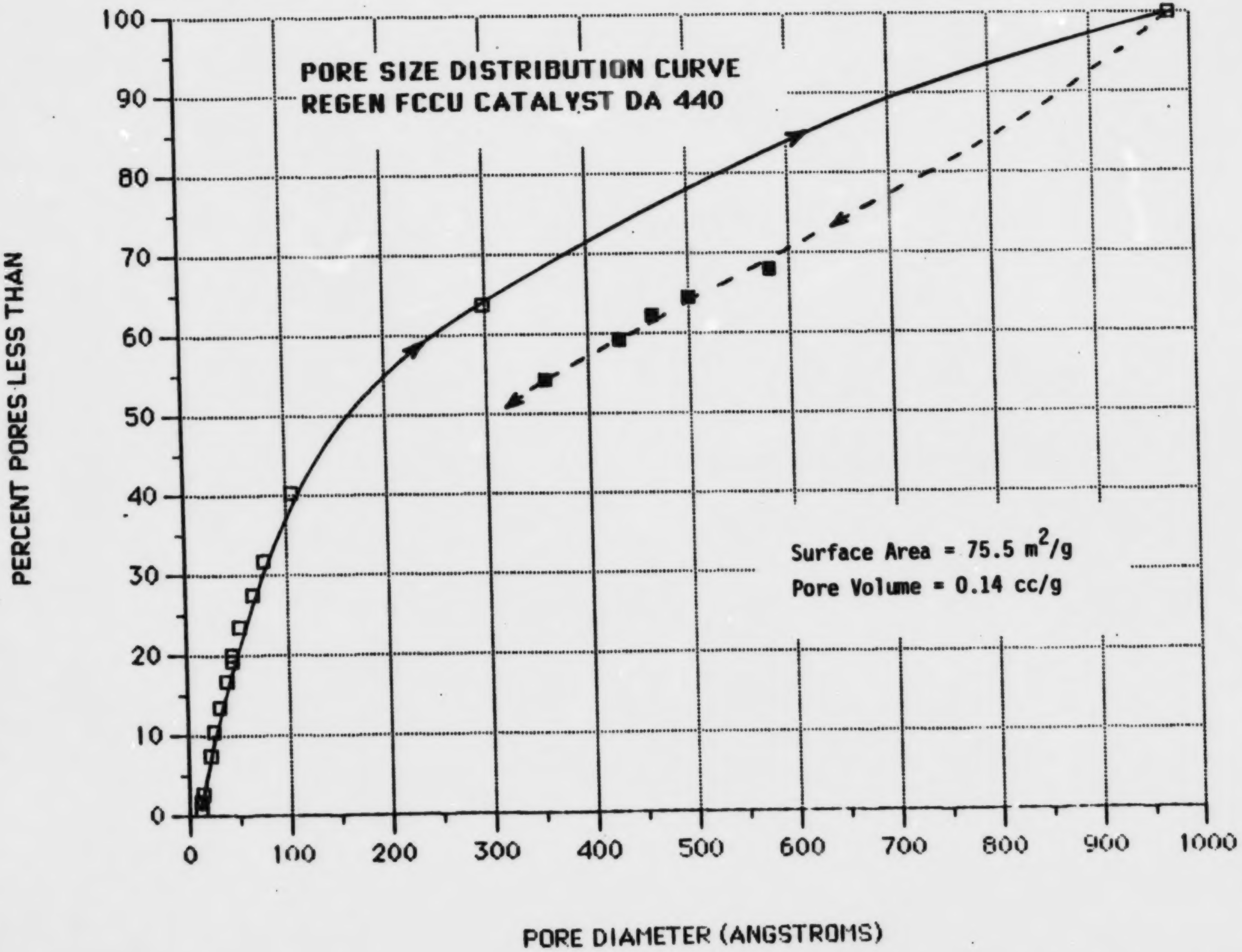
PORE SIZE DISTRIBUTION CURVE
REGEN FCCU CATALYST DA 440
Surface Area = 75.5 m²/g
Pore Volume = 0.14 cc/g
PERCENT PORES LESS THAN
100
90
80
70
60
50
40
30
20
10
0
0
100
200
300
400
500
600
700
800
900
1000
PORE DIAMETER (ANGSTROMS)

Figure 5

```
                 MICROMERITICS AUTO-PORE 9200 V2.02

ONTARIO RESEARCH FOUNDATION, FINE PARTICLE LAB           LP 10:31:4 1/19/87
REGEN-FCCU CATALYST DA-440, JAN 15, 87                   HP 10:55:55 1/19/87
PNTR NUMBER   +613

           CUMULATIVE PORE VOLUME (CC/G) VS. PORE DIAMETER
                        100% =      +0.5987
```

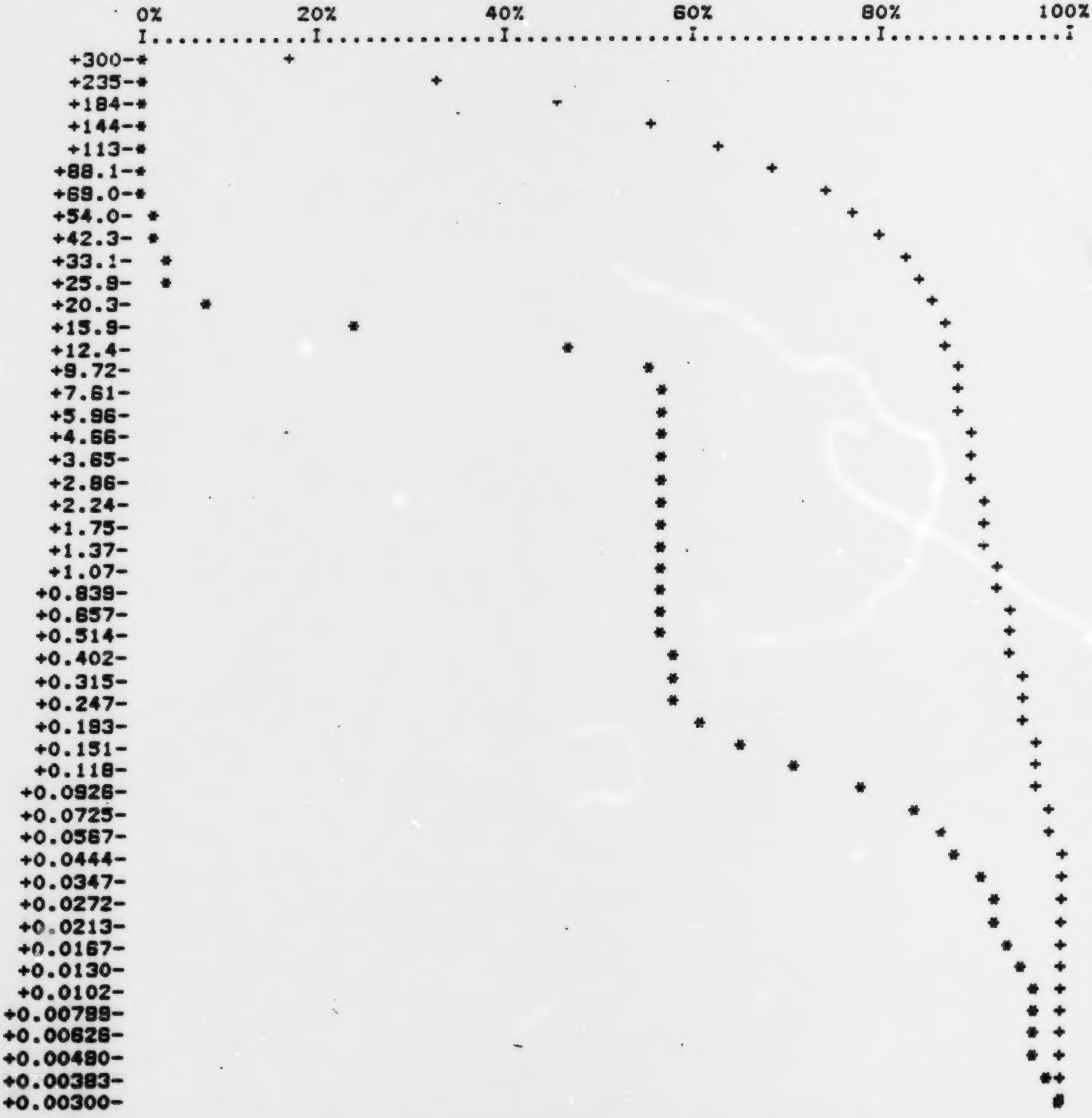

5. Deasphalting Experiments - Results and Discussion

Six deasphalting experiments were made initially with each of the VTBs (Athabasca and Lloydminster) to establish the effects on the deasphalted oils of the basic operating parameters such as solvent, solvent-VTB ratio and temperature-pressure.

Based on these initial results, a second series of deasphalting experiments was conducted, studying each solvent in turn, at a constant temperature and pressure, over a range of solvent-VTB ratios. The resulting phase envelope and tie lines developed for each solvent-VTB system provide the necessary data for carrying out an assessment of a complete multistage counterflow deasphalting process.

Half of the initial series of deasphalting experiments were incorporated into the second series, the remainder were combined with a final set of two runs with each of the VTBs, to form a miscellaneous data set. Combined with run data from the second series, the miscellaneous data set allowed the effects of solvent and temperature-pressure to be isolated and defined. These results will be described in later sections after a discussion of the phase envelopes obtained from the second series of measurements.

6. Generation of Phase Envelopes

Series of phase behaviour measurements, over a wide range of solvent/VTB ratios were carried out for both Lloydminster and Athabasca VTBs using the following solvents and conditions.

Propane	75°C	465 psia	Table 7
n-Butane	120°C	415 psia	Table 8
n-Pentane	160°C	365 psia	Table 9
n-Heptane	75°C	65 psia	Table 10

A complete set of measured phase splits and compositions are listed, solvent by solvent, in the indicated Tables. The system pressures for the phase behaviour measurements were selected so that the solvent would be undersaturated by at least 50 psia (i.e. 50 psia above the bubble point) at the desired operating temperature, to ensure that the systems would remain completely in the liquid phase. The required pressures were read off Pressure-Enthalpy diagrams such as the example, taken from reference 17, in Figure 6.

Some general observations regarding these experiments are in order. It soon became apparent that n-butane and n-pentane were the most economically viable solvents in terms of potential quantity and quality of deasphalted oil, so less emphasis was placed on developing comprehensive phase data for the propane and n-heptane systems.

Irrespective of solvent, there was much more difficulty in obtaining clean separation and analysis of the lower, VTB-rich, phase for the Lloydminster systems than for the Athabasca. This was a result of the less viscous nature of the Lloydminster residues and their tendency to smear over the inner surfaces of the cell during mercury pumping. The problems were particularly severe in instances where the volume of the lower phase was small, and are undoubtedly responsible for some of the ambiguities evident in the phase diagrams for the Lloydminster systems. For this reason, the following points will be made with reference to the Athabasca separations; similar observations apply to the Lloydminster results but are usually less clearly demonstrated.

Comparison of the phase behaviour for solvent-VTB systems is facilitated by plotting the phase data on pseudo-ternary phase diagrams of which Figures 7 and 8 are typical, although idealized, examples. In reducing the quaternary system solvent-oils-resins-asphaltenes to a pseudo-ternary the resins may be combined either with the oils, Figure 7, or with the asphaltenes as asphalt, Figure 8. With the first combination, leaving the asphaltenes segregated, the degree of separation of the asphaltenes is clearly evident at all stages. Combining the resins and asphaltenes, which are similar and tend naturally to associate, usually yields smoother curves and is preferred for general phase behaviour comparisons. In either representation, the dotted dilution line connecting the pure solvent apex and VTB composition on the baseline serves to indicate the solvent/VTB ratio associated with individual tie-lines.

As would be expected from Flory-Huggins theory, when the molecular weight of the solvent is increased, the region of immiscibility between solvent and VTB diminishes. On the pseudo-ternary diagrams this is evidenced by the shrinking area of the two phase region as we move to the solvent of higher molar mass. Comparing tie-lines at fixed solvent-VTB ratios, the tie-lines will be shorter, the greater the molar mass of solvent. For a particular solvent-VTB system, Flory-Huggins theory predicts that the miscible region will be approached by decreasing the solvent to VTB in the mixture. The effect is that the tie-lines get shorter, when the solvent/VTB ratio is reduced, and the compositions of the two phases approach each other, just prior to coalescing into a single phase as miscibility is achieved. The actual solvent/VTB ratio at the point of miscibility, where the pseudo-ternary phase envelope closes, will tend to increase for the higher molar mass solvents. The tie-line length has a significant effect on the composition of the deasphalted oil. With short tie-lines, where the 2 phase compositions are approaching each other, increasing quantities of the asphaltenes, and resins, will be retained in the upper phase, at the expense of solvent, and the quality of the deasphalted oil (DAO - the upper phase residue after solvent removal) will deteriorate.

Each of the above trends, deduced from liquid theory, is observed in the measured data for the Athabasca and Lloydminster VTB shown in Figures 9-12 and 13-16 respectively. (Analagous diagrams, except with the resins and asphaltenes combined as a single asphalt group, are contained in the Appendix).

Except for the propane systems, reducing the solvent-VTB ratio led to shortening of the tie-lines and, eventually, to closure of the phase envelope. The solvent-VTB ratio at, or close to, the point of closure increased in the solvent order, C_4, C_5, C_7. In the case of propane there was no evidence of the envelope closing even with a solvent-VTB ratio of 0.5, although it is likely that a single phase could have been achieved by further reducing the ratio.

While phase measurements at low solvent-VTB ratios were important to define the limits of the two phase region, equally necessary were runs at very high solvent-VTB ratios. The objective in these runs was particularly to define the lower phase composition. In any commercial process, this phase would represent the process residue - the ultimate limit to the overall recovery. The runs were carried out at a nominal 40:1 solvent-VTB (wt/wt) ratio, the highest value practicable with the experimental procedure, allowing just sufficient residue in the lower phase to determine the composition. It was anticipated that the quantities of DAO in the high dilution runs would be quite small. In all cases, however, while there was sufficient DAO to determine the composition, detailed inspections had to be omitted.

The conclusions are summarized below, where the mass % of the individual VTB components retained in the lower phase residue, along with the overall mass % of VTB left in the residue, is compared for the extractions with propane, butane and pentane. For all solvents the asphaltenes are essentially retained in the residue, but the decreasing retention of both oils and resins in the lower phase as the molecular weight of the solvent increases is quite marked. There is also a noticable difference between the Athabasca and Lloydminster VTB with a greater proportion of the oils and resins of the Athabasca VTB being retained in the lower phase residue, irrespective of the solvent. The overall retention of VTB in the lower phase residue is similarly affected by solvent and source, with low retention shown by the higher molar mass solvents and Lloydminster crude. The VTB retained in the lower phase residue sets the limit on the final stage recovery of deasphalted oil indicating that recoveries in the order of 80% would be possible with n-pentane.

Mass % Retention of VTB and Components in Lower Phase Residue

Solvent/VTB = 40 w/w

Solvent	Propane		nC_4		nC_5
VTB	Lloyd	Athabasca	Lloyd	Athabasca	Athabasca
Oils	23.1	64.8	3.6	7.3	1.5
Resins	76.5	90.4	38.3	50.1	11.8
Asphaltenes	99.1	100.0	99.5	100.0	98.7
VTB	48.1	80.3	26.2	39.0	22.1

7. Effects of Phase Behaviour on DAO

The variables that significantly affect the phase behaviour of the deasphalting process would also be expected to influence both the quality and the quantity of DAO produced. Using data from Table 11 along with selected data from the phase envelope measurements, Tables 7 to 10, these effects may be investigated and, with the aid of the Flory-Huggins liquid model, explained.

a. Solvent

The table below lists data for the runs made at 75°C, with a nominal Solvent-VTB ratio of 9 v/v, for each of the solvents. The overall mass % of the original VTB recovered as deasphalted oil in the upper phase increases rapidly as the solvent molar mass goes up. This is accompanied by higher recoveries, first of the oil fraction which levels off at about 90%, then of the resins fraction and ultimately, with n-heptane, of the asphaltene fraction. These observations are in accord with the conclusions from the liquid model, where increasingly heavier solvents give smaller regions of immiscibility with shorter tie-lines and heavier deasphalted oils (greater resin and asphaltene content).

Solvent Effect on Deasphalting

Mass % Recovery of VTB Components	Solvent C_3	 nC_4	 nC_5	 nC_7
Pressure, psia	465	205	105	65
Athabasca				
Overall	11.6	47.1	66.0	80.5
Oils	22.2	74.8	85.5	89.6
Resins	3.7	34.4	72.5	95.0
Asphaltenes	0.1	0.3	0.4	25.6
Lloydminster				
Overall	27.3	64.5	77.1	
Oils	41.7	83.0	89.8	
Resins	9.8	56.7	88.1	
Asphaltenes	0.0	0.5	0.6	

1. Solvent/VTB ratios all nominally 9:1 vol/vol
2. Temperature, 75°C

Additional to these generalized effects there is also noticeably better recovery of oil and resins from the Lloydminster VTB over the Athabasca at equivalent conditions. This no doubt reflects differences in the VTB constituent fractions of these two oils and their influence, as solutes, on the phase behaviour.

With regard to quality, it will be shown in later sections that the presence of asphaltenes, and to a lesser extent resins, in the deasphalted oil reduce its desirability as an FCCU feed. From the data above, quality and quantity of a deasphalted oil would appear to be mutually exclusive characteristics in the deasphalting process.

b. Temperature-Pressure

These variables were tied together insofar as the pressure at any selected temperature was set at least 50 psi in excess of the solvent bubble pressure in order to maintain a completely liquid system. The effects of the temperature-pressure combination is presented below for the solvents n-butane and n-pentane at a nominal volumetric solvent-VTB ratio of 9.

Temperature/Pressure Effect on Deasphalting

Mass % Recovery of VTB Components	Solvent			
	nC_4–		nC_5–	
Temperature, °C	120	75	160	75
Pressure, psia	415	205	365	105
Athabasca				
Overall	39.2	47.1	58.4	66.0
Oils	65.5	74.8	85.7	85.5
Resins	24.6	34.4	51.4	72.5
Asphaltenes	0.2	0.3	0.7	0.4
Lloydminster				
Overall	56.9	64.5	71.7	77.1
Oils	76.1	83.0	93.9	89.8
Resins	43.8	56.7	59.4	88.1
Asphaltenes	0.4	0.5	0.5	0.6

1. Solvent/VTB ratios all nominally 9:1 vol/vol

As mentioned in a previous section, over the temperature-pressure ranges involved in this work, the relative changes in solvent and VTB solubility parameters and molar volumes will lead to Flory-Huggins model predictions of increasing disparity between solvent and solutes as the temperature is raised. This leads to a larger region of immiscibility with a broader two phase envelope and longer tie-lines on a pseudo-ternary representation.

The results above concur with these general conclusions, with higher temperatures yielding lower overall recoveries of VTB as deasphalted oil. With n-butane, the recoveries of both the oils and resins fractions are depressed at the higher operating condition; with n-pentane the major effect is to lower the resins fraction recovery. It may be noted from these results that the solvent effects, discussed in the last section, predominate over temperature-pressure variations, with recoveries using n-pentane at the highest operating condition exceeding those for n-butane at the lowest temperature. Also, as was noted with the solvent effect, Lloydminster VTB recoveries, both overall and for the individual fractions, are better than the Athabasca VTB recoveries at comparable operating conditions.

c. Solvent-VTB Ratio

Data for the deasphalted oil composition and mass % extracted, as a function of solvent-VTB ratio, is given in the following table, for the Athabasca - pentane system. This system had the largest number of tie-line determinations over a solvent-VTB range from approximately 40 to less than 1. Over a large part of the range, from 20 to 5.2 there is little change in either the composition or the extracted mass of the deasphalted oil. Only as the phase envelope starts to close, at the lower solvent-VTB ratios, is there an obvious change in the composition, with a rapid increase in the asphaltenes at the expense of the oils. The overall mass extracted shows an increase at the low solvent-VTB ratio, however, this is system dependent and relates to the changes in composition required to bring the deasphalted oil and the lower phase residue to a common composition as the region of miscibility is approached.

Reviewing the data found on the next page, it can be seen that at certain stages in a multistage process there will be levels of asphaltenes present in the deasphalted oil. The question to be answered is how will the presence of asphaltenes, or even high levels of resins, influence the performance of the deasphalted oil in an FCC unit. The answer is found in the results of MAT tests made on deasphalted oil samples produced at the lower solvent-VTB ratios. Before covering these results in detail, the relation between the deasphalted oil composition and commonly measured inspection data, i.e. nitrogen content, Conradson Carbon, vanadium and nickel etc., will be discussed. Correlations between the deasphalted oil compositions, the inspection data and the FCC performance, provide the link between the phase behaviour and cat cracking and also form the basis for interpreting the microactivity test data.

Deasphalted Oil Compositions
(mass %)

Athabasca and n-Pentane at 160°C, 365 psia

Solvent-VTB w/w	37.1	20.0	6.8	5.2	1.0	0.9
Oils	58.5	65.6	64.0	67.5	53.7	46.8
Resins	40.9	34.4	35.9	32.3	38.9	38.3
Asphaltenes	0.6	0.0	0.1	0.2	7.4	14.9
% VTB	65.8	62.3	59.3	58.4	65.5	68.0

8. Deasphalted Oil Quality and Composition

The most desirable cat cracking feeds will contain low nitrogen, metals (nickel and vanadium) and Conradson Carbon since, in a different way, each of these materials will adversely affect the performance of the cracking catalyst. Given the polar nature of resins and asphaltenes, we might anticipate that deasphalted oils containing high levels of resins, or significant amounts of asphaltenes, will also be contaminated with the undesirable elements, nitrogen, metals and Conradson Carbon.

Data in the graphs, Figures 17 to 19, confirm this contention. Using the DAO inspection data for all the deasphalting runs, in Tables 12 to 19, the total nitrogen, metals (Ni + V) and Conradson Carbon are plotted against the asphalt (resins plus asphaltenes) content of the DAO. In each case there is a clear positive correlation. One interesting feature is that in all cases the correlations appear to be independent of the source of the DAO, no significant differences are evident between the properties for deasphalted oils produced from Athabasca or Lloydminster VTBs, at a given level of asphalt.

Although the abscissa in these plots is designated as asphalt, it is only above 35% that more than trace amounts of asphaltenes are present in the DAO. Levels of asphalt (resins) up to 15% can be tolerated before any significant metals content is observed, in the DAO, by contrast the DAO nitrogen levels show increases even at low asphalt levels. One might conjecture that metals are associated with the larger polar structures and therefore are found in the DAO only when the level of asphalt has risen sufficiently to indicate that the larger molecular structures, or their remnants, have started to find acceptance in the deasphalted phase. Conversely, the nitrogen is probably fairly well distributed over the whole molecular spectrum of the asphalt and therefore finds its way into the deasphalted phase just as soon as the resins are taken up.

TABLE 7 : Deasphalting Data for Propane at 75C, 465 PSIA

Lloydminster VTB	Run No	34L			5L						27L		
	Solvent/VTB												
	V/V	82.0			9.0						1.0		
	wt/wt	40.0			4.4						0.5		
		Feed	Phase1	Phase2	Feed	Phase1	Phase2				Feed	Phase1	Phase2
Residue MassZ	Oil		85.9	24.1		90.2	45.6					91.3	55.0
	Resin		13.5	41.4		9.8	32.0					8.5	29.2
	Asphaltene		0.6	34.5		0.0	22.4					0.2	15.8
Mass	Solvent	158.80	158.56	0.24	114.08	109.95	4.13				17.75	7.68	10.07
	Non-Solv	4.08	1.97	2.11	25.99	7.10	18.89				35.50	1.00	34.50
	TOTAL	162.88	160.53	2.35	140.07	117.05	23.02				53.25	8.68	44.57
Mass Z	Phase		98.56	1.44		83.57	16.43					16.30	83.70
Component Mass Z	Solvent	97.50	98.77	10.21	81.44	93.93	17.94				33.33	88.48	22.59
	Oil	1.35	1.05	21.64	10.72	5.47	37.42				37.35	10.52	42.57
	Resin	0.70	0.17	37.17	4.81	0.59	26.26				19.08	0.98	22.60
	Asphaltene	0.45	0.01	30.98	3.02	0.00	18.38				10.24	0.02	12.23
	TOTAL	100.00	100.00	100.00	100.00	100.00	100.00				100.00	100.00	100.00

Athabasca VTB	Run No	34A			5A			26A			27A		
	Solvent/VTB												
	V/V	86.0			9.1			2.2			1.1		
	wt/wt	40.0			4.2			1.0			0.5		
		Feed	Phase1	Phase2	Feed	Phase1	Phase2	Feed	Phase1	Phase2	Feed	Phase1	Phase2
Residue MassZ	Oil		78.6	30.0		89.3	44.7		88.1	42.2		86.9	44.3
	Resin		20.5	40.6		10.7	36.1		11.8	38.0		13.0	36.9
	Asphaltene		0.9	29.4		0.0	19.2		0.1	19.8		0.1	18.8
Mass	Solvent	137.74	137.33	0.41	114.48	112.50	1.98	58.14	50.34	7.80	29.07	18.47	10.60
	Non-Solv	3.70	0.64	3.06	27.14	3.14	24.00	58.14	2.11	56.03	58.13	0.93	57.20
	TOTAL	141.44	137.97	3.47	141.62	115.64	25.98	116.28	52.45	63.83	87.20	19.40	67.80
Mass Z	Phase		97.55	2.45		81.66	18.34		45.11	54.89		[illegible]	[illegible]
Component Mass Z	Solvent	97.38	99.54	11.82	80.84	97.28	7.62	50.00	95.98	12.22	33.34	[illegible]	5.63
	Oil	1.00	0.36	26.46	9.56	2.42	41.29	21.93	3.54	37.04	29.99	[illegible]	37.37
	Resin	0.97	0.10	35.80	6.36	0.29	33.35	18.52	0.47	33.36	24.34	[illegible]	31.13
	Asphaltene	0.64	0.00	25.93	3.25	0.00	17.74	9.54	0.00	17.38	12.33	0.00	15.86
	TOTAL	100.00	100.00	100.00	100.00	100.00	100.00	100.00	100.00	100.00	100.00	100.00	100.00

TABLE 7

Propane at
75° C, 465 PSIA

TABLE 8 : Deasphalting Data for n-Butane at 120C, 415 PSIA

Lloydminster VTB	Run No	33L			23L			20L			22L			32L		
	Solvent/VTB															
	V/V	70.9			13.0			9.0			4.0			1.6		
	wt/wt	40.0			7.3			5.1			2.3			0.9		
		Feed	Phase1	Phase2	Feed	Phase1	Phase2	Feed	Phase1	Phase2	Feed	Phase1	Phase2	Feed	Phase1	Phase2
Residue	Oil		75.6	5.9		77.1	17.5		78.9	21.0		74.3	27.9		62.3	51.1
Mass %	Resin		24.2	30.8		22.8	37.2		21.0	37.5		25.4	33.4		32.0	28.2
	Asphaltene		0.2	63.3		0.1	45.3		0.1	41.5		0.3	38.7		5.7	20.7
Mass	Solvent	158.80	158.61	0.19	152.92	151.51	1.41	131.34	128.84	2.50	58.06	55.23	2.83	27.79	8.62	19.17
	Non-Solv	4.15	2.80	1.35	20.86	12.68	8.18	25.87	14.71	11.16	25.74	14.12	11.62	31.02	7.84	23.18
	TOTAL	162.95	161.41	1.54	173.78	164.19	9.59	157.21	143.55	13.66	83.80	69.35	14.45	58.81	16.46	42.35
Mass %	Phase		99.05	0.95		94.48	5.52		91.31	8.69		82.76	17.24		27.99	72.01
Component	Solvent	97.45	98.27	12.34	88.00	92.28	14.70	83.54	89.75	18.30	69.28	79.64	19.58	47.25	52.37	45.27
Mass %	Oil	1.35	1.31	5.17	6.45	5.95	14.93	8.87	8.09	17.16	16.39	15.13	22.44	28.45	29.67	27.97
	Resin	0.67	0.42	27.00	3.41	1.76	31.73	4.63	2.15	30.64	8.91	5.17	26.86	15.38	15.24	15.44
	Asphaltene	0.53	0.00	55.49	2.14	0.01	38.64	2.96	0.01	33.90	5.42	0.06	31.12	8.92	2.71	11.33
	TOTAL	100.00	100.00	100.00	100.00	100.00	100.00	100.00	100.00	100.00	100.00	100.00	100.00	100.00	100.00	100.00

Athabasca VTB	Run No	33A			23A			20A			22A			28A		
	Solvent/VTB															
	V/V	74.8			13.0			9.0			4.0			0.9		
	wt/wt	40.0			7.0			4.8			2.1			0.5		
		Feed	Phase1	Phase2	Feed	Phase1	Phase2	Feed	Phase1	Phase2	Feed	Phase1	Phase2	Feed	Phase1	Phase2
Residue	Oil		72.0	7.0		72.9	18.6		76.9	25.9		73.9	28.8		45.2	43.4
Mass %	Resin		28.0	34.2		27.1	41.3		23.0	40.1		26.0	41.9		36.3	36.0
	Asphaltene		0.0	58.8		0	40.1		0.1	34.0		0.1	29.3		18.5	20.6
Mass	Solvent	172.17	171.89	0.28	152.51	150.50	2.01	130.93	127.93	3.00	79.98	76.71	3.27	16.96	16.49	0.47
	Non-Solv	4.50	2.48	2.02	21.93	8.91	13.02	27.19	10.66	16.53	37.38	10.75	26.63	33.91	32.14	1.77
	TOTAL	176.67	174.37	2.30	174.44	159.41	15.03	158.12	138.59	19.53	117.35	87.46	29.90	50.87	48.63	2.24
Mass %	Phase		98.70	1.30		91.38	8.62		87.65	12.35		74.53	25.47		95.60	4.40
Component	Solvent	97.45	98.58	12.17	87.43	94.41	13.37	82.80	92.31	15.36	68.15	87.71	10.94	33.34	33.91	20.98
Mass %	Oil	1.09	1.02	6.15	5.11	4.07	16.11	7.89	5.91	21.92	13.30	9.08	25.65	30.07	29.87	34.29
	Resin	0.78	0.40	30.04	4.47	1.51	35.78	5.74	1.77	33.94	11.89	3.20	37.32	24.19	23.99	28.45
	Asphaltene	0.67	0.00	51.64	2.99	0.00	34.74	3.56	0.01	28.78	6.66	0.01	26.10	12.41	12.23	16.28
	TOTAL	100.00	100.00	100.00	100.00	100.00	100.00	100.00	100.00	100.00	100.00	100.00	100.00	100.00	100.00	100.00

TABLE 8

n-Butane at
120 C
415 PSIA

TABLE 9 : Deasphalting Data for n-Pentane at 160C, 365 PSIA

Lloydminster VTB	Run No	29L			19L			24L			36L		
	Solvent/VTB												
	V/V	32.8			9.0			1.6			1.3		
	wt/wt	20.0			5.5			1.0			0.8		
		Feed	Phase1	Phase2	Feed	Phase1	Phase2	Feed	Phase1	Phase2	Feed	Phase1	Phase2
Residue Mass %	Oil		63.1	1.1		77.3	11.6		58.2	28.1		57.0	45.0
	Resin		34	0.5		22.6	25.0		32.2	19.2		27.1	26.4
	Asphaltene		2.9	98.4		0.1	63.4		9.6	52.7		15.9	28.6
Mass	Solvent	133.12	132.66	0.46	142.73	140.93	1.80	25.74	25.27	0.47	42.35	42.16	0.19
	Non-Solv	6.66	4.78	1.88	25.99	18.63	7.36	26.04	23.89	2.15	53.02	52.30	0.72
	TOTAL	139.78	137.44	2.34	168.72	159.56	9.16	51.78	49.16	2.62	95.37	94.46	0.91
Mass %	Phase		98.33	1.67		94.57	5.43		94.94	5.06		99.05	0.95
Component Mass %	Solvent	95.24	96.52	19.66	84.60	88.32	19.65	49.71	51.40	17.94	44.41	44.63	20.88
	Oil	2.17	2.19	0.88	9.04	9.03	9.32	28.02	28.28	23.06	31.60	31.56	35.60
	Resin	1.17	1.18	0.40	3.59	2.64	20.09	15.65	15.65	15.76	15.06	15.00	20.89
	Asphaltene	1.42	0.10	79.06	2.78	0.01	50.94	6.62	4.67	43.25	8.94	8.80	22.63
	TOTAL	100.00	100.00	100.00	100.00	100.00	100.00	100.00	100.00	100.00	100.00	100.00	100.00

Athabasca VTB	Run No	35A			29A			39A			19A			24A			25A		
	Solvent/VTB																		
	V/V	69.1			34.5			12.2			9.0			1.7			1.6		
	wt/wt	40.0			20.0			7.0			5.2			1.0			0.9		
		Feed	Phase1	Phase2	Feed	Phase1	Phase2	Feed	Phase1	Phase2	Feed	Phase1	Phase2	Feed	Phase1	Phase2	Feed	Phase1	Phase2
Residue Mass %	Oil		58.5	1.7		65.6	4.5		64.0	7.6		67.5	14.3		53.7	26.4		46.8	37.0
	Resin		40.9	10.5		34.4	29.1		35.9	28.0		32.3	31.0		38.9	30.1		38.3	33.9
	Asphaltene		0.6	87.8		0	66.4		0.1	64.4		0.2	54.7		7.4	43.5		14.9	29.1
Mass	Solvent	154.96	154.69	0.27	145.35	144.60	0.75	180.79	178.79	2.00	141.65	138.17	3.48	43.36	35.76	7.60	39.02	28.70	10.32
	Non-Solv	4.18	2.75	1.43	7.27	4.53	2.74	26.49	15.70	10.79	27.19	15.87	11.32	43.36	28.39	14.97	43.36	29.49	13.87
	TOTAL	159.14	157.44	1.70	152.62	149.13	3.49	207.28	194.49	12.79	168.84	154.04	14.80	86.72	64.15	22.57	82.38	58.19	24.19
Mass %	Phase		98.93	1.07		97.71	2.29		93.83	6.17		91.23	8.77		73.97	26.03		70.64	29.36
Component Mass %	Solvent	97.37	98.25	15.88	95.24	96.96	21.49	87.22	91.93	15.64	83.90	89.70	23.51	50.00	55.74	33.67	47.37	49.32	42.66
	Oil	1.03	1.02	1.43	2.03	1.99	3.53	5.24	5.17	6.41	7.30	6.95	10.94	22.14	23.77	17.51	22.98	23.72	21.21
	Resin	0.80	0.71	8.83	1.34	1.04	22.85	4.18	2.90	23.62	5.11	3.33	23.71	17.93	17.22	19.96	19.42	19.41	19.44
	Asphaltene	0.80	0.01	73.86	1.19	0.00	52.13	3.36	0.01	54.33	3.69	0.02	41.84	9.93	3.27	28.85	10.23	7.55	16.69
	TOTAL	100.00	100.00	100.00	100.00	100.00	100.00	100.00	100.00	100.00	100.00	100.00	100.00	100.00	100.00	100.00	100.00	100.00	100.00

TABLE 9

n-Pentane
at 160 C
365 PSIA

TABLE 10 : Deasphalting Data for n-Heptane at 75C, 65 PSIA

Lloydminster VTB	Run No	14L			31L		
	Solvent/VTB						
	V/V	17.5			4.5		
	wt/wt	11.7			3.0		
		Feed	Phase1	Phase2	Feed	Phase1	Phase2
Residue	Oil		63.2	11.4		62.5	16.5
Mass %	Resin		35.4	13.8		30.0	12.7
	Asphaltene		1.4	74.8		7.5	70.8
Mass	Solvent	222.27	214.01	8.26	79.87	77.48	2.39
	Non-Solv	19.06	15.74	3.32	26.62	23.33	3.29
	TOTAL	241.33	229.75	11.58	106.49	100.81	5.68
Mass %	Phase		95.20	4.80		94.67	5.33
Component	Solvent	92.10	93.15	71.33	75.00	76.86	42.08
Mass %	Oil	4.28	4.33	3.27	14.20	14.46	9.56
	Resin	2.50	2.43	3.96	6.96	6.94	7.36
	Asphaltene	1.12	0.10	21.45	3.83	1.74	41.01
	TOTAL	100.00	100.00	100.00	100.00	100.00	100.00

Athabasca VTB	Run No	14A			40A			30A		
	Solvent/VTB									
	V/V	17.5			9.0			3.2		
	wt/wt	11.1			5.6			2.0		
		Feed	Phase1	Phase2	Feed	Phase1	Phase2	Feed	Phase1	Phase2
Residue	Oil		50.5	3.2		51.2	3.2		43.4	18.7
Mass %	Resin		46.2	9.4		43.3	8.2		39.7	21.7
	Asphaltene		3.3	87.4		5.5	88.6		16.9	59.6
Mass	Solvent	222.38	218.75	3.63	215.44	211.39	4.05	54.60	52.84	1.76
	Non-Solv	20.08	16.11	3.97	29.09	23.41	5.68	27.13	25.25	1.88
	TOTAL	242.46	234.86	7.60	244.53	234.80	9.73	81.73	78.09	3.64
Mass %	Phase		96.87	3.13		96.02	3.98		95.55	4.45
Component	Solvent	91.72	93.14	47.76	88.10	90.03	41.62	66.81	67.67	48.35
Mass %	Oil	3:41	3.46	1.67	4.98	5.10	1.87	13.84	14.03	9.66
	Resin	3.22	3.17	4.91	4.34	4.32	4.79	12.76	12.84	11.21
	Asphaltene	1.65	0.23	45.66	2.58	0.55	51.72	6.59	5.46	30.78
	TOTAL	100.00	100.00	100.00	100.00	100.00	100.00	100.00	100.00	100.00

TABLE 10

n-Heptane at
75 c, 65 PSIA

TABLE 11 :Deasphalting Data -- Miscellaneous Conditions

Lloydminster VTB	Run No	21L			37L			10L			38L			15L		
	Solvent	C4			C4			C5			C5			C7		
	Temp C	140			75			140			75			180		
	Press psia	565			205			265			105			165		
	Solvent/VTB															
	V/V	9.0			9.0			9.0			9.0			12.1		
	wt/wt	5.1			5.1			5.5			5.5			8.1		
		Feed	Phase1	Phase2	Feed	Phase1	Phase2	Feed	Phase1	Phase2	Feed	Phase1	Phase2	Feed	Phase1	Phase2
Residue	Oil		81.0	26.9		75.9	14.5		67.6	7.5		68.7	8.3		63.5	4.4
Mass %	Resin		18.8	38.0		24.0	32.4		32.2	21.4		31.2	19.5		34.4	6.8
	Asphaltene		0.2	35.1		0.1	53.1		0.2	71.1		0.1	72.2		2.1	88.8
Mass	Solvent	130.65	128.61	2.04	157.48	148.63	8.85	140.77	138.29	2.48	173.77	172.40	1.37	185.48	183.84	1.64
	Non-Solv	25.74	13.40	12.34	30.89	19.92	10.97	25.63	19.23	6.40	31.38	24.18	7.20	23.00	20.12	2.88
	TOTAL	156.39	142.01	14.38	188.37	168.55	19.82	166.40	157.52	8.88	205.15	196.58	8.57	208.48	203.96	4.52
Mass %	Phase		90.81	9.19		89.48	10.52		94.66	5.34		95.82	4.18		97.83	2.17
Component	Solvent	83.54	90.56	14.19	83.60	88.18	44.65	84.60	87.79	27.93	84.70	87.70	15.99	88.97	90.14	36.28
Mass %	Oil	9.06	7.64	23.08	8.87	8.97	8.03	8.10	8.25	5.41	8.39	8.45	6.97	6.19	6.26	2.80
	Resin	4.61	1.77	32.61	4.42	2.84	17.93	4.54	3.93	15.42	4.36	3.84	16.38	3.41	3.39	4.33
	Asphaltene	2.79	0.02	30.12	3.10	0.01	29.39	2.76	0.02	51.24	2.55	0.01	60.66	1.43	0.21	56.58
	TOTAL	100.00	100.00	100.00	100.00	100.00	100.00	100.00	100.00	100.00	100.00	100.00	100.00	100.00	100.00	100.00

Athabasca VTB	Run No	21A			37A			10A			38A			15A		
	Solvent	C4			C4			C5			C5			C7		
	Temp C	140			75			140			75			180		
	Press psia	565			205			265			105			165		
	Solvent/VTB															
	V/V	9.0			9.0			9.0			9.0			12.1		
	wt/wt	4.8			4.8			5.2			5.2			7.7		
		Feed	Phase1	Phase2	Feed	Phase1	Phase2	Feed	Phase1	Phase2	Feed	Phase1	Phase2	Feed	Phase1	Phase2
Residue	Oil		73.9	26.3		73.1	14.7		58.9	6.9		59.6	7.0		47.6	3.8
Mass %	Resin		25.8	41.8		26.8	40.3		41.1	30.4		40.3	21.7		49.9	10.0
	Asphaltene		0.3	31.9		0.1	45.0		0.0	62.7		0.1	71.3		2.5	86.2
Mass	Solvent	131.11	129.12	1.99	156.99	150.80	6.19	140.89	137.99	2.90	170.12	166.68	3.44	184.60	183.13	1.47
	Non-Solv	27.23	8.51	18.72	33.98	16.00	17.98	26.09	15.53	10.56	33.80	22.29	11.51	24.67	20.28	4.39
	TOTAL	158.34	137.63	20.71	190.97	166.80	24.17	166.98	153.52	13.46	203.92	188.97	14.95	209.27	203.41	5.86
Mass %	Phase		86.92	13.08		87.34	12.66		91.94	8.06		92.67	7.33		97.20	2.80
Component	Solvent	82.80	93.82	9.61	82.21	90.41	25.61	84.38	89.88	21.55	83.42	88.20	23.01	88.21	90.03	25.09
Mass %	Oil	7.08	4.57	23.77	7.51	7.01	10.94	5.91	5.96	5.41	6.91	7.03	5.39	4.69	4.75	2.85
	Resin	6.33	1.60	37.78	6.04	2.57	29.98	5.75	4.16	23.85	5.63	4.75	16.71	5.05	4.98	7.49
	Asphaltene	3.79	0.02	28.83	4.25	0.01	33.48	3.97	0.00	49.19	4.04	0.01	54.89	2.05	0.25	64.58
	TOTAL	100.00	100.00	100.00	100.00	100.00	100.00	100.00	100.00	100.00	100.00	100.00	100.00	100.00	100.00	100.00

TABLE 11

Miscellaneous
Conditions

TABLE 12: DEASPHALTING EXPERIMENTS: CHARACTERIZATIONS
LLOYDMINSTER VTB WITH PROPANE

Run No.	34		5		27	
CONDITIONS						
Temperature, °C	75		75		75	
Pressure, psig	450		450		450	
Solvent/Oil Ratio, v/v	82.0		9.0		1.0	
w/w	40.0		4.4		0.5	
YIELDS						
DAO Extracted, wt%	48.3		27.0		2.8	
Residue, wt%	51.7		73.0		97.2	
Material Balance, wt%						
SOLVENT DISTRIBUTION						
Solvent Rich Phase, wt%	99.8		96.4		43.7	
Solvent Lean Phase, wt%	0.2		3.6		56.3	
PROPERTIES	DAO	RESIDUE	DAO	RESIDUE	DAO	RESIDUE
Density at 15°C			0.938			
°API			19.2			
Total Sulphur, wt%			2.84			
Total Nitrogen, ppm w/w			1120			
Basic Nitrogen, ppm w/w			398			
Aniline Point, °C			91.0			
Conradson Carbon, wt%			1.7			
Asphaltenes, wt%	0.6	34.5	0.0	22.4	0.2	15.8
Resins, wt%	13.6	41.4	9.8	32.0	8.5	29.2
Oils S/A, wt%	85.9	24.1	90.2	45.6	91.3	55.0
Nickel, ppm w/w			1	100		
Vanadium, ppm w/w			1.1	270		
GCD Boiling Range						
IBP			300			
5%			383			
10%			410			
20%			437			
30%			459			
Recovery to 554°C			78.3			

td = Too Dark

TABLE 13: DEASPHALTING EXPERIMENTS: CHARACTERIZATIONS
ATHABASCA VTB WITH PROPANE

Run No.	34		5		26		27
CONDITIONS							
Temperature, 'C	75		75		75		75
Pressure, psig	450		450		450		450
Solvent/Oil Ratio, v/v	86.0		9.1		2.2		1.1
w/w	40.0		4.2		1.0		0.5
YIELDS							
DAO Extracted, wt%	17.4		12.0		3.6		1.6
Residue, wt%	82.6		88.0		96.4		98.4
Material Balance, wt%							
SOLVENT DISTRIBUTION							
Solvent Rich Phase, wt%	99.7		95.7		91.7		82.5
Solvent Lean Phase, wt%	0.3		4.3		8.3		17.5
PROPERTIES	DAO	RESIDUE	DAO	RESIDUE	DAO	RESIDUE	DAO
Density at 15'C			0.956				
'API			16.4				
Total Sulphur, wt%			3.66				
Total Nitrogen, ppm w/w			1537				
Basic Nitrogen, ppm w/w			603				
Aniline Point, 'C							
Conradson Carbon, wt%			2.9				
Asphaltenes, wt%	0.9	29.4	0.0	19.2	0.1	19.8	0.1
Resins, wt%	20.5	40.6	10.7	36.1	11.8	38.0	13.0
Oils S/A, wt%	78.6	30.0	89.3	44.7	88.1	42.2	86.9
Nickel, ppm w/w							
Vanadium, ppm w/w							
GCD Boiling Range							
IBP			259		372		401
5%			466		471		465
10%			484		484		481
20%			502		503		498
30%			517		519		512
Recovery to 554'C			54.6		47.4		61.4

td = Too Dark

TABLE 14: DEASPHALTING EXPERIMENTS: CHARACTERIZATIONS
LLOYDMINSTER VTB WITH n-BUTANE

Run No.	33		23		20		22		32		21		37	
CONDITIONS														
Temperature, °C	120		120		120		120		120		140		75	
Pressure, psig	400		400		400		400		400		550		190	
Solvent/Oil Ratio, v/v	70.9		13.0		9.0		4.0		1.6		9.0		9.0	
w/w	40.0		7.3		5.1		2.3		0.9		5.1		5.1	
YIELDS														
DAO Extracted, wt%	67.4		60.8		57.5		55.5		25.3		52.7		64.5	
Residue, wt%	32.6		39.2		42.5		44.5		74.7		47.3		35.5	
Material Balance, wt%														
SOLVENT DISTRIBUTION														
Solvent Rich Phase, wt%	99.9								31.0				94.4	
Solvent Lean Phase, wt%	0.1								69.0				5.6	
PROPERTIES	DAO	RESIDUE	DAO	RESIDUE	DAO	RESIDUE	DAO	RESIDUE	DAO	RESIDUE	DAO	RESIDUE	DAO	RESIDUE
Density at 15°C			0.975		0.973		0.976		1.007		0.970		0.978	
API			13.5		13.8		13.4		8.9		14.3		13.1	
Total Sulphur, wt%			3.88		3.7		4.03		4.26		3.75		4.65	
Total Nitrogen, ppm w/w			2012		2080		2030		4238		2047		2623	
Basic Nitrogen, ppm w/w			845		876		881		956		1068		735	
Aniline Point, °C			td		td		td		td		td		-	
Conradson Carbon, wt%			5.43		6.1		6.35		12.4		4.57		7.22	
Asphaltenes, wt%	0.2	63.3	0.1	45.3	0.1	41.5	0.3	38.7	5.7	20.7	0.2	35.1	0.1	53.1
Resins, wt%	24.2	30.8	22.8	37.2	21.0	37.5	25.4	33.4	32.0	28.2	18.8	38.0	24.0	32.4
Oils S/A, wt%	75.6	5.9	77.1	17.5	78.9	21.0	74.3	27.9	62.3	51.1	81.0	26.9	75.9	32.4
Nickel, ppm w/w			7.3	180	8.4	150	9.3	160	36	100	4.3	155	13	150
Vanadium, ppm w/w			14	470	18	380	22	410	76	160	12	480	14	400
GCD Boiling Range														
IBP			351		339		334		359		328		352	
5%			407		402		406		415		401		407	
10%			435		429		433		446		427		432	
20%			468		464		466		480		462		463	
30%			497		491		494		514		488		490	
Recovery to 534°C			49.3		52.9		51.2		42.9		53.8		56.0	

td = Too Dark

TABLE 15: DEASPHALTING EXPERIMENTS: CHARACTERIZATIONS
ATHABASCA VTB WITH n-BUTANE

Run No.	33		23		20		22		28		21		37	
CONDITIONS														
Temperature, °C	120		120		120		120		120		140		75	
Pressure, psig	400		400		400		400		400		550		190	
Solvent/Oil Ratio, v/v	74.8		13.0		9.0		4.0		0.9		9.0		9.0	
w/w	40.0		7.0		4.8		2.1		0.5		4.8		4.8	
YIELDS														
DAO Extracted, wt%	55.2		40.4		39.0		28.5		94.8		31.5		47.1	
Residue, wt%	44.8		59.6		61.0		71.5		5.2		68.5		52.9	
Material Balance, wt%														
SOLVENT DISTRIBUTION														
Solvent Rich Phase, wt%	99.8								97.8				96.1	
Solvent Lean Phase, wt%	0.2								2.2				3.9	
PROPERTIES	DAO	RESIDUE	DAO	RESIDUE	DAO	RESIDUE	DAO	RESIDUE	DAO	RESIDUE	DAO	RESIDUE	DAO	RESIDUE
Density at 15°C			0.996		0.994		0.987		1.049		0.990		1.001	
API			10.5		10.8		11.8		3.3		11.4		9.7	
Total Sulphur, wt%			5.04		5.00		4.82		6.09		4.89		5.52	
Total Nitrogen, ppm w/w			2475		2906		2313		7053		2759		3392	
Basic Nitrogen, ppm w/w			1090		1163		1003		1957		1443		1039	
Aniline Point, °C			td		td		td		td		td		-	
Conradson Carbon, wt%			7.22		8.3		6.68		24		6.13		0.37	
Asphaltenes, wt%	0.1	38.8	0.0	40.1	0.1	34.0	0.1	29.3	18.5	20.6	0.3	31.9	0.1	45.0
Resins, wt%	28.0	34.2	27.1	41.3	23.0	40.1	26.0	41.9	36.3	36.0	25.8	41.8	26.8	40.3
Oils S/A, wt%	71.9	7.0	72.9	18.6	76.9	25.9	73.9	28.8	45.2	43.4	73.9	26.3	73.1	14.7
Nickel, ppm w/w			9.7	200	15	195	10	170	129	120	8	180	17	225
Vanadium, ppm w/w			22	500	33	520	23	480	250	210	17	490	38	600
GCD Boiling Range														
IBP			413		279		438		402		183		450	
5%			485		477		481		496		477		485	
10%			500		496		500		519		492		501	
20%			528		521		524		560		516		527	
30%			551		544		547				537		548	
Recovery to 554°C			31.7		34.5		33.8		18.8		38.1		32.7	

td = Too Dark

TABLE 16: DEASPHALTING EXPERIMENTS: CHARACTERIZATIONS
LLOYDMINSTER VTB WITH n-PENTANE

Run No.	29		19		24		36		10		38	
CONDITIONS												
Temperature, °C	160		160		160		160		140		75	
Pressure, psig	350		350		350		350		250		90	
Solvent/Oil Ratio, v/v	32.8		9.0		1.6		1.3		9.0		9.0	
w/w	20.0		5.5		1.0		0.8		5.5		5.5	
YIELDS												
DAO Extracted, wt%	72.6		71.9		91.8		98.6		75.1		77.0	
Residue, wt%	27.4		28.1		8.2		1.4		24.9		23.0	
Material Balance, wt%												
SOLVENT DISTRIBUTION												
Solvent Rich Phase, wt%	99.7		97.8		98.2		99.6		98.3		99.2	
Solvent Lean Phase, wt%	0.3		2.2		1.8		0.4		1.7		0.8	
PROPERTIES	DAO	RESIDUE	DAO	RESIDUE	DAO	RESIDUE	DAO	RESIDUE	DAO	RESIDUE	DAO	RESIDUE
Density at 15°C	1.003		0.988		1.008				0.991		0.994	
API	9.5		11.7		8.8				11.3		10.8	
Total Sulphur, wt%	4.20		4.37		5.01				3.99		4.74	
Total Nitrogen, ppm w/w	3769		2680		5304				3136		3395	
Basic Nitrogen, ppm w/w	778		979		1033				1145		926	
Aniline Point, °C	td				td				td		-	
Conradson Carbon, wt%	10.7		9.2		16.6				9.4		10.73	
Asphaltenes, wt%	2.9	98.4	0.1	63.4	9.6	52.7	15.9	28.6	0.2	71.1	0.1	72.2
Resins, wt%	34.0	0.5	22.6	25.0	32.2	19.2	27.3	26.6	32.2	21.4	31.2	19.5
Oils S/A, wt%	63.1	1.1	77.3	11.6	58.2	28.1	56.8	44.8	67.6	7.5	68.7	8.3
Nickel, ppm w/w	20	220	22	190	58	190			25	230	17	250
Vanadium, ppm w/w	46	545	48	490	110	300			55	550	43	600
GCD Boiling Range												
IBP	361		320		310				312		362	
5%	417		425		415				408		416	
10%	442		435		440				439		442	
20%	478		471		487				477		477	
30%	507		500		523				509		509	
Recovery to 554°C	46.2		47.7		38.3				42.4		45.0	

td = Too Dark

TABLE 17: DEASPHALTING EXPERIMENTS: CHARACTERIZATIONS
ATHABASCA VTB WITH n-PENTANE

Run No.	35		29		39		19		24		25		10		38	
CONDITIONS																
Temperature, °C	160		160		160		160		160		160		140		75	
Pressure, psig	350		350		350		350		350		350		250		90	
Solvent/Oil Ratio, v/v	69.1		34.5		12.2		9.0		1.7		1.6		9.0		9.0	
w/w	40.0		20.0		7.0		5.2		1.0		0.9		5.2		5.2	
YIELDS																
DAO Extracted, wt%	65.8		63.2		59.3		58.8		65.3		67.7		59.5		66.0	
Residue, wt%	34.2		36.8		40.7		41.2		34.7		32.3		40.5		34.0	
Material Balance, wt%																
SOLVENT DISTRIBUTION																
Solvent Rich Phase, wt%	99.8		99.5		98.9		97.6		82.5		73.5		97.9		98.0	
Solvent Lean Phase, wt%	0.2		0.5		1.1		2.4		17.5		26.5		2.1		2.0	
PROPERTIES	DAO	RESIDUE	DAO	RESIDUE	DAO	RESIDUE	DAO	RESIDUE	DAO	RESIDUE	DAO	RESIDUE	DAO	RESIDUE	DAO	RESIDUE
Density at 15°C			1.022		1.014		1.004		1.074		1.094		1.018		1.022	
API			6.9		7.9		9.4		0.2		-2.2		7.4		6.9	
Total Sulphur, wt%			5.68		5.73		5.67		6.15		6.77		5.23		6.30	
Total Nitrogen, ppm w/w			5361		4639		3615		5198		5154		3459		4784	
Basic Nitrogen, ppm w/w			1178		1092		1451		1323		1295		1222		1264	
Aniline Point, °C			td		-				td		td		td		-	
Conradson Carbon, wt%			12.30		12.11		12.8		19.9		22.3		12.4		14.33	
Asphaltenes, wt%	0.6	87.0	0.0	66.4	0.1	64.4	0.2	54.7	7.4	43.5	14.9	29.1	-	62.7	0.1	71.3
Resins, wt%	40.9	10.5	34.4	29.1	35.9	28.0	32.3	31.0	38.9	30.1	38.3	33.9	41.1	30.4	40.3	21.7
Oils S/A, wt%	58.5	1.7	65.6	4.5	64.0	7.6	67.5	14.3	53.7	26.4	46.8	37.0	58.9	6.9	59.6	7.0
Nickel, ppm w/w			30	210	49	260	44	313	86	273	118	186	32	251	40	280
Vanadium, ppm w/w			60	552	28	730	110	750	236	587	331	387	79	602	100	920
GCD Boiling Range																
IBP			386		339		283		432		346		297		446	
5%			485		481		486		497		494		477		489	
10%			503		499		506		523		521		503		507	
20%			530		526		537		577		565		533		538	
30%			556		547		576						563		563	
Recovery to 354°C			29.7		32.6		24.9		16.5		17.6		27.2		26.7	

td = Too Dark

TABLE 18: DEASPHALTING EXPERIMENTS: CHARACTERIZATIONS
LLOYDMINSTER VTB WITH n-HEPTANE

Run No.	14		31		15	
CONDITIONS						
Temperature, °C	75		75		180	
Pressure, psig	50		50		150	
Solvent/Oil Ratio, v/v	17.5		4.5		12.1	
w/w	11.7		3.0		8.9	
YIELDS						
DAO Extracted, wt%	82.7		87.8		87.5	
Residue, wt%	17.3		12.2		12.5	
Material Balance, wt%						
SOLVENT DISTRIBUTION						
Solvent Rich Phase, wt%	96.3		97.0		99.1	
Solvent Lean Phase, wt%	3.7		3.0		0.9	
PROPERTIES	DAO	RESIDUE	DAO	RESIDUE	DAO	RESIDUE
Density at 15°C	1.004		1.015		1.006	
API	9.3		7.8		9	
Total Sulphur, wt%	4.31		4.8		4.48	
Total Nitrogen, ppm w/w	3101		4846		3456	
Basic Nitrogen, ppm w/w	1116		1200		1523	
Aniline Point, °C	td		td		td	
Conradson Carbon, wt%	12.8		14.9		13.3	
Asphaltenes, wt%	1.4	74.8	7.5	70.8	2.1	88.8
Resins, wt%	35.4	13.8	30	12.7	34.4	6.8
Oils S/A, wt%	63.2	11.4	62.5	16.5	63.5	4.4
Nickel, ppm w/w	42	236	47	240	35	300
Vanadium, ppm w/w	93	520	79	596	83	626
GCD Boiling Range						
IBP	223		323		331	
5%	409		418		416	
10%	443		445		446	
20%	482		488		489	
30%	517		522		524	
Recovery to 554°C	39.8		39.2		37.0	

td = Too Dark

TABLE 19: DEASPHALTING EXPERIMENTS: CHARACTERIZATIONS
ATHABASCA VTB WITH n-HEPTANE

Run No.	14		40		30		15	
CONDITIONS								
Temperature, °C	75		75		75		180	
Pressure, psig	50		50		50		150	
Solvent/Oil Ratio, v/v	17.5		9.0		3.2		12.1	
w/w	11.1		5.6		2.0		7.7	
YIELDS								
DAO Extracted, wt%	80.3		80.5		93.1		82.2	
Residue, wt%	19.7		19.5		6.9		17.8	
Material Balance, wt%								
SOLVENT DISTRIBUTION								
Solvent Rich Phase, wt%	98.4		98.1		96.8		99.2	
Solvent Lean Phase, wt%	1.6		1.9		3.2		0.8	
PROPERTIES	DAO	RESIDUE	DAO	RESIDUE	DAO	RESIDUE	DAO	RESIDUE
Density at 15°C	1.026		1.038		1.055		1.035	
API	6.3		4.7		2.5		5	
Total Sulphur, wt%	5.44		6.53		6.56		5.83	
Total Nitrogen, ppm w/w	3500		5771		6904		3036	
Basic Nitrogen, ppm w/w	1570		1401		1729		1664	
Aniline Point, °C	td		-		td		td	
Conradson Carbon, wt%	18.4		19.38		22.3		18.3	
Asphaltenes, wt%	3.3	87.4	5.5	88.6	16.9	59.6	2.5	86.2
Resins, wt%	46.2	9.4	43.3	8.2	39.7	21.7	49.9	10
Oils S/A, wt%	50.5	3.2	51.2	3.2	43.4	18.7	47.6	3.8
Nickel, ppm w/w	73	311	80	300	110	210	69	313
Vanadium, ppm w/w	180	936	190	750	250	270	179	920
GCD Boiling Range								
IBP	308		321		298		314	
5%	490		486		493		494	
10%	515		507		516		518	
20%	555		538		556		562	
30%	-		567				-	
Recovery to 554°C	19.4		25.3		19.7		18.5	

td = Too Dark

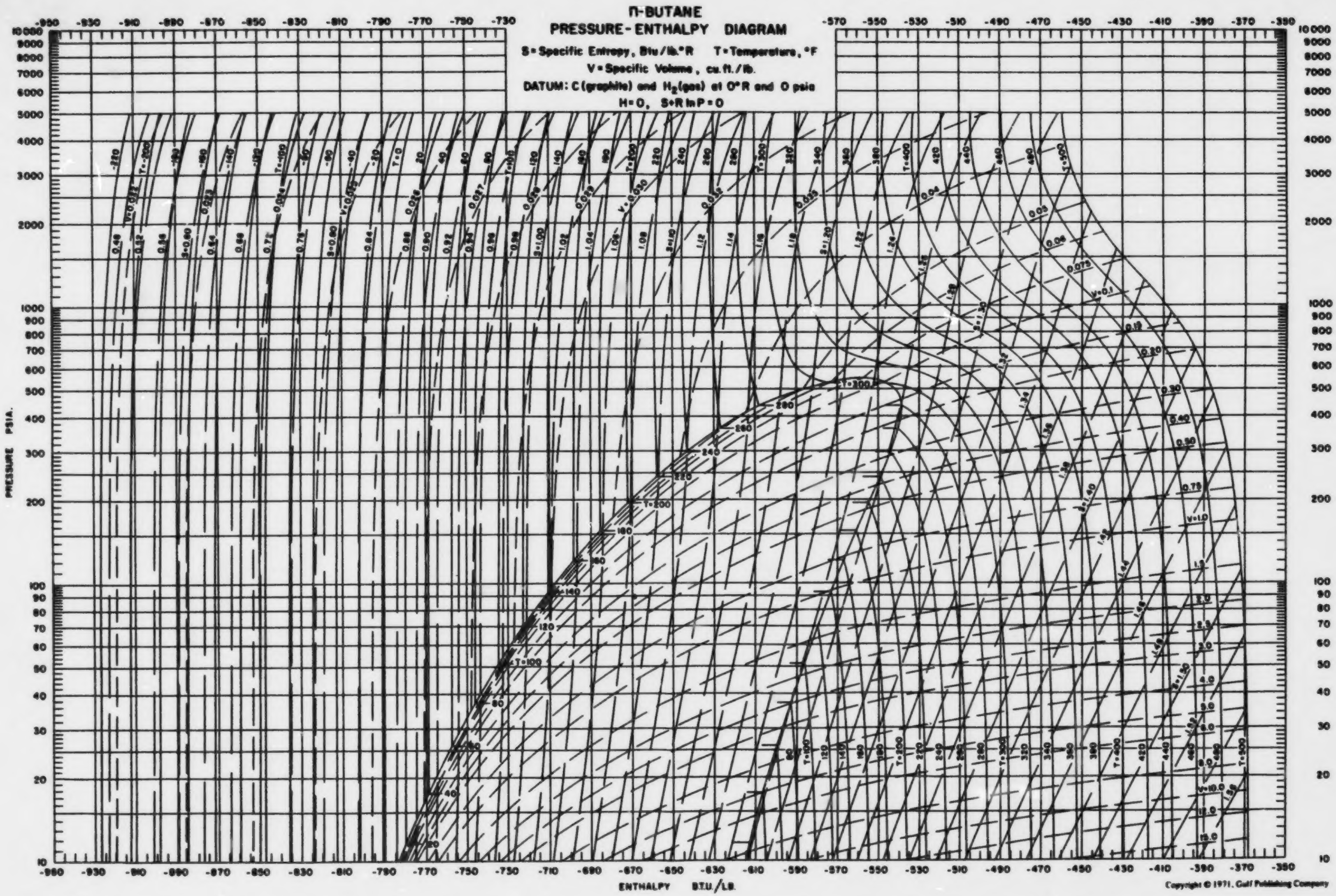

Taken from K.E. Starling's "Fluid Thermodynamic Properties for Light Petroleum Systems" (Ref. 17).

FIGURE 7

VTB Example

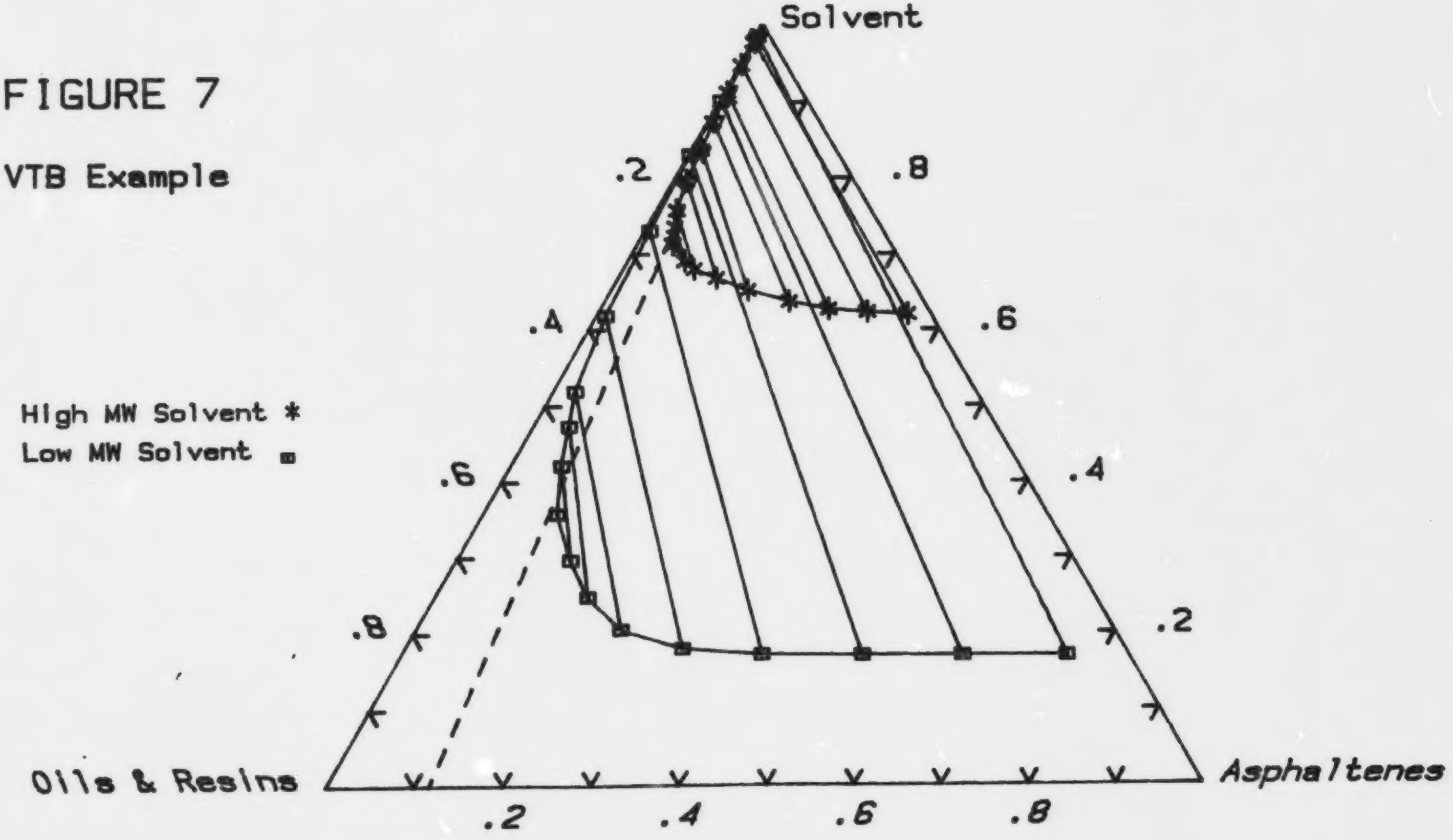

FIGURE 8

VTB Example

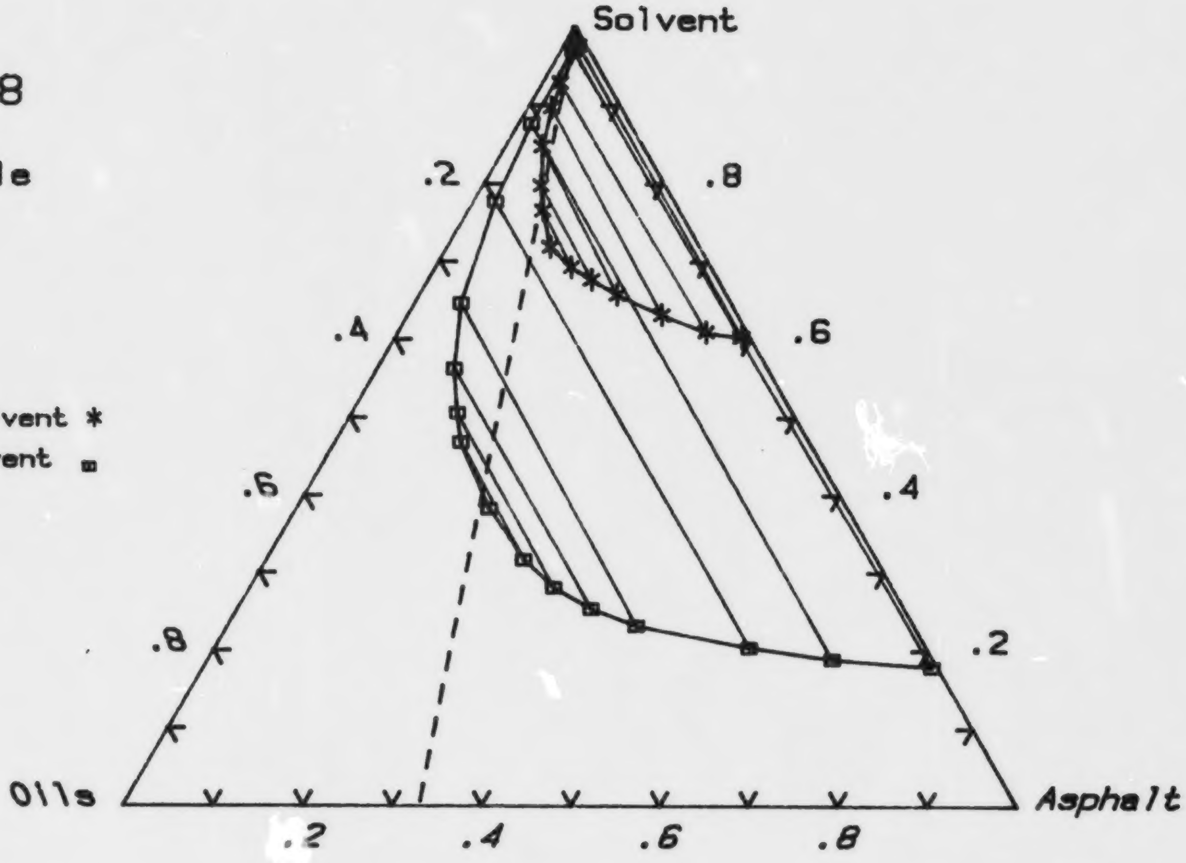

FIGURE 9

Athabasca - C3
75C 465 PSIA

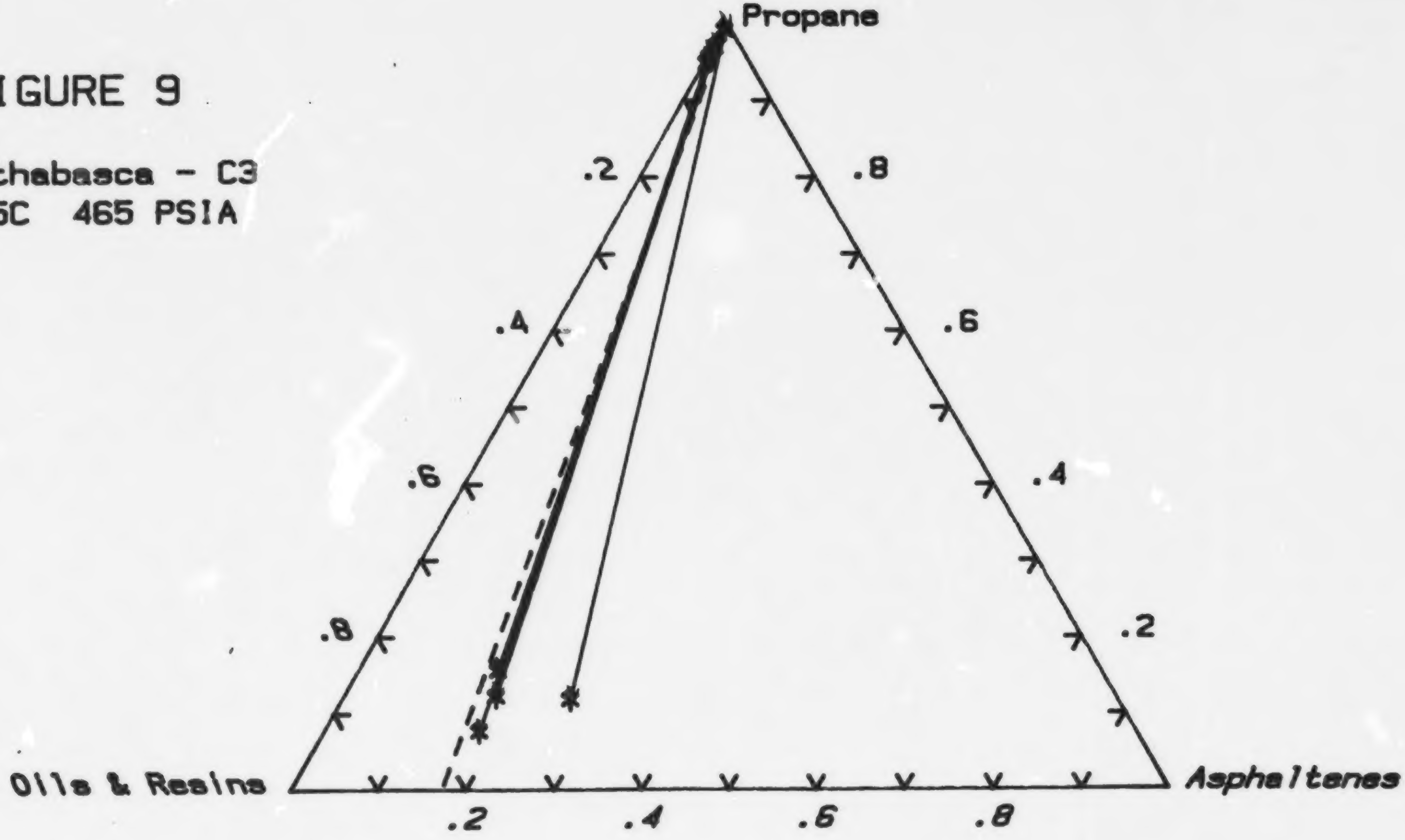

FIGURE 10

Athabasca - C4
120C 415 PSIA

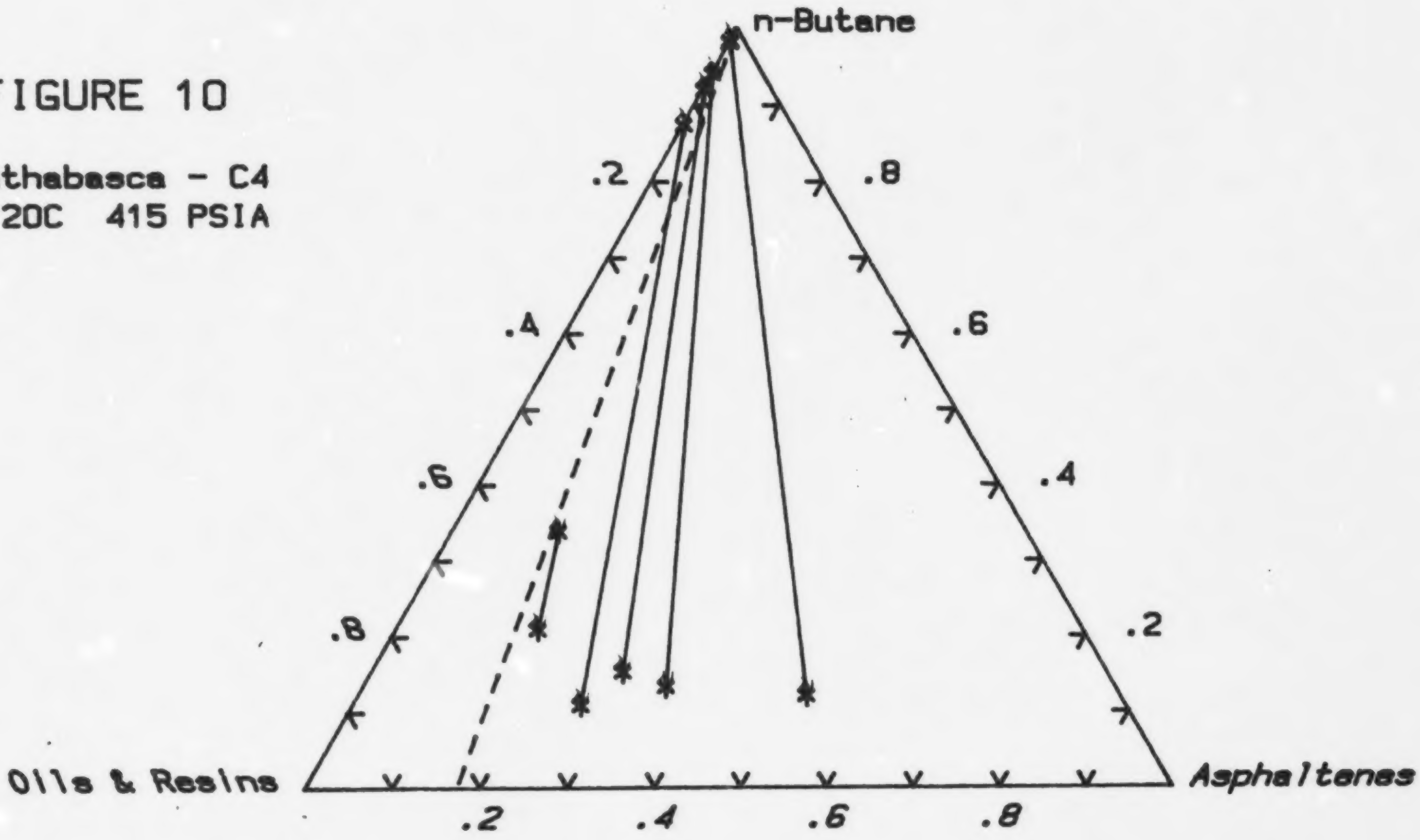

FIGURE 11

Athabasca - C5
160C 365 PSIA

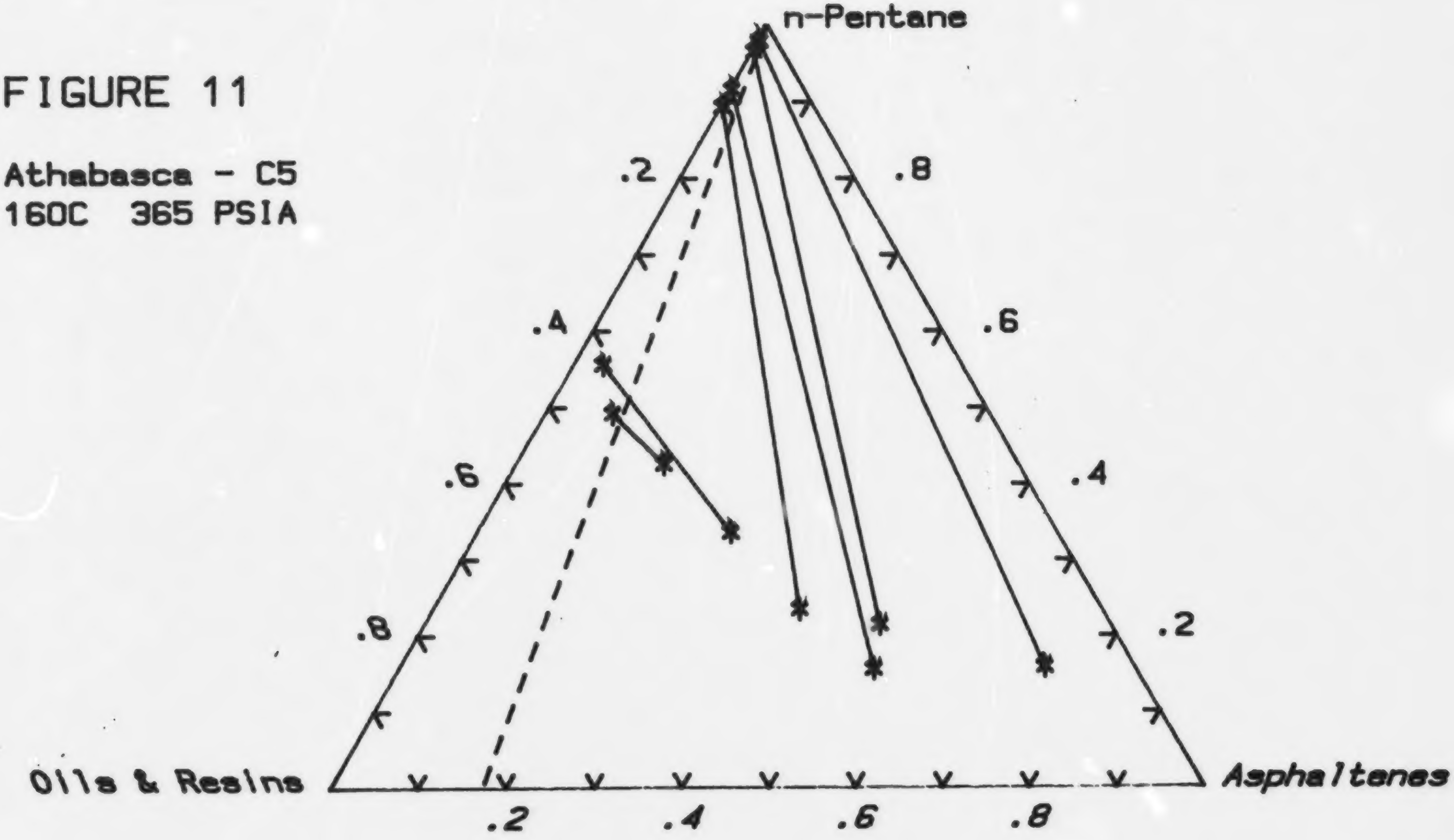

FIGURE 12

Athabasca - C7
75C 65 PSIA

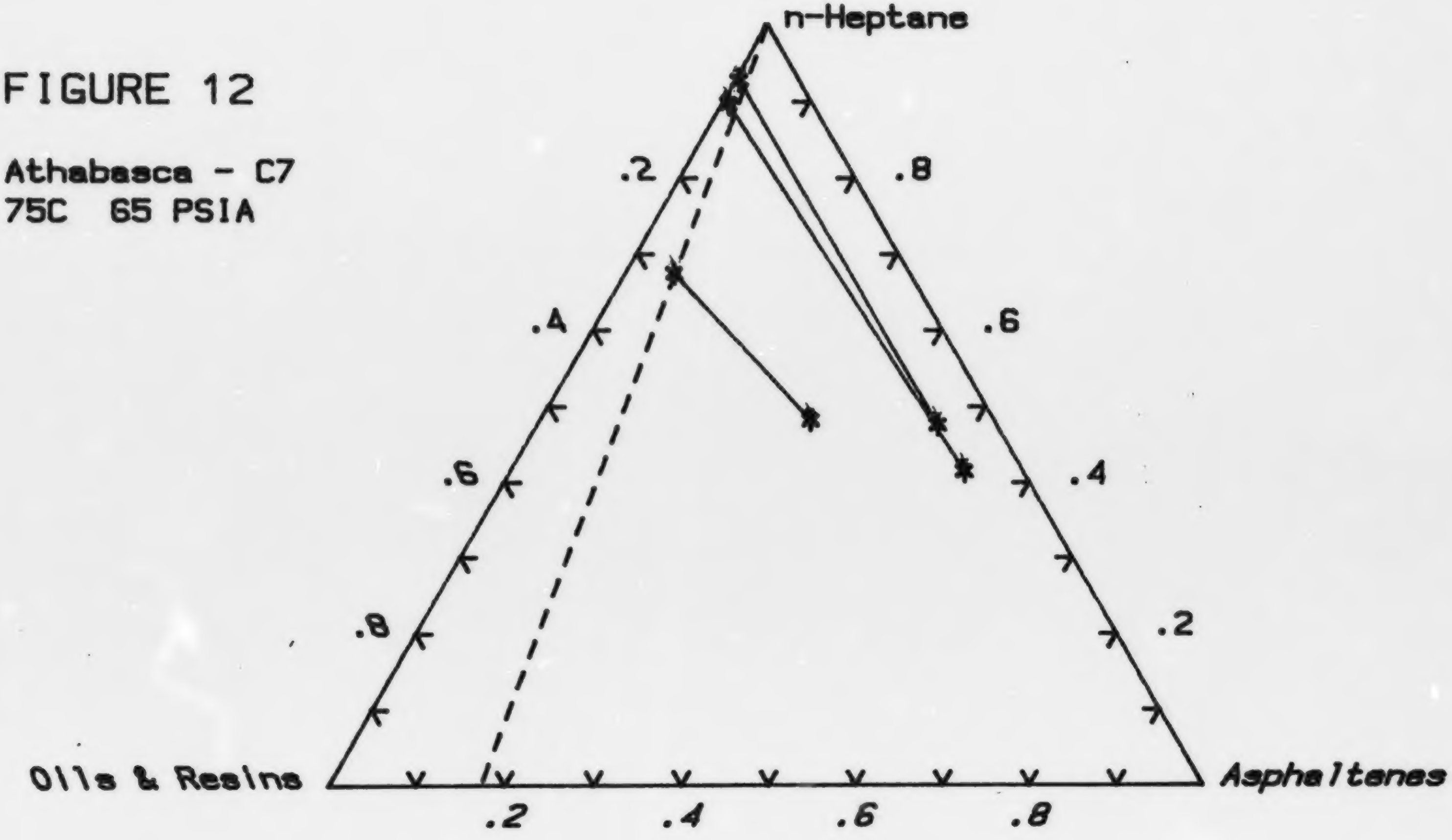

FIGURE 13

Lloydminster - C3
75C 465 PSIA

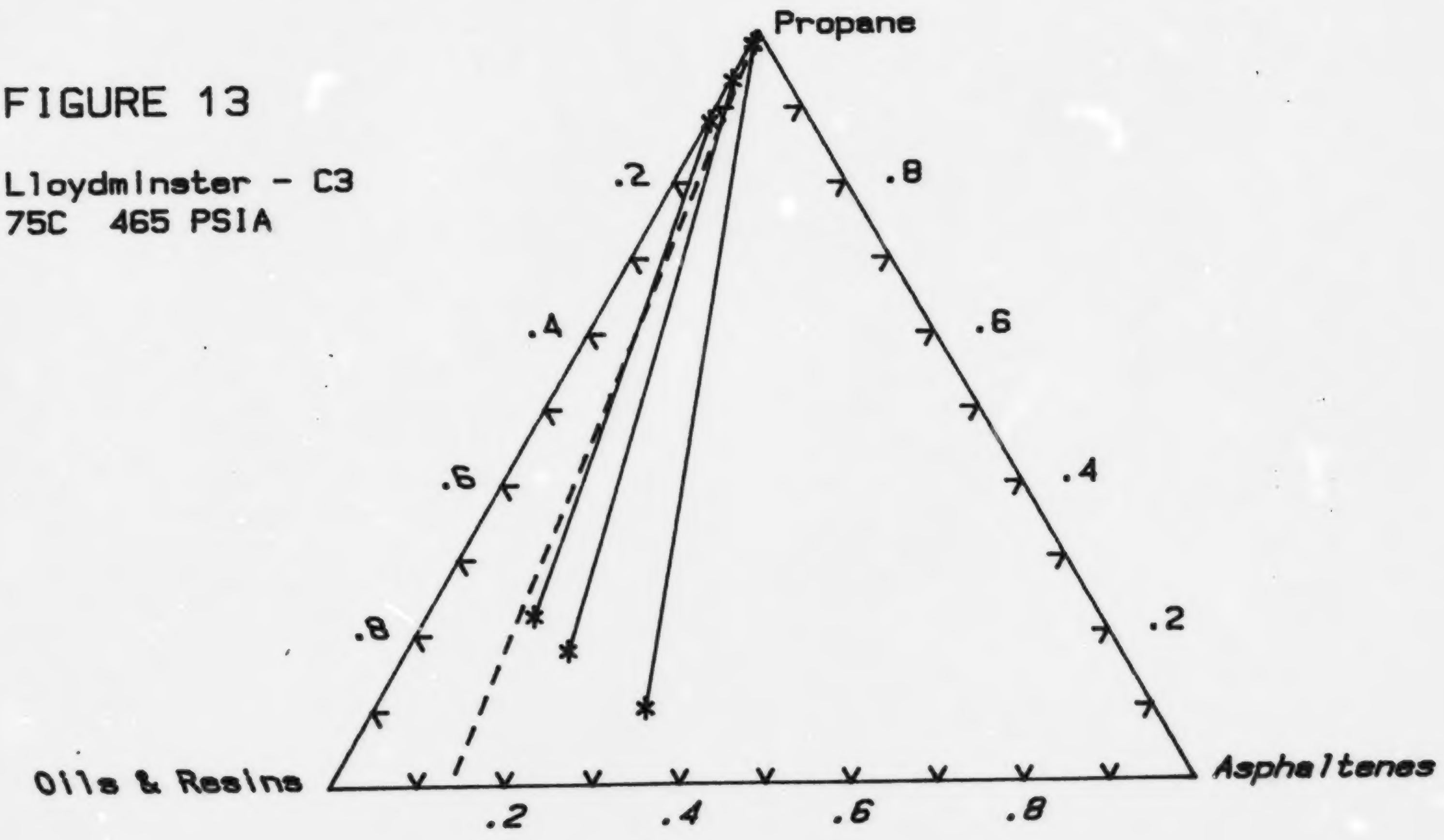

FIGURE 14

Lloydminster - C4
120C 415 PSIA

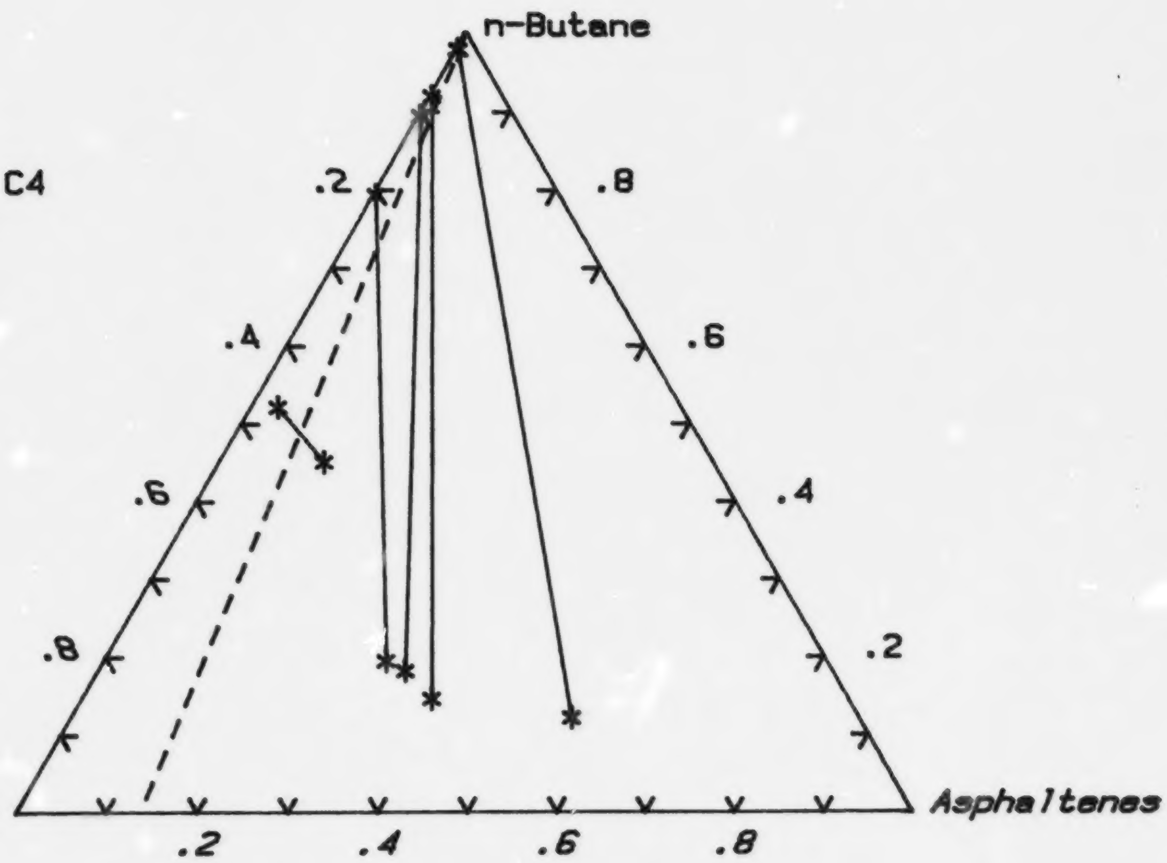

FIGURE 15

Lloydminster - C5
160C 365 PSIA

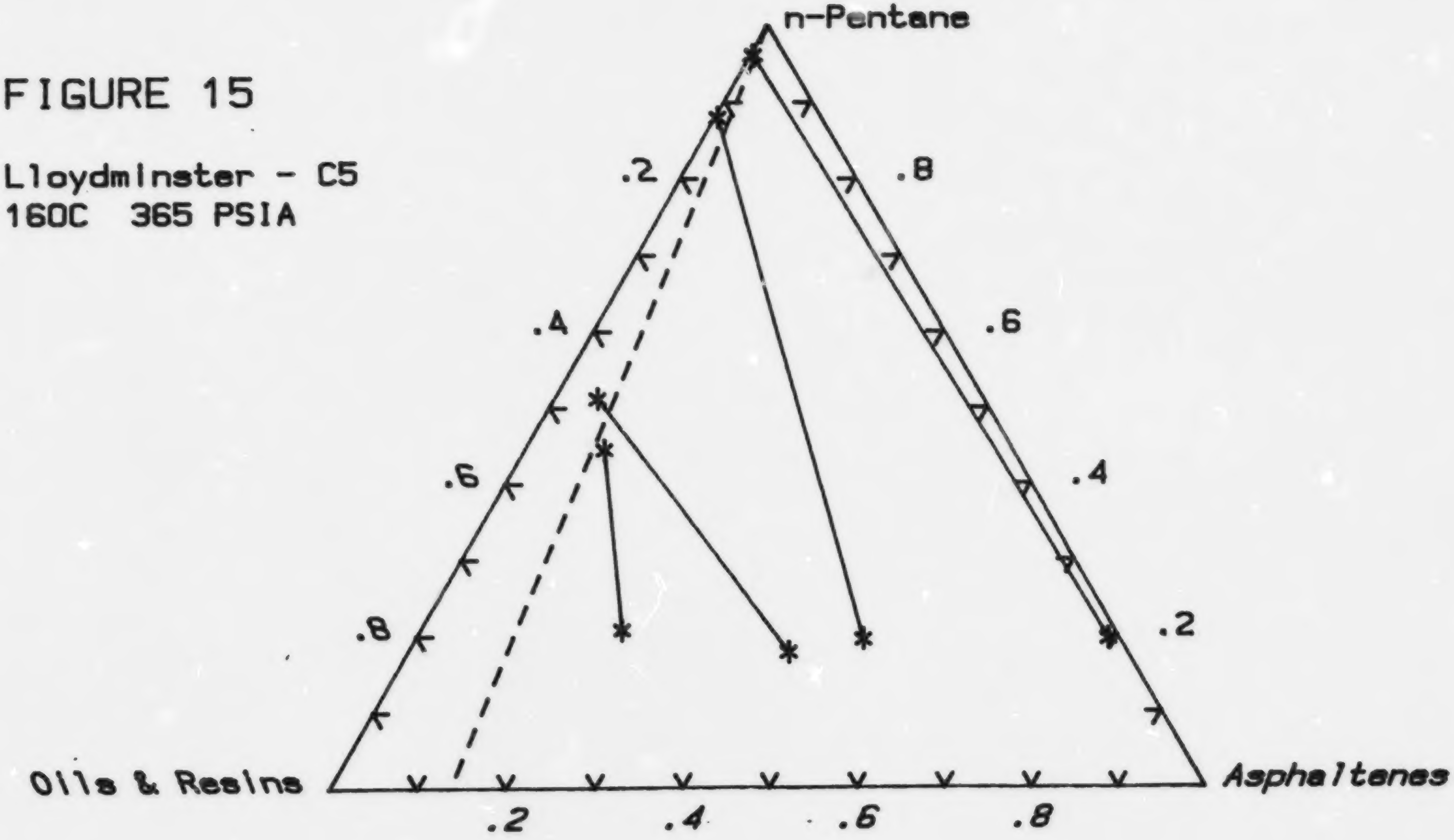

FIGURE 16

Lloydminster - C7
75C 65 PSIA

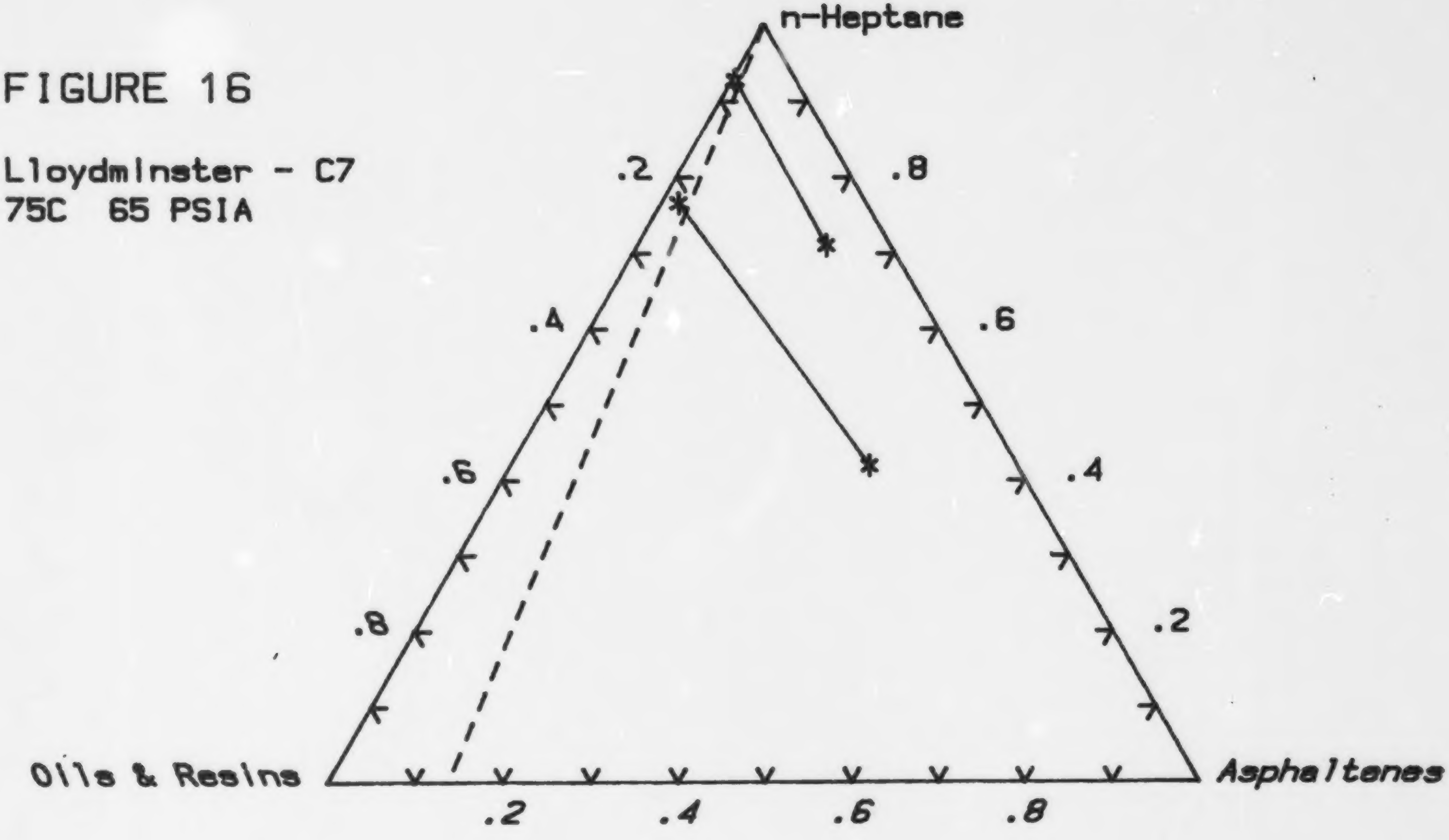

Figure 17

Nitrogen–Asphalt Correlation for DAO

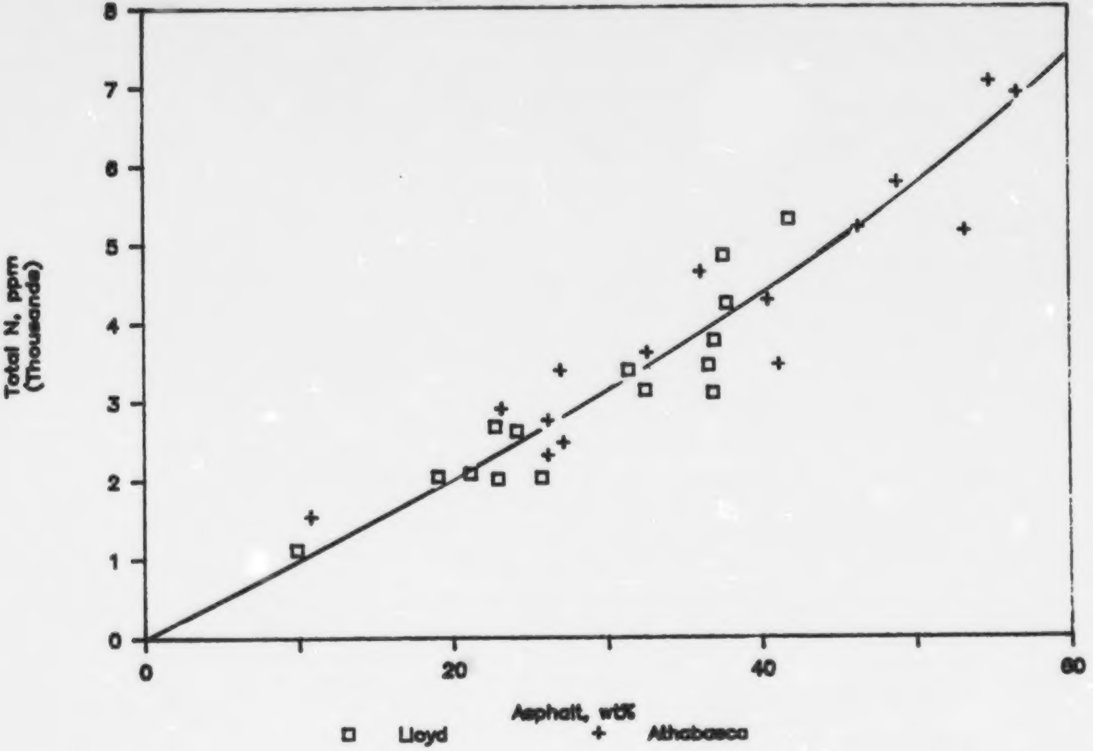

Figure 18

Metals–Asphalt Correlation for DAO

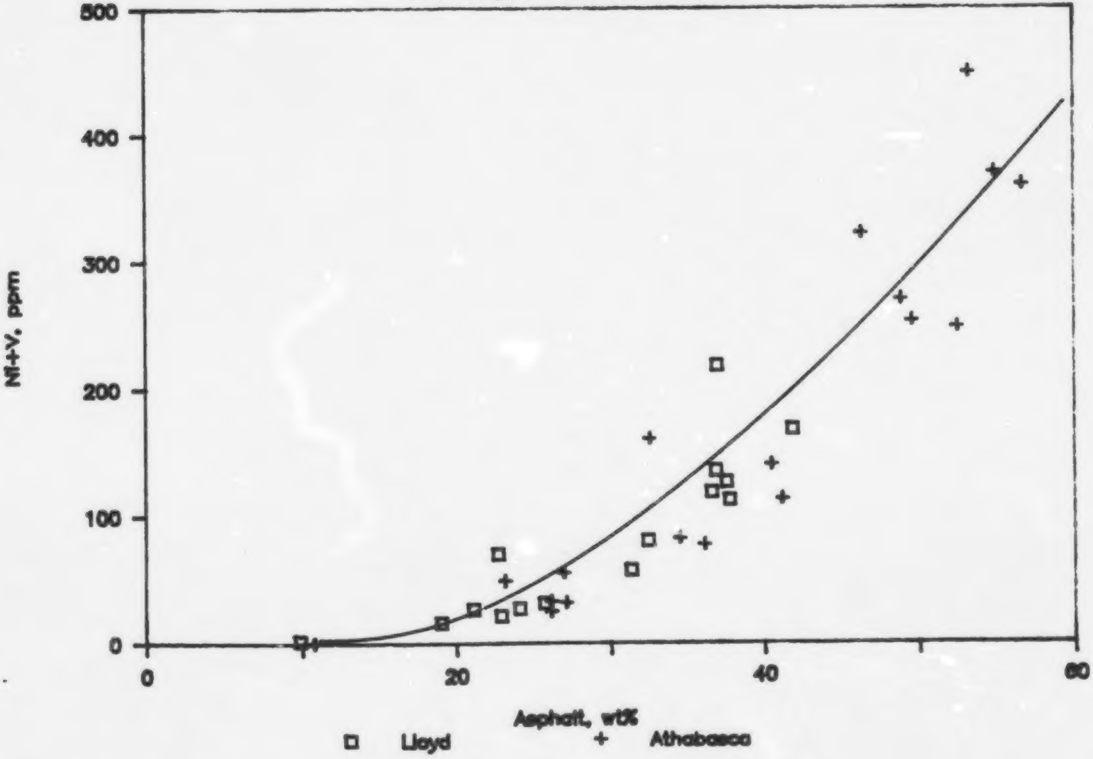

Figure 19

CCR-Asphalt Correlation for DAO

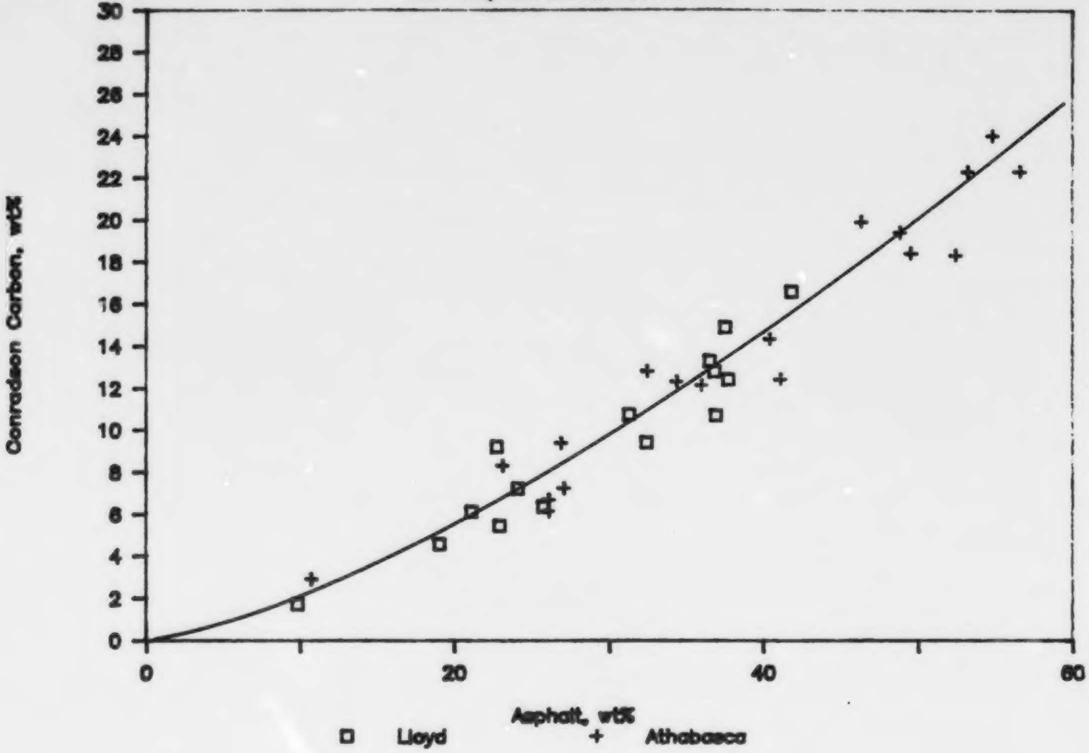

9. Results from the Microactivity Testing Program

A total of fourteen deasphalted oils prepared from Lloyd VTB, fifteen DA oils prepared from Athabasca VTB and two vacuum gas oils were evaluated for this contract. Each oil was cracked at three severities by varying the C/O ratio (2, 4 and 6) while maintaining a reactor temperature at 510°C and a WHSV of 20 h^{-1}.

DA oils ranged from low Conradson Carbon, low metals oils which could be considered as feed to a commercial FCC to highly asphaltic DA oils which were similar to the VTB feed material in terms of carbon residue and metals content.Studying such a wide range of feedstocks required some variation in the experimental technique and also in the manner in which the data was interpreted. The feed varied from free flowing liquids to solids which required heating to 130°C in order to inject the material into the MAT reactor. These high melting solids obviously posed problems in terms of achieving the correct C/O ratio without carrying out multiple repeat experiments.

These materials deposited large amounts of coke both on the catalyst and to a lesser extent on the reactor internals. In fact, over the range of deasphalted oils studied, the coke make varied by an order of magnitude from 3.56% for propane DAO to 35.4 for low quality butane DA oil. These variations in coke make were associated with similar variations in Conradson Carbon from 1.7 to 24.0%.

In the initial MAT work, the DA oils were of reasonable quality and standard experimental and computational procedures gave good material balances when calculating catalytic cracking yields. However, as the DA oils became more asphaltic the experimental procedures became more exacting and it was necessary to revise the computational procedures to account for the large coke makes associated with these asphaltic DA oils. These procedures are reviewed in the Experimental Section, 6.

To place this study into perspective, it is informative to briefly review literature data on the cracking of residual feedstocks. A.R. Johnson has recently reviewed the commercial performance of the Stone and Webster Residual Oil FCC Unit (3). This unit is designed to crack a combination of gas oil and VTB to produce high yields of gasoline. In the review, the heaviest feed processed was a mixture of 31 vol.% VTB in VGO. The blended feed and the VTB had the following properties.

	Feed	VTB
V + Ni, ppm	18.5	60
CCR, wt%	5.5	17.7

Yen et al of Kellog presented data correlating coke make with CCR for pilot plant and commercial operations (5). They studied feedstocks with CCR up to 8.7 wt%.

J. Bousquet et al evaluating propane, butane, and pentane deasphalted oils from light and heavy Arabian vacuum residues, as FCC feedstock (2). They were able to crack the neat propane and butane DA oils (CCR 2.5 and 5.6 wt% respectively) in their pilot plant but had to blend the pentane DA oil (CCR 11 wt%) with gas oil because experimentally it was very difficult to test the neat oil.

The above corresponds to what was observed in the present study. The propane and better quality butane DA oil were relatively easy to test in the microreactor while the other materials were progressively more difficult to test as the CCR increased. For the low CCR oils, the yields were calculated by the standard procedure while for the more asphaltic oils (all the pentane and heptane DA oils plus the butane DA oils from Runs 28 and 37) the coke was calculated as the difference in the material balance.

10. General Relationships Between MAT Yields and DA Oil Quality

Yield data obtained at a nominal constant severity (C/O ratio of 4) is compared here for all the Lloydminster and Athabasca DA oils. The two sets of data are summarized in Tables 26 and 27.

a. Coke Correlations

For these sets of data, the most obvious trend is the variation in coke make with both asphalt (resins + asphaltene content) and CCR. Figure 20 shows the excellent correlations between asphalt content and coke make over the range of 10 to 55 wt% asphalt. The concave curvature to the plot suggests that the heavier asphaltic material shows a greater propensity to form coke than the "lighter" resins. In the range to 10 - 25 wt% resins, the slope of Figure 20 suggests that for every one percent increase in the resin content of the feed above 10%, then there is a corresponding increase in the coke make by 0.4 wt%, i.e. 40% of the incremental resins are yielded as coke. In the range 48 - 55 wt% resins plus asphaltenes, the increased slope suggests that for every one percent increase in the asphalt content above 48% there is a corresponding one percent increase in the coke make, i.e. all the incremental resins and asphaltenes are yielded as coke.

Figure 21 shows that there is essentially a straight line relationship between the coke make and feedstock CCR. Moreover, the slope of the line (within the accuracy of measuring the coke) approximates to a 1:1 relationship between coke make and CCR. These data substantiate the claims of Yen et al (5) that the Conradson Carbon portion of the feed is essentially yielded as coke. Yen (5) plotted CCR ranging from 4 to 8.7% against coke makes ranging from 7.2 to 11.5%. These data fit the CCR vs. coke plot for Athabasca and Lloyd DA oils shown in Figure 21. This excellent agreement is somewhat surprising and suggests that the severity of a MAT unit operating at 510°C and C/O of 4/1 is similar to that of pilot and commercial plant operation.

Operating the MAT unit at a lower C/O of 2 yields less coke while at the higher C/O of 6 more coke is produced. However, for any set of results the difference in coke yield between a 2/1 and a 6/1 C/O ratio is relatively consistent at an average value of 7.3 wt%. This implies that the coke vs. CCR plots for the various C/O ratios are three parallel lines. To summarize this part of the discussion, the CCR is a most important property of DA oil as it sets the additive coke make for the MAT unit.

b. **Product Correlations**

Other general trends noted are a modest increase in dry gas make and a decrease in the C_3C_4, gasoline, and LCO yields as the asphalt content and CCR of the feed increase. The dry gas make for the two feeds is plotted against the feed asphalt (asphaltene + resin) content in Figure 22, while the three liquid products are plotted against oil content in Figures 23, 24 and 25. The dry gas yields are on average higher for the Athabasca DA oils.

As can be seen from Figure 23, there is some discrimination in terms of gasoline production from the two feedstocks, with the Lloydminster on average yielding more gasoline for a given oil content of a feed. Based on the mass spectrometric composition of the two oil fractions (Table 2) which shows the crackable components for the Lloyd and Athabasca fractions as 46.9 and 25.4 wt% respectively, it may have been expected that the difference in the gasoline yield would have been more significant. As discussed, when reviewing the feedstock analyses, it is expected that the lower polynuclear aromatics in the DA oil would be associated with significant paraffinic and cycloparaffinic structures thus providing an additional source of crackable components. Another source of crackable components are the lighter resins. It was earlier estimated that 40% of this material was yielded as coke leaving 60% available to be cracked. Although it was not the intent of this project to develop detailed correlations between gasoline yield and DA quality, it is interesting to note that the simple equation:

$$\text{Gasoline yield, wt\%} = \text{Oil content, wt\%} \times 0.5 + \text{Resin Content, wt\%} \times 0.165$$

provides a reasonable estimate of gasoline yield at a C/O ratio of 4/1. At this C/O ratio for DA oils the gasoline yield is normally close to its maximum value, making this a potentially useful method for evaluating DA oils. Obviously other yield, feed quality correlations can be developed using the present data base.

Both the C_3C_4 and LCO yields show a steady increase as the oil content of the feed increases. There is little discrimination between the two oils in either set of data.

c. Metal Effects

The MAT unit, unlike a commercial FCC unit is not affected by feed metals. Thus, care should be taken to include the deleterious effects of metals, when using this data to relate to potential commercial operation.

Figure 20

Coke Make vs DAO Asphalt (C/O=4)

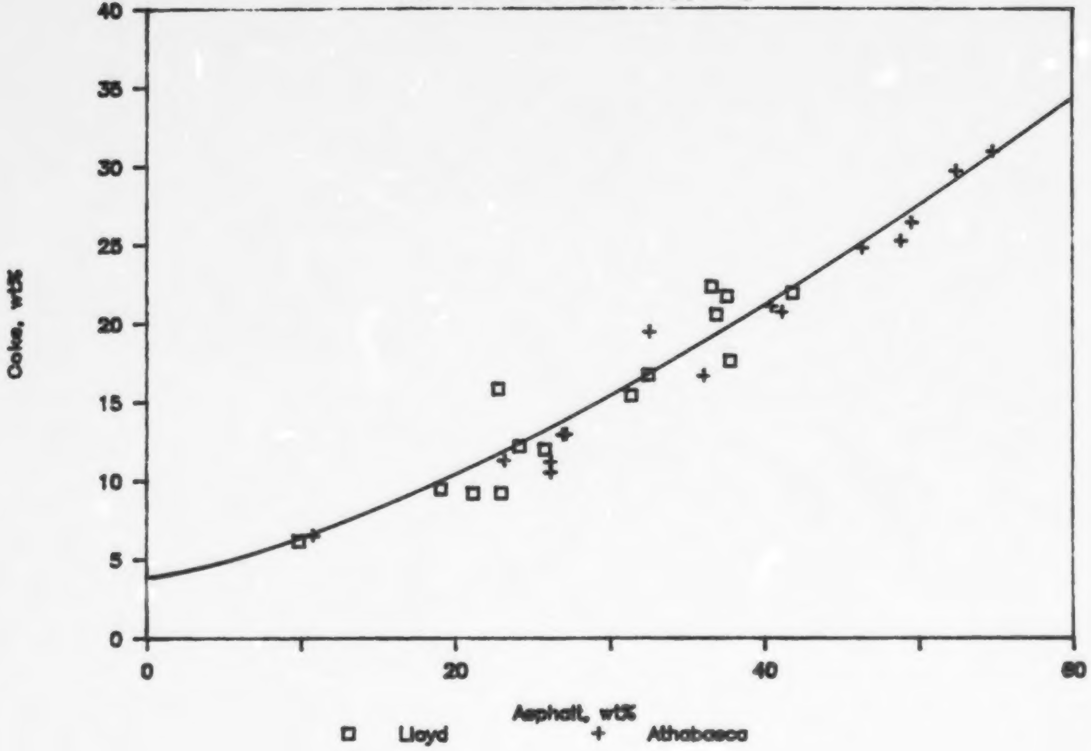

Figure 21

Coke Make vs DAO CCR (C/O=4)

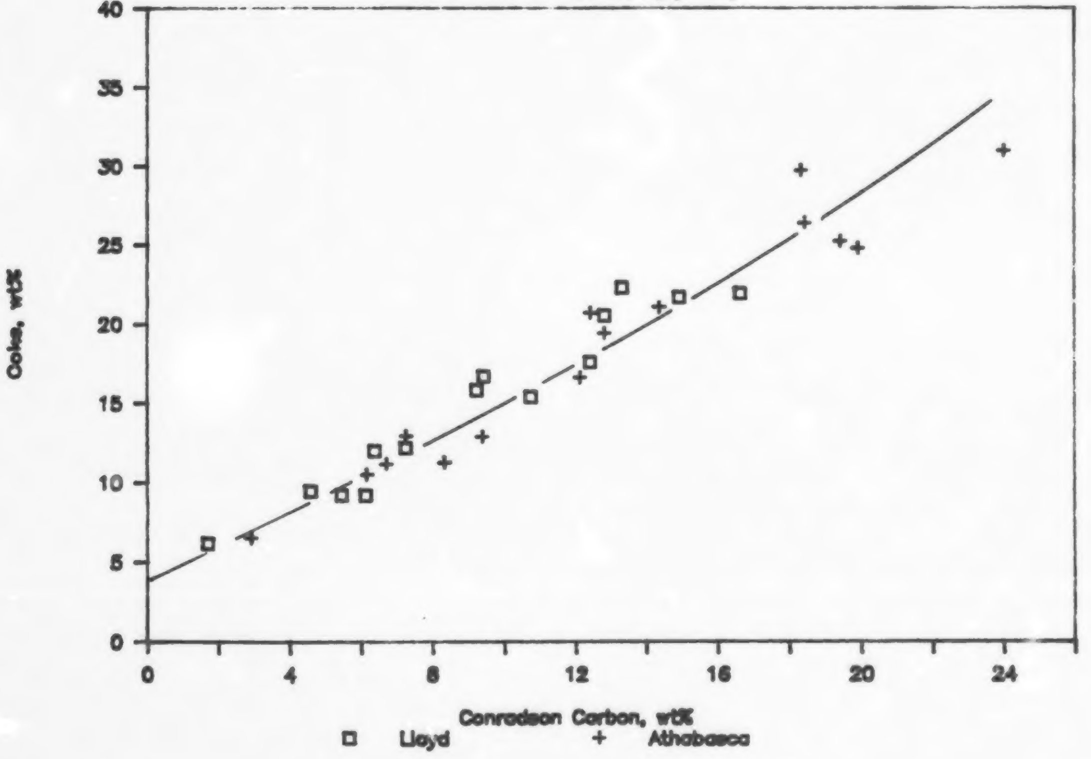

Figure 22

Dry Gas Make vs DAO Asphalt (C/O=4)

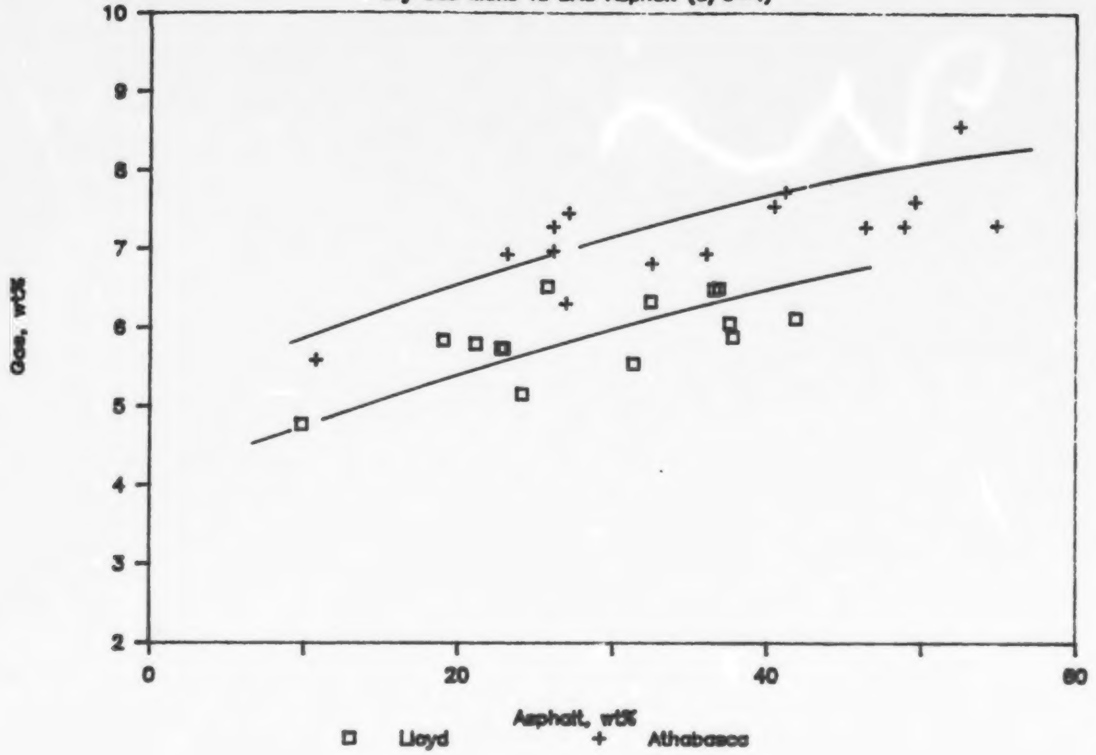

Figure 23

C5+ Gasoline vs DAO Oils (C/O=4)

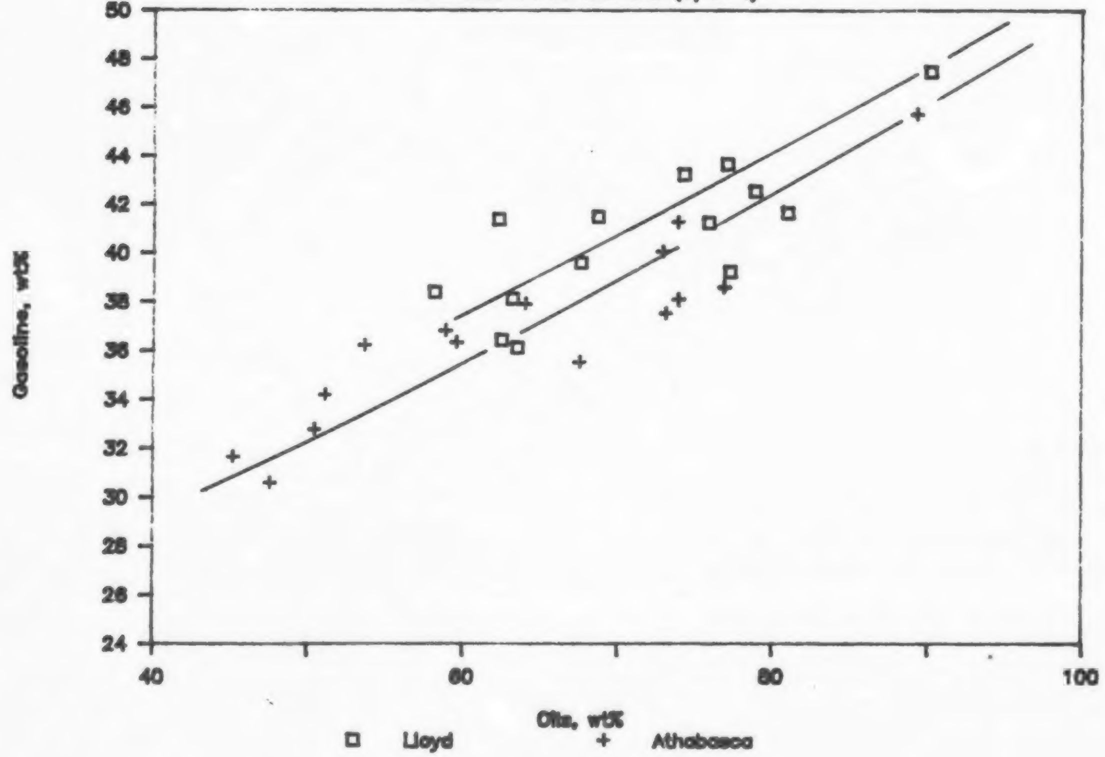

Figure 24

C3C4 Yield vs DAO Ofls(C/O=4)

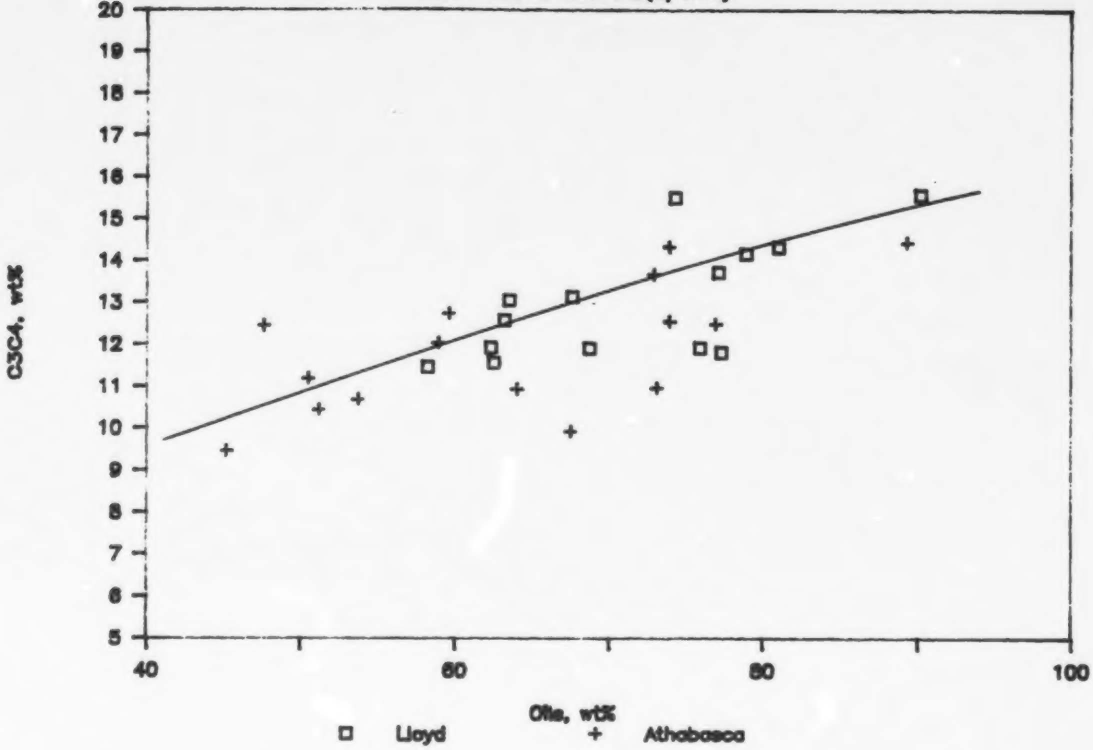

Figure 25

LCO Yield vs DAO Ofls (C/O=4)

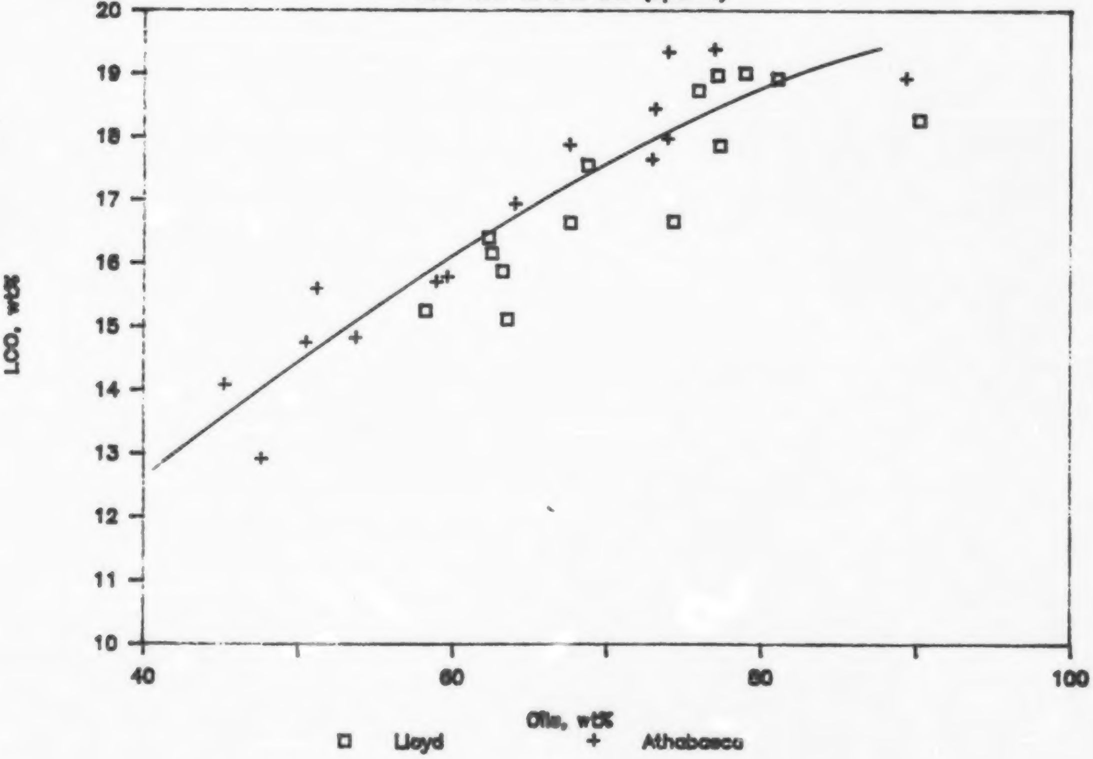

11. Cracking Characteristics of the Propane DA Oils and Associated VGOs

Propane deasphalted oils are normally recognized as good FCC feedstock. Here the Lloyd and Athabasca oils (LC3DAO, AC3DAO) will be compared with the two associated vacuum gas oils (LVGO and AVGO). The yield data are given in Tables 20 and Figures 26 to 33 show the severity and selectivity plots for the four oils.

The two gas oils are of significantly different composition and as expected, the Lloyd VGO gives much higher conversions and gasoline yields at the various operating severities. There is a much smaller difference in yield profiles obtained from cracking the two DA oils and both DA oils are much better cracking stocks than the Athabasca VGO.

Figure 26 shows the relationship between C/O and conversion for the four oils. The Athabasca VGO shows a much lower conversion than the other oils while the Lloyd VGO is 4-6 numbers lower than the DA oils at the higher C/O ratios. It is noted generally that DA oils crack more readily than the associated gas oils, and will give higher "ultimate" conversions. However, as conversions approach the mid 70's the major incremental product is coke.

The reactivity of DA oil products is illustrated by Figure 27 which shows the gasoline overcracking for the two DA oils at higher conversion. In contrast, the two VGOs do not show overcracking in the severity range studied. The Athabasca VGO gives a much lower yield of gasoline than the other materials while the Lloyd VGO produced the highest yield of gasoline. The maximum gasoline yield for the Lloyd DA oil was 1.8 wt% greater than the Athabasca material. As discussed previously this difference is due to the increase in the oil content and quality in the Lloyd sample.

Figure 29 shows that the C_3C_4 yield correlates extremely well with conversion data for the four feedstock fitting a common line. Since the DA oils give higher conversions at a given severity they also produce more C_3C_4 than the gas oils.

Both Athabasca samples make more dry gas for a given conversion than the Lloyd samples (Figure 28). Hydrogen sulphide is a major component in the dry gas as would be expected from the high sulphur contents of the feeds (LVGO 2.1, AVGO 3.7, LC3DAO 2.84, AC3DAO 3.66 wt%). As discussed earlier, dry gas make for DA oils is also related to the resin content and the propensity of the feedstock to form coke.

Both Lloyd samples show a regular decline in LCO production with increasing conversion (Figure 30). However the relationship is not as straight forward for the Athabasca samples and the VGO actually shows a maximum for LCO yield. It is suggested that at low conversions a significant amount of decant oil initially cracks to LCO before being cracked further to gasoline and other products at higher conversions.

The decant oil shows a more regular decline for the four oils (Figure 31). The Athabasca DA oil and VGO and the Lloyd DA oil essentially fit on one curve with the Lloyd VGO showing lower decant oil yields at equivalent conversion.

The coke make is plotted against conversion and C/O ratio in Figures 32 and 33. There is essentially a linear relationship between coke and C/O with the data points for the Athabasca VGO and DA oil and the Lloyd DA oil fitting on one line and the Lloyd VGO showing a significantly lower coke production.

The above discussion shows that the propane DA oil exhibits similar cracking characteristics to gas oils with the provision that it is easier to crack and at high conversion incremental converted material is yielded as coke. To complete the discussion on propane deasphalted oil the present results are compared to literature data on Arabian DA oil (2).

Comparison of Propane DA Oil Yields

	Light* Arabian	Heavy* Arabian	Lloyd	Athabasca
Dry Gas wt,%	3.5	3.7	4.8	5.6
C_3C_4	16.0	12.8	15.6	14.4
Gasoline	51.8	51.0	47.5	45.7
LCO	16.1	17.4	18.3	18.9
DO	6.5	7.7	7.7	8.8
Coke	5.5	7.4	6.15	6.5
Conversion, wt%	77	75	74.0	72.3

* J. Bousquet and T. Laboural, O&GJ, April 20, 1988, p. 62

It appears that the Arabian DA oil are not as reactive as the Lloyd and Athabasca oils and thus can be cracked at higher conversion without producing excessive coke or overcracking the gasoline fraction. The increased gasoline yield obtained from cracking the Arabian DA oils must be related to the improved quantity/quality of the oil fraction in the DA oil.

TABLE 20

MICROACTIVITY TEST RESULTS USING DA-440 EQUILIBRIUM CATALYST AND ATHABASCA AND LLOYDMINSTER VACUUM GAS OILS AND C_3 DA OILS

	Lloyd VGO			Atha VGO			LC_3 DAO			AC_3 DAO		
MAT #	114	115	116	117	118-R	119	3	1-R	2	50	10	11
Feed	-	-	-	–	-	-	5	5	5	5	5	5
WHSV. hr-1	18.30	19.50	20.60	20.10	19.80	22.60	18.90	20.20	21.40	19.40	20.10	17.60
Cat/Oil	2.18	4.00	5.82	1.99	3.95	5.30	2.12	3.86	5.27	2.06	3.89	6.81
H2	0.02	0.03	0.04	0.03	0.04	0.05	0.02	0.03	0.04	0.04	0.05	0.07
H2S	1.31	1.51	1.53	1.87	2.04	2.52	1.89	2.07	1.74	2.26	2.83	3.25
C1	0.32	0.44	0.54	0.40	0.55	0.78	0.68	0.93	1.02	0.71	0.91	1.29
C2	0.30	0.40	0.52	0.36	0.50	0.67	0.67	0.86	0.95	0.70	0.96	1.17
C2=	0.46	0.63	0.80	0.40	0.38	0.78	0.62	0.88	1.02	0.54	0.83	1.20
TOTAL	2.41	3.01	3.43	3.06	3.71	4.80	3.88	4.77	4.77	4.25	5.58	6.98
C3	0.89	1.29	1.50	0.66	0.85	1.36	1.24	1.44	2.21	1.10	1.50	2.59
C3=	2.77	3.41	3.57	2.08	2.95	3.10	3.55	4.18	4.59	2.65	3.98	4.51
iC4	3.45	4.62	5.10	1.94	3.26	3.74	3.65	5.02	6.18	2.53	4.11	6.31
nC4	0.73	1.02	1.21	0.44	0.68	0.92	0.96	1.38	1.71	0.79	1.18	1.97
C4=	2.41	2.87	3.11	1.78	2.25	2.65	3.31	3.56	3.60	2.45	3.67	3.19
TOTAL C3C4	10.25	13.21	14.49	6.90	9.99	11.77	12.71	15.58	18.29	9.52	14.44	18.57
iC5	4.10	4.90	5.61	2.01	2.94	3.79	4.26	5.42	6.58	2.97	4.81	6.99
nC5	0.40	0.40	0.38	0.29	0.34	0.36	0.44	0.47	0.58	0.33	0.53	0.70
C5=	1.61	1.89	2.32	1.55	1.75	1.42	1.42	1.61	0.73	1.38	2.10	0.57
TOTAL C5	6.11	7.19	8.31	3.85	5.03	5.57	6.12	7.50	7.89	4.68	7.44	8.26
C5-216C	45.73	49.03	50.10	30.29	38.28	41.36	45.12	47.49	47.44	35.67	45.73	43.93
C6-216C	39.62	41.84	41.79	26.44	33.25	35.79	39.00	39.99	39.55	30.99	38.29	35.47
216-343C	25.74	22.40	20.15	19.98	22.17	21.56	20.64	18.27	16.25	20.18	18.93	15.21
343C-EP	13.24	8.28	6.38	36.51	20.21	13.17	13.99	7.74	5.66	26.81	8.81	5.27
Coke	2.63	4.07	5.45	3.26	5.64	7.34	3.66	6.15	7.59	3.57	6.51	10.04
Conv. wt%	61.02	69.32	73.47	43.51	57.62	65.27	65.37	73.99	78.09	53.01	72.26	79.52
Mat Balance	100.27	100.01	100.09	99.12	99.89	99.74	98.98	99.67	101.34	96.71	98.28	98.31

Figure 26

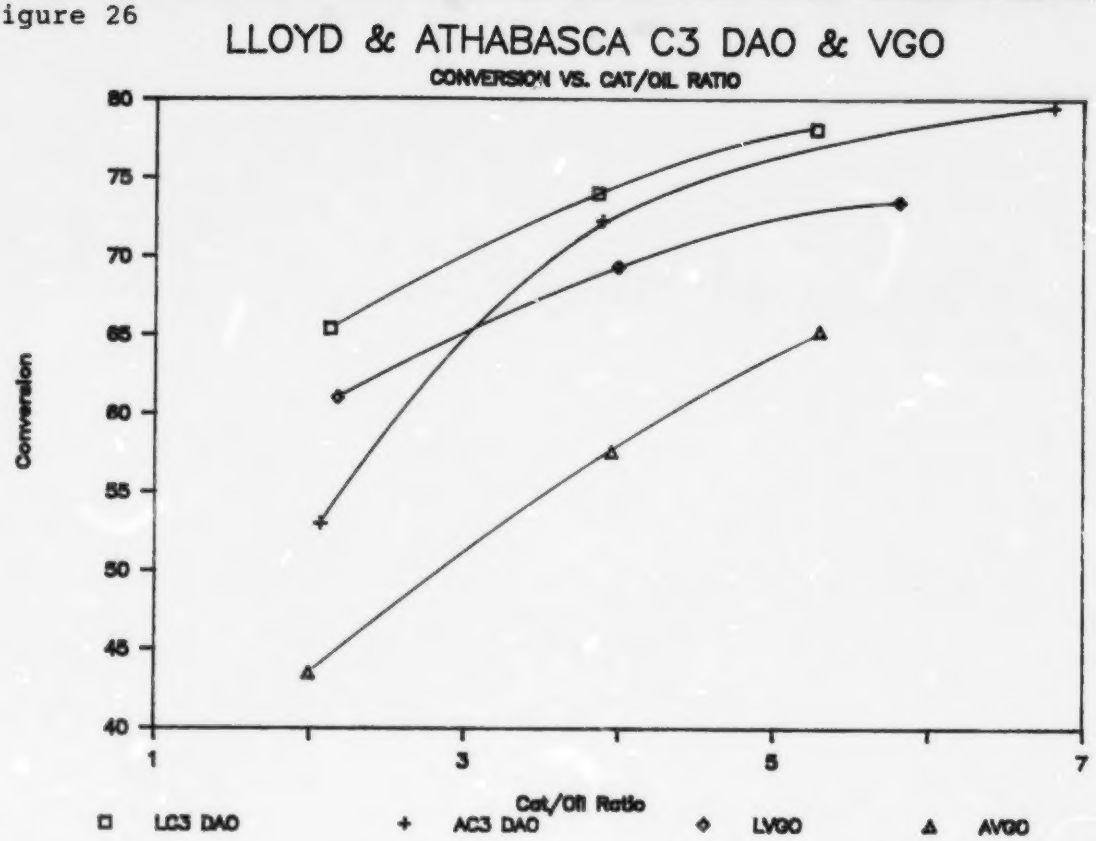

Figure 27

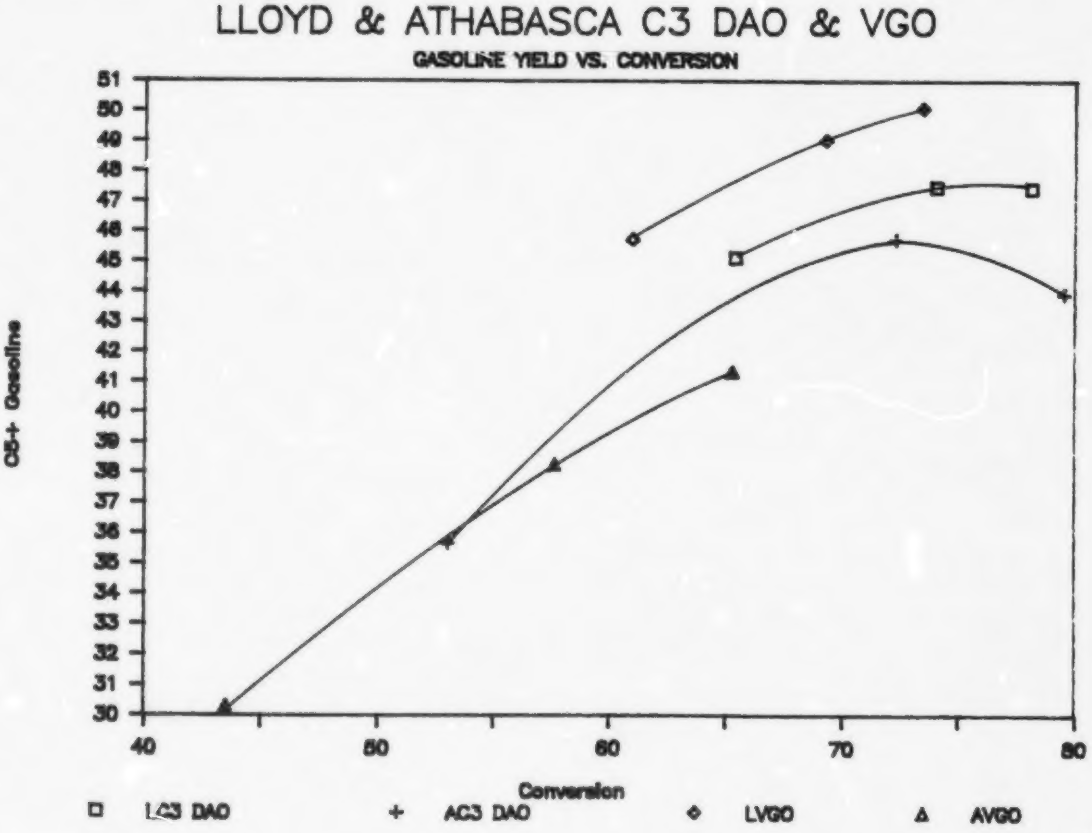

Figure 28

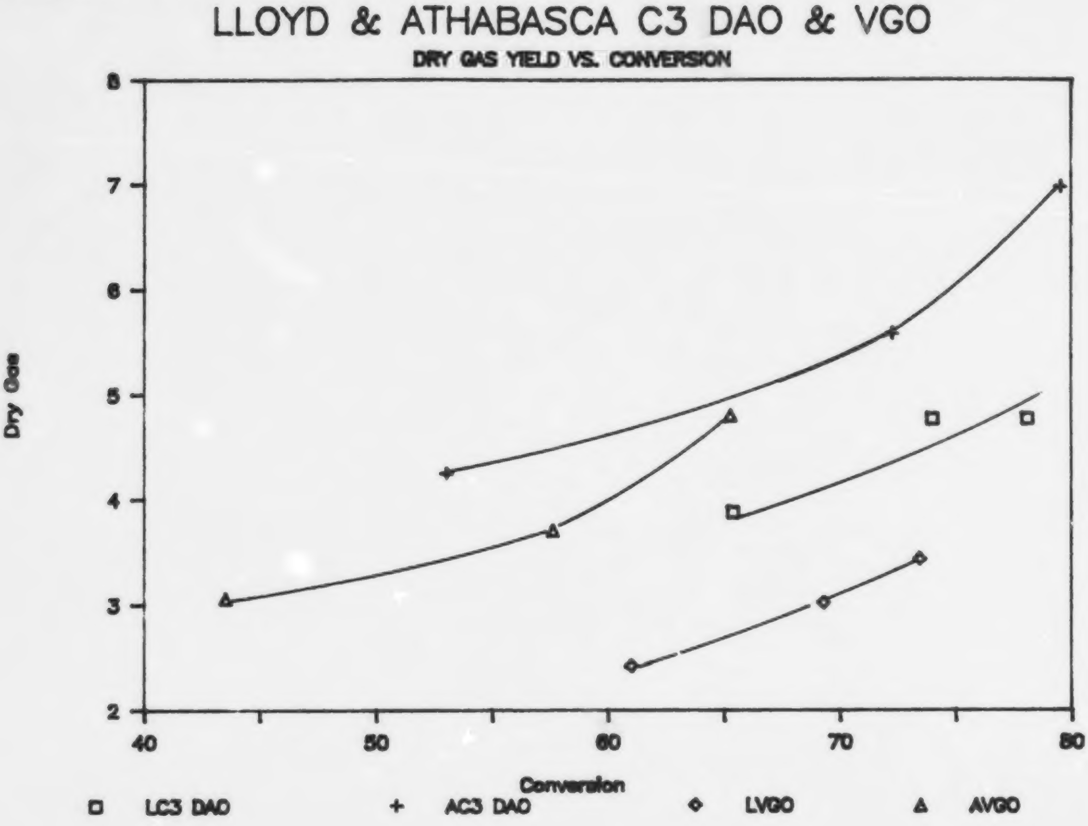

Figure 29

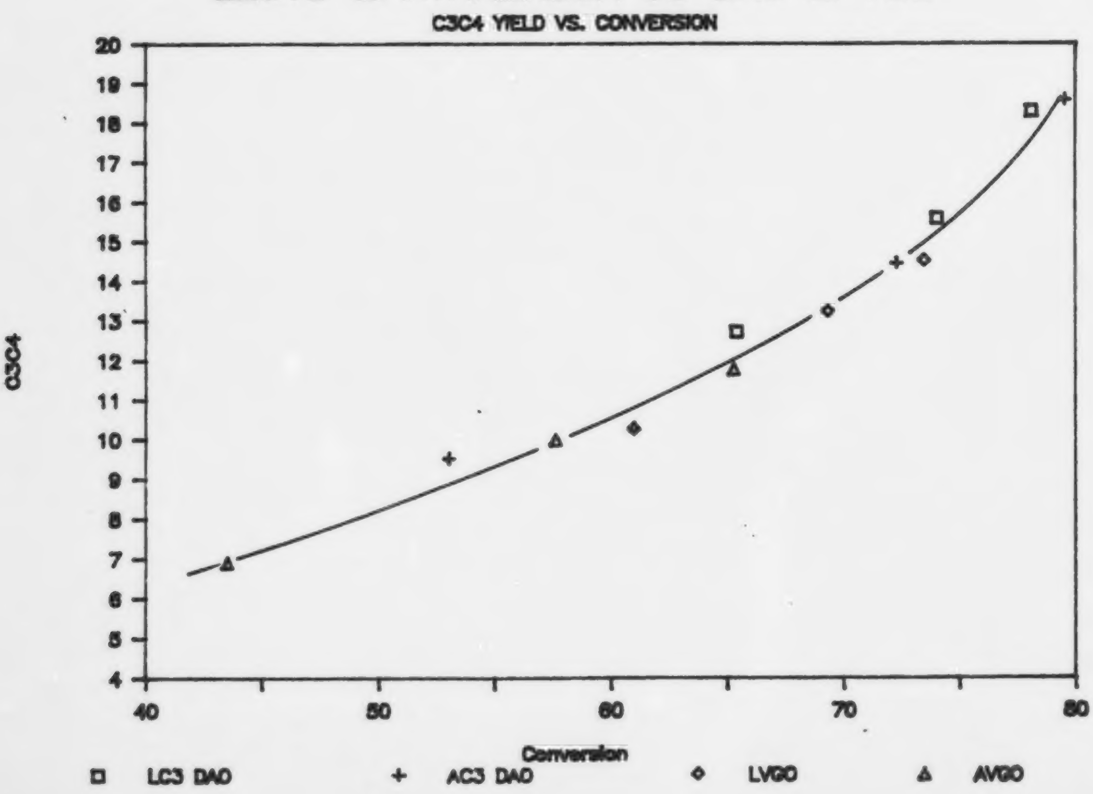

Figure 30

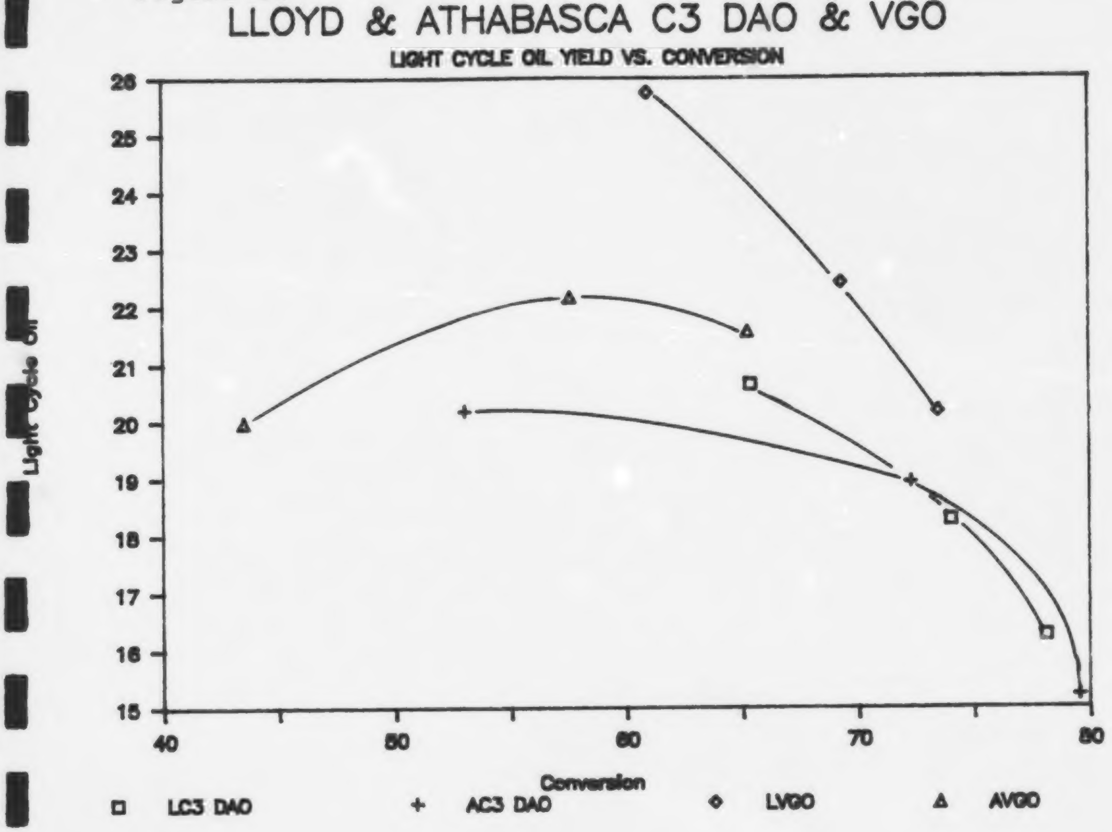
LLOYD & ATHABASCA C3 DAO & VGO

LIGHT CYCLE OIL YIELD VS. CONVERSION

Figure 31

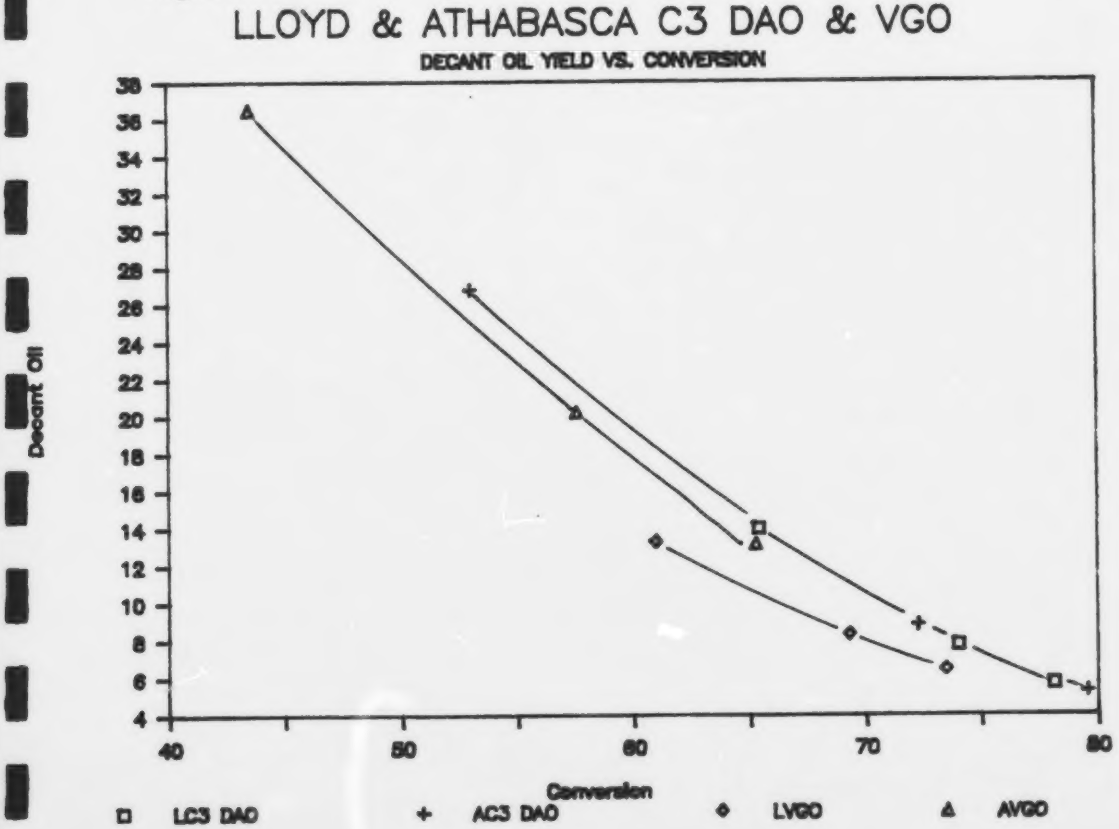
LLOYD & ATHABASCA C3 DAO & VGO

DECANT OIL YIELD VS. CONVERSION

Figure 32

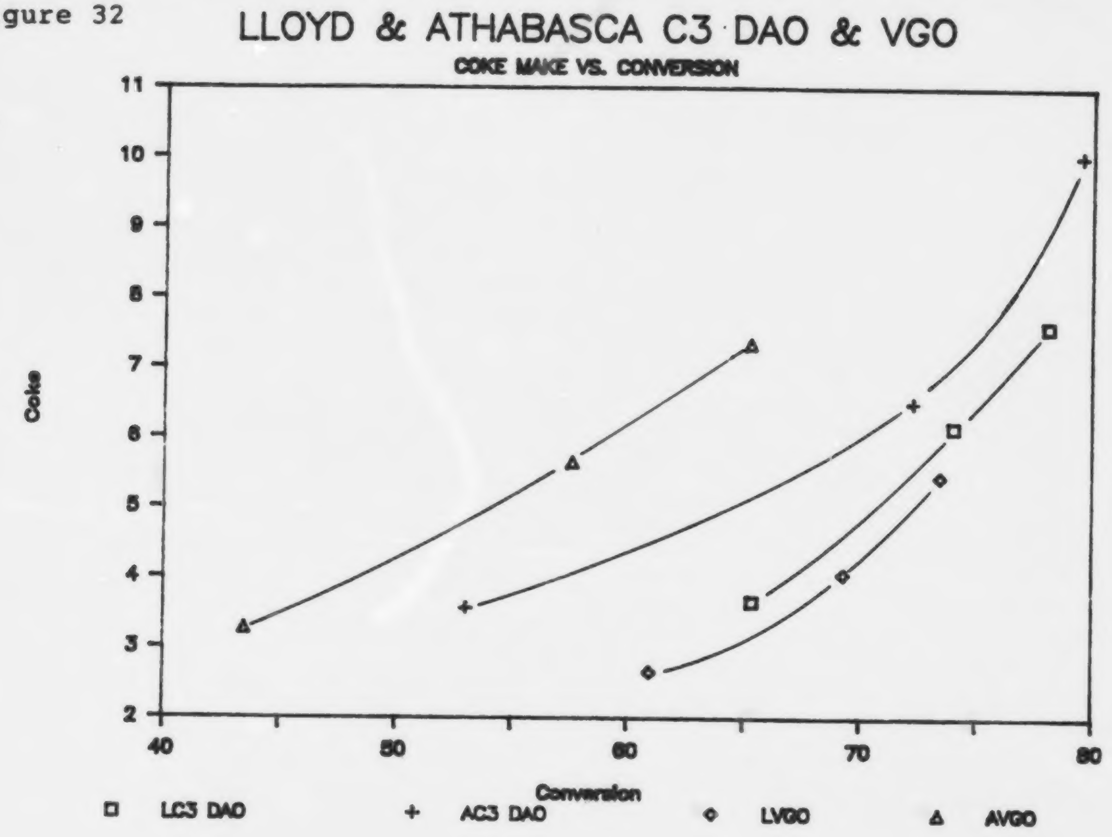

Figure 33

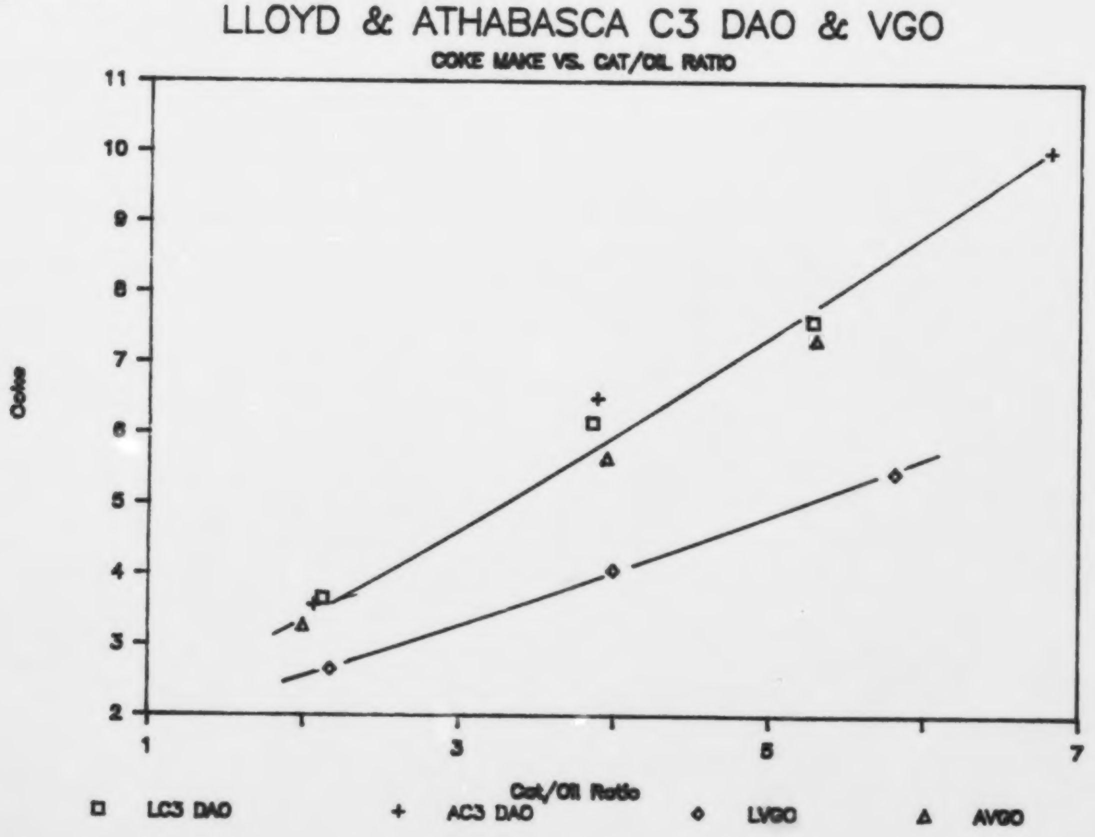

12. Cracking Characteristics of the Butane DA Oils

Six Athabasca and six Lloyd DA oils were tested in the MAT unit. The yields are given in Tables 21 and 22 while a summary of the principle properties and yields at a C/O ratio of 4 are given in Tables 26 and 27. The major difference between propane and butane DA oils is the increase in the resin content of the DA oil. This in turn reduces the yield of gasoline and substantially increases the coke yield. With the increased CCR and metals content the butane DA oils could not be considered as a neat charge to an FCC unit but would have to be blended with gas oil.

The general change in yield profile discussed for the propane DA oils also apply to the butane extracts. These are illustrated in Figures 34 to 41 using the oil from DA test 23 (120°C S/O 13/1 v/v). As the conversion is increased, the gasoline yield shows a maximum at a conversion of 72 wt%, then declines as the rate of gasoline cracking becomes greater than the rate of gasoline production. The dry gas make and the C_3C_4 make increases with increasing conversion while the LCO and DO yields decline. The major effect is the significant increase in coke make with increasing severity. Comparing the two DA oils, the Lloyd is more selective for gasoline and LCO production and less selective for dry gas and coke. The two oils show similar selectivity towards C_3C_4 and decant oil production, i.e. the points on the yield vs. conversion plot form a single line.

A series of four deasphalting experiments were carried out at 120°C by varying the butane/oil ratio from 13/1 v/v to the minimum practical ratio, and the resulting oils were evaluated in the MAT unit. Tables 26 and 27 contain the pertinent data which are summarized below.

	LLOYD C_4 DAO				ATHABASCA C_4 DAO			
Run No.	23	20	22	32	23	20	22	28
S/O Ratio, w/w	7.3	5.1	2.3	0.9	7.0	4.8	2.1	0.5
Yield, wt%	60.8	57.5	55.5	25.9	40.4	39.0	28.5	94.8
Resin, wt%	22.8	21.0	25.4	32.0	27.1	23.0	26.0	36.3
Asphaltene, wt%	0.1	0.1	0.3	5.7	-	0.1	0.1	18.5
CCR, wt%	5.4	6.1	6.35	12.4	7.2	8.3	6.7	24
Gasoline, wt%	43.7	42.5	43.2	41.4	40.1	38.6	41.3	31.7
Coke, wt%	9.2	9.2	12.0	17.6	12.9	11.3	11.2	30.9
Conversion, wt%	72.3	71.7	77.2	76.8	74.1	69.3	74.0	79.4
C/O, w/w	3.9	3.6	4.3	3.9	4.6	3.8	4.0	3.7

When operating in a commercially accepted solvent/oil ratio range (13/1 - 4/1 v/v or 7/1 - 2/1 w/w) the ratio has only a minor effect on product quality and it is difficult to determine any significant changes in the cracking patterns. However below a

2/1 wt. ratio, the S/O ratio significantly affects the quality of the extracted DA oil as the two phase system tends towards a single phase. This is illustrated in Figures 42 and 43 where the gasoline and coke yields are plotted against the S/O ratio. In the case of the 0.5/1 solvent/oil ratio Athabasca DA oil, the properties were closely similar to that of Athabasca VTB.

A series of three deasphalting experiments were carried out to quantify the effect of temperature on oil yield and quality at constant solvent/oil ratio. It is generally accepted that an increase in the deasphalting temperature decreases the oil yield but increases the oil quality.

The pertinent experimental results are presented in Tables 26 and 27 and summarized below.

	Lloyd			Athabasca		
Run No.	37	20	21	37	20	21
Temp., °C	75	120	140	75	120	140
Yield, wt%	64.5	57.5	52.7	47.1	39.0	31.5
Asphaltenes, wt%	0.1	0.1	0.2	0.1	0.1	0.3
Resins, wt%	24.0	21.0	18.8	26.8	23.0	25.8
CCR, wt%	7.2	6.1	4.57	9.4	8.3	6.1
Gasoline, wt%	41.2	42.5	41.7	37.5	38.6	38.1
Coke, wt%	12.2	9.2	9.5	12.9	11.3	10.5
Conversion, wt%	70.5	71.7	71.3	67.7	69.3	68.1
C/O Ratio, w/w	4.2	3.6	4.0	4.1	3.8	3.8

There is a general decrease in yield and decrease in the CCR content as the extraction temperature is increased. The poorer quality DA oils yield more coke when cracked but there is little change in gasoline yield. It is modern practice to deasphalt at temperatures near the critical point in order that the oil and solvent can be separated under supercritical conditions thus making the process energy efficient.

To complete the discussion on butane DA oils, the yields are compared to pilot plant literature data on Arabian DA oils (2).

Comparison of Butane DA Oil Yields

	Light* Arabian	Heavy* Arabian	Lloyd (23)	Athabasca (23)
Dry Gas	4.2	4.6	5.7	7.45
C_3C_4	14.2	9.7	13.7	13.7
Gasoline	47.3	44.4	43.7	40.05
LCO	18.2	20.9	19.0	17.6
DO	7.8	13.1	8.7	8.3
Coke	8.2	7.4	9.2	12.9
Conversion	74	66	72.3	74.1
CCR, wt%	5.6	5.3	5.4	7.2
Resins, wt%	4.3	6.7	22.8	27.1

* J. Bousquet and T. Laboural, O&GJ, April 20, 1988, p. 62

The Arabian oils are better feedstocks containing less resins and metals and yield more gasoline and less coke. One surprising difference between the two types of feedstock is the relationship between resin content and Conradson Carbon Residue. The asphaltic DA oils show much larger resin contents but an almost equivalent CCR.

TABLE 21: MICROACTIVITY TEST RESULTS USING DA-440 EQUILIBRIUM CATALYST AND LLOYDMINSTER BUTANE DA OILS

MAT #	65	64	63	5	4	6	62	61	60	126	127	128	16-R	15	17	135	136	137
Feed	23	23	23	20	20	20	22	22	22	32	32	32	21	21	21	37	37	37
WHSV, hr-1	18.30	19.90	20.40	19.50	21.70	18.90	17.90	18.10	21.00	19.80	20.00	19.10	18.40	19.70	19.40	20.00	18.70	14.10
Cat/Oil	2.19	3.93	5.88	2.05	3.61	6.34	2.23	4.31	5.72	2.02	3.91	6.25	2.17	3.96	6.17	1.99	4.18	8.48
H2	0.03	0.04	0.06	0.03	0.04	0.06	0.03	0.05	0.07	0.03	0.06	0.08	0.03	0.05	0.07	0.02	0.06	0.10
H2S	2.45	2.84	3.11	2.14	2.77	3.03	2.34	3.02	3.28	2.01	2.78	3.09	2.20	2.88	3.05	1.70	2.34	2.03
C1	1.05	1.08	1.51	0.86	1.14	1.44	0.98	1.34	1.73	0.89	1.24	1.33	0.82	1.10	1.44	0.69	1.11	1.52
C2	0.86	0.97	1.24	0.73	1.03	1.29	0.87	1.19	1.53	0.76	1.06	1.34	0.73	1.01	1.39	0.63	0.98	1.29
C2=	0.59	0.80	1.04	0.50	0.81	1.11	0.59	0.92	1.21	0.42	0.74	1.00	0.51	0.80	1.10	0.37	0.66	1.13
TOTAL	4.98	5.73	6.96	4.26	5.79	6.93	4.81	6.52	7.82	4.11	5.88	7.04	4.29	5.84	7.05	3.41	5.15	6.07
C3	1.24	1.63	2.23	1.21	1.70	2.39	1.24	2.06	2.53	0.98	1.54	2.34	1.05	1.65	2.13	0.82	1.35	2.41
C3=	2.75	3.66	4.18	2.47	3.88	4.17	2.80	3.99	4.45	1.81	3.18	3.37	2.51	3.91	4.59	1.89	3.34	3.99
iC4	2.55	3.89	5.05	2.33	3.97	5.26	2.62	4.61	5.50	1.63	3.30	4.61	2.28	4.11	5.26	1.57	3.02	6.28
nC4	0.90	1.20	1.65	0.75	1.22	1.76	0.89	1.52	1.89	0.66	1.12	1.62	0.73	1.21	1.63	0.58	0.95	1.77
C4=	2.70	3.34	3.33	2.29	3.39	2.98	2.71	3.32	3.38	1.75	2.78	2.39	2.49	3.44	3.68	2.04	3.26	2.50
TOTAL C3C4	10.14	13.72	16.44	9.05	14.16	16.56	10.26	15.50	17.75	6.83	11.92	14.33	9.06	14.32	17.29	6.90	11.92	16.95
iC5	3.42	4.71	5.78	2.91	4.48	5.97	3.49	5.53	6.12	1.91	3.86	5.17	2.79	4.64	5.87	1.85	3.32	6.01
nC5	0.39	0.48	0.65	0.37	0.50	0.67	0.39	0.56	0.63	0.39	0.54	0.62	0.37	0.53	0.65	0.41	0.63	0.69
C5=	1.50	2.01	1.18	1.42	1.44	0.84	1.49	0.93	1.24	1.44	2.17	1.73	1.55	1.69	1.41	1.52	2.16	1.38
TOTAL C5	5.31	7.20	7.61	4.70	6.42	7.48	5.37	7.02	7.99	3.74	6.57	7.52	4.71	6.86	7.93	3.78	6.11	8.08
C5-216C	38.13	43.66	41.96	36.12	42.53	42.96	38.07	43.23	40.89	29.06	41.40	39.65	35.79	41.65	40.16	31.82	41.23	40.43
C6-216C	32.82	36.46	34.35	31.42	36.11	35.48	32.70	36.21	32.90	25.32	34.83	32.13	31.08	34.79	32.23	28.04	35.12	32.35
216-343C	21.16	18.98	15.58	20.80	19.01	15.53	20.42	16.66	15.32	17.62	16.40	14.18	21.28	18.92	15.36	19.77	18.73	13.42
343C-EP	18.79	8.69	5.81	23.58	9.31	4.99	19.24	6.12	5.27	28.40	6.83	5.11	23.99	9.81	6.74	27.91	10.80	3.79
Coke	6.80	9.22	13.25	6.19	9.20	13.03	7.20	11.97	12.95	13.98	17.57	19.69	5.59	9.46	13.20	10.19	12.17	19.34
Conv, wt%	60.04	72.33	78.61	55.62	71.68	79.48	60.34	77.23	79.41	53.98	76.76	80.71	54.73	71.27	77.69	52.32	70.46	82.79
Mat Balance	98.00	98.40	98.60	99.59	99.27	97.57	98.21	98.61	96.02	97.32	96.58	98.49	98.82	98.55	98.27	98.36	102.88	101.07

TABLE 22: MICROACTIVITY TEST RESULTS USING DA-440 EQUILIBRIUM CATALYST AND ATHABASCA BUTANE DA OILS

MAT # Feed	71 23	70 23	69 23	8 20	7 20	9 20	68 22	67 22	66 22	132 28	133 28	134 28	13 21	12 21	14 21	141 37	142 37	143 37
WHSV, hr-1	21.30	17.00	21.30	14.10	20.30	17.80	18.10	19.70	20.10	17.10	21.30	16.40	19.00	20.60	19.50	19.50	19.20	19.90
Cat/Oil	2.22	4.61	5.62	2.74	3.84	6.75	2.21	3.98	5.97	2.33	3.67	7.30	2.10	3.79	6.15	2.05	4.07	6.02
H2	0.03	0.05	0.07	0.03	0.05	0.07	0.03	0.05	0.07	0.06	0.09	0.10	0.02	0.05	0.07	0.03	0.05	0.07
H2S	3.19	3.67	4.01	3.00	3.44	3.76	2.88	3.63	3.90	3.06	3.46	4.05	2.56	3.41	3.76	2.14	3.15	3.64
C1	0.70	1.46	1.91	1.01	1.38	1.76	1.17	1.44	1.71	1.38	1.66	1.99	0.86	1.40	1.51	0.86	1.26	1.47
C2	0.65	1.34	1.61	0.97	1.22	1.57	1.04	1.27	1.46	1.19	1.38	1.63	0.84	1.27	1.36	0.80	1.10	1.27
C2=	0.45	0.93	1.15	0.63	0.84	1.14	0.62	0.89	1.10	0.49	0.71	1.00	0.53	0.84	1.08	0.44	0.74	0.92
TOTAL	5.02	7.45	8.75	5.64	6.93	8.30	5.74	7.28	8.24	6.18	7.30	8.77	4.81	6.97	7.78	4.27	6.30	7.37
C3	1.57	1.90	2.42	1.30	1.73	2.34	1.36	1.88	2.33	1.25	1.50	2.43	1.12	1.32	2.25	1.00	1.56	1.97
C3=	2.55	3.66	4.07	2.48	3.42	4.11	2.70	3.90	4.09	2.03	2.49	2.80	2.10	3.65	3.92	1.80	2.95	3.49
iC4	2.12	3.66	4.43	2.27	3.14	4.38	2.21	3.69	4.65	1.48	2.02	3.75	1.86	3.13	4.53	1.32	2.83	3.80
nC4	0.65	1.30	1.61	0.85	1.16	1.65	0.91	1.33	1.66	1.08	1.23	1.88	0.75	1.19	1.61	0.61	1.05	1.36
C4=	1.61	3.14	3.22	2.19	3.03	3.01	2.63	3.52	3.14	2.07	2.21	1.84	2.02	3.25	2.94	1.66	2.56	2.73
TOTAL C3C4	8.50	13.66	15.75	9.09	12.48	15.69	9.81	14.32	15.87	7.91	9.45	12.70	7.85	12.54	15.25	6.39	10.95	13.35
iC5	2.67	4.27	4.80	2.71	3.48	5.10	2.93	4.40	5.32	1.74	2.21	4.09	2.30	3.68	5.03	1.55	3.18	4.34
nC5	0.34	0.55	0.65	0.44	0.56	0.69	0.41	0.56	0.68	0.46	0.53	0.73	0.36	0.54	0.73	0.36	0.55	0.60
C5=	1.14	1.79	2.05	1.34	1.60	1.08	1.52	1.71	1.24	1.70	1.90	1.03	1.31	1.66	1.01	1.46	1.68	1.69
TOTAL C5	4.15	6.61	7.50	4.49	5.64	6.87	4.86	6.67	7.24	3.90	4.64	5.85	3.97	5.88	6.77	3.37	5.41	6.63
C5-216C	31.72	40.05	38.25	33.14	38.60	37.08	33.64	41.26	39.70	29.54	31.66	29.05	30.03	38.09	38.36	27.08	37.53	40.04
C6-216C	27.57	33.44	30.75	28.65	32.96	30.21	28.78	34.59	32.46	25.64	27.02	23.20	26.06	32.21	31.59	23.71	32.12	33.41
216-343C	20.03	17.64	15.34	19.95	19.39	16.37	19.44	17.97	15.59	16.02	14.08	10.73	19.51	19.34	16.29	18.09	18.44	16.12
343C-EP	27.25	8.26	7.08	23.92	11.31	6.36	23.72	8.00	6.02	12.15	6.58	3.33	31.43	12.55	8.58	33.32	13.88	5.55
Coke	7.48	12.94	14.83	8.26	11.29	16.20	7.65	11.17	14.58	28.20	30.93	35.42	6.37	10.51	13.74	10.85	12.90	17.57
Conv, wt%	52.72	74.10	77.58	56.13	69.30	77.27	56.84	74.03	78.40	71.83	79.35	85.95	49.06	68.11	75.13	48.59	67.68	70.33
Mat Balance	98.92	99.45	97.59	98.77	99.97	97.72	97.22	97.92	98.66	86.22	82.27	83.78	99.81	98.34	97.57	98.97	101.80	101.61

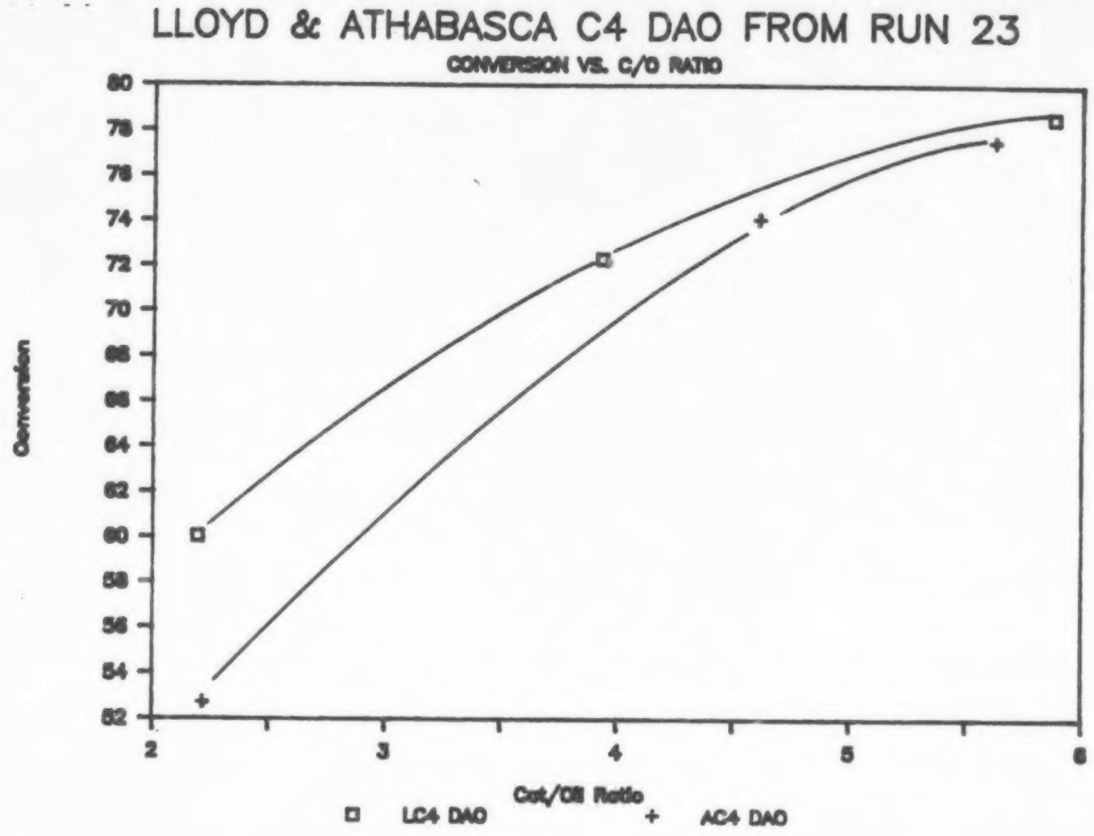
LLOYD & ATHABASCA C4 DAO FROM RUN 23
CONVERSION VS. C/O RATIO
80
78
76
74
72
70
68
66
64
62
60
58
56
54
52
Conversion
2
3
4
5
6
Cat/Oil Ratio
LC4 DAO
AC4 DAO

Figure 35

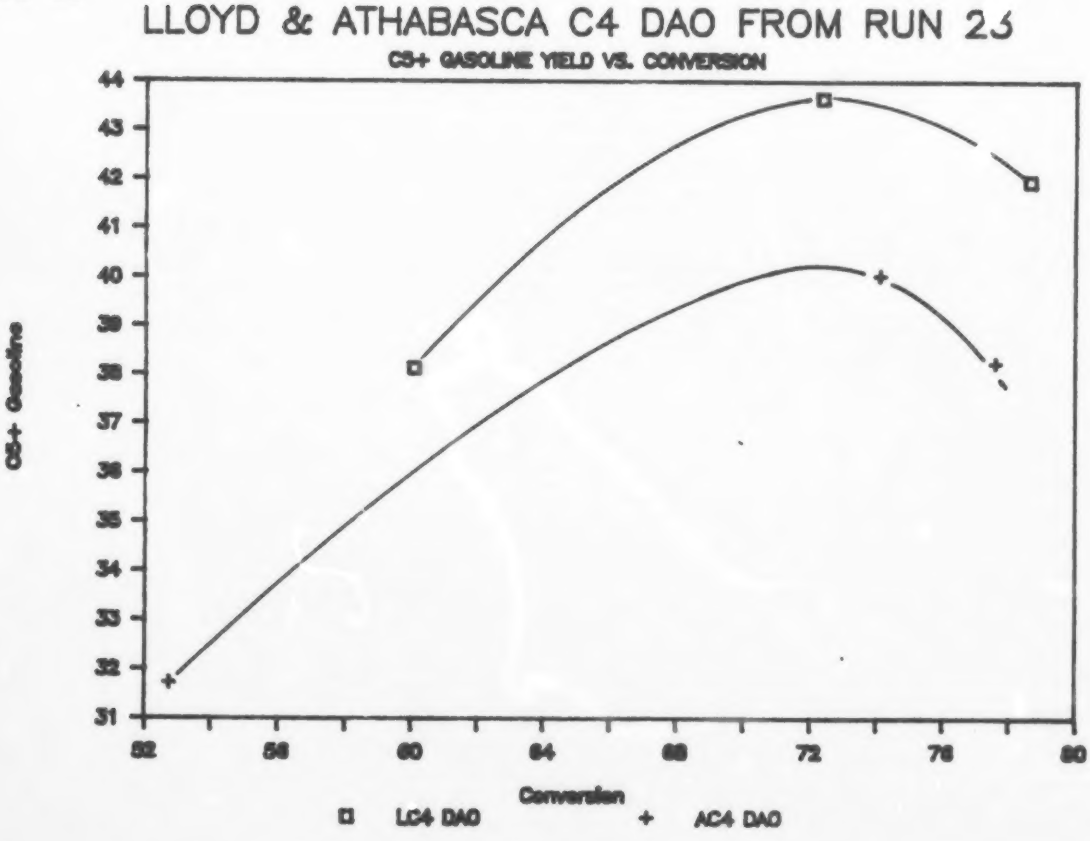
LLOYD & ATHABASCA C4 DAO FROM RUN 23
C5+ GASOLINE YIELD VS. CONVERSION
44
43
42
41
40
39
38
37
36
35
34
33
32
31
C5+ Gasoline
52
56
60
64
68
72
76
80
Conversion
LC4 DAO
AC4 DAO

Figure 36

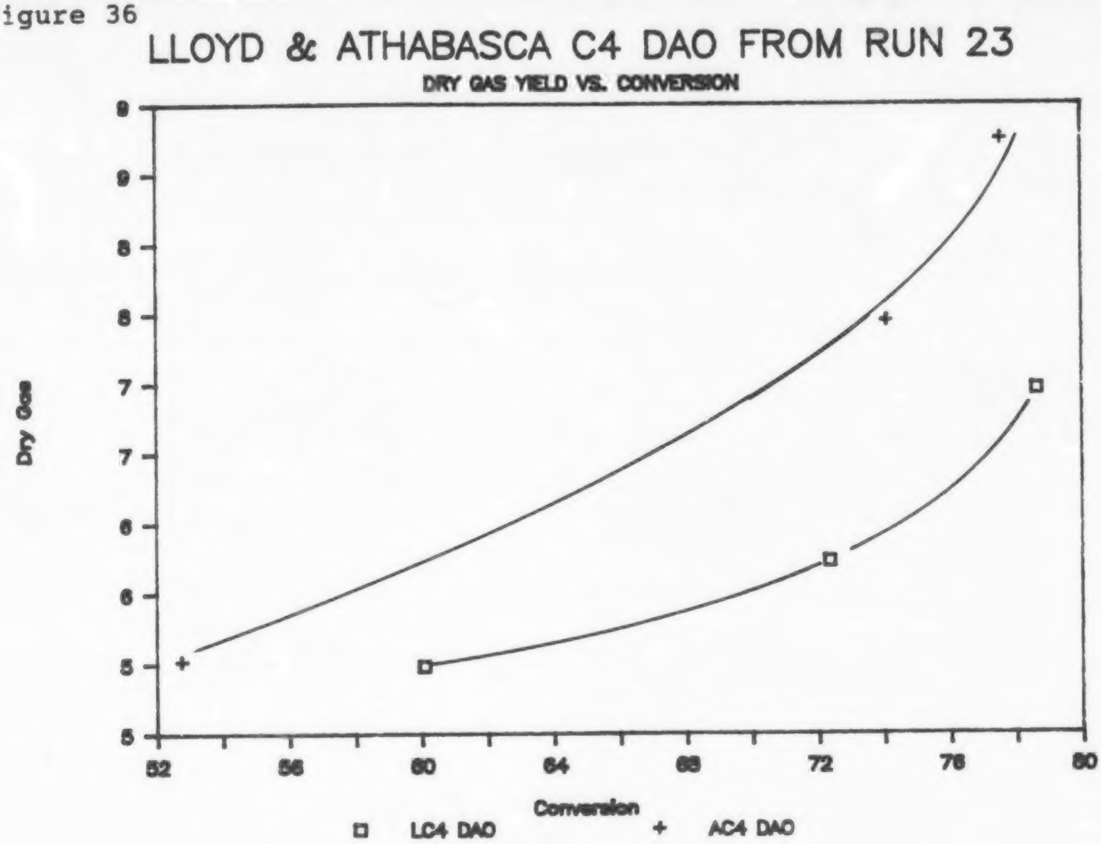

Figure 37

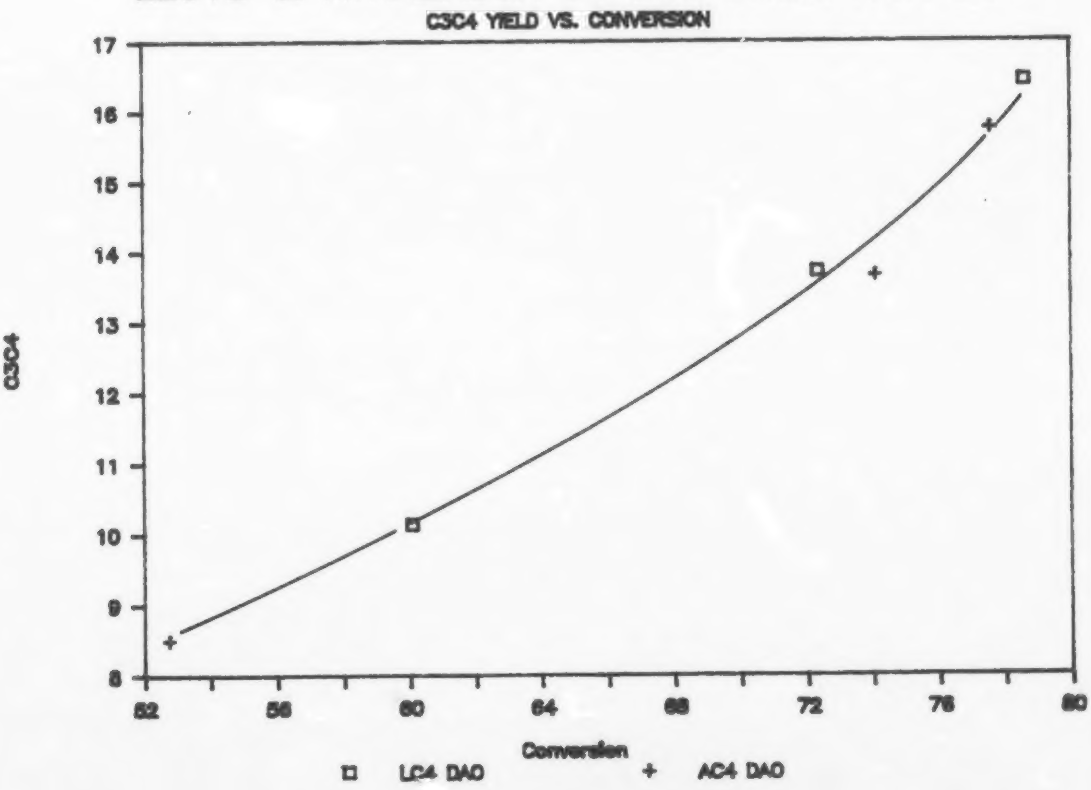

Figure 38

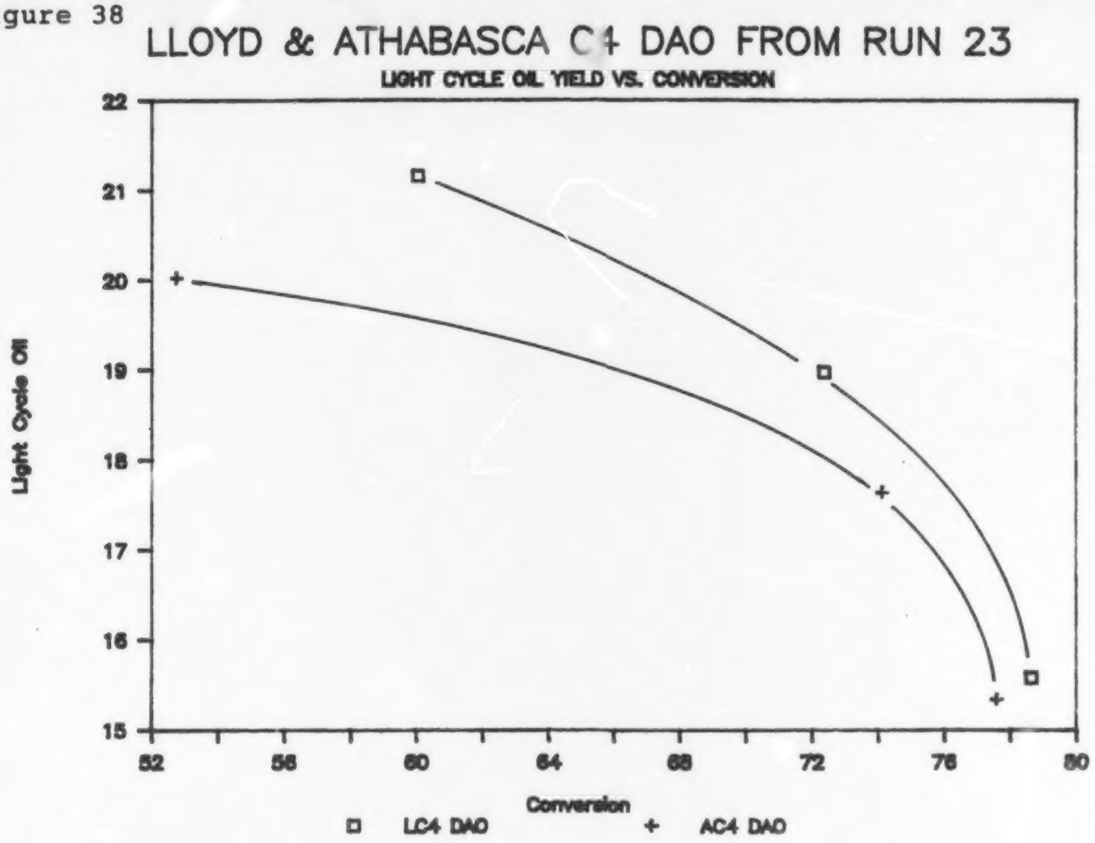

Figure 39

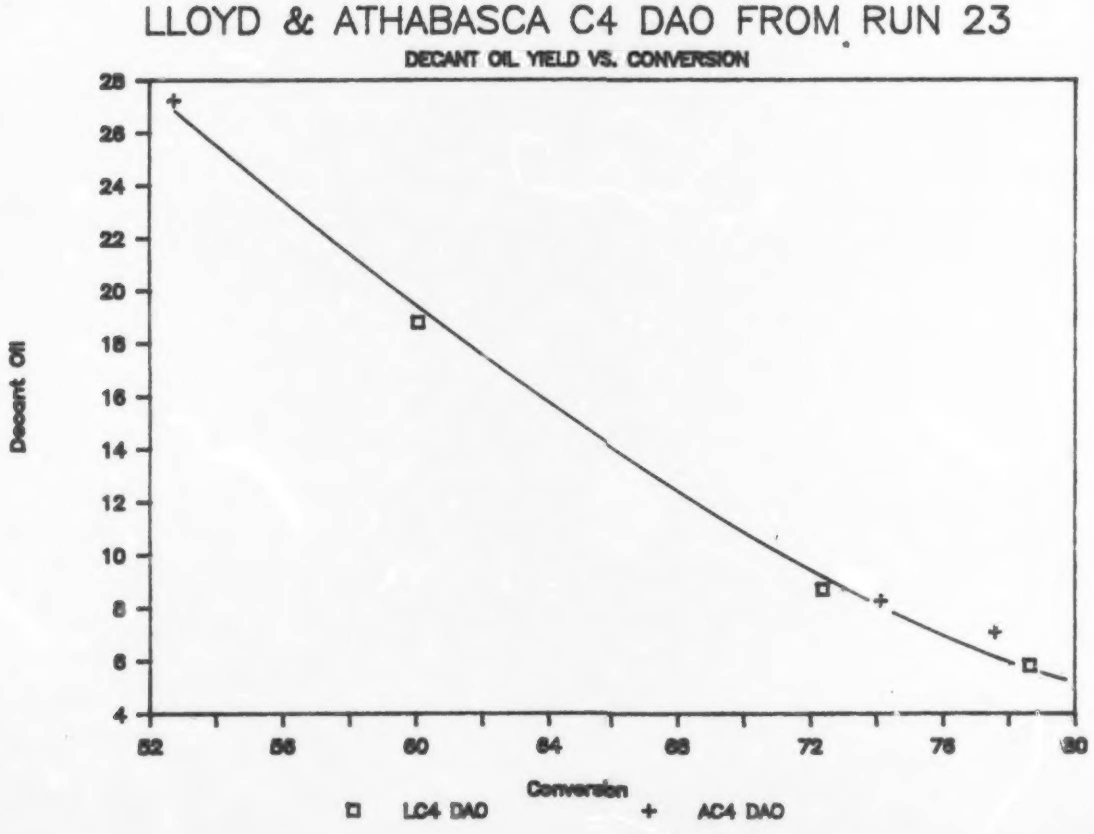

Figure 40

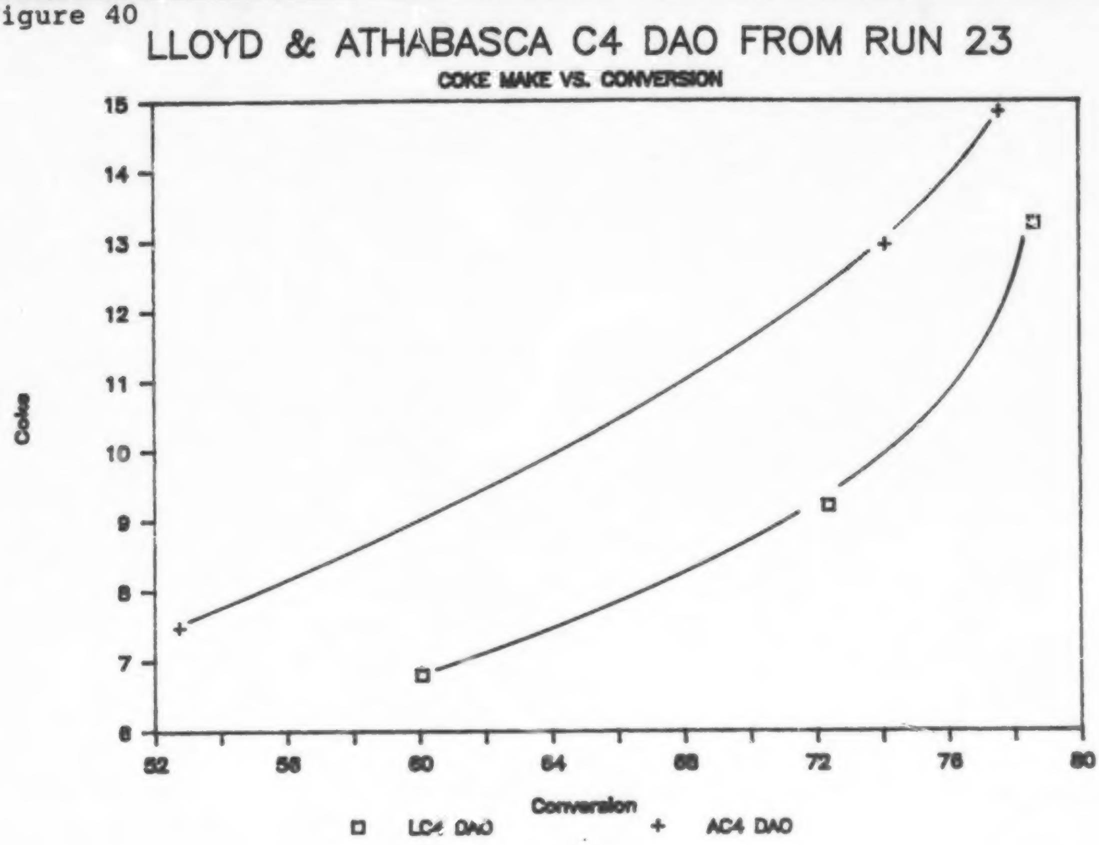

Figure 41

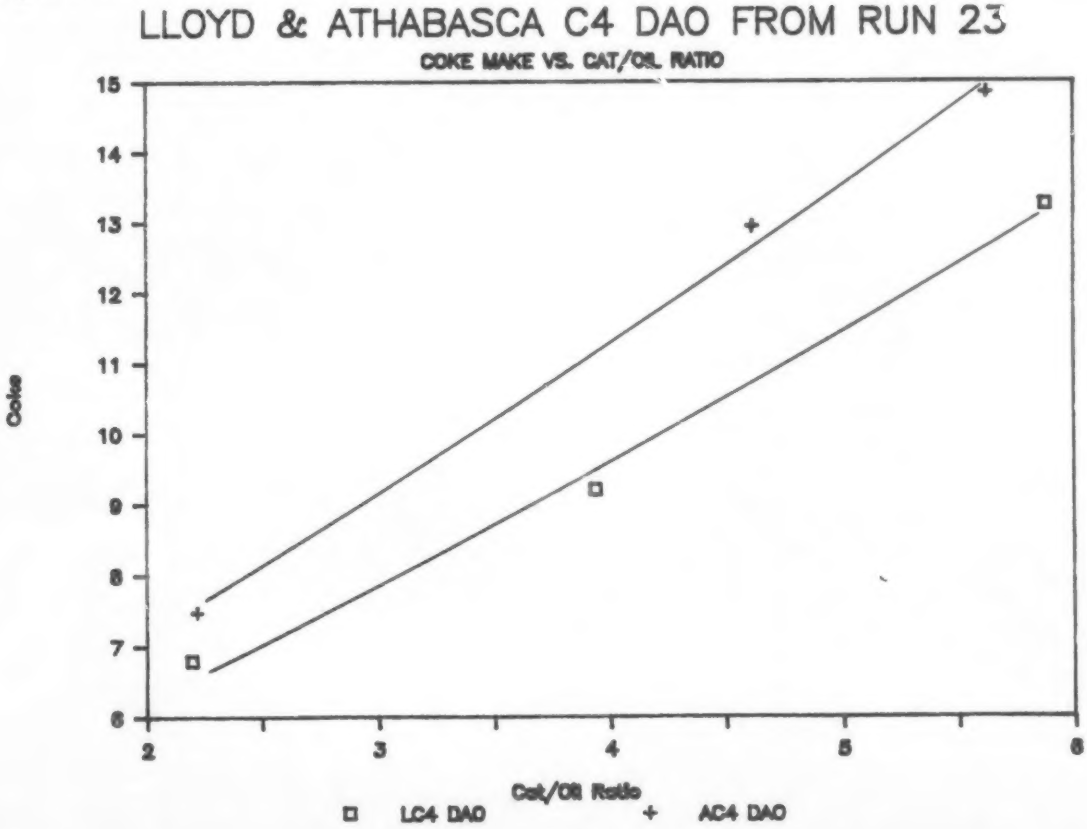

Figure 42

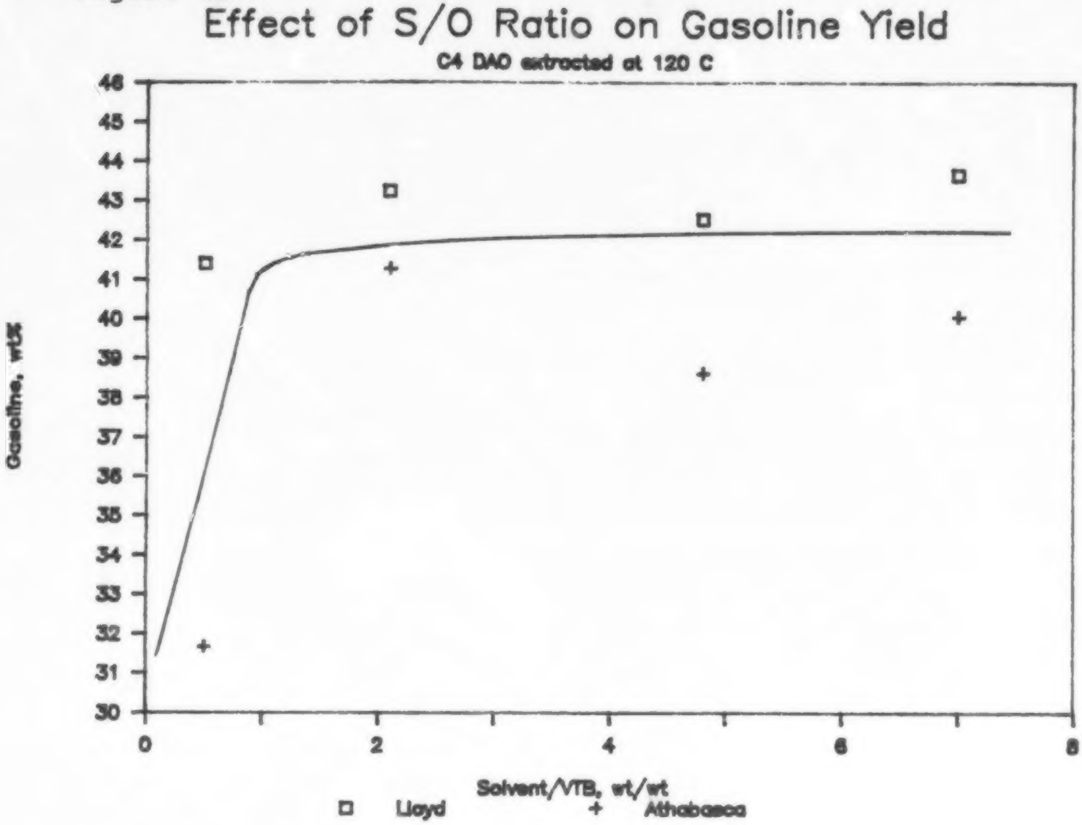
Effect of S/O Ratio on Gasoline Yield

C4 DAO extracted at 120 C

Figure 43

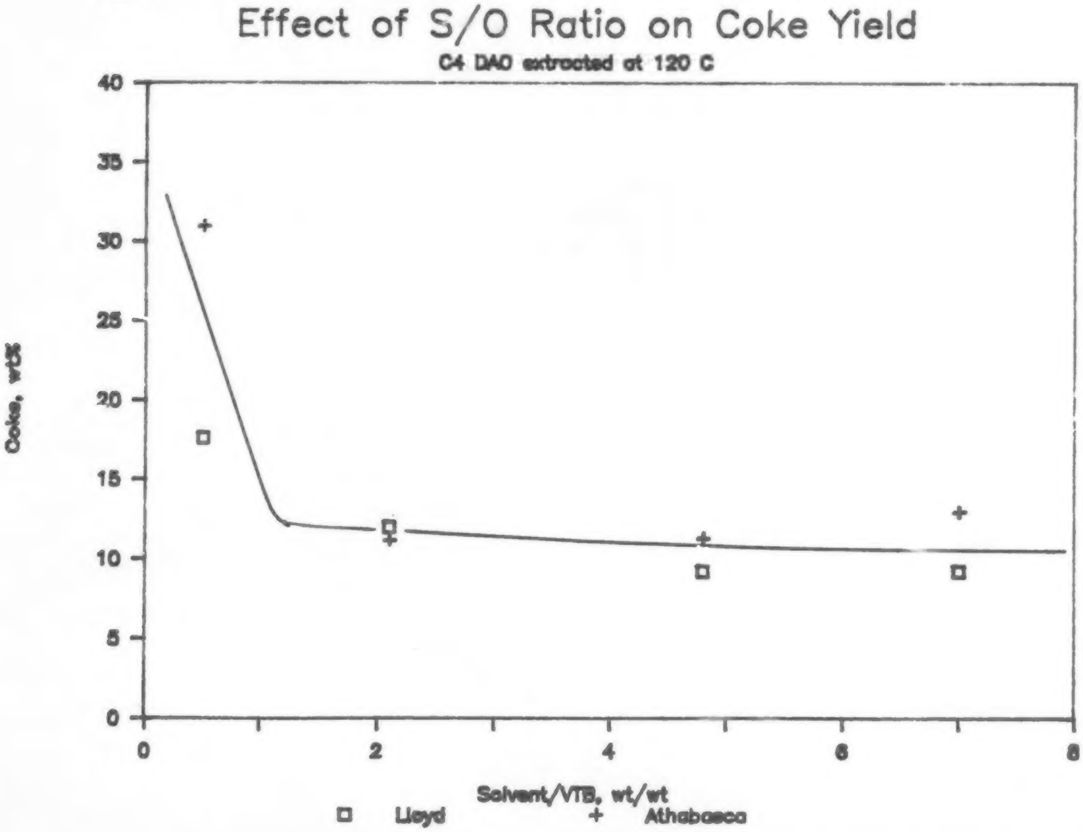
Effect of S/O Ratio on Coke Yield

C4 DAO extracted at 120 C

13. Cracking Characteristics of the Pentane DA Oils

MAT runs were carried out for five Athabasca and four Lloyd pentane DA oils. The yield data is given in Tables 23 and 24 while a summary of the properties of the DAO oils along with their cracking yield profile at a C/O of 4 are presented in Tables 26 and 27. Because of the high resin content, these DA oils were experimentally quite difficult to test in the MAT unit. At times it was impossible to obtain good material balances by standard procedures because of the build-up of carbon deposits in the reactor. For all these runs, the coke make was estimated as the difference in the material balance.

These oils still show similar trends to those noted for the propane and butane DA oils, but the higher resin content increases the average coke make and decreases the gasoline yields. The severity and selectivity plots for a typical pentane DA oil (DA test 10, 140°C S/O 5.2 w/w) are presented in Figures 44 to 51. The dry gas, coke and C_3C_4 yields increase with conversion while the LCO and DO yields decrease with conversion. The gasoline shows signs of overcracking at higher conversions as the gasoline yield peaks at a C/O ratio of 4.

For a given conversion, the Lloyd DA oil produces more gasoline and less dry gas and coke. There is little difference in the selectivity to C_3C_4, LCO and decant oil production for the two DA oils. Both DA oils give similar conversion at an equivalent severity (C/O ratio).

A series of experiments were carried out at 160°C to determine the effect of S/O ratio one DA oil yield and quality. The resulting oils were tested in the MAT unit at three C/O ratios (see Tables 23 and 24). The results from the DA experiments and the MAT runs carried out at a C/O of 4 are given in Tables 26 and 27 are summarized below.

	Lloyd C_5 DAO		Athabasca C_5 DAO		
Run No.	19	24	39	19	24
S/O Ratio, w/w	5.5	1.0	6.8	5.2	1.0
Yield, wt%	71.9	91.8	59.3	58.8	65.3
Resin, wt%	22.6	32.2	35.9	32.3	38.9
Asphaltene, wt%	0.1	9.6	0.1	0.2	7.4
CCR, wt%	9.2	16.6	12.1	12.8	19.9
Gasoline, wt%	39.2	38.4	37.9	35.5	36.2
Coke, wt%	15.8	21.9	16.6	19.4	24.8
Conversion, wt%	72.6	77.9	72.4	71.7	78.9
C/O, w/w	3.8	4.1	4.3	3.8	4.3

As the solvent/oil ratio decreases, there is a large increase in the resin and asphaltene content of the DAO. This leads to a significant increase in coke make and conversion. However there is no significant variation in the gasoline yield. This is illustrated in Figures 52 and 53.

A set of three experiments were carried out for both Lloyd and Athabasca VTBs, to determine the effect of deasphalting temperature (75, 140 and 160°C) on product yield and quality at a constant solvent/oil ratio. Each of the six pentane DA oils was cracked at three C/O ratios and the results are reported in Tables 23 and 24. Results from the DA experiments along with yield data from the MAT testing at a C/O ratio of 4 are given in Tables 26 and 27. These data are summarized below.

	Lloyd C_5 DAO			Athabasca C_5 DAO		
Run No.	38	10	19	38	10	19
Temp., °C	75	140	160	75	140	160
Yield, wt%	77.0	75.1	71.9	66.0	59.5	58.8
Asphaltenes, wt%	0.1	0.2	0.1	0.1	-	0.2
Resins, wt%	31.2	32.2	22.6	40.3	41.1	32.3
CCR, wt%	10.7	9.4	9.2	14.3	12.4	12.8
Gasoline, wt%	41.5	39.6	39.2	36.3	36.8	35.5
Coke, wt%	15.4	16.7	15.8	19.6	18.1	19.4
Conversion, wt%	74.3	75.7	72.6	77.7	77.3	71.7
C/O Ratio, w/w	3.9	4.1	3.8	4.3	4.3	3.8

Over this operating temperature range there is a small change in the DA oil yield and quality in the expected direction, i.e. yield decreases and quality increases as the deasphalting temperature increases. However, these quality changes are not large enough for the MAT yield profiles to show any significant trends.

TABLE 23: MICROACTIVITY TEST RESULTS USING DA-440 EQUILIBRIUM CATALYST AND LLOYDMINSTER PENTANE DA OILS

MAT #	19	18	20	123	124	125	74	73	72	138	139	140
Feed	19	19	19	24	24	24	10	10	10	38	38	38
WHSV, hr-1	18.70	20.60	20.00	17.00	19.20	19.40	18.60	19.20	22.30	19.60	19.80	18.80
Cat/Oil	2.13	3.81	6.00	2.35	4.07	6.17	2.16	4.09	5.37	2.04	3.94	6.36
H2	0.03	0.05	0.06	0.05	0.06	0.07	0.03	0.05	0.07	0.02	0.05	0.07
H2S	2.22	2.73	2.99	2.40	2.76	3.09	2.16	2.96	3.18	1.89	2.67	2.90
C1	0.94	1.18	1.46	1.22	1.35	1.54	0.98	1.35	1.60	0.82	1.16	1.49
C2	0.83	1.05	1.29	1.02	1.18	1.26	0.83	1.15	1.38	0.71	0.99	1.32
C2=	0.49	0.72	1.00	0.52	0.77	0.90	0.48	0.82	0.98	0.40	0.67	1.02
TOTAL	4.51	5.73	6.80	5.21	6.12	6.86	4.48	6.33	7.21	3.84	5.54	6.80
C3	1.06	1.45	1.53	1.17	1.64	2.21	1.33	1.79	2.09	0.94	1.58	2.14
C3=	2.26	3.30	3.77	2.27	2.97	2.99	2.29	3.45	3.41	1.81	3.27	3.46
iC4	1.97	3.13	4.59	1.90	3.22	4.20	2.14	3.68	4.06	1.64	3.36	4.42
nC4	0.76	1.05	1.56	0.79	1.13	1.51	0.80	1.25	1.43	0.63	1.09	1.53
C4=	2.17	2.88	2.73	2.23	2.49	2.07	2.22	2.96	2.62	1.75	2.60	2.62
TOTAL C3C4	8.22	11.81	14.18	8.36	11.45	12.98	8.78	13.13	13.61	6.77	11.90	14.17
iC5	2.63	3.77	5.07	2.29	3.57	4.60	2.88	4.43	4.68	1.98	3.63	5.06
nC5	0.39	0.49	0.68	0.51	0.59	0.61	0.36	0.58	0.63	0.43	0.59	0.73
C5=	1.49	1.54	0.75	1.90	1.76	1.50	1.36	1.24	1.01	1.68	2.33	1.66
TOTAL C5	4.51	5.80	6.50	4.70	5.92	6.71	4.60	6.25	6.32	4.09	6.55	7.45
C5-216C	34.80	39.22	39.46	34.02	38.40	35.80	35.19	39.60	37.32	30.37	41.49	40.80
C6-216C	30.29	33.42	32.96	29.32	32.48	29.09	30.59	33.35	31.00	26.28	34.94	33.35
216-343C	20.45	17.86	14.90	17.61	15.25	13.17	20.10	16.64	14.52	18.14	17.55	15.14
343C-EP	20.74	9.56	5.63	14.06	6.88	4.86	19.11	7.61	6.17	29.02	8.12	5.15
Coke	11.28	15.82	19.03	20.74	21.90	26.33	12.34	16.69	21.17	11.86	15.40	17.94
Conv, wt%	58.81	72.58	79.46	68.32	77.87	81.97	60.80	75.74	79.31	52.83	74.33	79.71
Mat Balance	98.24	98.12	100.18	93.02	96.64	97.35	99.30	98.72	96.52	98.81	103.01	102.48

TABLE 24: MICROACTIVITY TEST RESULTS USING DA-440 EQUILIBRIUM CATALYST AND ATHABASCA PENTANE DA OILS

MAT #	22-R	21	23	129	130	131	144	145	146	77	76	75	147	148	149
Feed	19	19	19	24	24	24	39	39	39	10	10	10	38	38	38
WHSV, hr-1	18.10	20.50	19.70	13.80	18.10	22.50	17.80	18.00	22.00	18.60	18.10	20.10	19.50	16.90	16.80
Cat/Oil	2.21	3.82	6.09	2.90	4.34	5.31	2.24	4.34	5.43	2.15	4.33	5.96	2.04	4.64	7.14
H2	0.03	0.04	0.06	0.05	0.06	0.09	0.03	0.05	0.07	0.03	0.05	0.07	0.02	0.07	0.08
H2S	2.88	3.21	3.97	2.67	3.59	3.59	1.98	3.46	3.80	2.77	3.65	3.72	2.25	3.66	3.98
C1	1.17	1.48	2.10	1.24	1.55	1.82	1.05	1.50	1.68	1.28	1.72	1.97	0.99	1.58	1.93
C2	1.04	1.31	1.53	1.04	1.33	1.48	0.96	1.19	1.49	1.08	1.41	1.57	0.88	1.39	1.66
C2=	0.54	0.77	0.99	0.47	0.75	0.84	0.48	0.74	0.95	0.55	0.89	0.99	0.41	0.84	1.07
TOTAL	5.66	6.81	8.65	5.47	7.28	7.82	4.50	6.94	7.99	5.71	7.72	8.32	4.55	7.54	8.72
C3	1.18	1.24	2.12	1.11	1.64	1.83	1.11	1.61	2.08	1.26	1.83	2.18	0.96	2.06	2.59
C3=	2.06	2.86	3.50	1.95	2.79	3.00	1.76	2.91	3.33	1.96	3.25	3.23	1.46	3.51	3.00
iC4	1.61	2.30	3.65	1.37	2.66	2.95	1.96	2.73	3.56	1.57	3.02	3.58	1.15	3.43	4.14
nC4	0.78	0.91	1.41	0.70	1.10	1.17	0.69	1.10	1.36	0.71	1.23	1.40	0.60	1.23	1.68
C4=	2.03	2.61	2.64	2.03	2.48	2.39	1.78	2.57	2.69	2.42	2.69	2.36	1.49	2.50	1.94
TOTAL C3C4	7.66	9.92	13.32	7.16	10.67	11.34	7.30	10.92	13.02	7.92	12.02	12.75	5.66	12.73	13.35
iC5	2.19	2.84	4.18	1.63	3.07	3.31	1.66	3.06	4.00	2.20	3.56	3.98	1.53	3.46	4.43
nC5	0.45	0.53	0.69	0.57	0.64	0.65	0.43	0.87	0.66	0.33	0.57	0.60	0.55	0.61	0.67
C5=	1.51	1.44	1.27	2.43	2.45	1.50	1.52	3.37	1.96	1.15	1.55	1.02	1.97	1.16	1.24
TOTAL C5	4.15	4.81	6.14	4.63	6.16	5.46	3.61	7.30	6.62	3.68	5.68	5.60	4.05	5.23	6.34
C5-216C	30.80	35.52	35.42	30.02	36.22	33.88	27.21	37.92	38.45	29.60	36.83	35.84	26.53	36.34	34.84
C6-216C	26.65	30.71	29.28	25.39	30.06	28.42	23.60	30.62	31.83	25.92	31.15	30.24	22.48	31.11	28.50
216-343C	19.22	17.87	14.24	16.86	14.82	13.72	17.44	16.94	16.02	19.32	13.70	15.12	17.00	15.78	13.27
343C-EP	23.62	10.46	6.67	15.26	6.25	5.36	30.11	10.65	6.41	22.34	7.04	5.80	31.59	6.53	4.12
Coke	13.04	19.42	21.70	25.23	24.76	27.88	13.44	16.63	18.11	15.11	20.69	22.17	14.67	21.08	25.70
Conv, wt%	57.16	71.67	79.10	67.88	78.93	80.91	52.45	72.41	77.58	58.34	77.26	79.08	51.41	77.70	82.61
Mat Balance	98.09	95.15	97.64	91.76	91.61	91.52	99.10	101.43	102.89	99.90	98.94	97.77	98.49	99.88	101.71

Figure 44

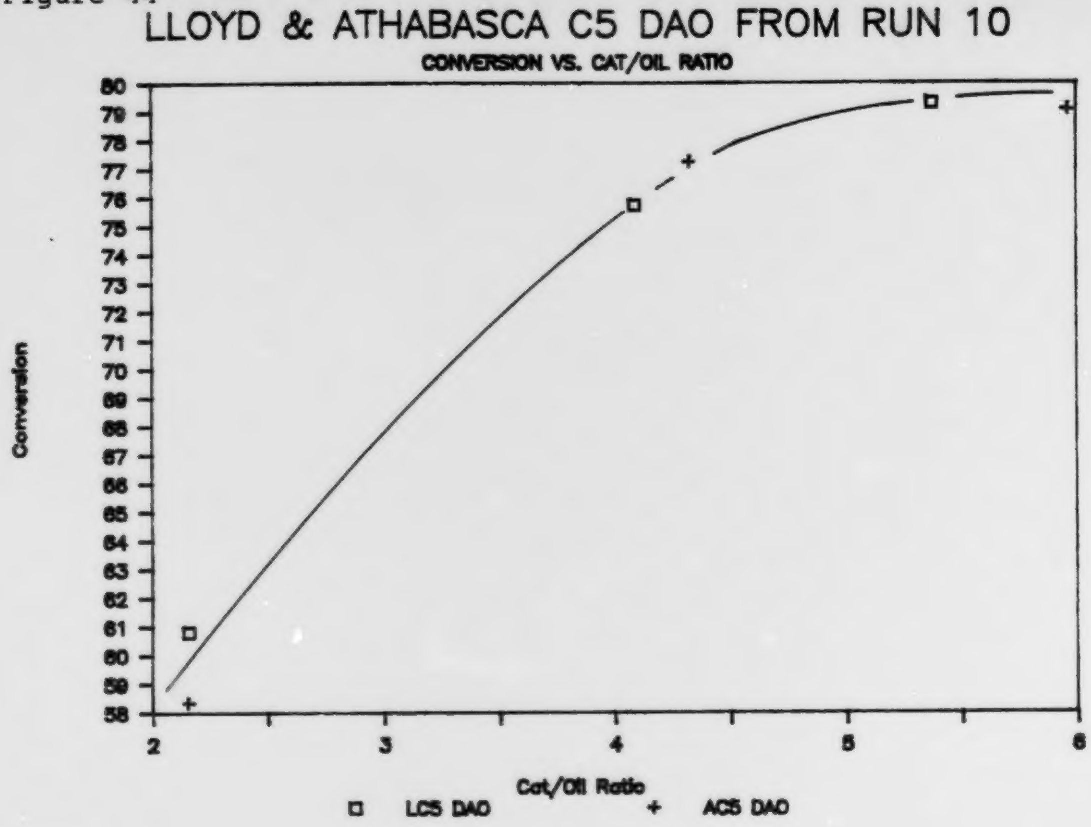

Figure 45

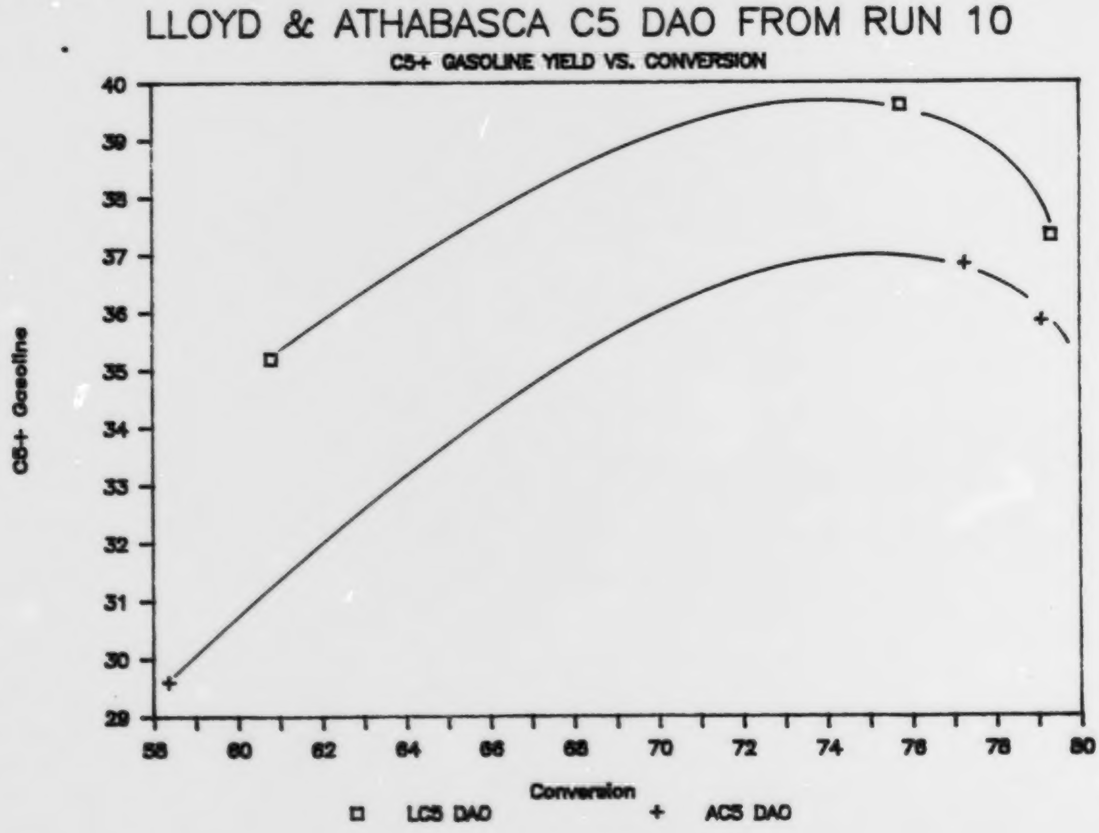

Figure 46

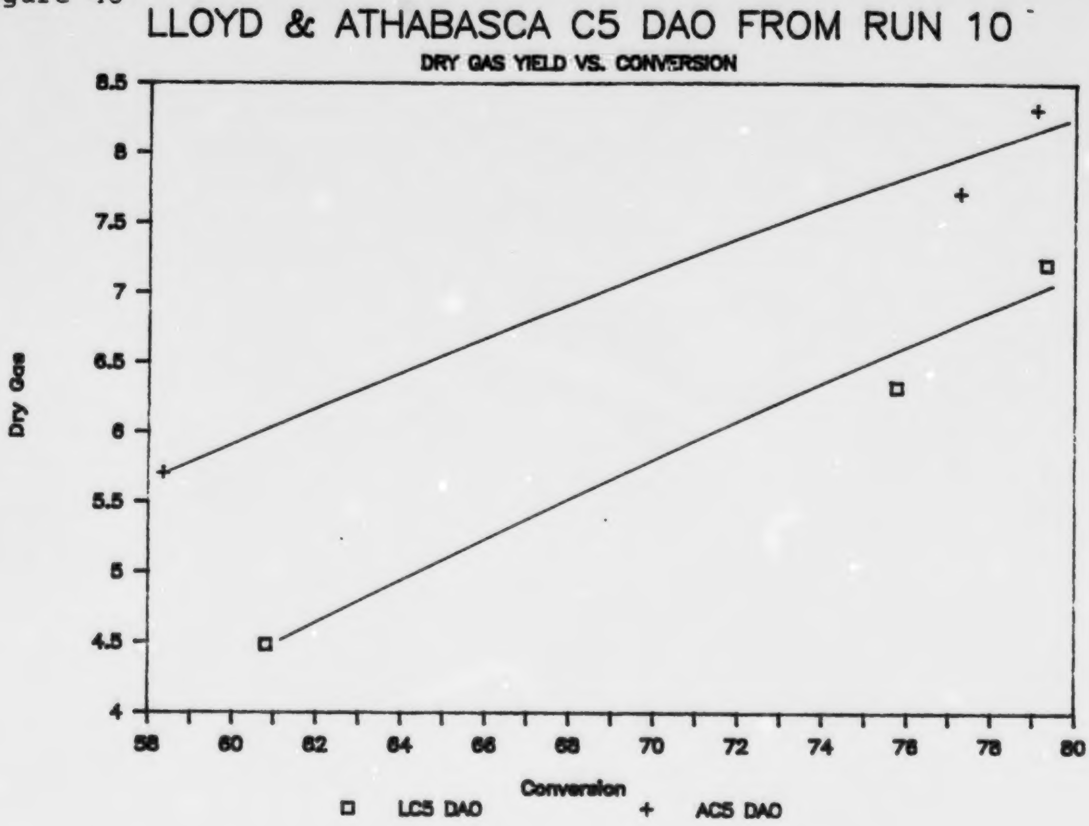

Figure 47

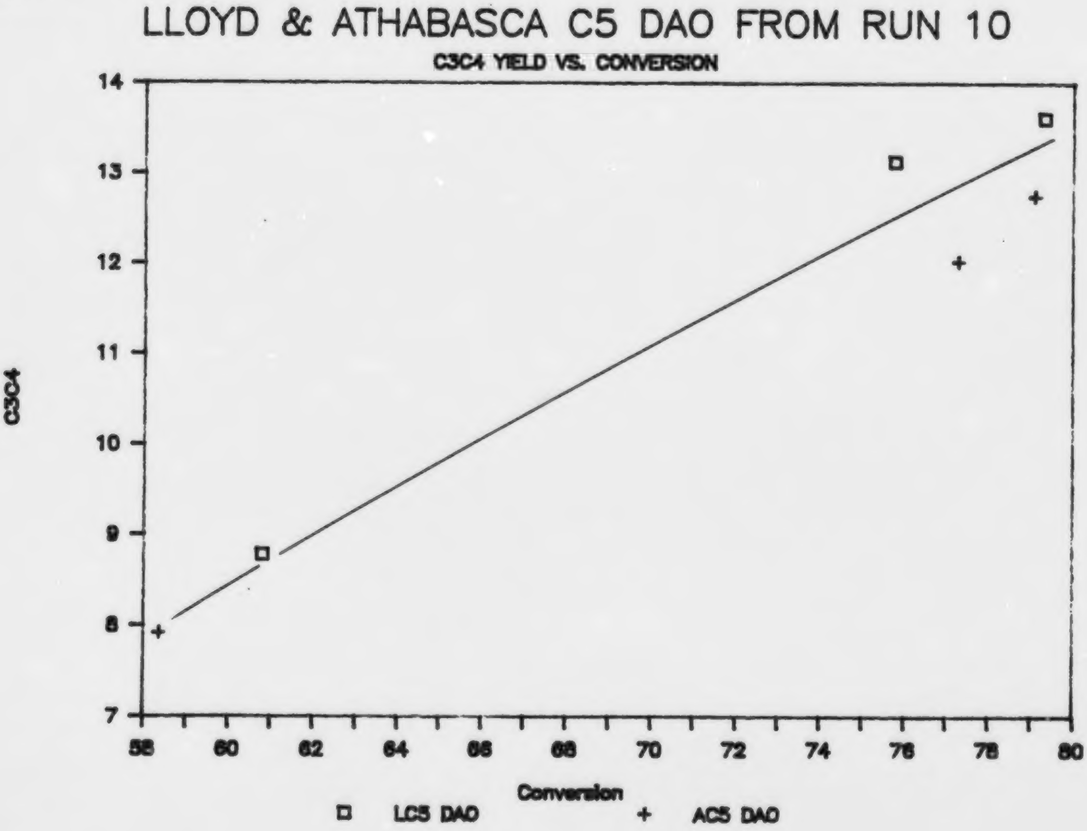

Figure 48

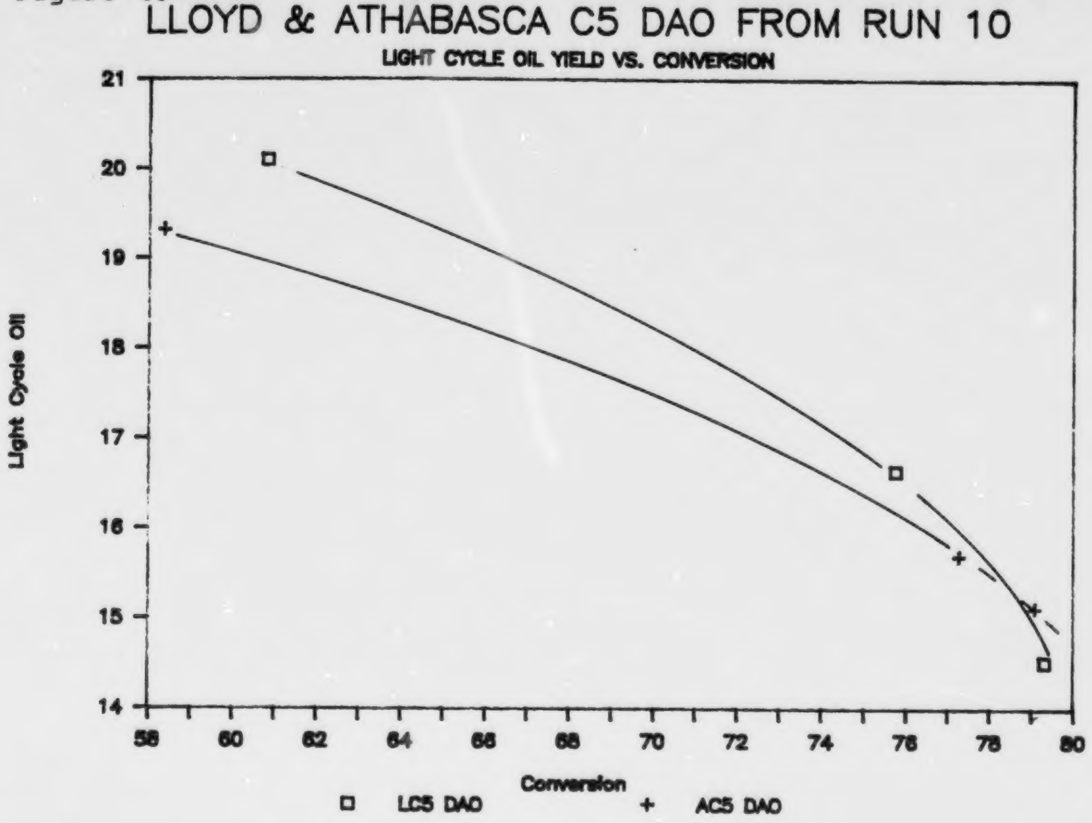

LLOYD & ATHABASCA C5 DAO FROM RUN 10

LIGHT CYCLE OIL YIELD VS. CONVERSION

Figure 49

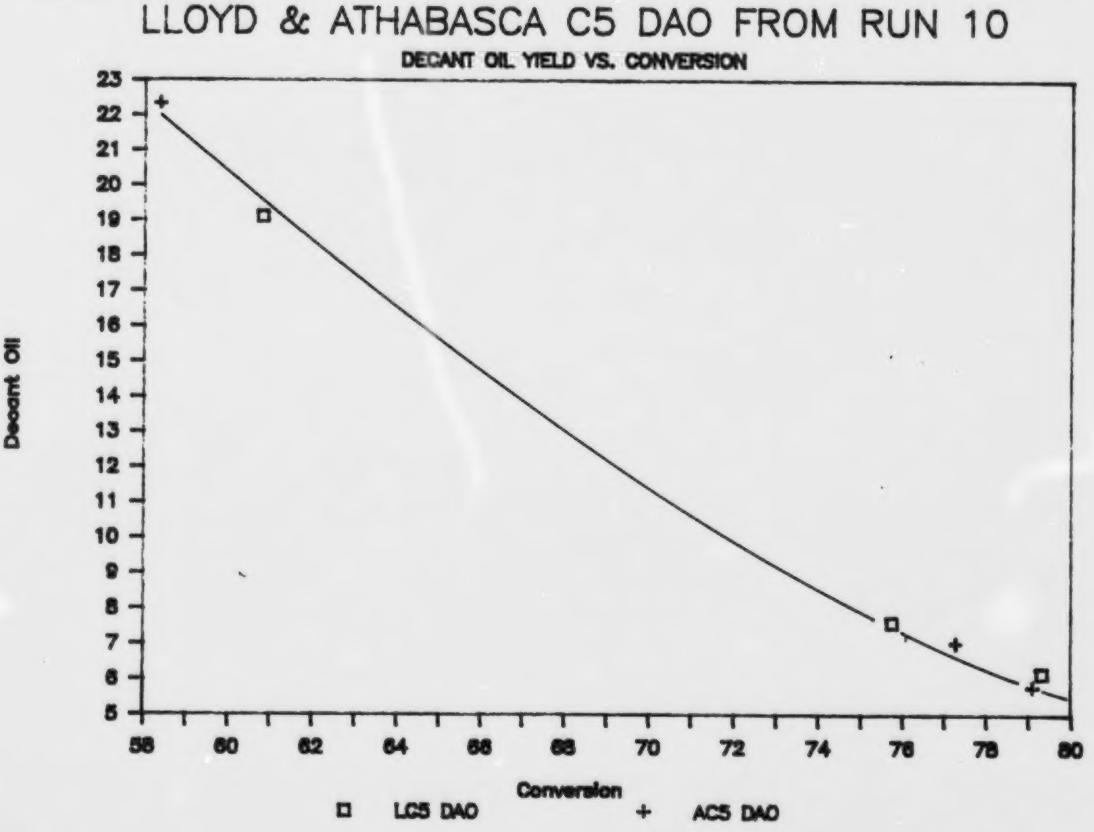

LLOYD & ATHABASCA C5 DAO FROM RUN 10

DECANT OIL YIELD VS. CONVERSION

Figure 50

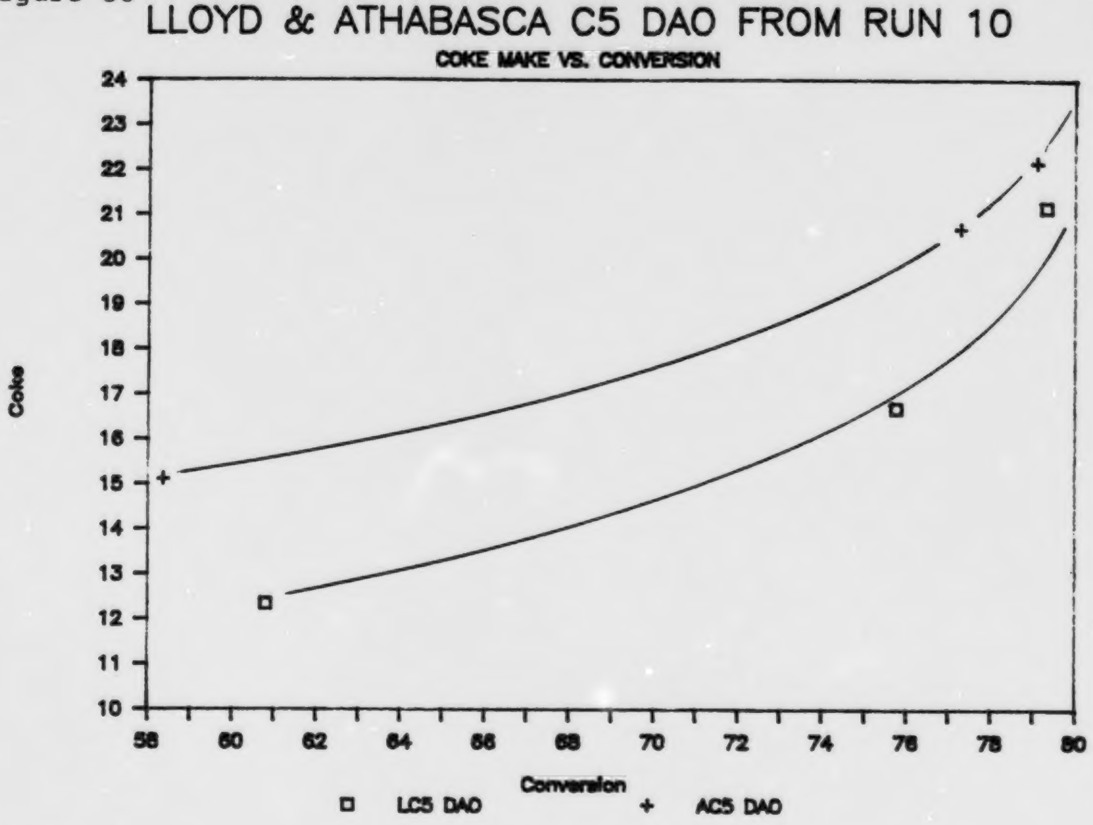

Figure 51

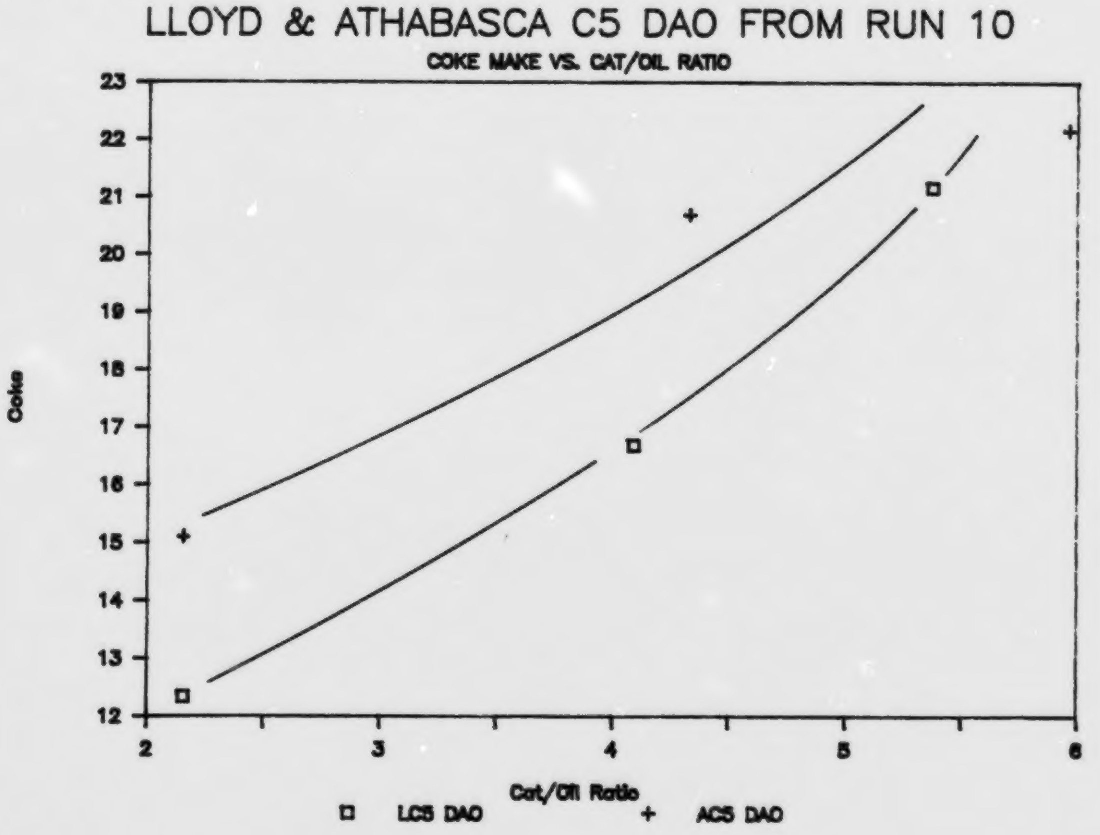

Figure 52

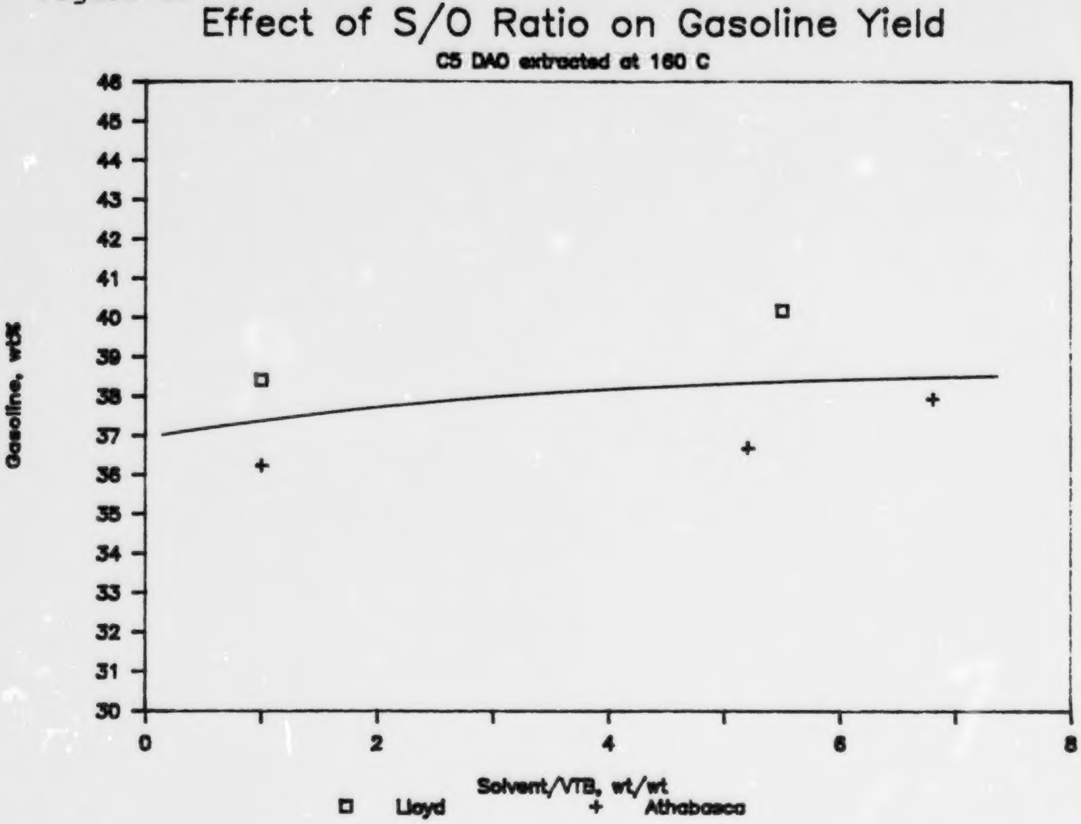

Figure 53

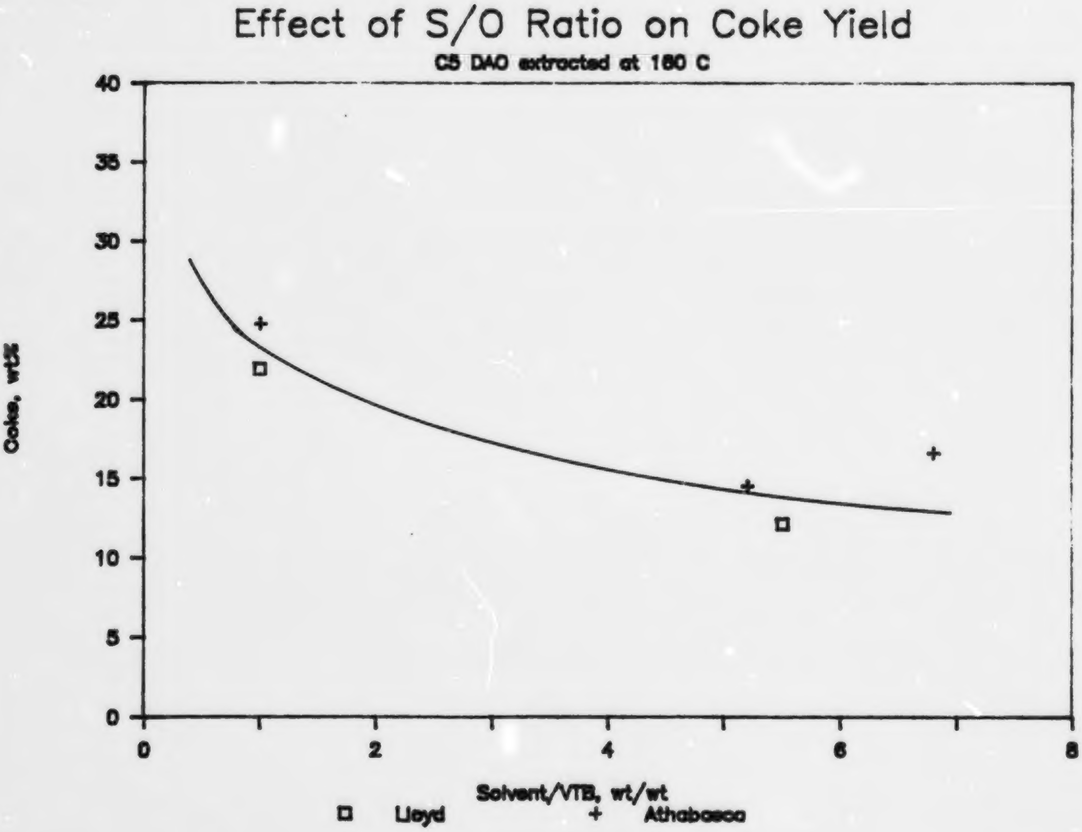

14. Cracking Characteristics of the Heptane DA Oils

The MAT experiments carried out using six heptane DA oils (3 Athabasca, 3 Lloyd) are reported in Table 25. All the heptane DA oils contained asphaltenes as well as large amounts of resins. These highly asphaltic oils required heating to 130°C in order to inject them into the MAT unit and produced large amounts of coke when cracked. These experimental difficulties increase the uncertainty in interpreting the experimental results.

Three deasphalting experiments were carried out to quantify the effect of temperature and solvent/oil ratio on DA oil yields and quality. Each oil was then cracked in the MAT unit at three C/O ratios. The MAT results are presented in Table 25 and the results from the deasphalting experiments, along with the MAT yields for a C/O of 4 are given in Tables 26 and 27. These results are summarized below.

	Lloyd C_7 DAO			Athabasca C_7 DAO		
Run No.	14	31	15	14	40	15
Temp., °C	75	75	180	75	75	180
S/O Ratio, w/w	11.7	3.0	8.1	11.1	7.7	7.7
Yield, wt%	82.7	87.8	87.5	80.3	80.5	82.2
Asphaltenes, wt%	1.4	7.5	2.1	3.3	5.5	2.5
Resins, wt%	35.4	30.7	34.4	46.2	43.2	49.9
CCR, wt%	12.8	14.9	13.3	18.4	19.4	18.3
Gasoline, wt%	38.1	36.4	36.1	32.8	34.2	30.6
Coke, wt%	20.5	21.7	22.3	26.4	25.2	29.7
Conversion, wt%	77.7	75.7	78.0	77.9	77.1	81.3
C/O Ratio, w/w	3.9	3.9	4.1	4.4	4.5	4.7

Over the range of deasphalting conditions studied, the changing of temperatures from 75 to 180°C and solvent/oil ratio from 11.7 to 3 w/w did not greatly change the oil yield and quality. Thus the MAT yield profiles did not show any significant variations.

To finalize this part of the discussion, the severity and selectivity plots obtained when cracking Lloyd and Athabasca DA oil from experiment 14 (extracted at 75°C at a S/O ratio of 11.1 w/w) are presented in Figures 54 to 61.

When compared to the pentane DA oils heptane extracts yield more coke and dry gas, less gasoline and liquids and are more easy to convert. Unfortunately the additional conversion is yielded as coke.

For a given conversion, the Lloyd DA oil again produces more gasoline, less coke and dry gas, and equivalent amounts of C_3C_4 and decant oil. Both DA oils give the same conversion at an equivalent severity.

TABLE 25: MICROACTIVITY TEST RESULTS USING DA-440 EQUILIBRIUM CATALYST AND HEPTANE DA OILS

	LLOYDMINSTER									ATHABASCA								
MAT #	101	100	99	120	121	122	104	103	102	107	106	105	150	151	152	113	109	108
Feed	14	14	14	31	31	31	15	15	15	14	14	14	40	40	40	15	15	15
WHSV, hr-1	18.20	20.00	20.20	18.30	20.10	19.30	17.20	19.10	22.10	18.50	19.60	6.90	20.40	20.10	20.40	17.10	16.80	19.70
Cat/Oil	2.20	3.91	5.59	2.18	3.90	6.25	2.33	4.09	5.44	2.16	4.40	6.69	1.96	2.92	4.52	2.34	4.66	6.08
H2	0.03	0.05	0.07	0.03	0.06	0.08	0.04	0.05	0.07	0.03	0.04	0.09	0.03	0.07	0.05	0.03	0.06	0.07
H2S	2.53	2.96	3.00	2.06	2.86	3.13	2.69	2.93	2.85	2.93	3.75	3.92	2.38	3.57	3.50	3.02	4.11	3.95
C1	1.20	1.46	1.71	0.97	1.30	1.67	1.23	1.45	1.72	1.35	1.65	2.16	1.12	1.88	1.63	1.36	1.90	2.04
C2	1.05	1.22	1.38	0.84	1.13	1.42	1.03	1.23	1.37	1.09	1.37	1.70	0.96	1.45	1.35	1.14	1.59	1.63
C2=	0.57	0.81	0.94	0.44	0.71	1.03	0.57	0.82	0.92	0.50	0.79	1.00	0.38	0.85	0.76	0.53	0.90	0.98
TOTAL	5.38	6.50	7.10	4.34	6.06	7.33	5.56	6.48	6.93	5.90	7.60	8.87	4.87	7.82	7.29	6.08	8.56	8.67
C3	1.24	1.80	2.18	1.13	1.90	2.33	1.28	1.99	2.11	1.21	1.71	2.47	0.95	1.95	1.73	1.27	2.09	2.27
C3=	2.51	3.30	3.48	2.16	3.01	3.24	2.60	3.37	3.32	1.87	3.00	3.10	1.51	3.00	2.86	1.98	3.23	3.14
iC4	2.20	3.45	4.12	1.88	3.32	4.50	2.32	3.71	3.97	1.46	2.75	3.71	0.91	3.24	2.54	1.52	3.28	3.52
nC4	0.85	1.23	1.48	0.69	0.93	1.59	0.89	1.26	1.42	0.73	1.15	1.58	0.58	1.29	1.05	0.76	1.33	1.43
C4=	2.34	2.79	2.57	1.75	2.40	2.18	2.46	2.72	2.52	1.78	2.57	2.06	1.55	2.67	2.25	1.84	2.51	2.19
TOTAL C3C4	9.14	12.57	13.83	7.61	11.56	13.84	9.55	13.05	13.34	7.05	11.18	12.92	5.50	12.15	10.43	7.37	12.44	12.55
iC5	2.42	3.80	4.41	2.01	3.19	4.94	2.58	3.77	4.31	1.59	2.94	3.86	1.16	3.61	2.78	1.66	3.46	3.87
nC5	0.50	0.59	0.63	0.43	0.64	0.64	0.50	0.55	0.51	0.44	0.54	0.63	0.36	0.64	0.54	0.42	0.63	0.66
C5=	1.77	1.77	0.88	1.62	0.76	0.79	1.82	1.46	1.16	1.59	1.41	1.09	1.18	1.81	1.45	1.53	1.37	1.28
TOTAL C5	4.69	6.16	5.92	4.06	4.59	6.37	4.90	5.78	5.98	3.62	4.89	5.58	2.70	6.06	4.77	3.61	5.46	5.81
C5-216C	35.08	38.14	34.55	31.17	36.43	36.05	36.04	36.12	34.09	28.77	32.78	30.40	23.96	33.05	34.19	27.63	30.59	30.45
C6-216C	30.39	31.98	28.63	27.11	31.84	29.68	31.14	30.34	28.11	25.15	27.89	24.82	21.26	26.99	29.42	24.02	25.13	24.64
216-343C	19.21	15.87	13.61	18.02	16.16	13.49	18.55	15.11	13.09	17.80	14.74	11.79	16.05	13.02	15.59	17.35	12.91	11.46
343C-EP	14.65	6.41	4.94	24.40	8.10	5.47	13.21	6.94	4.67	20.01	7.32	4.06	26.95	4.45	7.28	19.29	5.82	4.88
Coke	16.54	20.51	25.97	14.46	21.69	23.82	17.09	22.30	27.88	20.47	26.38	31.96	22.67	29.51	25.22	22.28	29.68	31.99
Conv, wt%	66.14	77.71	81.45	57.59	75.74	81.04	68.24	77.95	82.24	62.19	77.93	84.16	57.00	82.53	77.12	63.37	81.27	83.66
Mat Balance	97.94	97.76	95.28	98.50	94.91	95.92	96.02	97.03	90.18	96.10	96.23	88.91	95.66	87.58	91.77	98.17	92.65	91.45

Figure 54

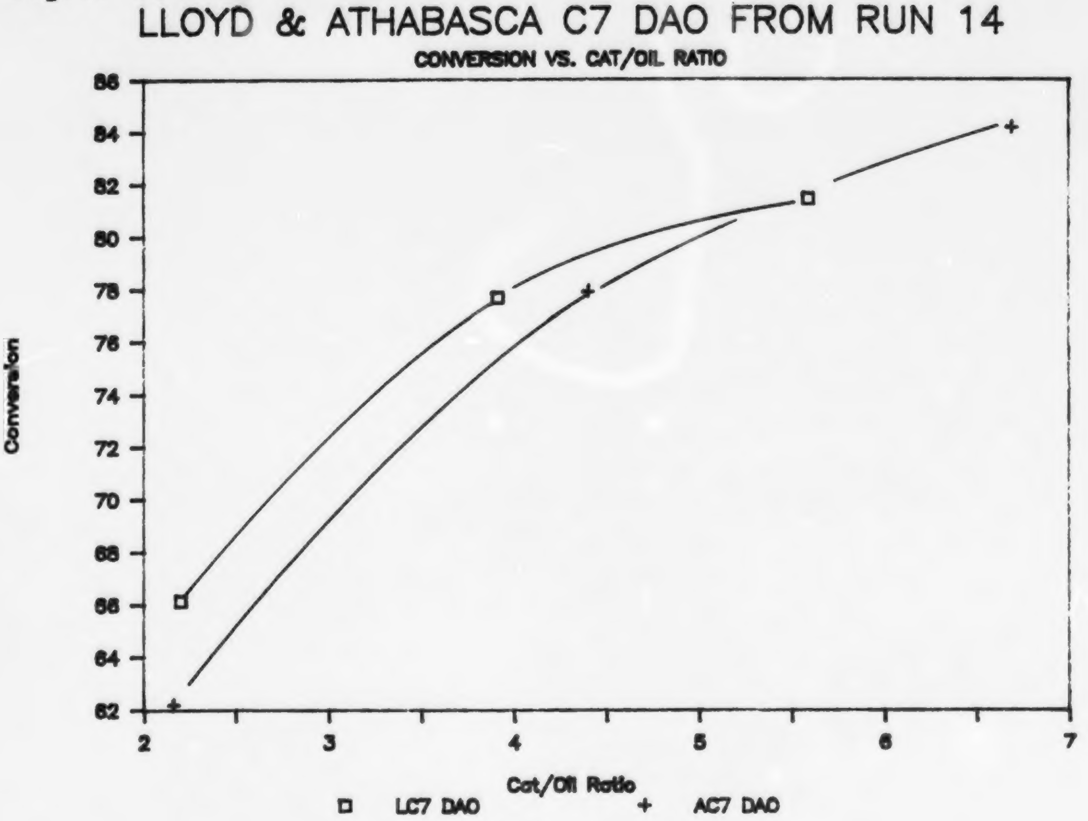

Figure 55

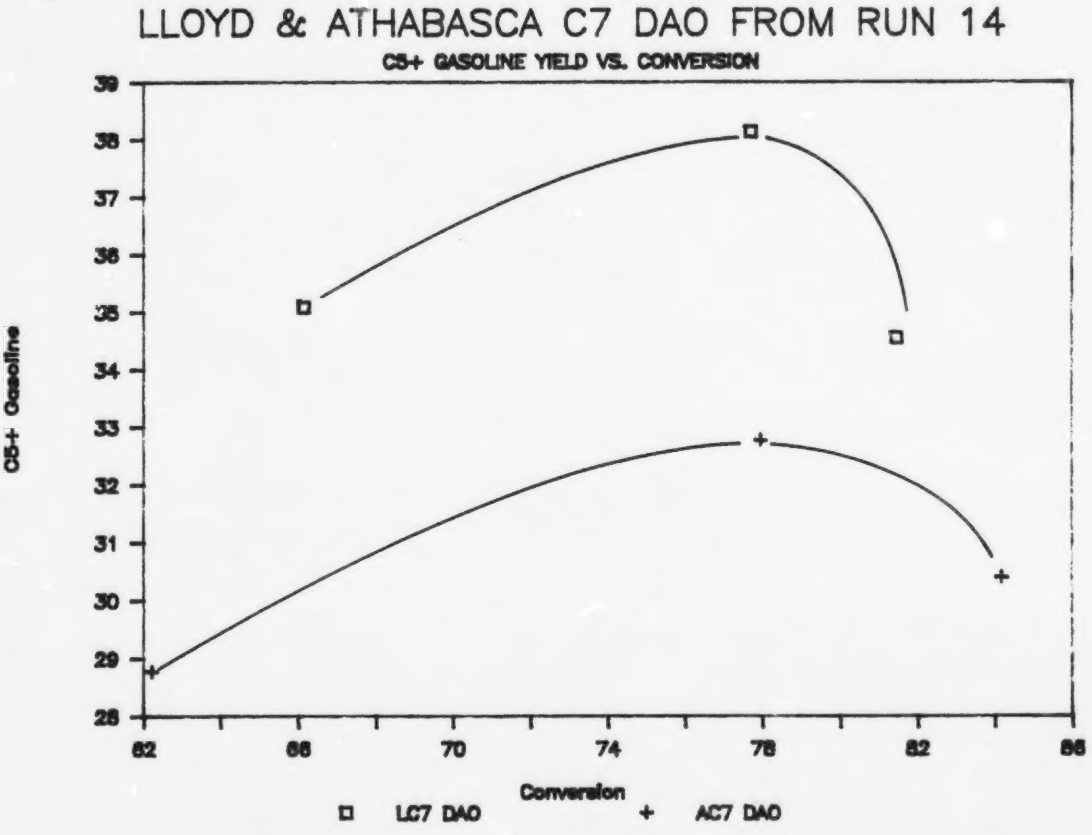

Figure 56

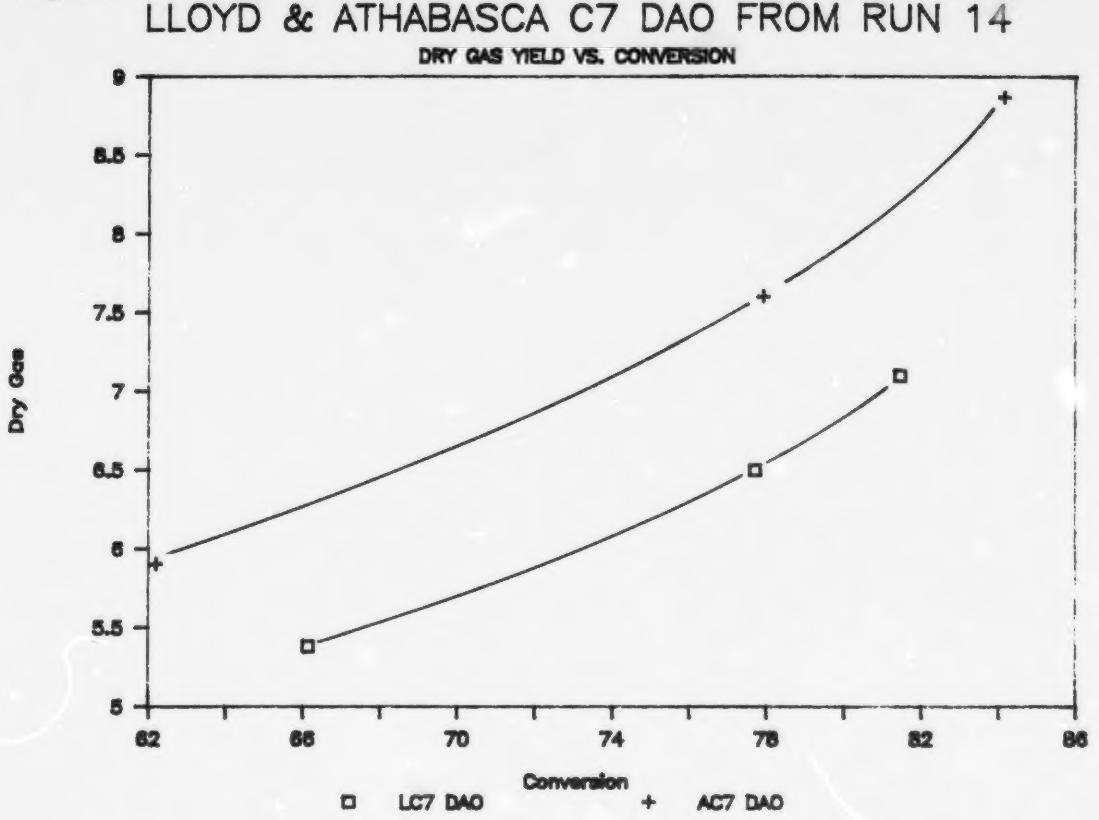

Figure 57

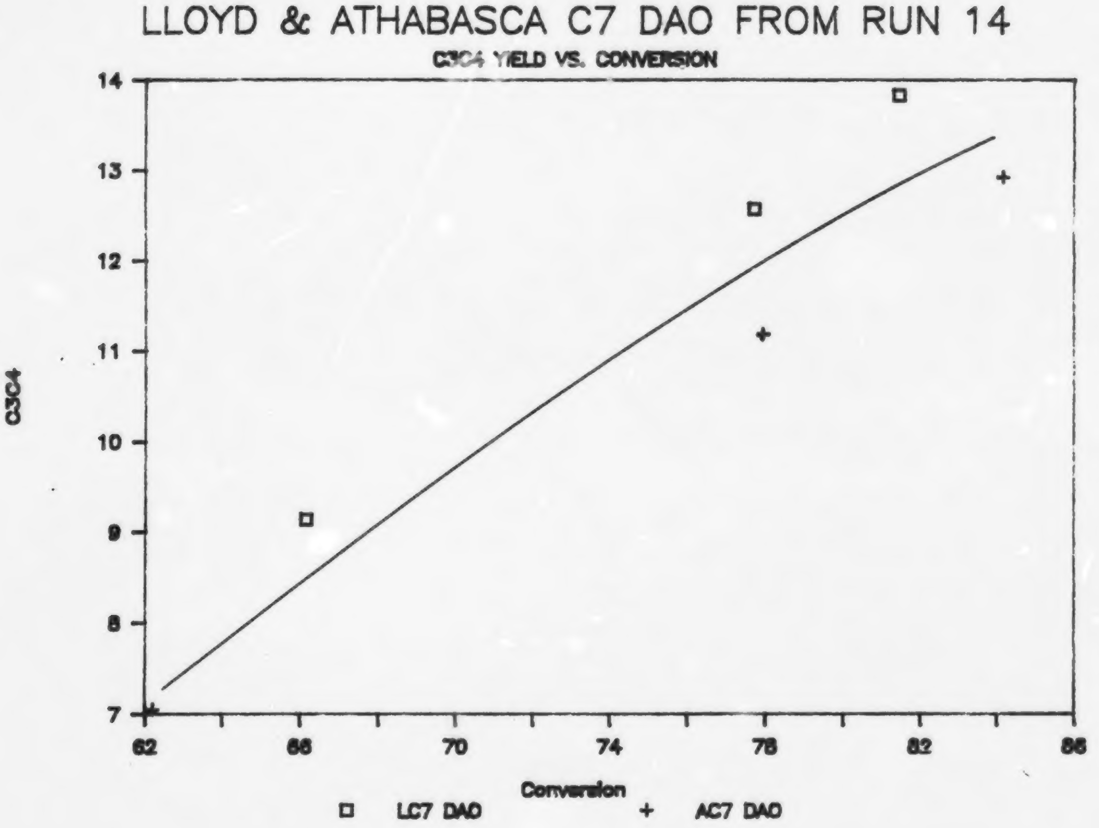

Figure 58

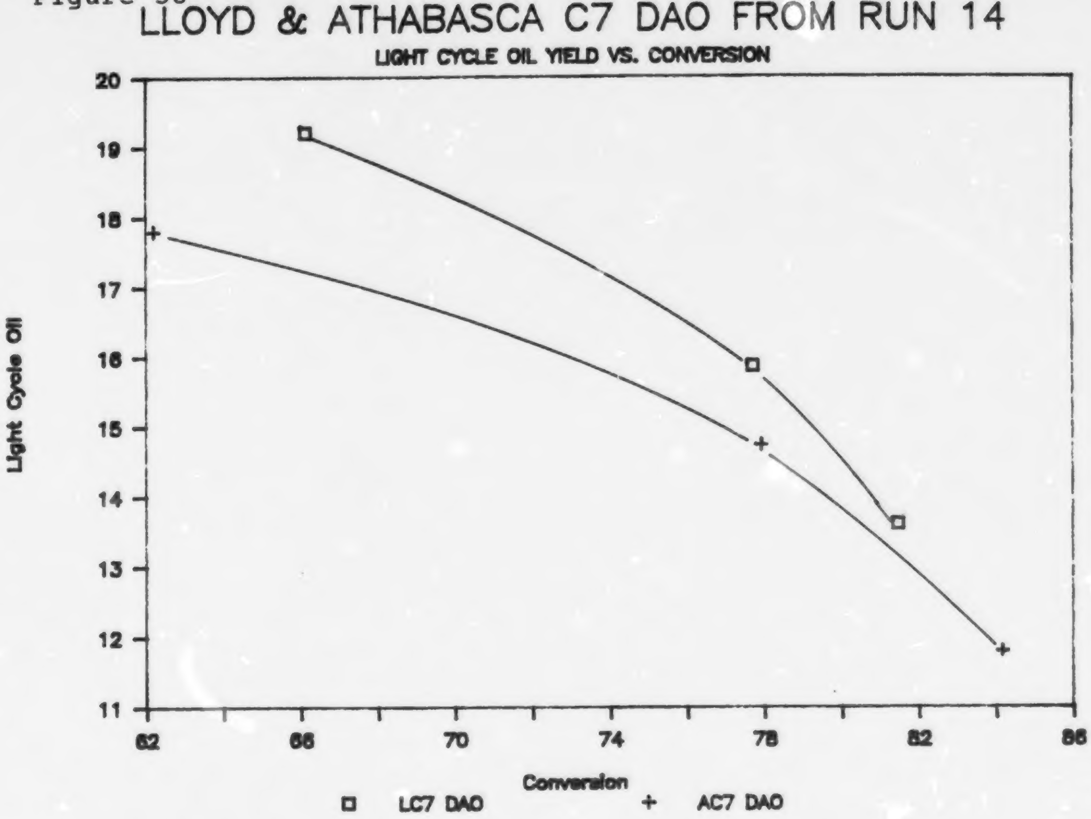

LLOYD & ATHABASCA C7 DAO FROM RUN 14

LIGHT CYCLE OIL YIELD VS. CONVERSION

Figure 59

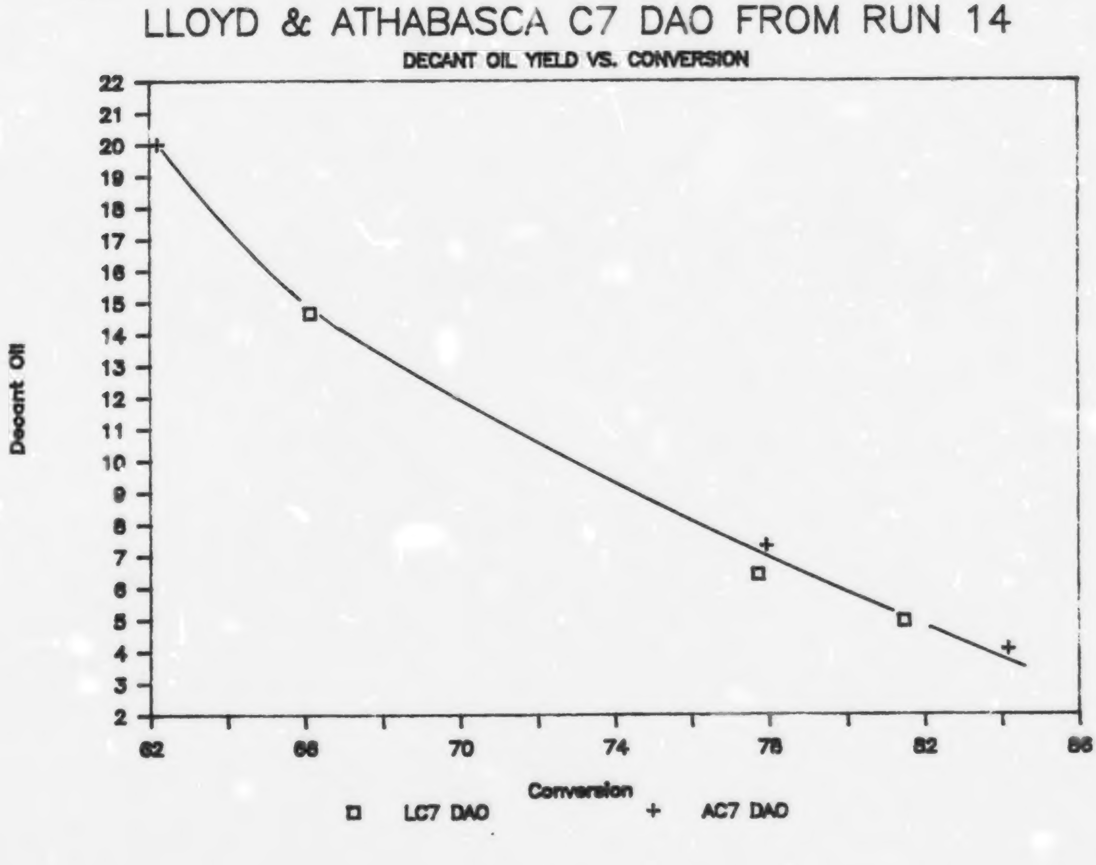

LLOYD & ATHABASCA C7 DAO FROM RUN 14

DECANT OIL YIELD VS. CONVERSION

Figure 60

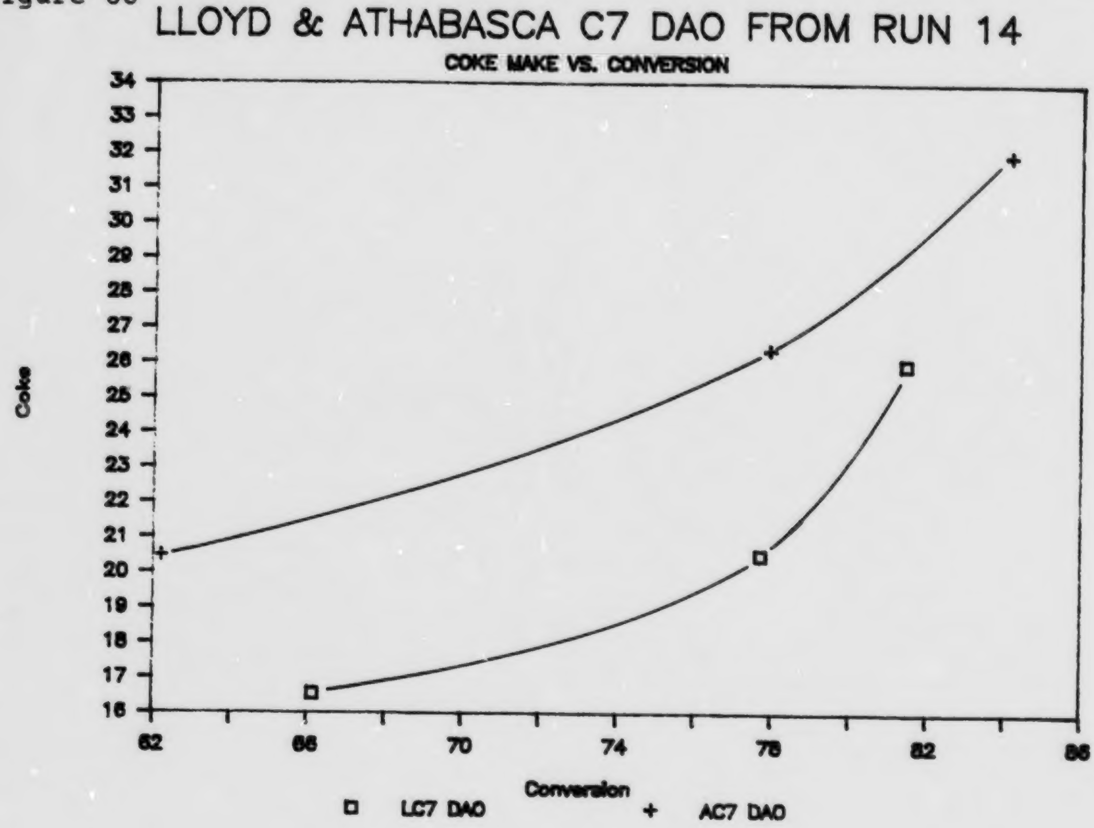

Figure 61

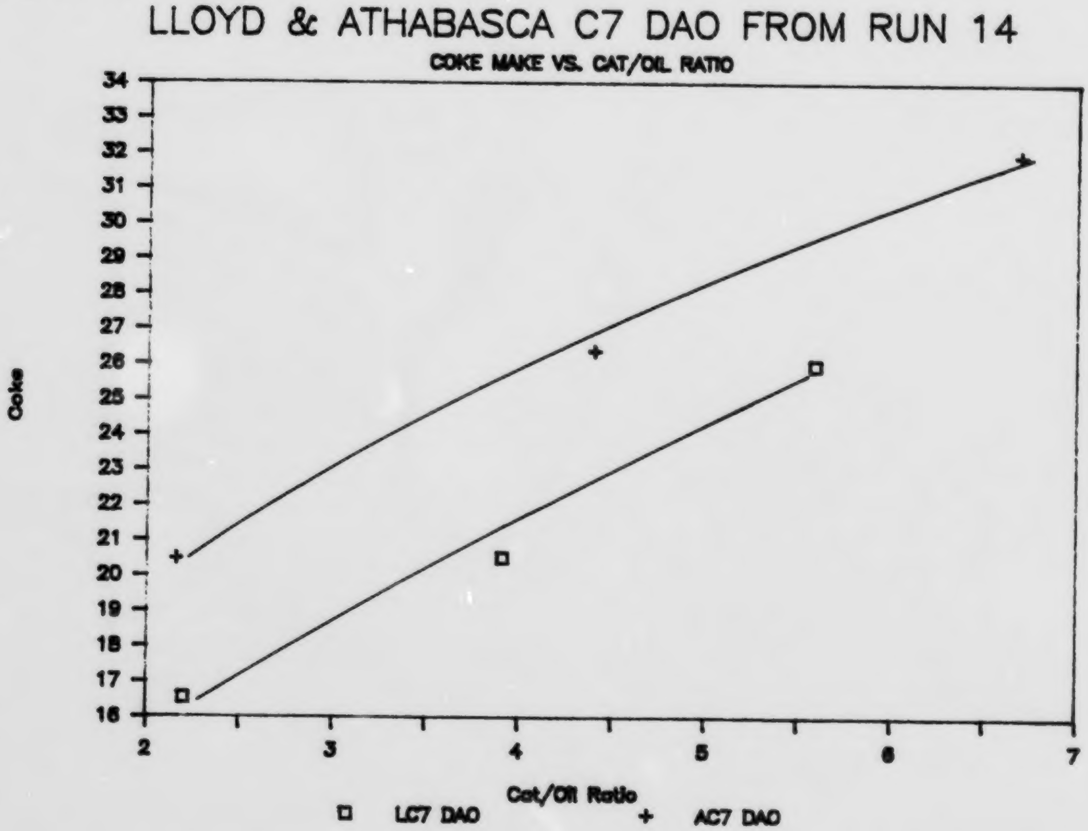

TABLE 26

Summary of Deasphalting and MAT Results -- Lloydminster Data

Run #	5	23	20	22	32	21	37	19	24	10	38	14	31	15
MAT #	1	64	4	61	127	15	136	18	124	73	139	100	121	103
Solvent	C3	C4	C4	C4	C4	C4	C4	C5	C5	C5	C5	C7	C7	C7
Ratio w/w	4.4	7.3	5.1	2.3	0.9	5.1	5.1	5.5	1	5.5	5.5	11.7	3	8.1
Temp C	75	120	120	120	120	140	75	160	160	140	75	75	75	180
Press psia	465	415	415	415	415	565	205	365	365	265	105	65	65	165
Yield DAO wt%	27	60.8	57.5	55.5	25.3	52.7	64.5	71.9	91.8	75.1	77	82.7	87.8	87.5
Density g/cc	0.9385	0.9751	0.973	0.9756	1.0069	0.9701	0.978	0.9876	1.0077	0.9906	0.9939	1.0043	1.0155	1.0065
N ppm w/w	1120	2012	2080	2030	4238	2047	2623	2680	5304	3136	3395	3101	4846	3456
Basic N ppm	398	845	876	881	956	1068	735	979	1033	1145	926	1116	1200	1523
Con Carbon wt%	1.7	5.43	6.1	6.35	12.4	4.57	7.22	9.2	16.6	9.4	10.73	12.8	14.9	13.3
Asphaltene	0	0.1	0.1	0.3	5.7	0.2	0.1	0.1	9.6	0.2	0.1	1.4	7.5	2.1
Resins	9.8	22.8	21	25.4	32	18.8	24	22.6	32.2	32.2	31.2	35.4	30.7	34.4
Oils	90.2	77.1	78.9	74.3	62.3	81	75.9	77.3	58.2	67.6	68.7	63.2	62.5	63.5
Ni+V ppm w/w	2	21	26	31	112	16	27	70	168	80	60	135	126	118
MAT Yields wt%														
Gas	4.77	5.73	5.79	6.52	5.88	5.84	5.15	5.73	6.12	6.33	5.54	6.50	6.06	6.48
C3C4	15.58	13.72	14.16	15.50	11.92	14.32	11.92	11.81	11.45	13.13	11.90	12.57	11.56	13.05
Gasoline	47.49	43.66	42.53	43.23	41.40	41.65	41.23	39.22	38.40	39.60	41.49	38.14	36.43	36.12
LCO	18.27	18.98	19.01	16.66	16.40	18.92	18.73	17.86	15.25	16.64	17.55	15.87	16.16	15.11
DO	7.74	8.69	9.31	6.12	6.83	9.81	10.80	9.56	6.88	7.61	8.12	6.41	8.10	6.94
Coke	6.15	9.22	9.20	11.97	17.57	9.46	12.17	15.82	21.90	16.69	15.40	20.51	21.69	22.30
Conversion	73.99	72.33	71.68	77.23	76.76	71.27	70.46	72.59	77.87	75.74	74.33	77.71	75.74	77.95
216 Conversion	67.84	63.11	62.48	65.25	59.2	61.81	58.3	56.76	55.97	59.06	58.93	57.21	54.05	55.65
Cat/Oil	3.86	3.93	3.61	4.31	3.91	3.96	4.18	3.81	4.07	4.09	3.94	3.91	3.90	4.09

TABLE 27

Summary of Deasphalting and MAT Results -- Athabasca Data

Run #	5	23	20	22	28	21	37	19	24	39	10	38	14	40	15
MAT #	10	70	7	67	133	12	142	21	130	145	76	148	106	152	109
Solvent	C3	C4	C4	C4	C4	C4	C4	C5	C5	C5	C5	C5	C7	C7	C7
Ratio w/w	4.2	7	4.8	2.1	0.5	4.8	4.6	5.2	1	6.8	5.2	5	11.1	7.7	7.7
Temp C	75	120	120	120	120	140	75	160	160	160	140	75	75	75	180
Press psia	465	415	415	415	415	565	205	365	365	365	265	105	65	65	165
Yield DAO wt%	12	40.4	39	28.5	94.8	31.5	47.1	58.8	65.3	59.3	59.5	66	80.3	80.5	82.2
Density g/cc	0.9562	0.9957	0.9937	0.9869	1.0489	0.9897	1.0014	1.0035	1.0736	1.0144	1.018	1.022	1.026	1.0381	1.0359
N ppm w/w	1537	2475	2906	2313	7053	2759	3392	3615	5198	4639	3459	4284	3500	5771	3036
Basic N ppm	603	1090	1163	1003	1957	1445	1039	1451	1523	1092	1222	1264	1570	1401	1664
Con Carbon wt%	2.9	7.22	8.3	6.68	24	6.13	9.37	12.8	19.9	12.11	12.4	14.33	18.4	19.4	18.3
Asphaltene	0	0	0.1	0.1	18.5	0.3	0.1	0.2	7.4	0.1	0	0.1	3.3	5.5	2.5
Resins	10.7	27.1	23	26	36.3	25.8	26.8	32.3	38.9	35.9	41.1	40.3	46.2	43.3	49.9
Oils	89.3	72.9	76.9	73.9	45.2	73.9	73.1	67.5	53.7	64	58.9	59.6	50.5	51.2	47.6
Ni+V ppm w/w	0	32	48	24	370	25	43	154	322	77	111	140	253	195	248
MAT Yields wt%															
Gas	5.58	7.45	6.93	7.28	7.30	6.97	6.30	6.81	7.28	6.94	7.72	7.54	7.60	7.29	8.56
C3C4	14.44	13.66	12.48	14.32	9.45	12.54	10.95	9.92	10.67	10.92	12.02	12.73	11.18	10.43	12.44
Gasoline	45.73	40.05	38.60	41.26	31.66	38.09	37.53	35.52	36.22	37.92	36.83	36.34	32.78	34.19	30.59
LCO	18.93	17.64	19.39	17.97	14.08	19.34	18.44	17.87	14.82	16.94	15.70	15.78	14.74	15.59	12.91
DO	8.81	8.26	11.31	8.00	6.58	12.55	13.88	10.46	6.25	10.65	7.04	6.53	7.32	7.28	5.82
Coke	6.51	12.94	11.29	11.17	30.93	10.51	12.90	19.42	24.76	16.63	20.69	21.08	26.38	25.22	29.68
Conversion	72.26	74.10	69.30	74.03	79.35	68.11	67.68	71.67	78.93	72.41	77.26	77.70	77.93	77.12	81.27
216 Conversion	65.75	61.16	58.01	62.86	48.41	57.6	54.78	52.25	54.17	55.78	56.57	56.61	51.56	51.91	51.59
Cat/Oil	3.89	4.61	3.84	3.98	3.67	3.79	4.07	3.82	4.34	4.34	4.33	4.64	4.40	4.52	4.66

15. Solvent Effects

As discussed earlier, there is a good correlation between the CCR and resin content of a DAO and the coke and gas produced when the DA oil is cracked in the MAT unit. In addition, the gasoline yield correlates with the oil content of the DA oil. It has also been established that the composition of the DA oil is strongly dependent upon the choice of solvent. Table 28 further illustrates how solvent choice affects the DA oil yield and quality and the associated MAT results. The deasphalting runs selected for this comparison were carried out at similar solvent/oil ratios (v/v) and reduced temperatures (operating temp./critical temp.). The MAT data is at a nominal C/O ratio of 4. The data shows clearly that as the solvent molecular weight is decreased from _n_-heptane through to propane

- the DA oil yield decreases
- the Conradson Carbon and metals content of the DA oil decreases
- the density decreases and the oil content of the DA oil increases

As the DA oil quality increases (decrease in CCR and resin content), the coke and gas make decrease, while the gasoline, C_3C_4 and LCO yields increase.

Although the poorer quality DA oils yield less gasoline when calculated as a wt% of oil charged to the reactor, they yield substantially more gasoline when calculated as a wt% of VTB. A reason for this is that the heavier solvents (nC_7 and nC_5) extract a greater amount of oil than the lighter solvents in this single stage extraction process. A properly designed multicontacting process using the lighter solvents would recover substantially more of the oil fraction than the single stage process.

It was noted earlier that the resin fraction may contribute to gasoline production, thus increasing gasoline yields for the DA oils obtained from the heavier solvents over that which would be expected based on the oil content of the DA oil. The validity of this can be tested using data from Table 28 and the following equation.

$$\text{Gasoline} = \text{Oil content, wt\%} \times 0.5 + (100 - \text{Oil Content, wt\%}) \times 0.165$$

	Athabasca Gasoline Yield, wt%		Lloyd Gasoline Yield, wt%	
	Measured	Calc.	Measured	Calc.
nC_7 DA Oil	30.6	32.4	36.1	37.4
nC_5 DA Oil	36.8	36.2	39.6	39.1
nC_4 DA Oil	38.6	42.3	42.5	42.9
C_3 DA Oil	45.7	46.4	47.5	46.7

It is obvious that this simple relationship between gasoline yield and the oil and resin content can be improved. However, it does serve to show that the resin fraction contributes to gasoline production.

To complete the discussion, the data in Table 29 shows the solvent effects at a constant deasphalting temperature (75°C). The trends with decreasing solvent molecular weight are closely similar to those described above; decreasing DA oil yield, increasing oil quality and improved in the MAT yield profiles.

TABLE 28

SOLVENT EFFECTS ON DAO QUALITY AND MAT YIELDS

	ATHABASCA					LLOYDMINSTER				
Run No.	15	10	20	5	-	15	10	20	5	-
Solvent	nC_7	nC_5	nC_4	C_3	VGO	nC_7	nC_5	nC_4	C_3	VGO
T_R	0.84	0.88	0.925	0.94		0.84	0.88	0.925	0.94	
Temperature, °C	180	140	120	75	-	180	140	120	75	-
Ratio, v/v	12.1	9	9	9	-	12.1	9	9	9	-
Yield, wt%	82.2	59.5	39.0	12	38*	87.5	75.1	57.5	27	35.6*
DAO Density	1.0359	1.018	0.9937	0.9562	0.9785	1.0155	0.9906	0.9730	0.9385	0.9265
Conradson Carbon, wt%	18.3	12.4	8.3	2.9	0.92	13.3	9.4	6.1	1.7	0.07
Ni + V, ppm w/w	248	113	49	-	4	118	80	26	1	0.3
Oils, wt%	47.6	58.9	76.9	89.3	-	63.5	67.6	78.9	90.2	-
Yields, wt%										
Gas	8.56	7.72	6.93	5.58	3.71	6.48	6.33	5.79	4.77	3.01
C_3C_4	12.44	12.02	12.48	14.44	9.99	13.05	13.13	14.16	15.58	13.21
Gasoline	30.59	36.83	38.60	45.73	38.23	36.12	39.60	42.53	47.49	49.03
LCO	12.91	15.70	19.39	18.93	33.25	15.11	16.64	19.01	18.27	22.40
DO	5.82	7.04	11.31	8.81	9.13	6.94	7.62	9.31	7.74	8.30
Coke	29.68	20.69	11.29	6.50	5.65	22.30	16.69	9.21	6.15	4.05
Conversion, wt%	81.27	77.26	69.30	72.26	57.62	77.95	75.74	71.68	73.99	69.30
C/O	4.66	4.33	3.84	3.89	3.95	4.09	4.09	3.61	3.86	4.0
Yield Gasoline /100g VTB	25.1	21.9	15.1	5.5		31.6	29.7	24.5	12.8	
Vol Cat Cracked Gasoline/100 vol VTB	35	30	20	7		43	40	32	16	

* Calculated from distillation data as (wt% VGO x 100 / wt% VTB)

TABLE 29

SOLVENT EFFECTS ON DAO QUALITY AND MAT YIELDS
CONSTANT DA TEMPERATURE

	ATHABASCA				LLOYDMINSTER			
Run No.	40	38	37	5	14	38	37	5
Solvent	nC_7	nC_5	nC_4	C_3	nC_7	nC_5	nC_4	C_3
Temperature, °C	75	75	75	75	75	75	75	75
Ratio, v/v	12.1	9	9	9	17	9	9	9
Yield, wt%	80.5	66.0	47.1	12	82.7	77.0	64.5	27
DAO Density	1.038	1.022	1.0014	0.9562	1.0043	0.9939	0.9780	0.9385
Conradson Carbon, wt%	19.4	14.33	9.37	2.9	12.8	10.73	7.22	1.7
Ni + V, ppm w/w	195	117	43	-	135	57	27	1.1
Oils, wt%	51.2	59.6	73.1	89.3	63.2	68.7	75.9	90.2
Yields, wt%								
Gas	7.29	7.54	6.30	5.58	6.50	5.54	5.15	4.77
C_3C_4	10.43	12.73	10.95	14.44	12.57	11.90	11.92	15.58
Gasoline	34.19	36.34	37.53	45.73	38.14	41.49	41.23	47.49
LCO	15.59	15.78	18.44	18.93	15.87	17.55	18.73	18.27
DO	7.28	6.53	13.88	8.81	6.42	8.12	10.80	7.74
Coke	25.22	21.08	12.90	6.50	20.51	15.40	12.17	6.15
Conversion, wt%	77.12	77.70	67.68	72.26	77.71	74.33	70.46	73.99
C/O	4.50	4.64	4.07	3.89	3.91	3.94	4.18	3.86
Yield Gasoline /100g VTB	27.5	24.0	17.7	5.5	31.5	31.9	26.6	12.8
Vol Cat Cracked Gasoline/100 vol VTB	38	32.7	23.6	7	42	42.3	34.7	16

REFERENCES

1. S.R. Nelson, Chem. Eng. Progress, May, 1985 p. 63
2. J. Bousquet and T. Laboural, O&GJ, April 20, 1987, p. 62
3. A.R. Johnson, NPRA Annual Meeting, Los Angeles, 1986, AM-86-42
4. Anon, Hydrocarbon Processing, September, 1987, p. 67
5. L.C. Yen, R.E. Wrench and A.S. Ong, O&GJ, January 11, 1988, p. 67
6. N. Cyr, D.D. McIntyre, G. Toth and O.P.Strausz, Fuel, Vol. 66, p. 1709, December, 1987
7. P.K. Dutta and R.J. Holland, Fuel, Vol. 63, p. 197, February, 1984
8. J.F. McKay, P.J. Amend and T.E. Cogswell, A.C.S. Division of Petroleum Chemistry, Tar Sands and Oil Shales, March 20, 1977, p. 708
9. J.G. Speight, A.C.S. Division of Petroleum Chemistry, Polynuclear Aromatic Hydrocarbons, September 7, 1986, p. 818
10. R.A. Flinn, H. Beuther and B.K. Schmid, Petroleum Refinery, p. 139, April, 1961
11. H. Sawatsky, S.M. Ahmed, A.E. George and G.T. Smiley, A.C.S. Division of Petroleum Chemistry, March 12, 1987, p. 11
12. M.J.L. Johnson, J. Catal. 52, p. 425, 1978
13. R.T. Penning, A.G. Vickers and B.R. Shah, Hydrocarbon Processing, May, 1982, p. 145
14. D.L. Mitchell and J.G. Speight, Fuel 52, pp 149-152, 1973
15. A. Hirschberg, L.N.J. deJong, B.A. Schipper and J.G. Meijer, SPEJ, pp 283-293, June, 1984
16. G.A. Mansoori, T.S. Jiang and S. Kawanaka, Arab. J. for Sci. & Eng., 13(1), pp 17-34, 1988
17. K.E. Starling, "Fluid Thermodynamic Properties for Light Petroleum Systems", Gulf Publishing Co., Houston, Texas, 1973

APPENDIX

Pseudo-Ternary Diagrams

Solvent-Oils-Asphalt

FIGURE 9A

Athabasca - C3
75C 465 PSIA

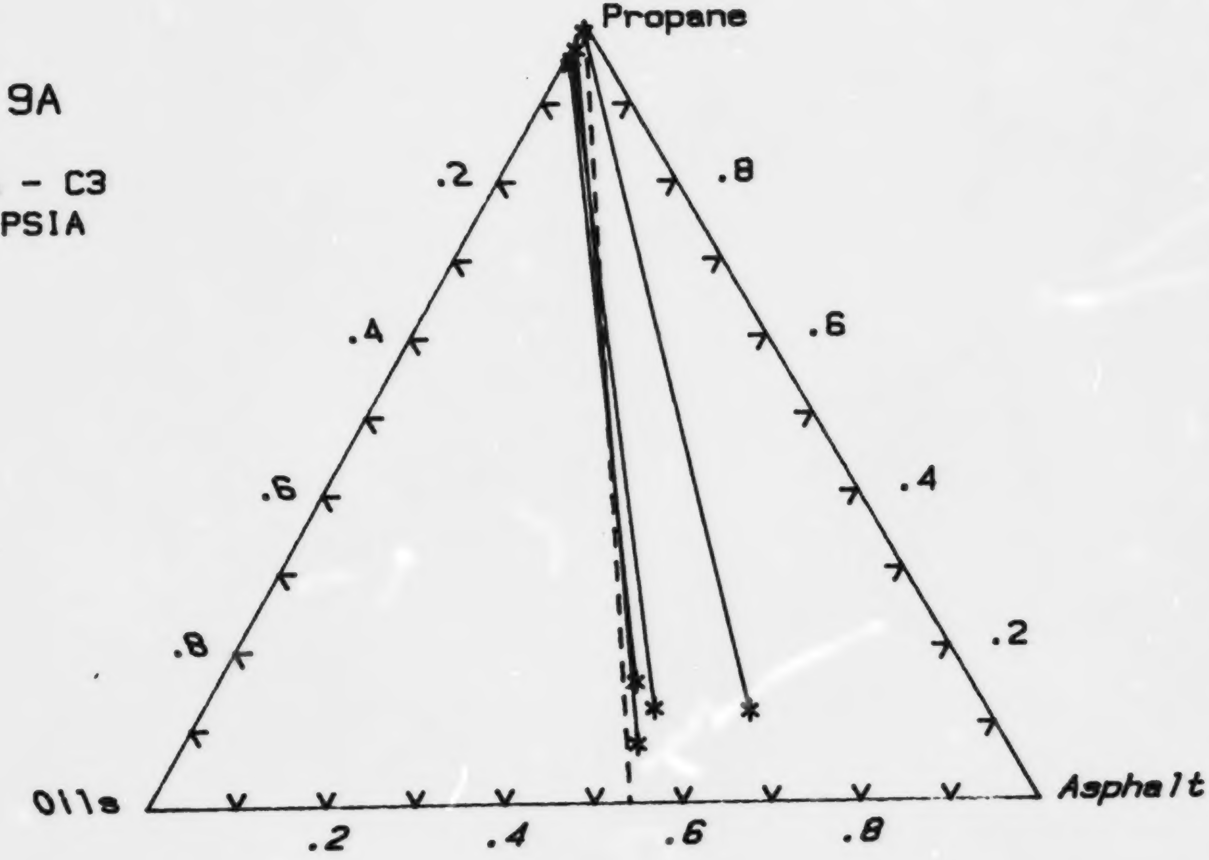

FIGURE 10A

Athabasca - C4
120C 415 PSIA

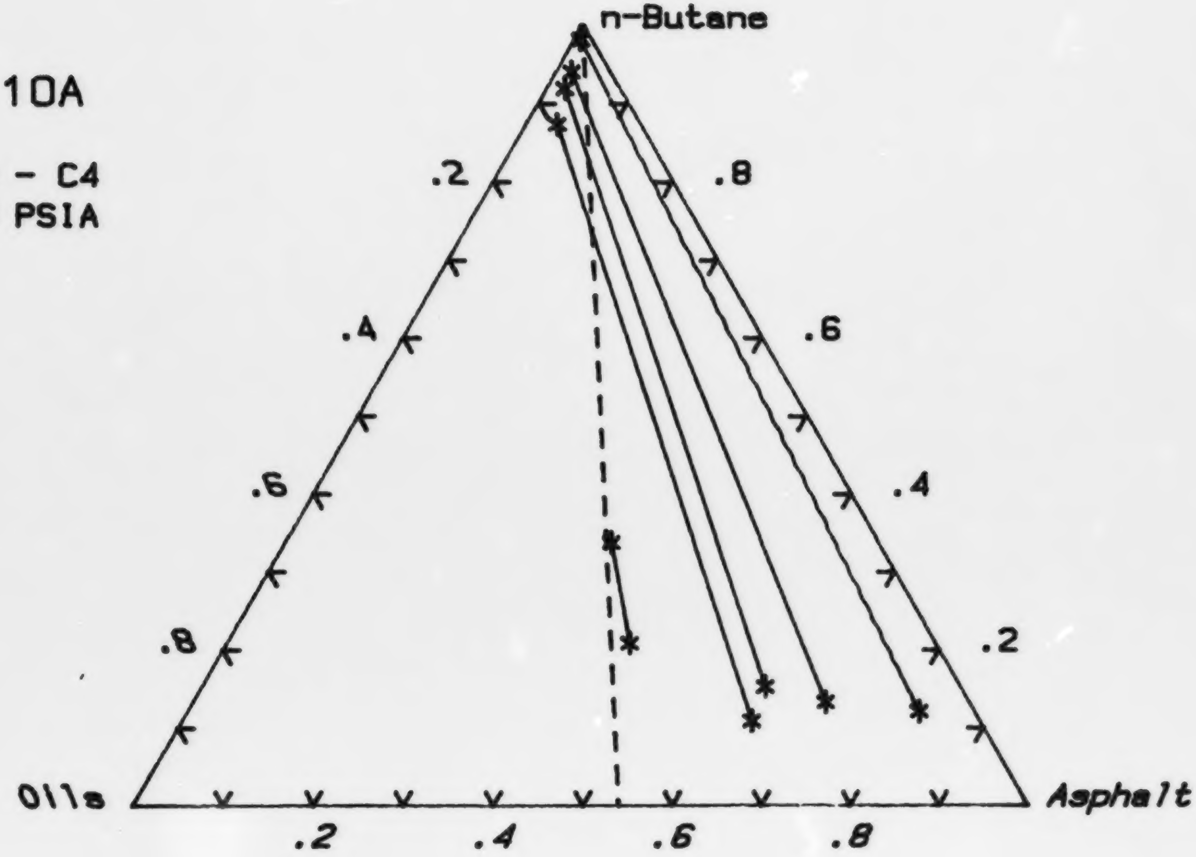

FIGURE 11A

Athabasca - C5
160C 365 PSIA

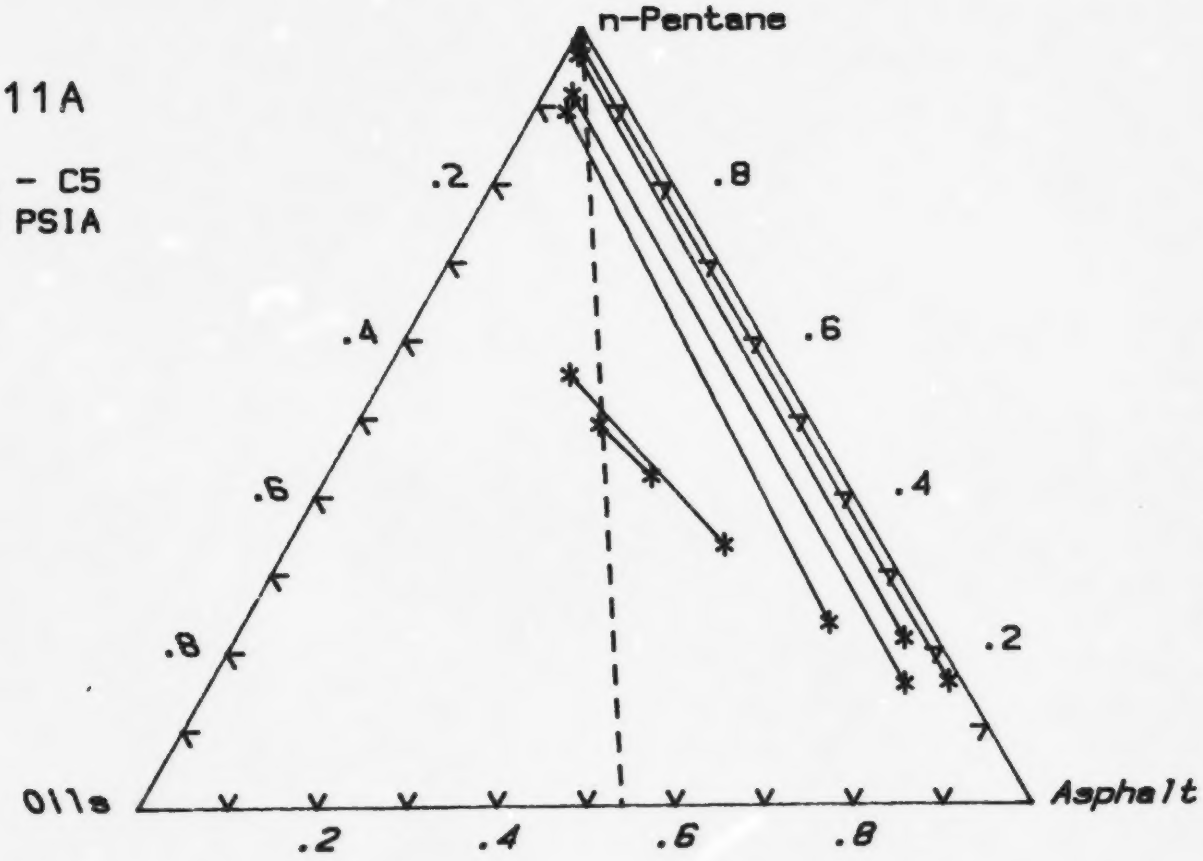

FIGURE 12A

Athabasca - C7
75C 65 PSIA

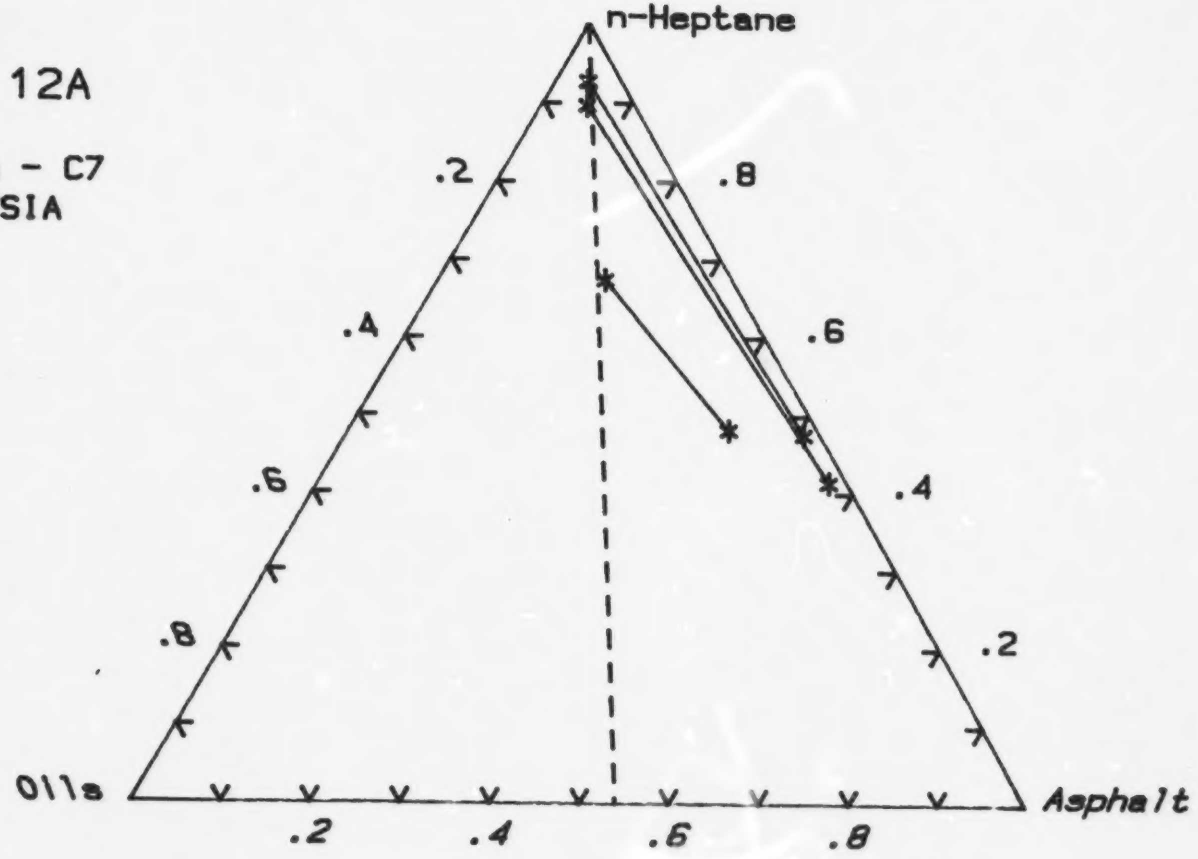

FIGURE 13A

Lloydminster - C3
75C 465 PSIA

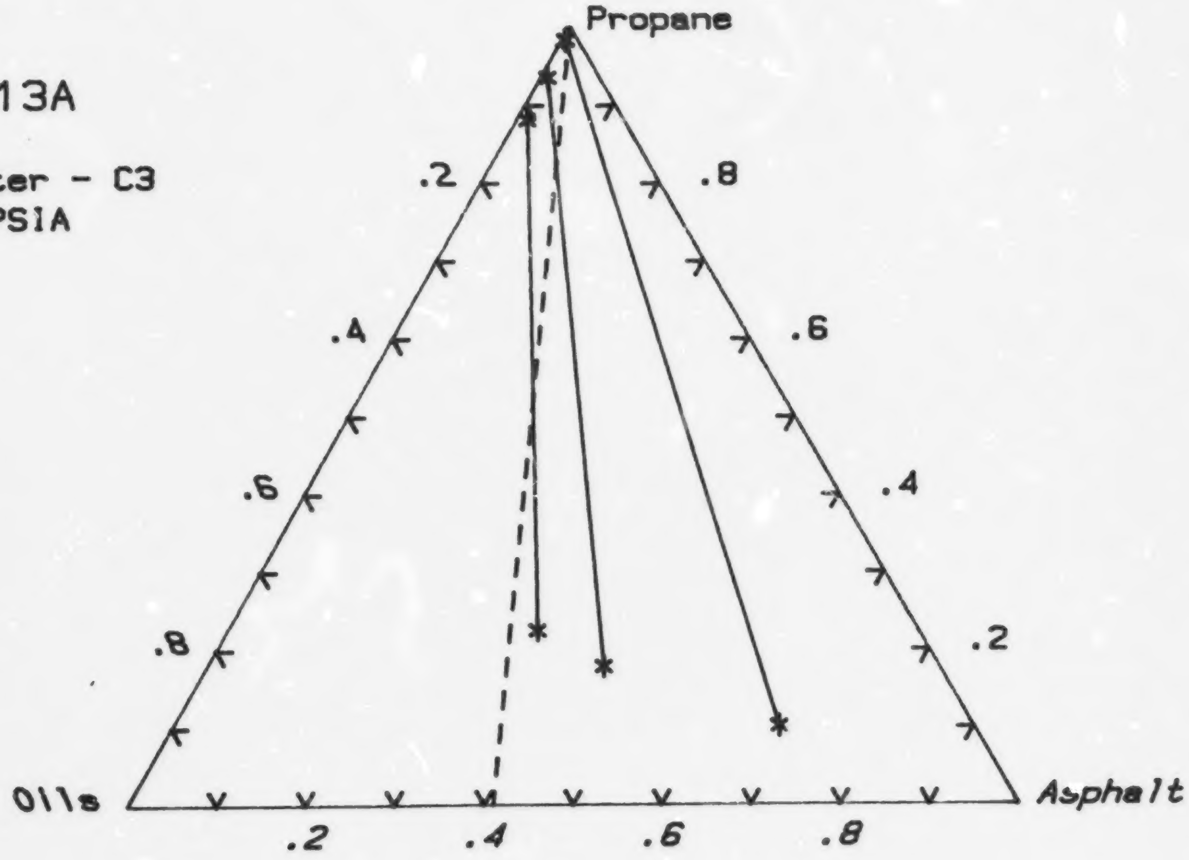

FIGURE 14A

Lloydminster - C4
120C 415 PSIA

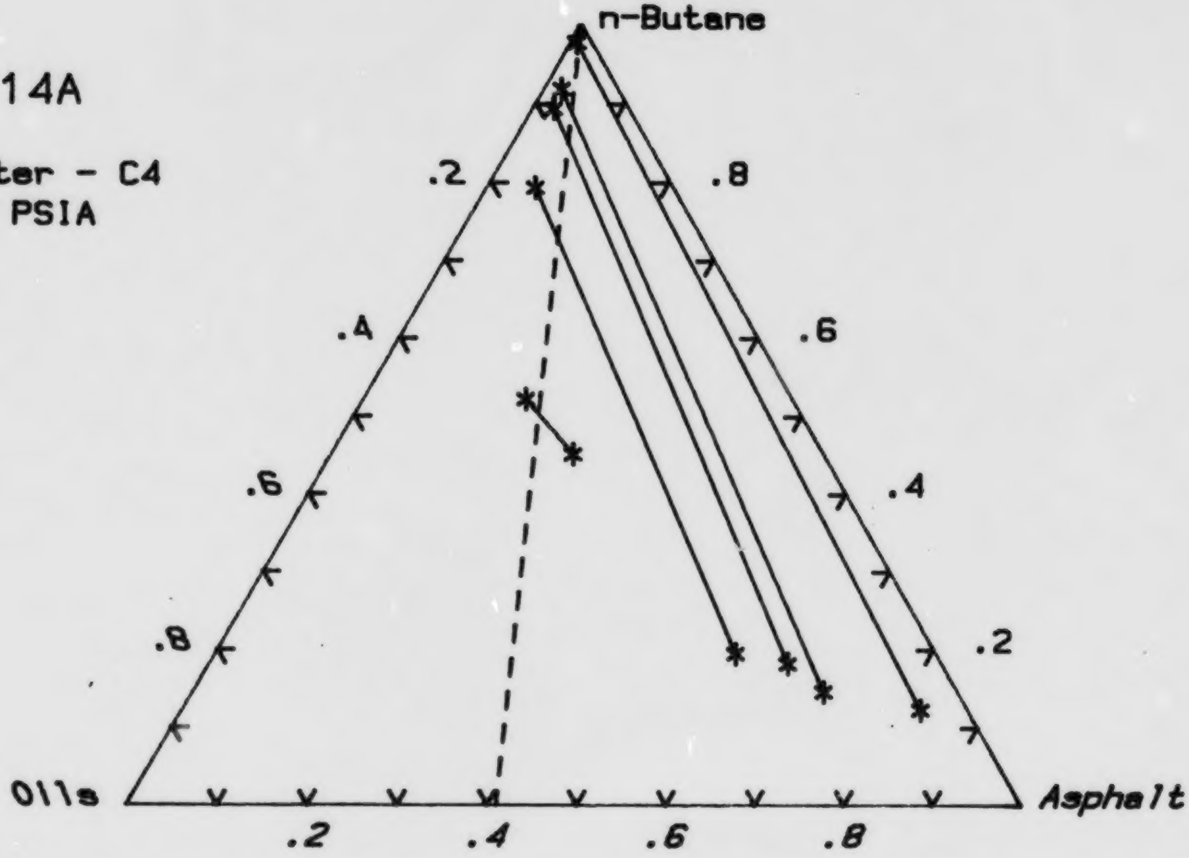

FIGURE 15A

Lloydminster - C5
160C 365 PSIA

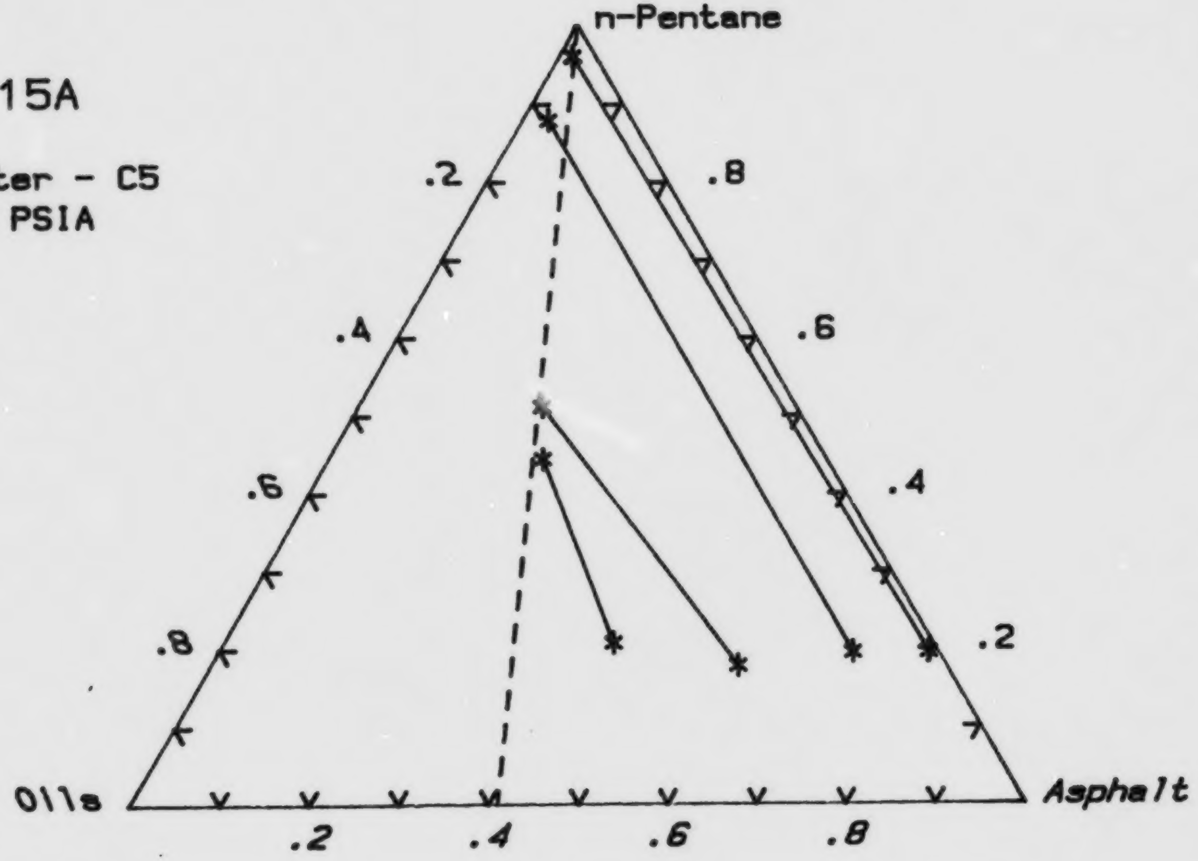

FIGURE 16A

Lloydminster - C7
75C 65 PSIA

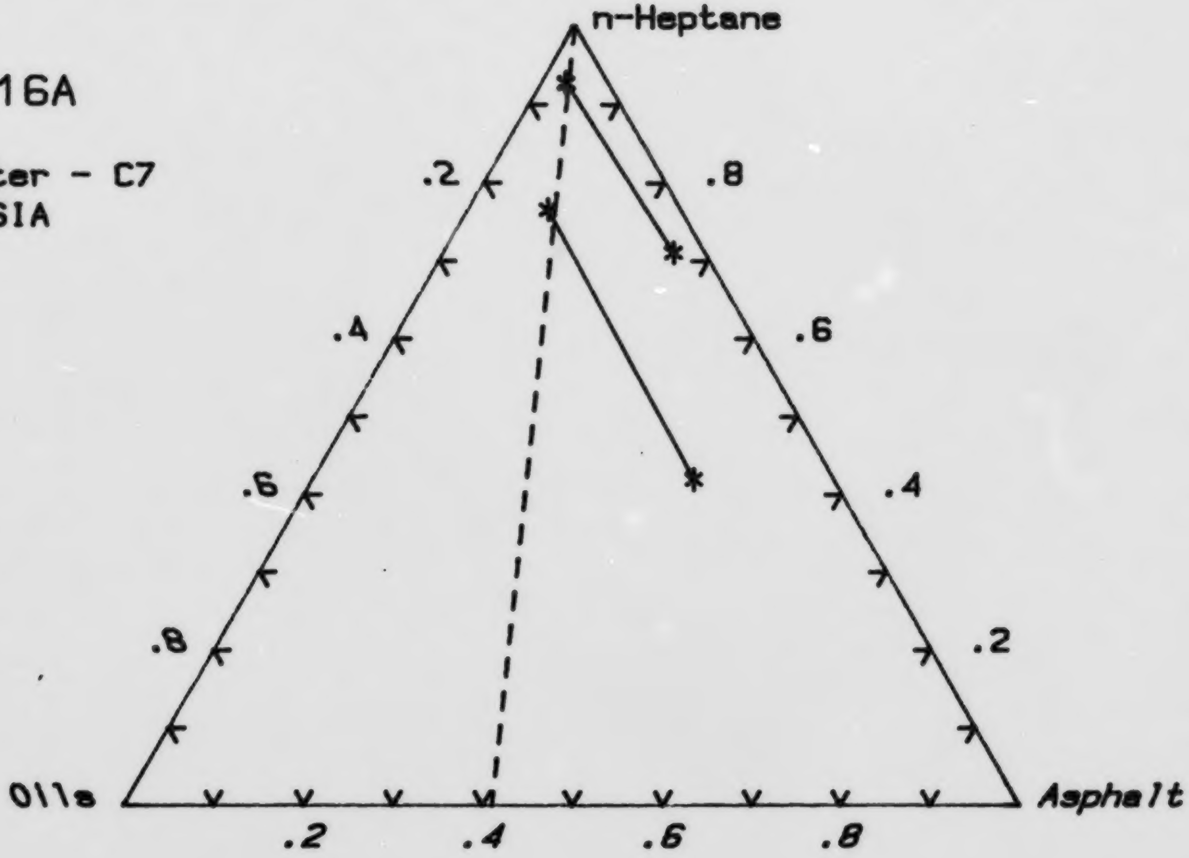

SHERIDAN TECHNICAL ASSOCIATES INC.

Consulting Research Laboratory Services

DEASPHALTING OF NON-CONVENTIONAL RESIDUES AND CATALYTIC CRACKING OF DE-ASPHALTED OILS BY METAL-TOLERANT CATALYST

(Part of the Program of the Federal Panel on
Energy R&D [PERD])

TASK 8

DA AND FCC PROCESS MODELLING

FINAL REPORT

MARCH, 1989

S.C.C. FILE NUMBER: 07SQ.23440-7-9126

CONTRACT SERIAL NUMBER: 23440-7-9126/01SQ

SCIENTIFIC AUTHORITY: DR. S.H. NG

STA FILE NUMBER: 190-89-30

SHERIDAN TECHNICAL ASSOCIATES INC.

333 WYECROFT ROAD, UNITS 6 & 7

OAKVILLE, ONTARIO

L6K 2H2

94pp

MARCH, 1989

MICROMEDIA

INTRODUCTION

The work described in this report is an addendum to the experimental deasphalting phase behaviour and catalytic cracking studies which were reported in December 1988. (" Final Report, Deasphalting of Non-Conventional Residues and Catalytic Cracking of Deasphalted Oils by a Metals-Tolerant Catalyst"). Two of the recommendations contained in the Final Report concerned fully utilizing the experimental data via modelling and correlation; it was to address these recommendations that the contract was modified to include the current model applications as Task 8.

Task 8 consists of four separate model applications

(a) Match the experimental phase behaviour observed during deasphalting to permit calculation of phase behaviour over a complete range of solvent-VTB ratios.

(b) Fit a kinetic model to the experimental catalytic cracking data for the deasphalted oils to derive rate constants for gas oil cracking, gasoline formation and gasoline cracking.

(c) Using the rate constants from 8b, model the performance of a commercial heat-balanced riser FCCU with selected deasphalted oils as feedstock.

(d) Repeat the kinetic model fitting described in 8b to the cracking data for the special feeds produced during Task 6 of the contract (final report entitled "Task 6: Special Deasphalting/MAT Runs", issued in July, 1988.)

Each of the applications is dealt with in a separate section of the report. A summary of the salient features of the model used for the application is included in each section with a more detailed description, together with examples of the computer program outputs, given in the Appendices.

TASK 8A Deasphalting Phase Behaviour

Experimental phase behaviour was reported in Task 4 during the deasphalting of Lloydminister and Athabasca vacuum tower bottoms (VTB) with solvents ranging from propane to n-heptane. Temperature and pressure conditions were selected so that the systems were undersaturated (i.e. below the bubble point) resulting ,usually, in two liquid phases: an upper, solvent-rich, deasphalted phase accompanied by a lower phase in which the asphaltenes were concentrated. Weight compositions of each phase, in terms of four components (solvent, oils, resins and asphaltenes), were obtained during deasphalting with initial solvent-VTB ratios lying between 40:1 and 0.5:1 wt/wt. Detailed data was reported previously (Tables 7 to 10 of the Final Report on the experimental program).

1. FHRS Model

The FHRS model is a two phase equilibrium program which calculates the equilibrium compositions and relative amounts of the two phases for any specified feed composition at a given temperature and pressure. Initial phase composition estimates are refined until the equilibrium requirement that a component has the same activity in both phases i.e.

$$\ln a_i^1 = \ln a_i^2$$

is satisfied for all components in the system. The logarithm of the molar activity is calculated for all components, in both phases, using the FHRS (Flory-Huggins-Regular Solution) equation.

$$\ln a_i = \frac{v_i}{RT} (\delta_i - \bar{\delta})^2 + \ln\phi_i + 1 - v_i/v$$

V_i and δ_i are the component molar volumes and solubility parameters, respectively; v is the phase molar volume and ϕ_i is the volume fraction of the component in the phase. $\bar{\delta}$ is the volumetric average solubility parameter for the phase.

As is evident from the equation (and as detailed in Appendix I) the component properties influencing the activity, and hence the phase compositions, are the molar volume and solubility parameter.

2. Phase Data Matching

The procedure used was common to all eight of the solvent-VTB systems studied, and involved the following steps: -

(a) For each solvent-oil ratio, the measured weight compositions for the equilibrium phases were converted to a molar basis, and the material balance molar feed composition calculated.

(b) For each system, the molar feed compositions were used in the FHRS model and the component molar volumes and solubility parameters were adjusted systematically to obtain the closest agreement between the calculated phase compositions (K values) and the experimental values at one or more solvent-oil ratios.

(c) For a particular VTB composition, varying levels of solvent were recombined mathematically to produce feed compositions at exact solvent-VTB ratios from 40:1 to 0.5:1. After conversion to mole %, the phase splits and phase compositions were calculated with the FHRS program using the component properties from the matching step (b).

(d) The calculated phase compositions at each of the solvent-VTB ratios were converted back to a mass basis for tabulation and comparison plotting with the experimental data.

With respect to the component properties in step (b), no attempt was made to use 'rational values', except in the case of the solvents for which molar volumes and solubility parameters were calculated at the run conditions. For the remaining components, oils, resins and asphaltenes, the physical significance of any of the molar quantities becomes increasingly tenuous as the distribution of species constituting a 'component' becomes wider. Given this lack of definition, treating the component molar volumes and solubility parameters as straight fitting parameters is justified.

3. Phase Matching Results

Before covering in detail the results of each of the systems matched, some comments about the practical limitations involved in this matching exercise should be made.

(a) Since the phase equilibrium conditions are defined in molar terms, the matching is carried out on this basis. The disparity between the solvent molecular weight and that of the other system components causes distortions which complicate the matching. In molar terms all of the feeds, and the equilibrium phases, tend to be heavily solvent weighted. Feeds usually contain in excess of 90 mole % solvent and, for the high solvent-oil ratios, solvent often exceeds 99 mole %. Performing iterative phase equilibrium calculations under these conditions puts great demands on the numerical stability of the algorithm. Also, what appears as reasonable agreement between calculated and experimental compositions, in molar terms, can become much less reasonable when converted to weight percent (e.g. 70 mole % solvent with 2 mole % asphaltene converts to 10 wt % solvent with 30 wt % asphaltene).

(b) A quaternary system consisting of solvent, oils, resins and asphaltenes has been assumed throughout, and the K values for these four components have been matched. This poses a problem in the case of the asphaltenes, which in most of the runs with propane, butane and pentane are present in the upper phases only in trace quantities. This results in experimental K values which are very small and imprecise, with errors possibly orders of magnitude greater than the quoted K value. Accepting this reality, no effort was made to match the asphaltene K values in such situations. Consequently, the asphaltene-resin split calculated for the lower phase is not to be taken literally.

(c) The final comment concerns the experimental data. Determining the phase compositions, particularly of the lower phases, by material balance on the solvent, is exacting and error-prone given the relative weights of solvent in the two phases. For the Lloydminister experiments, the situation was further complicated by the physical nature of the residue in the lower phase which enhanced the difficulty in obtaining clean separation and analysis of the phase. Some discretion is required in selecting what to match in order to avoid duplicating what ultimately may turn out to be inconsistency rather than reality.

Despite these limitations, matches were obtained for all eight of the systems studied experimentally. These comments will, however, serve to temper the expectations of how much can be achieved, given the complexity of the actual systems and the conceptual simplicity of the model.

3.1 Propane Deasphalting

The calculated phase compositions for solvent-oil ratios from 40:1 down to 0.5:1 are given in Tables 1 and 2 for Lloydminster and Athabasca VTB deasphalting with propane. The compositions were obtained using the component properties listed in Table 3. The data from Tables 1 and 2 are plotted in Figures 1 and 2 with the experimental data points included for comparison. Due to the difficulties with the asphaltene-resin split calculated for the lower phase (Phase 2 in Tables 1 & 2) in systems with nonexistent asphaltene K values, the data are plotted with asphaltenes and resins combined into the single pseudo-ternary component - asphalt. (Corresponding plots with the asphaltenes separated are given in Appendix IV; the lower phase asphaltene/resin ratios in these plots were based on the experimental values, assuming the calculated asphaltenes+resins to be correct.)

In general the agreement between calculated and measured phases is reasonable; for the upper phase it is within the experimental error. In both Athabasca and Lloydminster systems the only major discrepancy is at the high solvent-oil ratio (40:1) where the model is unable to duplicate the extremely low K values (typically less than 0.005) observed for the oils and resins. This translates into a significantly reduced oils content in the calculated lower phase composition.

Reducing the solvent-VTB ratio much below 0.5 indicated a single phase system without closure of the phase envelope - confirming the speculation made in the December Final Report on the experimental work.

3.2 n-Butane Deasphalting

Using the component properties from Table 3, the phase compositions in Tables 1 and 2 were generated for solvent-oil ratios from 40:1 to 0.9:1 for Lloydminster VTB deasphalting with n-butane, and for solvent-oil ratios down to 0.4:1 for Athabasca VTB deasphalting. Figures 3 and 4 are comparison plots of the data in Tables 1 & 2 with the experimental data.

The only problem with matching these systems revolved around how much weight to give the experimental tie lines at solvent-oil ratios below 1. The Athabasca run 28A at 0.5 wt/wt solvent-oil ratio had almost identical oil-resin-asphaltene ratios in the upper and lower phases and these ratios were just about the same as the ratios in the original VTB, suggesting that the system was at, or very close to, a single phase condition. Lloydminster run 32L at 0.9 wt/wt solvent oil ratio was the only deasphalting run in which the lower phase was significantly larger than the upper phase. A replicate run produced the more routine large upper phase and a small lower phase with a different composition from the original run. Again the evidence suggests instabilities associated with a system very close to the phase boundary. As a result of these uncertainties the matching was restricted to the higher solvent-oil ratio runs.

Aside from the low solvent-oil ratio runs (ratios below 1), the agreement between calculated and observed phase compositions is quite satisfactory for both upper and lower phases with the Athabasca and Lloydminster systems. Again there was difficulty for the model predicting the low oil and resin K values observed at the highest solvent-oil ratios, but the discrepancies were smaller, and the effects on the tie lines were less dramatic, than with propane deasphalting.

The model data supports the experimental evidence of proximity to the single phase at solvent-VTB ratios less than 1. Single phases were predicted below 0.9 ratio for Lloydminster and 0.5 for Athabasca. Contrary to the experimental data, the model does not indicate closure of the two phase envelope before the single phase is reached for either system.

3.3 n-Pentane Deasphalting

The calculated phase compositions for solvent-oil ratios from 40:1 down to 0.8:1 are given in Tables 1 and 2 and plotted in Figures 5 and 6 along with the experimental data.

The pentane systems exhibited features significantly different from the lighter solvent systems, and these differences are reflected in the molar volume terms for the oils and resins, in Table 3, required to match the data. For solvent oil ratios of 5 and below the asphaltenes had measurable K values and an effort was made to match them. It was this process that necessitated adjustment of the oils and resins properties and, in the case of Lloydminster, the asphaltene molar volume.

The match obtained for the Athabasca system in Figure 6 is quite reasonable. The model predicts closure of the phase envelope with two short tie lines at solvent-oil ratios of 1 and 0.9. It is noticeable that the model is slightly overpredicting the oils content in the lower phase at these low solvent-oil ratios, while the oils are being underpredicted (K values too high) at the high solvent-oil ratios. This effect is not evident in the Lloydminster system. In the latter case the discrepancies are in the lower liquid phase solvent compositions, with the model 'averaging out' the almost constant level of 20 wt% solvent observed experimentally, but showing more curvature than the experimental data. Recognizing the practical problems that attended the measurement of these lower phase compositions for Lloydminster, the model predictions are probably within the range of experimental error.

3.4 n-Heptane Deasphalting

Phase compositions calculated for solvent-oil ratios from 10:1 down to 1:1, are reported in Tables 1 and 2 and compared to the experimental data in Figures 7 and 8.

Matching these systems with the usual procedure was not feasible given the limited, and sometimes contradictory, nature of the experimental data. The parameters for the oils, resins and asphaltenes were taken from the n-pentane deasphalting matches; the solvent solubility parameter was then increased so that thermodynamically stable phase separation was limited to the range observed experimentally.

The resulting calculated phase compositions agree reasonably well with the experimental tie lines at the lower solvent-oil ratios but indicate lower solvent content in the bottom phase when the solvent-oil ratios exceed 3. For the Lloydminster case, the model prediction may be correct since the experimental tie line at 11.7 solvent-oil ratio with a solvent content of 71.3 wt% in the lower phase is obviously suspect. With the Athabasca system there are also inconsistencies, not as obvious but, nevertheless, still present. The tie line at 11.1 solvent-oil ratio is not in line with the other tie lines; a reduction in the solvent level of the lower phase below 40 wt% is required for consistency. Whether the solvent in the lower phase should be closer to the 30% level indicated by the model will have to remain an open question.

While it may not be possible to reconcile model and observed compositions for the lower liquid phase, it is perhaps worth noting that no such reconciliation is required for the upper phase. Generally there is good agreement between calculation and experiment for the upper phase compositions in both Lloydminster and Athabasca systems.

Propane/VTB wt/wt	40			20			10			5			1			0.5		
	Feed	Phase1	Phase2	Feed	Phase1	Phase2	Feed	Phase1	Phase2	Feed	Phase1	Phase2	Feed	Phase1	Phase2	Feed	Phase1	Phase2
Phase Split mass %		98.501	1.499		98.108	1.892		96.240	3.740		88.780	11.220		44.633	55.367		21.342	78.658
Solvent	96.75	98.11	7.03	94.73	96.38	8.77	90.97	94.03	12.53	83.43	92.06	15.08	50.01	90.17	17.64	33.29	89.97	17.91
Oils	1.38	1.36	3.13	2.79	2.70	7.70	5.39	4.85	19.25	9.84	7.05	31.89	29.52	9.25	45.86	39.27	9.48	47.35
Resins	0.66	0.53	9.30	1.29	0.92	20.89	2.50	1.12	37.78	4.62	0.89	34.15	13.69	0.58	24.25	18.18	0.55	22.96
Asphaltenes	1.21	0.00	80.55	1.19	0.00	62.64	1.14	0.00	30.45	2.12	0.00	16.87	6.78	0.00	12.25	9.27	0.00	11.78
TOTAL		100.00	100.00		100.00	100.00		100.00	100.00		100.00	100.00		100.00	100.00		100.00	100.00

n-Butane/VTB wt/wt	40			20			10			5			1			0.9		
	Feed	Phase1	Phase2	Feed	Phase1	Phase2	Feed	Phase1	Phase2	Feed	Phase1	Phase2	Feed	Phase1	Phase2	Feed	Phase1	Phase2
Phase Split mass %		99.028	0.972		98.951	1.049		97.415	2.585		94.020	5.980		43.600	56.400		39.162	60.838
Solvent	97.00	97.87	8.39	94.97	95.87	9.47	90.41	92.49	11.81	83.24	87.46	16.88	50.01	78.43	28.04	47.18	79.54	26.35
Oils	1.41	1.40	1.69	2.82	2.81	3.67	5.34	5.27	7.95	9.80	9.32	17.30	29.50	18.42	38.06	28.42	17.23	35.62
Resins	0.67	0.64	3.87	1.31	1.24	8.02	2.52	2.17	15.59	4.54	3.18	26.03	13.63	3.12	21.75	15.38	3.19	23.23
Asphaltenes	0.92	0.08	86.04	0.90	0.07	78.83	1.73	0.06	64.64	2.42	0.04	39.78	6.86	0.03	12.14	9.01	0.03	14.79
TOTAL		100.00	100.00		100.00	100.00		100.00	100.00		100.00	100.00		100.00	100.00		100.00	100.00

n-Pentane/VTB wt/wt	40			20			10			5			1			0.8		
	Feed	Phase1	Phase2	Feed	Phase1	Phase2	Feed	Phase1	Phase2	Feed	Phase1	Phase2	Feed	Phase1	Phase2	Feed	Phase1	Phase2
Phase Split mass %		99.659	0.341		99.260	0.740		98.431	1.569		96.670	3.330		77.708	22.292		69.969	30.031
Solvent	97.56	97.84	13.17	95.21	95.82	13.51	90.90	92.12	14.19	83.32	85.66	15.53	49.98	57.23	24.71	44.43	51.80	27.24
Oils	1.44	1.44	1.26	2.83	2.84	2.49	5.37	5.38	4.82	9.84	9.87	9.09	29.51	29.61	29.17	32.79	32.90	32.52
Resins	0.67	0.66	1.54	1.30	1.29	2.96	2.48	2.44	5.49	4.56	4.39	9.49	13.66	12.23	18.63	15.17	13.64	18.75
Asphaltenes	0.34	0.05	84.04	0.65	0.05	81.05	1.25	0.06	75.49	2.28	0.09	65.88	6.85	0.93	27.50	7.61	1.66	21.49
TOTAL		100.00	100.00		100.00	100.00		100.00	100.00		100.00	100.00		100.00	100.00		100.00	100.00

n-Heptane/VTB wt/wt	10			5			4			3		
	Feed	Phase1	Phase2	Feed	Phase1	Phase2	Feed	Phase1	Phase2	Feed	Phase1	Phase2
Phase Split mass %		99.955	0.045		99.342	0.658		99.298	0.702		98.849	1.151
Solvent	90.91	90.94	29.86	83.33	83.67	33.15	80.00	80.32	34.85	74.58	75.01	37.83
Oils	5.36	5.36	5.12	9.83	9.84	9.48	11.79	11.79	11.41	14.67	14.67	14.30
Resins	2.48	2.48	3.96	4.55	4.54	6.71	5.45	5.43	7.72	6.83	6.80	9.09
Asphaltenes	1.25	1.22	61.06	2.28	1.96	50.66	2.77	2.46	46.01	3.93	3.52	38.78
TOTAL		100.00	100.00		100.00	100.00		100.00	100.00		100.00	100.00

CALCULATED PHASE COMPOSITIONS -- DEASPHALTING LLOYDMINSTER VTB

TABLE 1

Lloydminster VTB

Propane/VTB wt/wt	40			20			10			5			1			0.5		
	Feed	Phase1	Phase2	Feed	Phase1	Phase2	Feed	Phase1	Phase2	Feed	Phase1	Phase2	Feed	Phase1	Phase2	Feed	Phase1	Phase2
Phase Split mass %		97.997	2.003		96.841	3.159		92.651	7.349		85.074	14.926		45.671	54.329		25.414	74.586
Solvent	96.83	98.66	7.20	94.89	97.71	8.67	90.31	96.71	9.65	83.09	95.74	11.02	49.99	94.87	12.27	33.36	94.77	12.43
Oils	1.08	1.00	4.72	2.19	1.90	11.03	4.12	2.96	18.75	7.63	3.98	28.42	23.00	4.92	38.20	30.69	5.02	39.43
Resins	0.88	0.33	27.62	1.73	0.39	42.73	3.30	0.33	40.72	6.12	0.28	39.42	18.29	0.21	33.48	24.46	0.21	32.73
Asphaltenes	1.21	0.00	60.45	1.19	0.00	37.57	2.27	0.00	30.88	3.16	0.00	21.14	8.72	0.00	16.05	11.49	0.00	15.41
TOTAL		100.00	100.00		100.00	100.00		100.00	100.00		100.00	100.00		100.00	100.00		100.00	100.00

n-Butane/VTB wt/wt	40			20			10			5			1			0.5		
	Feed	Phase1	Phase2	Feed	Phase1	Phase2	Feed	Phase1	Phase2	Feed	Phase1	Phase2	Feed	Phase1	Phase2	Feed	Phase1	Phase2
Phase Split mass %		98.784	1.216		98.259	1.741		95.075	4.925		87.436	12.564		44.819	55.181		21.676	78.324
Solvent	97.13	98.22	8.56	95.10	96.60	10.39	90.76	94.82	12.30	83.02	92.91	14.19	49.91	90.12	17.25	33.38	89.70	17.80
Oils	1.11	1.10	2.64	2.19	2.12	6.15	4.20	3.77	12.47	7.65	5.78	20.71	22.94	8.84	34.39	30.72	9.31	36.65
Resins	0.84	0.69	13.15	1.81	1.29	31.39	3.31	1.41	39.99	6.12	1.31	39.59	18.32	1.04	32.36	24.53	0.99	31.04
Asphaltenes	0.92	0.00	75.65	0.91	0.00	52.07	1.74	0.00	35.24	3.21	0.00	25.52	8.83	0.00	16.00	11.37	0.00	14.51
TOTAL		100.00	100.00		100.00	100.00		100.00	100.00		100.00	100.00		100.00	100.00		100.00	100.00

n-Pentane/VTB wt/wt	40			20			10			5			1			0.9		
	Feed	Phase1	Phase2	Feed	Phase1	Phase2	Feed	Phase1	Phase2	Feed	Phase1	Phase2	Feed	Phase1	Phase2	Feed	Phase1	Phase2
Phase Split mass %		99.640	0.360		99.100	0.900		97.956	2.044		95.418	4.582		61.628	38.372		51.630	48.370
Solvent	97.56	97.85	19.20	95.24	95.93	19.83	90.95	92.41	21.05	83.34	86.22	23.37	50.02	56.86	39.03	47.39	52.38	42.05
Oils	1.12	1.12	0.97	2.19	2.19	1.92	4.18	4.19	3.75	7.66	7.68	7.10	22.98	23.07	22.83	24.19	24.27	24.10
Resins	0.89	0.89	2.09	1.75	1.73	4.00	3.30	3.22	7.25	6.12	5.82	12.35	18.35	16.64	21.11	19.32	18.06	20.66
Asphaltenes	0.42	0.14	77.74	0.82	0.16	74.25	1.57	0.19	67.96	2.89	0.28	57.18	8.65	3.43	17.03	9.11	5.28	13.19
TOTAL		100.00	100.00		100.00	100.00		100.00	100.00		100.00	100.00		100.00	100.00		100.00	100.00

n-Heptane/VTB wt/wt	10			5			2		
	Feed	Phase1	Phase2	Feed	Phase1	Phase2	Feed	Phase1	Phase2
Phase Split mass %		98.581	1.419		97.965	2.035		95.871	4.129
Solvent	90.52	91.36	32.23	83.37	84.36	35.71	66.72	67.60	46.31
Oils	4.15	4.15	3.87	7.68	7.69	7.29	13.82	13.83	13.56
Resins	3.31	3.27	5.68	6.11	6.04	9.58	12.73	12.61	15.51
Asphaltenes	2.02	1.21	58.22	2.84	1.91	47.42	6.73	5.95	24.62
TOTAL		100.00	100.00		100.00	100.00		100.00	100.00

CALCULATED PHASE COMPOSITIONS -- DEASPHALTING ATHABASCA VTB

TABLE 2

Athabasca VTB

TABLE 3

FHRS Model - Matching Parameters

Temp °C	Press PSIA	Solvent	Solvent Vm	Solvent SP	Oils Vm	Oils SP	Resins Vm	Resins SP	Asphaltenes Vm	Asphaltenes SP
Lloydminster										
75	465	C_3	120	4.67	550	7.35	1100	7.35	3200	7.35
120	415	C_4	140	4.90	550	7.40	1100	7.45	3000	7.45
160	365	C_5	150	4.95	350	7.42	800	7.45	4000	7.45
75	65	C_7	150	5.41	350	7.42	800	7.45	4000	7.45
Athabasca										
75	465	C_3	119	4.60	550	7.40	1100	7.45	4200	7.45
120	415	C_4	140	4.75	550	7.40	1100	7.45	4200	7.45
160	365	C_5	140	4.96	350	7.35	900	7.42	4200	7.42
75	65	C_7	150	5.39	350	7.35	900	7.42	4200	7.42

Vm = Molar volume
SP = Solubility Parameter

FIGURE 1

Lloydminster - C3
75C 465 PSIA

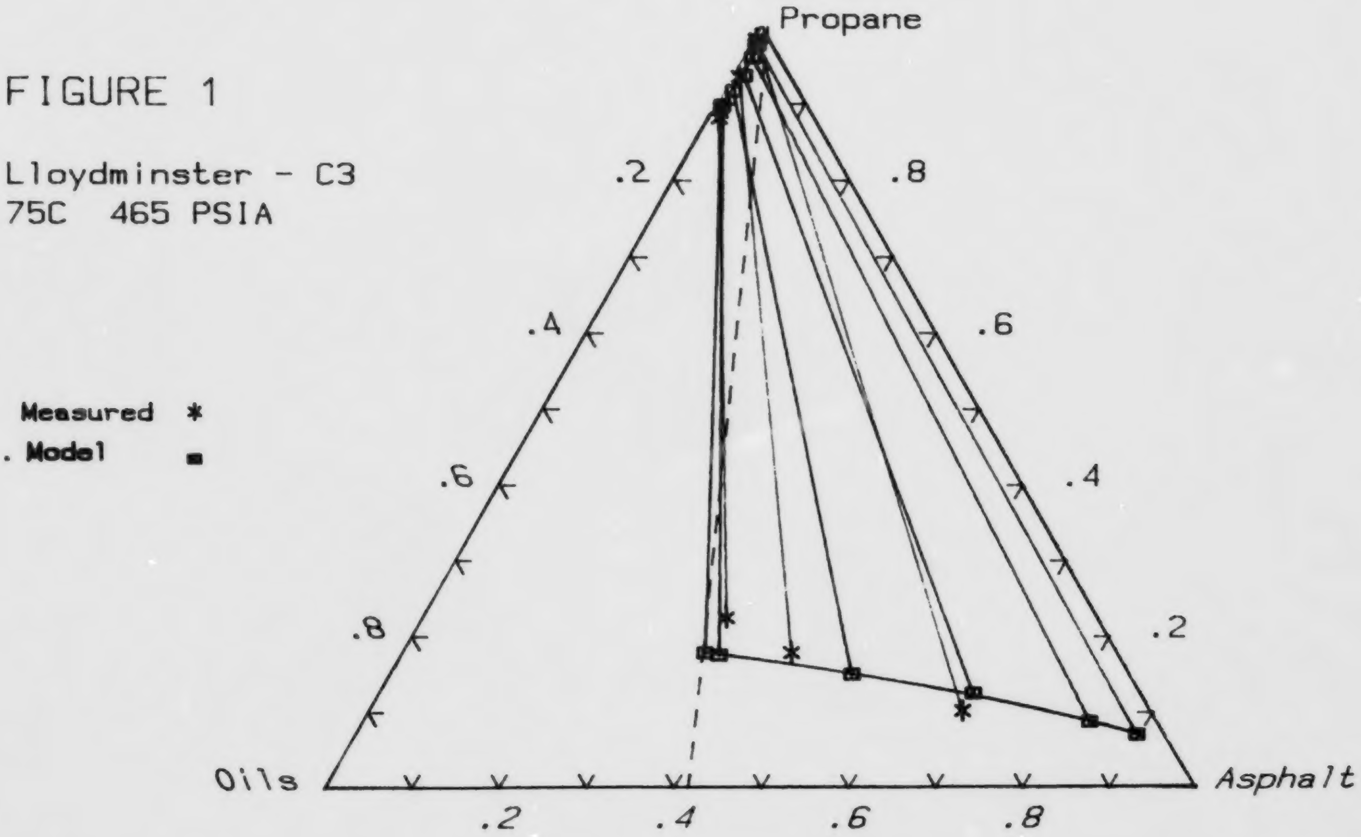

FIGURE 2

Athabasca - C3
75C 465 PSIA

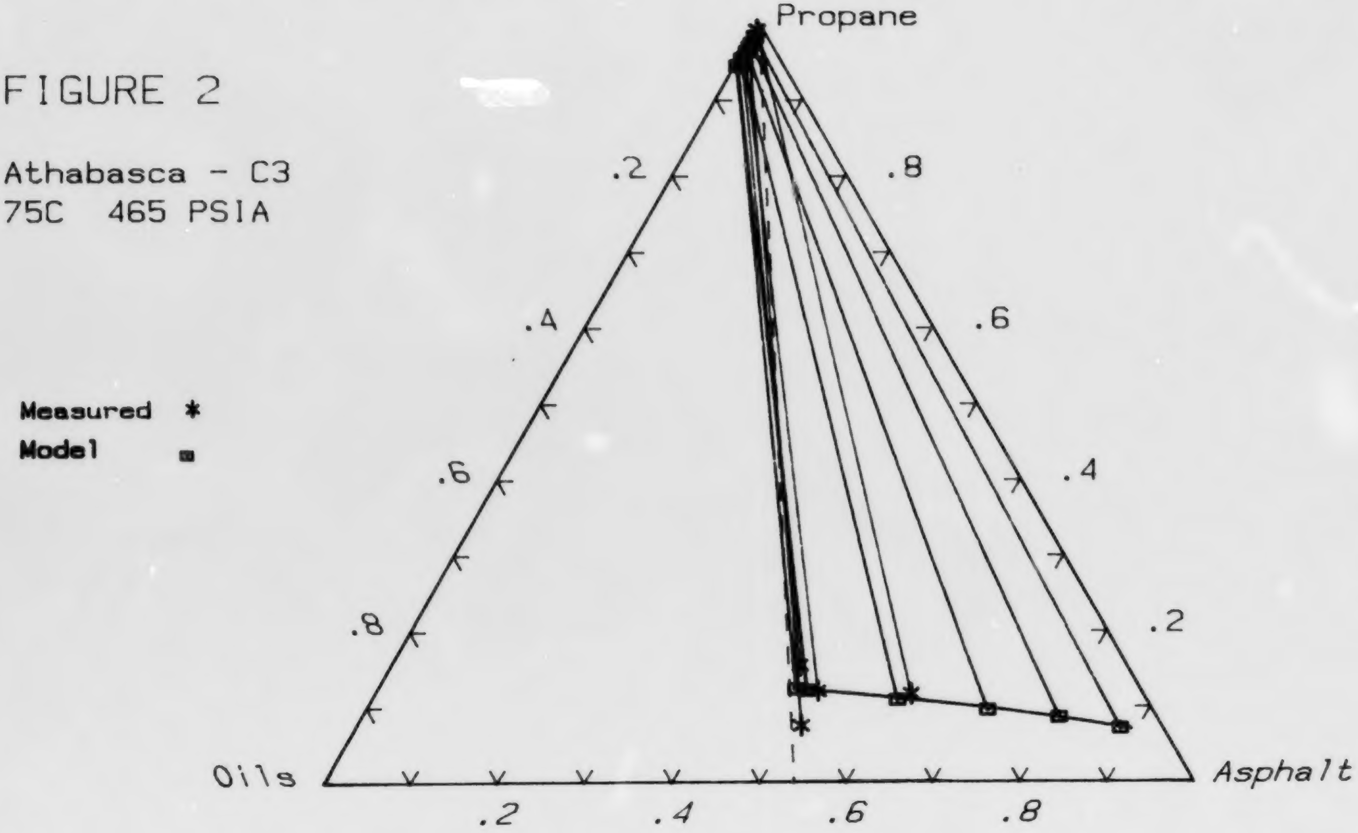

FIGURE 3

Lloydminster - C4
120C 415 PSIA

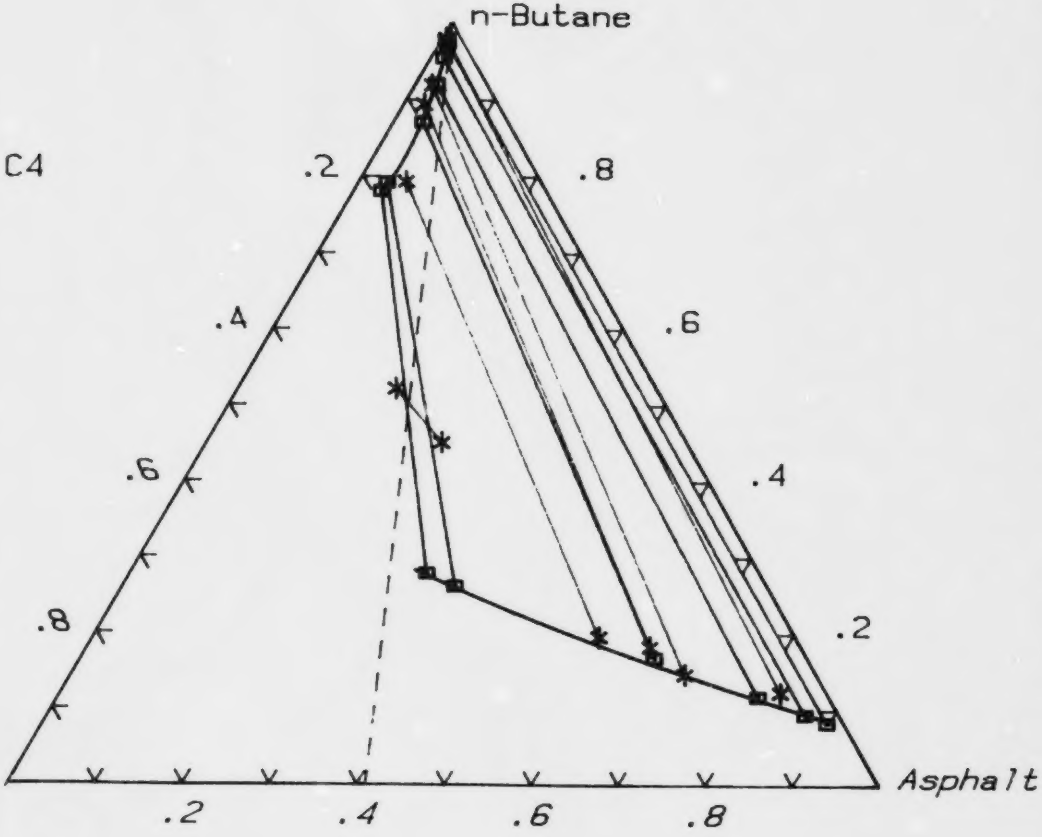

FIGURE 4

Athabasca - C4
120C 415 PSIA

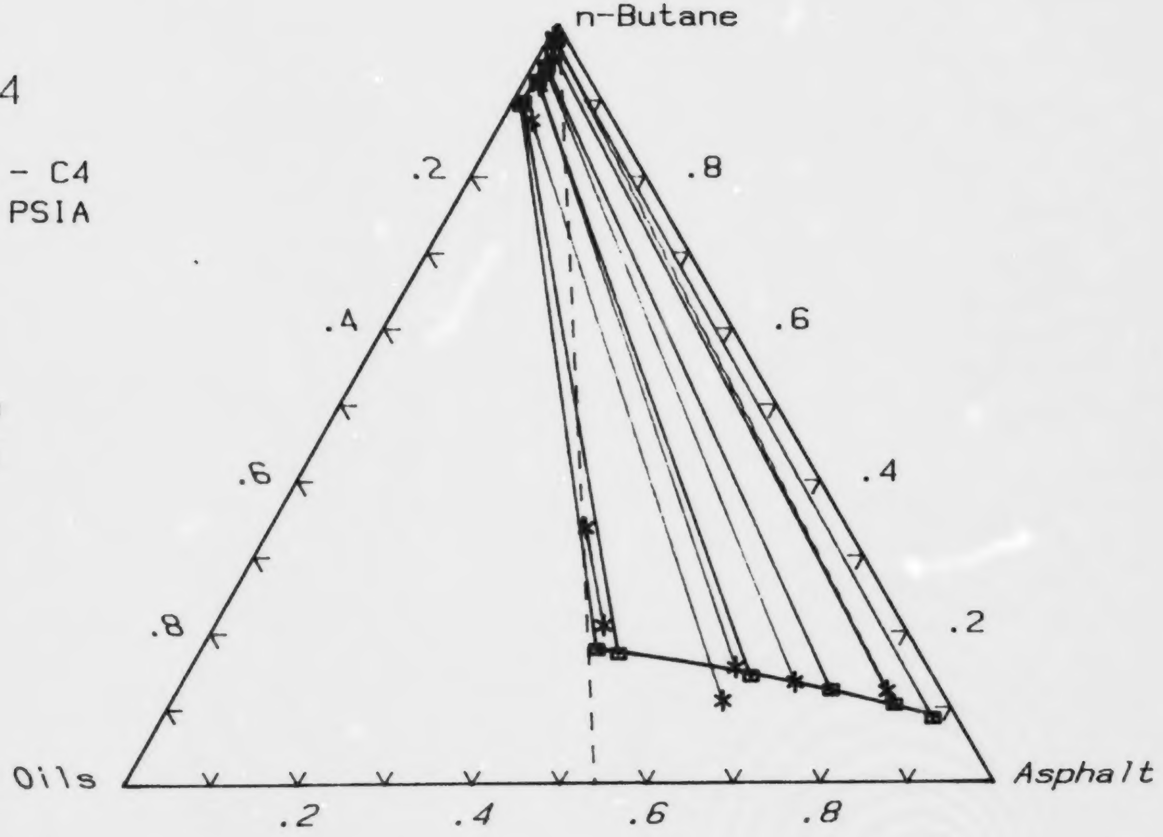

FIGURE 5

Lloydminster - C5
160C 365 PSIA

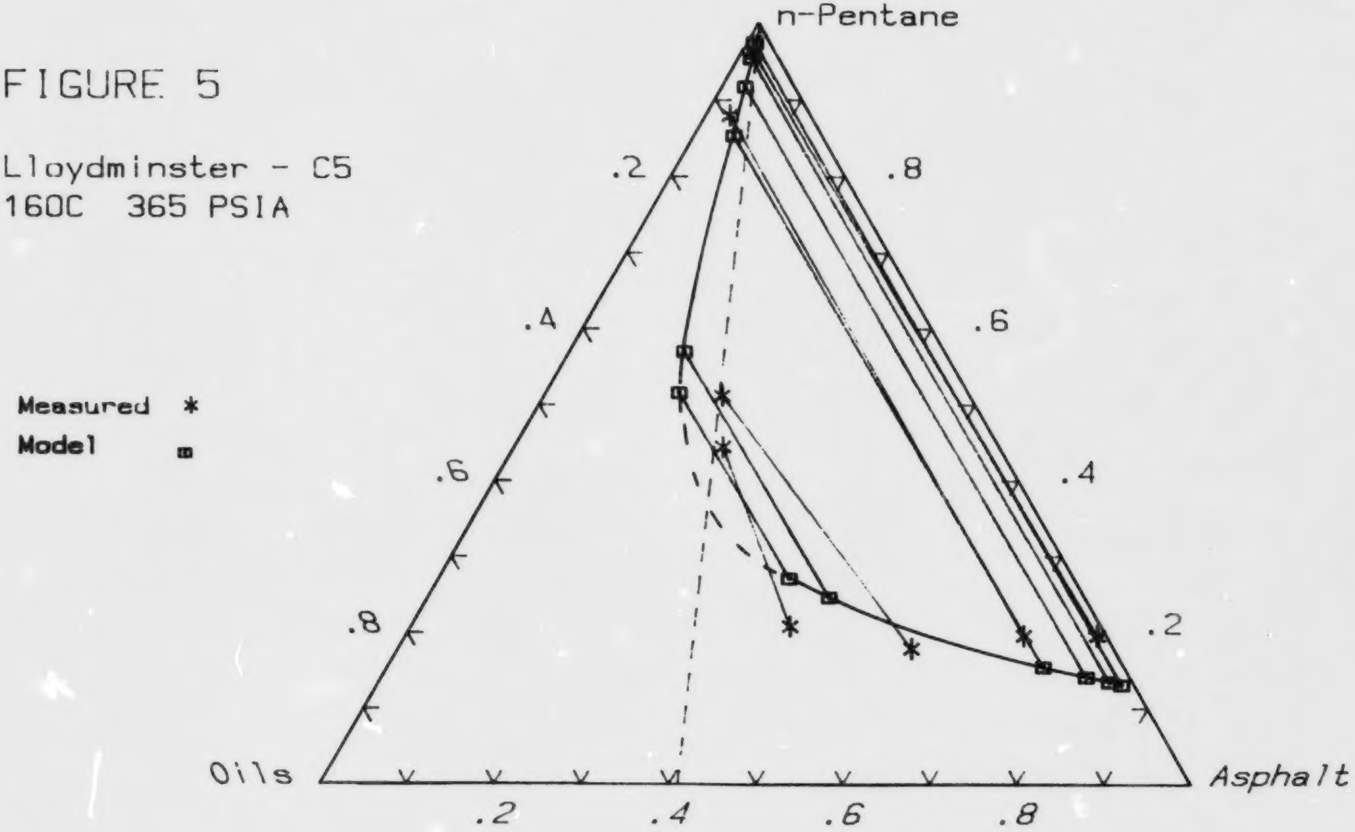

FIGURE 6

Athabasca - C5
160C 365 PSIA

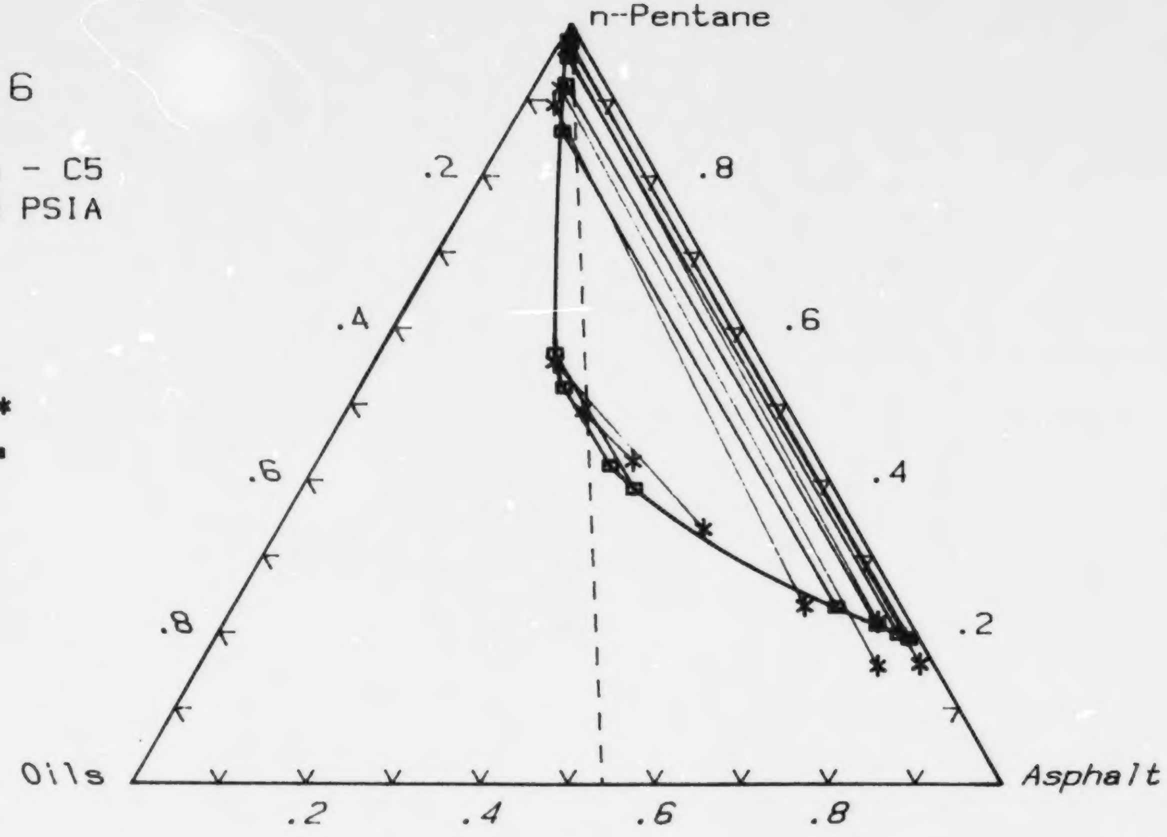

FIGURE 7

Lloydminster - C7
75C 65 PSIA

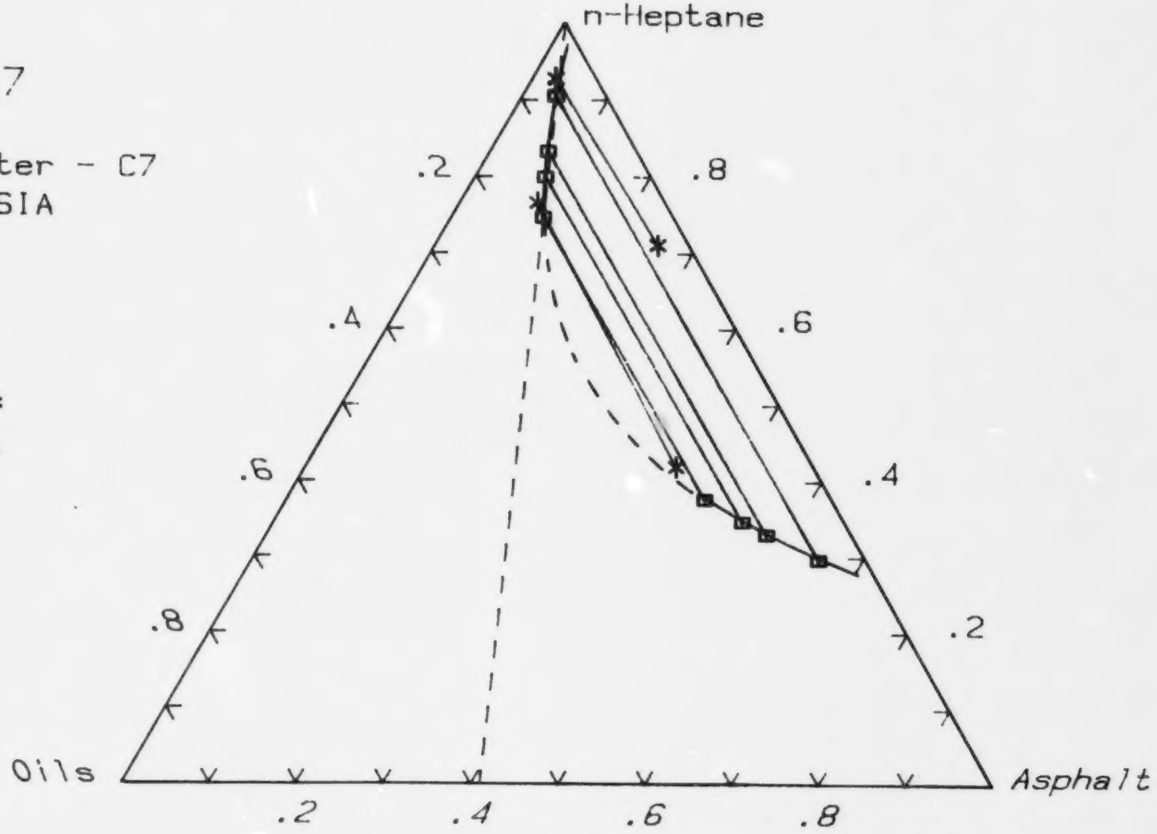

FIGURE 8

Athabasca - C7
75C 65 PSIA

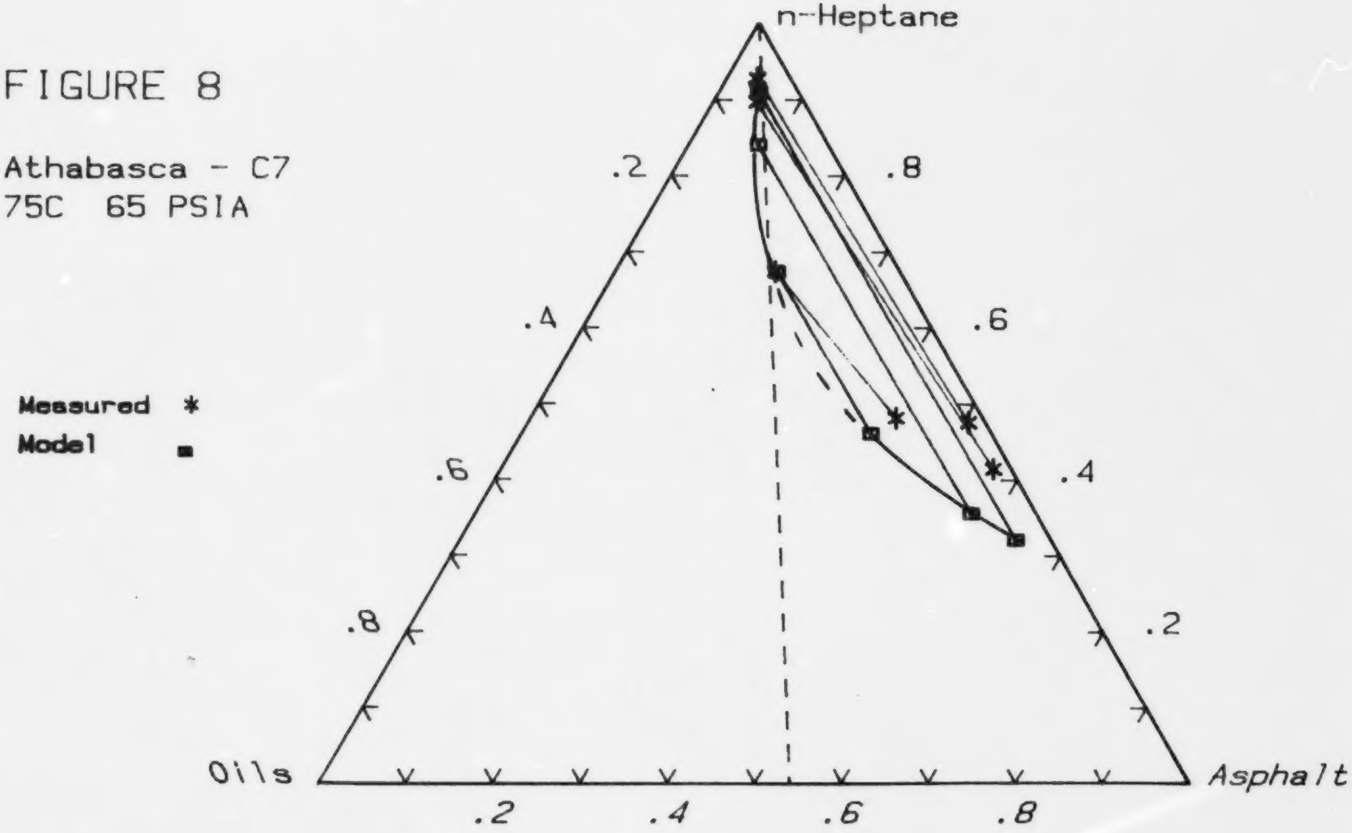

TASK 8B -- FCC Rate Constants for Deasphalted Oils

The FCC kinetic model of Weekman and Nace was fitted to the experimental MAT data from 29 deasphalted (DA) oils and 2 vacuum gas oils (VGO) from Lloydminster heavy oil and Athabasca bitumen reported previously, to derive rate content parameters for gas oil cracking, gasoline formation and cracking, and catalyst activity decay.

1. Model and Fitting Procedure

The Weekman-Nace model for gas oil cracking and the resulting equations applicable to a fixed bed reactor, as used in microactivity testing, are summarized in Appendix II. The nonlinear regression procedure used to fit the Weekman-Nace equations to the experimental data and to calculate the rate constant parameters is also outlined in Appendix II.

2. Results

The rate constant parameters and parameter ratios are given for the VGO and C_3 DA oils in Table 4, which also contains the average values for the C_4 to C_7 DA oils. Details for the individual C_4, C_5 and C_7 DA oils are given in Tables 5-7.

3. Discussion

Referring to the average rate constant parameters listed in Table 4, the general trend is for all the rate constants to increase as the progression is made to the heavier solvents - DA oils. In order to discriminate between feeds, and crude sources, it is therefore necessary to compare the ratios rather than the individual rate constants.

The decay ratios for the DA oils are generally less than for the corresponding VGO, but with the heavier feeds the selectivity ratio also decreases, an indication that the increased cracking rate is a result of direct cracking to coke and gas rather than to gasoline. Comparing the Lloydminster and Athabasca feeds, the Lloydminster oils in every case have superior decay and selectivity ratios over the corresponding Athabasca feeds, due to the propensity of the latter for coking rather than gasoline cracking.

For both Lloydminster and Athabasca, the propane deasphalted oils have cracking characteristics comparable to, or better than, the parent gas oil. For the C_4 and C_5 DA oils there is noticeably more coking and loss of selectivity (Note: Rate constants for feeds 32, 28 and 24, which had significant asphaltenes content, were obviously atypical and were omitted from the averages in Table 4). The C_7 DA feeds all contained proportions of asphaltenes; the Athabasca feeds have noticeably poorer selectivity, with coking and gasoline cracking occurring at almost the same rates.

One effect of the increase in direct cracking of the gas oil to coke and gas appears to be some inhibition of gasoline cracking. The gasoline formation ratios for the Athabasca feeds are generally greater than those for Lloydminster, despite the lower rate constants for gasoline formation with most of the Athabasca feeds. These lower formation rates are more than offset by the lower gasoline cracking rates.

TABLE 4

SUMMARY OF WEEKMAN-NACE RATE CONSTANTS

Averages for DA Oils at 510 C

```
        K1                  K2
GO --------->Gasoline -------> Gas+coke
 :                                ^
 :              K3                :
 :                                :
 :--------------------------------:
```

K0 = K1 + K3

FEED		K0 hr-1	Alpha hr-1	K1 hr-1	K2 hr-1	K3 hr-1	Decay Ratio Alph/K0	Selectivity Ratio K1/K0	Cracking Ratio K2/K3	Gasoline Formation K1/K2
Lloyd	VGO	76.7	76.7	71.7	12.5	5.0	1.00	0.93	2.50	5.7
	C3	106.0	84.3	96.6	16.5	9.4	0.79	0.91	1.76	5.9
	C4	118.8	125.8	99.1	18.6	19.7	1.06	0.83	0.94	5.3
	C5	132.1	131.1	100.2	18.2	31.9	0.99	0.76	0.57	5.5
	C7	139.6	117.5	108.3	23.7	31.3	0.84	0.78	0.76	4.6
Athabasca	VGO	64.4	125.6	56.6	16.5	7.8	1.95	0.88	2.12	3.4
	C3	128.0	140.4	108.4	16.9	19.6	1.10	0.85	0.86	6.4
	C4	111.9	143.1	85.3	17.0	26.6	1.28	0.76	0.64	5.0
	C5	134.7	147.5	84.7	12.6	50.0	1.10	0.63	0.25	6.7
	C7	163.0	138.2	90.3	14.4	72.7	0.85	0.55	0.20	6.3

TABLE 5

SUMMARY OF WEEKMAN-NACE RATE CONSTANTS

n-Butane DA Oils at 510 C

FEED	K0 hr-1	Alpha hr-1	K1 hr-1	K2 hr-1	K3 hr-1	Decay Ratio Alph/K0	Selectivity Ratio K1/K0	Cracking Ratio K2/K3	Gasoline Formation K1/K2
Lloyd C4 23	110.7	111.2	94.8	18.9	15.9	1.00	0.86	1.19	5.0
20	125.3	130.2	99.0	15.5	26.3	1.04	0.79	0.59	6.4
22	135.7	125.4	120.7	23.5	15.0	0.92	0.89	1.56	5.1
32	163.4	156.5	105.9	11.3	57.5	0.96	0.65	0.20	9.4
21	114.4	131.1	104.1	24.4	10.3	1.15	0.91	2.37	4.3
37	108.0	130.9	76.9	10.6	31.1	1.21	0.71	0.34	7.2
Athab C4 23	119.1	133.7	90.2	17.6	28.9	1.12	0.76	0.61	5.1
20	105.2	136.3	90.2	23.2	15.0	1.30	0.86	1.54	3.9
22	117.3	133.0	91.4	16.9	25.9	1.13	0.78	0.65	5.4
28	124.0	91.8	64.8	10.8	59.2	0.74	0.52	0.18	6.0
21	100.1	147.1	79.2	18.4	20.9	1.47	0.79	0.88	4.3
37	117.9	165.4	75.7	8.8	42.2	1.40	0.64	0.21	8.6

TABLE 6

SUMMARY OF WEEKMAN-NACE RATE CONSTANTS

n-Pentane DA Oils at 510 C

FEED	K0 hr-1	Alpha hr-1	K1 hr-1	K2 hr-1	K3 hr-1	Decay Ratio Alph/K0	Selectivity Ratio K1/K0	Cracking Ratio K2/K3	Gasoline Formation K1/K2
Lloyd C5 19	119.3	120.1	90.2	17.2	29.1	1.01	0.76	0.59	5.2
24	121.0	95.4	78.2	12.8	42.8	0.79	0.65	0.30	6.1
10	133.0	121.5	111.1	25.2	21.9	0.91	0.84	1.15	4.4
38	143.9	151.7	99.3	12.3	44.6	1.05	0.69	0.28	8.1
Athab C5 19	118.4	129.1	83.4	18.6	35.0	1.09	0.70	0.53	4.5
24	142.7	126.7	62.7	0.0	80.0	0.89	0.44	0.00	NA
39	137.9	161.4	79.0	5.9	58.9	1.17	0.57	0.10	13.4
10	127.4	127.7	77.4	11.4	50.0	1.00	0.61	0.23	6.8
38	155.1	171.8	99.0	14.4	56.1	1.11	0.64	0.26	6.9

TABLE 7

SUMMARY OF WEEKMAN-NACE RATE CONSTANTS

n-Heptane DA Oils at 510 C

FEED	K0 hr-1	Alpha hr-1	K1 hr-1	K2 hr-1	K3 hr-1	Decay Ratio Alph/K0	Selectivity Ratio K1/K0	Cracking Ratio K2/K3	Gasoline Formation K1/K2
Lloyd C7 14	132.3	104.3	102.1	22.6	30.2	0.79	0.77	0.75	4.5
31	147.2	142.4	102.3	18.6	44.9	0.97	0.69	0.41	5.5
15	139.4	105.7	120.5	30.0	18.9	0.76	0.86	1.59	4.0
Athab C7 14	151.8	128.4	92.2	18.1	59.6	0.85	0.61	0.30	5.1
40	168.6	148.6	81.0	6.5	87.6	0.88	0.48	0.07	12.5
15	168.7	137.7	97.7	18.3	71.0	0.82	0.58	0.26	5.4

Task 8C Riser FCCU Simulations

The STA FCCU kinetic riser model has been used to simulate cracking under commercial conditions for four feeds: IPL and Lloydminster vacuum gas oils (VGO) plus two deasphalted oils (DAO) obtained by propane (Feed 5) and butane (Feed 20) deasphalting of Lloydminster vacuum tower bottoms (VTB).

1. STA FCCU Model

The STA FCCU model consists of four linked units. A feed-catalyst mixing section is followed by a dilute phase riser where the conversion, debutanized gasoline yield and temperature profiles are determined from the reaction kinetics. A heat balance is carried out in the stripper-regenerator section to determine the temperature of the circulating catalyst before it returns to the feed-catalyst mixing section, at the base of the riser, through an optional flow control slide valve. A detailed description of each unit is given in Appendix III. Various modes of operation are possible with the model:

(a) Riser Profiles

A single pass through the mixing section and riser is used to generate profiles of conversion, temperature and gasoline yield along the riser, together with design information such as catalyst and vapour residence times, catalyst hold-up volumes and slip factors. This mode is generally used once the heat balanced operating conditions are known, in order to examine riser profiles for optimization potential. Adiabatic riser operation may be simulated by setting the heat loss term to zero. Even simpler, both the heat loss and heat of reaction terms may be set to zero to simulate the isothermal conditions frequently met with in pilot unit or laboratory operations.

(b) Heat Balanced Unit

Starting with an estimate of the circulating catalyst temperature, successive passes through the mixing section-riser-stripper-regenerator circuit are made until the catalyst temperature from the regenerator is constant and the unit is heat balanced.

(c) Slide Valve Option

Once the unit is heat balanced, the catalyst circulation rate is adjusted to bring the riser exit temperature, or the feed conversion level, to some target value. After each adjustment a new heat balance condition is established.

2. FCC Unit Description

The basis for comparing the test feeds was a nominal 60,000 BPD conventional riser-regenerator unit operating under typical conditions for processing VGO from Western Canadian crude. Since laboratory data for all feeds tested was available at 510°C, this was taken as the operating temperature at the riser exit. Details of the unit dimensions and conditions common to all simulations, based on actual design or operating practice, are given in Table 8, along with the catalyst and feed properties.

For a valid comparison of different feeds, it is important that the vapour velocity in the riser be maintained close to the design value of 50 ft/sec. Preliminary calculations were made to establish the correct rate for each feed to satisfy this requirement, based on the feed density and the vapour density at the anticipated conversion level. The feed rates are listed along with the results in Tables 12 and 13.

3. Feed Characterization

In the riser simulation, the feed is characterized by the rate constants for overall cracking, catalyst activity decay, gasoline formation and cracking. These were determined from laboratory cracking data using the Weekman-Nace reaction scheme. It should be noted that the riser model uses actual chemical rate constants, k, rather than the lumped constant, K, defined by Weekman and Nace for catalyst bed applications. Also, the rate constants are required in the Arrhenius form i.e.

$$k = A \exp(-E/RT)$$

defined by the pre-exponential factor, A, and activation energy, E. As the laboratory measurements for the test feeds were available at only one temperature, it was necessary to assume common activation energies for all the feeds, and then to calculate the factors A from the rate constants derived at 510°C. The values of A, E and the various rate constants, k, are listed for each feed in Table 9.

Other feed characterization parameters used in the riser model, i.e. Voorhies coke equation constants and coefficients in the correlations for the relative yields of dry gas and C_3C_4 in the gas make are listed in Tables 10 and 11. These parameters were obtained by fitting MAT data for the individual feeds.

4. Results

The IPL feed was run first to establish a base case and to check that the conditions listed in Table 1 did lead to a realistic simulation in terms of predicted yields, temperatures and flow rates. Once this had been verified the remaining three feeds were compared under two sets of conditions.

In the first set, the regenerator temperature was controlled at the same operating level predicted for the IPL feed, by withdrawing any excess heat from the regenerator using quench steam. Usually an FCC unit is operated so that the regenerator temperature stays within a reasonable range around its 'normal' operating point. For the purposes of this comparison, it was assumed that the regenerator temperature operating with IPL was normal, but to keep the comparison completely equitable, no deviation from this norm was allowed for the other feeds. The results are compared in Table 12.

In the second set, no restriction was placed on regenerator temperature, in effect assuming operation in different units - or at least with different regenerators - for those feeds exhibiting large deviations in operating conditions from the IPL base case. These results are set out in Table 13.

5. Discussion

Before making a detailed comparison of the results in Tables 12 and 13, some general observations can be made. In order to stay close to the design velocity of 50 ft/sec. in the riser, the throughput of heavier feeds has to be reduced by a significant margin. While there is a variation of about 6% in the final actual velocities, the variation in feed rates necessary to maintain this range is nearly 17%. This factor should be kept in mind when comparing the yields as a percentage of feed. A second observation, usually surprising initially, is the extremely short duration of reaction. While the vapour residence time is the order of 2 seconds, any given volume of vapour will be in contact with catalyst for only 30 - 40 milliseconds of its traverse of the riser. Upon reflection that the vapour occupies, typically, 97% of the volume in the riser, while the catalyst is limited to the remaining 3% of the volume, it is not difficult to visualise why the reaction times are so short.

5(a) Simulations at Constant Regenerator Conditions

As a result of the constant regenerator temperature the catalyst/oil ratio for all feeds is virtually constant. This leads to high coke yields on fresh feed for the two deasphalted feeds because of the increased coke on the spent catalyst produced by these feeds.

Comparing the Lloydminister and IPL gas oils, it is evident that Lloydminster is harder to crack, resulting in a lower conversion, gasoline yield and coke and gas make. This is not true of the deasphalted feeds which show high conversions with increasing degrees of overcracking leading to high coke and gas production at the expense of debutanized gasoline.

5(b) Unconstrained Regenerator Operation

Removing the regenerator temperature constraint has essentially no effect on the Lloydminster VGO which operates under almost the same conditions as the IPL gas oil. Given that the level of coke on spent catalyst is the same for these two feeds this might be expected.

As the coke on spent catalyst increases, with the deasphalted feeds, more heat is produced during regeneration raising the regenerator temperature and causing a reduction in the catalyst circulation rate required to satisfy the heat duty in the riser. This has two beneficial effects. Since the catalyst/oil ratio is lower, there is a corresponding decrease in the yield of coke on fresh feed. Also, the catalyst holdup volume in the riser decreases, lowering the vapour - catalyst contact time and reducing the overcracking evident at lower regenerator temperatures. This results in a noticeable improvement in the gasoline yield for the C_3 DAO and a significant increase for the C_4 DAO. At the same time, the yields of dry gas and C_3C_4 are lowered by virtue of the moderation in overall conversion.

Under the conditions listed in Table 13, the yields for the C_3 DAO are approaching those of the parent gas oil. For the C_4 DAO further optimization of conditions could give the required improvement, although the high regenerator temperatures associated with this feed would necessitate special regenerator design considerations. It is probable that the full potential of both deasphalted oils will only be realized in a unit designed for high temperature regeneration, where the high coke on spent catalyst, characteristic of these feeds, would be less of a liability.

TABLE 8(i)

FCCU Riser Dimensions and Operating Conditions

Riser Conditons	
Length, ft.	110
Diameter, ft.	4.42
Throughput, BPD	60,000
Riser pressure, PSIG	25
Vapour velocity, ft/s	50
Feed preheat, °C	350
Dispersion steam	0.015 x Feed rate
Pressure, PSIG	50
Heat loss, cal/g feed	5
Regenerator/Stripper Conditions	
Stripping steam	.003 x catalyst circulation
Pressure, PSIG	50
Air inlet temp., °C	150
Air moisture, wt. %	1.3
Regenerator pressure, PSIG	20
Flue gas, CO/CO_2	0.66
Regenerated catalyst coke, wt%	0.2
Heat loss, kcal/hour	3×10^6
Catalyst Properties	
Bulk density, g/cm^3	0.93
Particle density, g/cm^3	1.43
Fall velocity ft/s	2
Specific heat, cal/(g. °C)	0.26
Miscellaneous	
Enthalpy of cracking, cal/g feed	120
Feed vapour	
Specific heat, cal/(g. °C)	0.75

TABLE 8(ii)

Feed Characterization Properties

Feed	API Gravity	Watson K Factor	Molar Mass
IPL	24.2	12.0	410
Lloydminster	21.1	11.5	332
C3 DAO, 5	19.2	11.8	440
C4 DAO, 20	13.8	11.5	470

TABLE 9

Rate Constants (510°C) and Arrhenius Parameters

$$k = A \exp(-E/RT)$$

Feed	Overall Cracking	Catalyst Decay	Gasoline Formation	Gasoline Cracking
1. Rate Constant k, hr-1				
IPL	201 E03	92.6	227 E03	42.7E03
Lloydminister	154 E03	95.2	163 E03	34.9E03
C3 DAO, 5	239 E03	104.5	252 E03	51.1E03
C4 DAO,20	346 E03	172.7	330 E03	62.5E03
2. Pre-Exponent, A				
IPL	5.44E08	12.63	1.09E09	1.08E08
Lloydminister	4.17E08	13.55	7.82E08	8.86E07
C3 DAO, 5	6.48E08	14.25	1.22E09	1.30E08
C4 DAO,20	9.36E08	23.56	1.59E09	1.58E08
3. Activation Energy E, kcal/mole				
All feeds	12.3	-3.1	13.2	12.2

TABLE 10

Voorhies Parameters

$$m_s = A_v t^n$$

Feed	A_v	n
IPL	0.59	0.29
Lloydminster	0.62	0.23
C3 DAO,5	0.71	0.25
C4 DAO,20	0.91	0.29

Note: A_v factors include contribution of coke on regenerated catalyst.

TABLE 11

Gas Yield Correlation Coefficients

Yield % = A1 + A2.Conv + A3.Con Carb + A4.T

	Feed	A1	A2	A3	A4
1.	Dry Gas				
	IPL	-7.827	0.050	0.0	0.012
	Lloydminster	-4.143	0.1044	0.088	0.0
	C3 DAO, 5	-3.100	0.1044	0.088	0.0
	C4 DAO, 20	-2.070	0.1044	0.088	0.0
2.	C3C4				
	IPL	-36.092	0.3710	0.0	0.047
	Lloydminster	-7.859	0.3022	-0.3300	0.0
	C3 DAO,5	-5.495	0.3008	-0.3902	0.0
	C4 DAO,20	-5.095	0.3008	-0.3902	0.0

TABLE 12

OPERATE TO 510 C RISER EXIT, REGENERATOR 662 C

	IPL VGO	LLOYD VGO	C3 DAO 5	C4 DAO 20
Regenerator Conditions				
Temperature, C	662	662	662	662
Dry Air Rate, 1000kg/hr	234	219	226	230
Flue Gas CO/CO2, molar	0.66	0.66	0.66	0.66
Cat Circ Rate, t/min	44.81	42.00	41.48	40.20
Riser Conditions				
Feed Rate, t/hr	357.1	346.9	330.9	317.9
MBPD	59.3	56.5	53.2	49.3
Feed Preheat, C	350	350	350	350
Dispersion Steam, kg/hr	5356	5204	4964	4768
Outlet Temperature, C	510	511	510	510
Cat/Oil Ratio, kg/kg	7.5	7.3	7.5	7.6
Spent Catalyst Coke, wt%	0.9	0.9	1.1	1.3
Residence Time, s				
Vapour	2.05	2.17	2.08	2.06
Catalyst	2.12	2.25	2.15	2.13
Vap-Cat Contact Time, ms	42.4	43.6	40.3	38.9
Vapour Velocity, ft/s	53.7	50.7	52.9	53.4
Yields, wt% Feed				
Dry Gas	1.8	2.7	5.1	9.0
C3C4	13.6	11.3	17.0	21.9
C5+ Gasoline	54.4	51.8	48.9	42.7
Cycle Oil + Decant	24.6	28.7	22.4	17.8
Coke	5.5	5.4	6.7	8.6
Conversion, wt%	75.4	71.3	77.6	82.2

TABLE 13

OPERATE TO 510 C RISER EXIT

	IPL VGO	LLOYD VGO	C3 DAO 5	C4 DAO 20
Regenerator Conditions				
Temperature, C	662	664	691	737
Dry Air Rate, 1000kg/hr	234	217	224	227
Flue Gas CO/CO2, molar	0.66	0.66	0.66	0.66
Cat Circ Rate, t/min	44.81	40.91	35.27	27.86
Riser Conditions				
Feed Rate, t/hr	357.1	346.9	330.9	317.9
MBPD	59.3	56.5	53.2	49.3
Feed Preheat, C	350	350	350	350
Dispersion Steam, kg/hr	5356	5204	4964	4768
Outlet Temperature, C	510	510	510	510
Cat/Oil Ratio, kg/kg	7.5	7.1	6.4	5.3
Spent Catalyst Coke, wt%	0.9	0.9	1.1	1.3
Residence Time, s				
Vapour	2.05	2.18	2.13	2.15
Catalyst	2.12	2.26	2.20	2.23
Vap-Cat Contact Time, ms	42.4	43.4	35.6	29.1
Vapour Velocity, ft/s	53.7	50.46	51.6	51.2
Yields, wt% Feed				
Dry Gas	1.8	2.6	4.5	7.4
C3C4	13.6	11.0	15.0	17.9
C5+ Gasoline	54.4	51.9	50.6	47.3
Cycle Oil + Decant	24.6	29.2	24.1	21.3
Coke	5.5	5.3	5.7	6.0
Conversion, wt%	75.4	70.8	75.9	78.7

TASK 8D FCC Rate Constants for Treated Gas Oils

The FCC kinetic model of Weekman and Nace was fitted to the experimental MAT data measured, during Task 6, for the clay extracted derivatives and DMSO-acid treated raffinates from CANMET, Coprocessing and Shale oils. The model and fitting procedures were the same as in Task 8B, detailed in Appendix II.

1. Results

The rate constants and parameter ratios for each oil and its extracts and derivatives are given in Tables 14, 15 and 16. Single temperature cracking data over GX-30 catalyst are also included in each Table. Rate constant data for the CANMET and Shale oils were taken from a previous project ("Fluid Catalytic Cracking of Non-Conventional Gas Oils by an Octane-Enhancing Catalyst and a Metals Tolerant Catalyst", Final Report, October 1987).

2. Discussion

All three of the original feeds, CANMET, Coprocessing and Shale oils are characterized by high nitrogen content. The adverse effect of the nitrogen presence is clearly evident in Tables 14-16 with extremely high alpha values, indicative of rapid catalyst activity decay, leading to high decay ratios and low overall cracking rates. Additionally, the Coprocessing oil and Shale oil (at the lower temperatures) have poor selectivity ratios so that a disproportionate amount of what little cracking takes place is yielding gas and coke rather than gasoline. As the cracking temperature is raised, the rate of catalyst decay diminishes. This might be expected if the catalyst poisoning is caused by adsorption phenomena.

In an effort to alleviate the effect of catalyst poisoning, the high zeolite content GX-30 catalyst was substituted for the DA-440. While this noticeably improves the overall cracking rate constant for the Shale and Coprocessing Oils, there is no improvement in the catalyst decay characteristics. CANMET reacts differently, with all of the improvement in the decay ratio being attributable to a lower alpha. In all cases the decay ratios remain on the high side with GX-30 catalyst. But there is some improvement in the selectivity ratio for the Coprocessing oil with this catalyst.

Clay extraction has a similar effect on the ratios for the Coprocessing oil and Shale oil over DA-440 catalyst. In fact, the decay and selectivity ratios for the two clay extracted derivatives are virtually the same, with the ratios showing considerable improvement over those for the base oils. Even better improvement is shown by the DMSO-acid raffiniate derived from CANMET oil, with the decay and selectivity ratios, in this instance, approaching those associated with a viable FCC feedstock.

TABLE 14

SUMMARY OF WEEKMAN-NACE RATE CONSTANTS

CANMET and Treated CANMET Oils

CATALYST	FEED	TEMP DEG C	K0 hr-1	Alpha hr-1	K1 hr-1	K2 hr-1	K3 hr-1	Decay Ratio Alph/K0	Selectivity Ratio K1/K0	Cracking Ratio K2/K3	Gasoline Formation K1/K2
DA-440	CANMET	490	58.2	293.9	38.2	0.1	20.0	5.0	0.7	0.0	382.0
		510	74.7	304.6	77.2	45.5	NA	4.1	1.0	NA	1.7
		530	62.2	236.7	50.8	22.6	11.4	3.8	0.8	2.0	2.2
	DMSO/Raf	490	45.2	86.0	47.3	21.5	NA	1.9	1.0	NA	2.2
		510	70.8	116.3	72.4	24.7	NA	1.6	1.0	NA	2.9
		530	62.3	101.7	53.7	14.2	8.6	1.6	0.9	1.7	3.8
	Clay Extr	490	NA	NA	NA	NA	NA	NA	NA	NA	NA
		510	48.5	79.2	47.4	19.9	1.1	1.6	1.0	17.6	2.4
		530	NA	NA	NA	NA	NA	NA	NA	NA	NA
GX 30	CANMET	490	NA	NA	NA	NA	NA	NA	NA	NA	NA
		510	NA	NA	NA	NA	NA	NA	NA	NA	NA
		530	55.6	164.6	53.9	35.7	1.7	3.0	1.0	21.4	1.5

TABLE 15

SUMMARY OF WEEKMAN-NACE RATE CONSTANTS

Coprocessing and Treated Coprocessing Oils

CATALYST	FEED	TEMP DEG C	KO hr-1	Alpha hr-1	K1 hr-1	K2 hr-1	K3 hr-1	Decay Ratio Alph/KO	Selectivity Ratio K1/KO	Cracking Ratio K2/K3	Gasoline Formation K1/K2
DA-440	Copro Oil	490	37.2	235.8	21.4	4.6	15.8	6.3	0.6	0.3	4.7
		510	44.7	257.8	27.3	8.2	17.4	5.8	0.6	0.5	3.3
		530	32.6	182.6	20.0	8.5	12.6	5.6	0.6	0.7	2.4
	DMSO/Raf	490	NA	NA	NA	NA	NA	NA	NA	NA	NA
		510	50.6	146.2	43.0	19.1	7.6	2.9	0.8	2.5	2.2
		530	NA	NA	NA	NA	NA	NA	NA	NA	NA
	Clay Extr	490	45.1	97.8	41.5	18.1	3.5	2.2	0.9	5.2	2.3
		510	42.2	93.3	39.3	19.4	2.9	2.2	0.9	6.8	2.0
		530	42.6	84.4	32.5	11.4	10.1	2.0	0.8	1.1	2.8
GX 30	Copro Oil	490	NA	NA	NA	NA	NA	NA	NA	NA	NA
		510	NA	NA	NA	NA	NA	NA	NA	NA	NA
		530	52.9	190.8	45.2	33.1	7.8	3.6	0.9	4.3	1.4

TABLE 16

SUMMARY OF WEEKMAN-NACE RATE CONSTANTS

Shale and Treated Shale Oils

CATALYST	FEED	TEMP DEG C	K0 hr-1	Alpha hr-1	K1 hr-1	K2 hr-1	K3 hr-1	Decay Ratio Alph/K0	Selectivity Ratio K1/K0	Cracking Ratio K2/K3	Gasoline Formation K1/K2
DA 440	Shale Oil	470	36.3	273.1	22.4	0.0	13.9	7.5	0.6	0.0	NA
		490	29.5	195.6	18.4	0.1	11.1	6.6	0.6	0.0	NA
		510	33.3	177.8	26.3	15.6	7.0	5.3	0.8	2.2	1.7
		530	35.6	161.9	32.4	29.7	3.2	4.6	0.9	9.3	1.1
	DMSO/Raf	490	NA	NA	NA	NA	NA	NA	NA	NA	NA
		510	44.9	159.2	40.4	23.1	4.5	3.5	0.9	5.2	1.7
		530	NA	NA	NA	NA	NA	NA	NA	NA	NA
	Clay Extr	490	68.1	177.7	61.0	17.7	7.1	2.6	0.9	2.5	3.4
		510	89.4	200.6	84.8	27.1	4.6	2.2	0.9	5.9	3.1
		530	91.9	187.4	80.9	22.4	11.0	2.0	0.9	2.0	3.6
GX 30	Shale Oil	490	NA	NA	NA	NA	NA	NA	NA	NA	NA
		510	NA	NA	NA	NA	NA	NA	NA	NA	NA
		530	55.0	163.3	53.2	32.9	1.8	3.0	1.0	18.6	1.6

APPENDIX I

FHRS Model Formulation

FHRS Phase Model Formulation

1. Thermodynamic Considerations

For any system containing a mixture of components i, the Gibbs energy is given by

$$G = \sum n_i g_i^\circ + \Delta H^m - T\Delta S^m \qquad (1)$$

n_i is the number of moles of component i with a pure component molar Gibbs energy, g_i°; ΔH^m and ΔS^m are the changes in enthalpy and entropy on mixing the i components, and T is the temperature. The chemical potential of component i is defined by

$$\mu_i = \left[\partial G/\partial n_i \right]_{T,P,n_j} \qquad (2)$$

Other related variables conveniently used in solution thermodynamics are the fugacity, f_i, and activity, a_i. The relating expressions are

$$(\mu_i - g_i^\circ) = RT\ln(f_i/f_i^\circ) \qquad (3)$$

and

$$a_i = f_i/f_i^\circ \qquad (4)$$

whence

$$\ln a_i = (\mu_i - \mu_i^\circ)/RT \qquad (5)$$

since $\mu_i = g_i^\circ$ for a pure component.

If a system exists in more than one phase at equilibrium then the overall Gibbs energy of the system will be the sum of the individual phase Gibbs energies, G^j, as given in equation 1,

$$G_{total} = \sum_j G^j \qquad (6)$$

For equilibrium between the phases, a necessary condition is equality of the component chemical potentials across the phases so that

$$\mu_i^1 = \mu_i^2 = \text{———} = \mu_i^j \qquad (7)$$

Given the definition of the activity from equation 5, alternative expressions for the equilibrium conditions in a two phase system are

$$\mu_i^1 = \mu_i^2 \qquad \text{or,} \qquad \ln a_i^1 = \ln a_i^2 \tag{8}$$

To determine whether a particular two phase system satisfies condition 8, the component activity in each phase is calculated by differentiating equation 1 with respect to n_i. This yields, for the component activity in any phase

$$\ln a_i = (\mu_i - \mu_i^\circ)/RT = \frac{1}{RT} \cdot \frac{\partial \Delta H^m}{\partial n_i} - \frac{1}{R} \cdot \frac{\partial \Delta S^m}{\partial n_i} \tag{9}$$

Expressions for the enthalpy and entropy of mixing, and the derivatives with respect to the mole numbers (i.e. the partial molar mixing properties), are furnished by the phase model selected for the particular phase.

2. FHRS Liquid Phase Model

Flory (1942) and Huggins (1942) independently derived an equation to describe the large deviations from Raoult's law which result from the entropy of mixing of long chain molecules with small molecule solvents. For the binary system solvent(1) - polymer(2), the entropy of mixing is

$$\Delta S^m = -R(n_1 \ln\phi_1 + n_2 \ln\phi_2) \tag{10}$$

where ϕ is the volume fraction defined in terms of the polymer-solvent segment size ratio, m,

$$\phi_1 = n_1/(n_1+n_2m) \qquad \text{and,} \qquad \phi_2 = n_2m/(n_1+n_2m) \tag{11}$$

Usually, the segment size ratio is based on the relative molar volumes of the polymer and solvent,

$$m = v_2/v_1 \tag{12}$$

Subsitution for m in the equations for ϕ leads to the conventional definition of the volume fraction.

Generalizing the equations above to a multicomponent system gives

$$\Delta S^m = -R\ \Sigma n_j \ln\phi_j \tag{13}$$

with

$$\phi_j = n_j m_j / \Sigma n_j m_j \qquad (14)$$

and

$$m_j = v_j / v_{ref} \qquad (15)$$

where v_{ref} is the molar volume of a selected reference component, generally the one with the smallest molar volume.

Differentiation of equation 13 yields

$$\frac{\partial \Delta S^m}{\partial n_i} = -R\left[\ln\phi_i + \sum_j \frac{n_j}{\phi_j} \cdot \frac{\partial \phi_j}{\partial n_i} \right] \qquad (16)$$

Noting that the derivatives of the volume fractions, after substituting for m, are

$$\frac{\partial \phi_j}{\partial n_i} = \frac{v_i}{\Sigma n_j v_j} \cdot (\delta_{ij} - \phi_i) \qquad (17)$$

where δ_{ij} is Kronecker delta, which is unity for i = j, and zero otherwise, equation 16 for the partial molar entropy of mixing becomes

$$\frac{\partial \Delta S^m}{\partial n_i} = -R(\ln\phi_i + 1 - v_i/v) \qquad (18)$$

v is the phase molar volume, $\Sigma n_i v_i / \Sigma n_i$.

In the original equations of Flory and Huggins it was assumed that the entropy change constituted all, or at least the major part, of the Gibbs energy change on mixing. This assumption of athermal solution proved too restrictive so an approximate enthalpy of mixing term was subsequently added to complete the equation. The final equation for a binary mixture is

$$\Delta G^m/RT = n_1 \ln\phi_1 + n_2 \ln\phi_2 + \varkappa\phi_1\phi_2(n_1 + mn_2) \qquad (19)$$

The first two terms are the entropy contribution; the final term results from expressing the energy of the binary as a general quadratic in the volume fractions. The Flory interaction parameter $\varkappa$ represents the interaction energy between the solvent and solute(polymer). While useful and flexible for binaries, extension of this approach to multicomponent mixtures proves less convenient, requiring definition of separate $\varkappa$ values for each possible interacting pair in the mixture. At the expense of an additional assumption, the geometric mean assumption, a simpler and more practical form for the enthalpy of mixing is available from regular solution theory. As described by

Prausnitz (1969), the enthalpy of mixing for a regular binary solution is given by the equation

$$\Delta H^m = \Delta E^m = (n_1 v_1 + n_2 v_2)\phi_1 \phi_2 (\delta_1 - \delta_2)^2 \qquad (20)$$

The equality of enthalpy and energy is valid for a regular solution since the excess volume of mixing is zero. The solubility parameters, δ, in equation 20 are defined as the square root of the cohesive energy density,

$$\delta = (\Delta E^v / v)^{1/2} \qquad (21)$$

ΔE^v is the vaporization energy of the compound from the condensed state to the ideal gas state (i.e. where molecular interactions are zero).

Differentiation of equation 20 yields

$$\frac{\partial \Delta H^m}{\partial n_i} = v_i (1 - \phi_i)(\delta_1 - \delta_2)^2 \qquad (22)$$

The analagous equation for a multicomponent system gives the partial molar enthalpy of mixing required for the activity equation 9,

$$\frac{\partial \Delta H^m}{\partial n_i} = v_i (\delta_i - \bar{\delta})^2 \qquad (23)$$

with $\bar{\delta} = \Sigma \phi_i \delta_i$.

The derivation of equation 23 is quite involved and is presented in the book by Prausnitz.

Inserting equation 23 for the partial molar enthalpy and equation 18 for the partial molar entropy into equation 9 gives a working equation for calculating the activity of any component in the phase.

$$\ln a_i = \frac{v_i}{RT} (\delta_i - \bar{\delta})^2 + \ln\phi_i + 1 - v_i / v \qquad (24)$$

Equation 24 is essentially the same as that used by Hirschberg et al. In this work it will be used to calculate component activities in all the liquid phases of the systems studied. For convenience in the remainder of the report, equation 24 will be referred to as the Flory-Huggins Regular Solution (FHRS) model, or equation.

3. Computational Considerations

In order to use the FHRS equation in the determination of the equilibrium phase behaviour of systems containing heavy fractions, a computational procedure is required. For testing purposes, a two phase equilibrium program, previously used for vapour-liquid equilibrium calculations with equations of state, was modified by replacing the equation of state package with an FHRS subroutine. In the current application it was assumed that the systems under consideration would be either single phase or would form two liquid phases at the temperature and pressure of operation.

To calculate the two equilibrium phases, an initial estimate of the compositions of the two phases is provided in the form of component equilibrium ratios,

$$K_i = y_i/x_i \tag{25}$$

with y_i as the mole fraction of component i in the upper liquid phase while x_i is the mole fraction in the lower phase. Assuming that overall system composition is known - mole fractions z_i - the fraction of the total system moles present in the lower phase, θ, may be calculated. For each component there is a mass balance such that

$$z_i = \theta x_i + (1 - \theta)y_i \tag{26}$$

or

$$z_i = x_i[\theta(1 - K_i) + K_i] \tag{27}$$

so that

$$x_i = z_i/[\theta(1 - K_i) + K_i] \tag{28}$$

and

$$y_i = K_i z_i/[\theta(1 - K_i) + K_i] \tag{29}$$

By definition, the mole fractions in each phase sum to unity, thus

$$\Sigma y_i = 1 \ , \ \Sigma x_i = 1 \ , \quad \text{and} \quad \Sigma y_i - \Sigma x_i = 0 \tag{30}$$

Substituting for x_i and y_i in this last equation one obtains

$$\sum \frac{z_i(K_i - 1)}{[\theta(1 - K_i) + K_i]} = 0 \tag{31}$$

Given the values for z_i and K_i this single implicit equation is readily solved for θ using one of the standard nonlinear equation solution techniques such as Newton's method. Once θ is known, x_i and y_i follow from equations 28 and 29.

The next stage of the calculation is to determine the component activities in each of the phases in turn. Using the upper phase as an example:

$$v = \Sigma y_i v_i \tag{32}$$

$$\phi_i = y_i v_i/v \tag{33}$$

$$\bar{\delta} = \Sigma \phi_i \delta_i \tag{34}$$

FIGURE 1

Phase Equilibrium Calculation Sequence

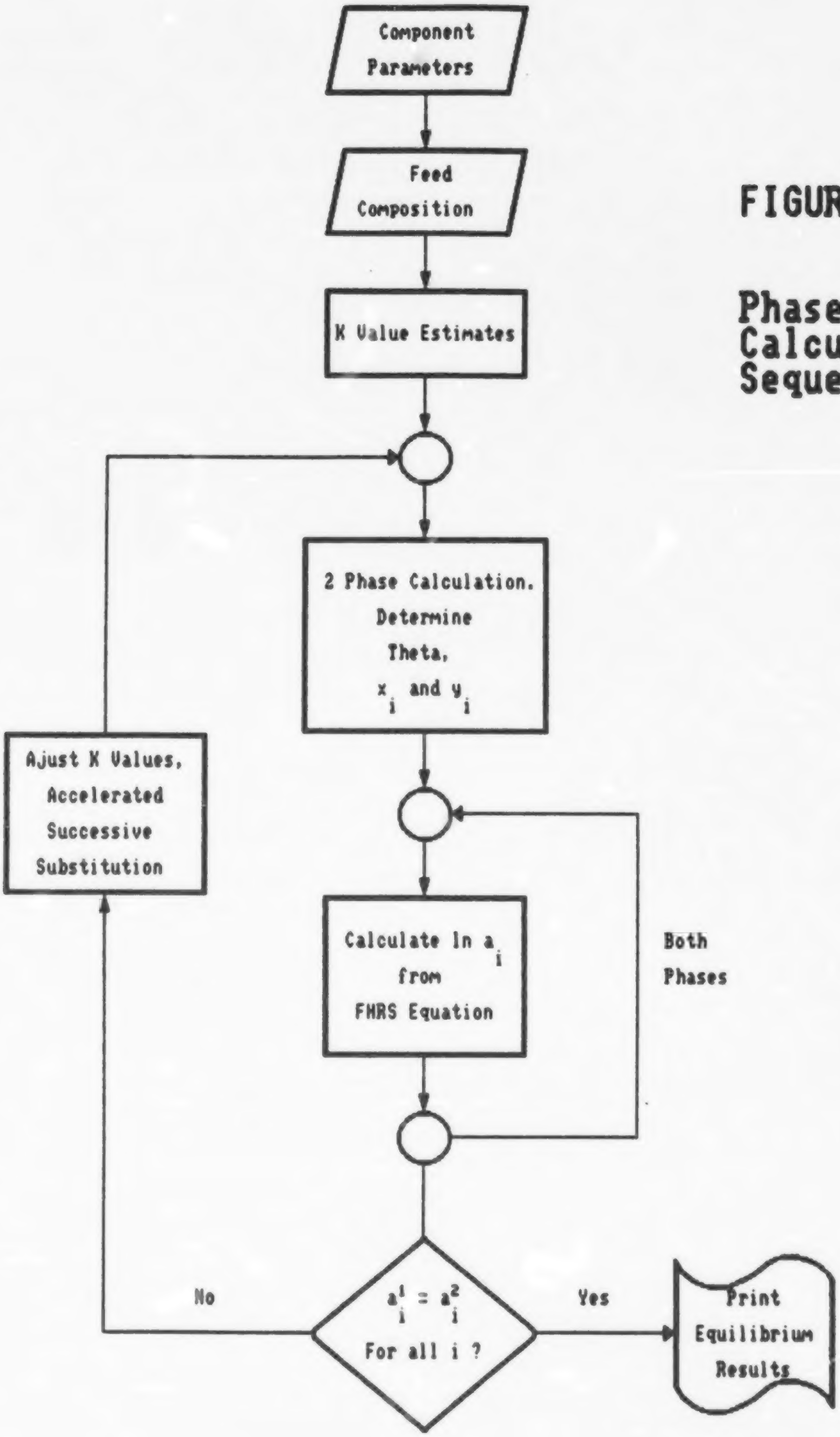
Component Parameters
Feed Composition
K Value Estimates
2 Phase Calculation. Determine Theta, x_i and y_i
Ajust K Values, Accelerated Successive Substitution
Calculate ln a_i from FHRS Equation
Both Phases
$a_i^1 = a_i^2$ For all i ?
No
Yes
Print Equilibrium Results

$$\ln a_i = \frac{v_i}{RT} (\delta_i - \bar{\delta})^2 + \ln\phi_i + 1 - v_i/v \qquad (24)$$

Analagous equations apply to the lower phase, replacing y_i by x_i .

Finally, the component activities in each phase are compared individually. If equality of component activity between the phases exists (within a small tolerance) for all the components, the system is at equilibrium. Otherwise, the equilibrium ratios are adjusted and the calculation is repeated until equilibrium is attained. The technique used to adjust the equilibrium ratios is an accelerated succesive substitution procedure developed by Mehra, Heidemann and Aziz (1983). This method has rapid and stable convergence properties and was specifically developed for phase equilibrium calculations.

The complete calculation sequence described above is summarized in Figure 1. In addition to the basic calculation sequence, other features were included in the program and should be noted.

Before attempting to solve equation 31 for the phase split, checks are made to ensure that two phases are feasible with the current K_i values; if not, the iteration is completed by calculating the properties of the indicated single phase before terminating the calculation. Using this feature it is also possible to restrict calculations to a single phase deliberately. This may be useful for comparing the properties of the system in a single phase with those of the system in two phases from a subsequent calculation. In particular this feature provides a check that the two phase system really is more stable than a single phase. During the calculations the Gibbs energy per mole of feed is calculated for each phase present using the following relations.

$$g = \Sigma z_i g_i{}^{\circ} + \Delta g^m = \Sigma z_i \mu_i{}^j \qquad (34)$$

$$g = \Sigma z_i \mu_i{}^{\circ} + \Sigma z_i (\mu_i{}^j - \mu_i{}^{\circ}) = \Sigma z_i \mu_i{}^{\circ} \;\text{[illegible]}\; RT\Sigma z_i \ln a_i{}^j \qquad (35)$$

Comparing g calculated for the single and two phase system makes it simple to check that the thermodynamic criterion for stability is being met and that g is decreasing. When two phases are present, comparison of g for each phase indicates how closely the equilibrium requirement for equality of the Gibbs energies is being satisfied.

As it turned out, most of the systems studied with this program were characterized by narrow ranges of two phase stability and extreme sensitivity to the K value of the solvent. Under these circumstances goood initial estimates of the K values were imperative if the correct phase behaviour was to be calculated. While the Gibbs energy comparison was useful in detecting stability problems it could not provide solutions to these problems. For these answers a stability program described by Michelsen (1982) was adapted for use with the FHRS model. The stability analysis in the program generates the number of phases present and their approximate compositions. K values calculated from these approximate compositions proved to be reliable initial estimates for use in the two phase equilibium program.

5. References

P. J. Flory, J. Chem. Phys. 10, 51 (1942).

A. Hirschberg, L. N. J. deJong, B. A. Schipper and J. G. Meijer, SPEJ, 283-293 (June,1984).

M. L. Huggins, J Phys. Chem. 46, 151 (1942).

R. K. Mehra, R. A. Heidemann and K. Aziz, Can. J. Chem. Eng. 61, 590-596 (1983).

M. L. Michelsen, Fluid Phase Equilibria 9, 1-19 (1982).

J. M. Prausnitz, Molecular Thermodynamics of Fluid Phase Equilibria', Prentice-Hall Inc., Englewood Cliffs NJ, 1969.

PROGRAM EXAMPLE

A copy of the input data file and the output from FHRS is given for a typical example.

The input data file consists of a problem title line, control integers - 04 indicates 4 components and the 01 specifies a copy of the input data - and three tolerance settings in E format. The latter defines the limits of convergence required for the component activities and in the solution of the phase split equation 31; these tolerances are not usually altered. The fourth line contains the system temperature (75°C) and pressure (65 PSIA) while the fifth line contains the feed molar composition. Component data follows for the four components consisting of a label, the molar mass, molar volume and the solubility parameter. The final line in the file contains the starting K values for each of the four components.

The output from the converged calculation consists of an echo check of the input data followed by summary table of the component molar compositions and the calculated K values. Phase 1 refers to the dense phase (lower phase). The overall molar and volume splits between the upper and lower phases are listed together with the phase molar mass and other calculated phase properties. The final line gives the number of K value iterations required to achieve the required convergence.

Matching Procedure - Parameter Adjustment

The matching procedure consists of carrying out a series of runs, such as that described above, using a particular feed composition, with the objective of obtaining calculated K values in reasonable agreement with the experimental data. Starting with an initial set of component molar volumes and solubility parameters the first calculation is made, the K values are compared to the experimental values and then one, or more, of the component properties is adjusted to try and improve the agreement between calculation and experiment. A further calculation is made and then the process is repeated until a satisfactory match between experimental and calculated K values is obtained.

The process of varying the component properties to obtain the required movement in calculated K values is largely one of experience and familiarity, since varying any of the component properties will affect all of the component K values to some degree. An initial series of calculations in which each of the component properties is varied, in turn, by a fixed percentage allows K value sensitivity matrices to be built up, as shown below. This serves as a useful guide as to which component parameters should be varied, and the extent of the variation required to achieve a match.

Sensitivity Matrices
(% Change in K Value)

Component Adjusted	Solvent	Oils	Resins	Asphaltenes
Molar Volume, +5%				
Solvent	2.7	0.0	0.0	-0.2
Oils	-11.2	-4.2	-0.1	-1.0
Resins	-16.5	1.3	-5.3	-0.9
Asphaltenes	-40.5	1.6	-1.4	-19.6
Solubility Parameter, +1%				
Solvent	- 1.7	0.3	0.6	2.6
Oils	20	-7.1	-2.6	-10.2
Resins	37	-1.7	-13	- 8.1
Asphaltenes	534	-6.0	-10.5	-35

Perhaps not surprisingly, K values are most sensitive to the solvent properties and there is a much greater sensitivity to the solubility parameters than to the molar volumes. Given the high level of solvent (in molar terms) present in the systems and the occurrence of the solubility parameter in the activity equation as a squared term, these traits are understandable.

SAMPLE FROM PROGRAM FHRS

Input Data File

```
Demonstration Calculation, Solvent/VTB 3:1
04        00        00        01
 1.000E-05 1.000E-06 1.000E-04
75.       65.
93.78     5.28      0.86      0.09
SOLV      100.2     150.      5.40
OILS      350.      350.      7.42
RESN      1000.     800.      7.45
ASPH      5500.     4000.     7.45
1.12      0.33      0.21      0.014
```

Sample Output

```
                         DATA ECHO CHECK
                         ---------------

       .100E-04  .100E-05  .100E-03
        75.0000   65.0000
     SOLV        100.2000  150.0000    5.4000
     OILS        350.0000  350.0000    7.4200
     RESN       1000.0000  800.0000    7.4500
     ASPH       5500.0000 4000.0000    7.4500
         1.1200     .3300     .2100     .0140


     Demonstration Calculation, Solvent/VTB 3:1
     FLORY-HUGGINS REGULAR SOLUTION MODEL


     PRESSURE   65.000 PSIA       TEMPERATURE  75.00 DEG. C


               COMPONENT           FEED      PHASE 1      PHASE 2      K-VALUE

                   SOLV      .93771E+02   .86882E+02   .93814E+02   .10798E+01
                   OILS      .52795E+01   .94056E+01   .52533E+01   .55853E+00
                   RESN      .85991E+00   .20909E+01   .85210E+00   .40753E+00
                   ASPH      .89991E-01   .16226E+01   .80268E-01   .49468E-01
                            -----------  -----------  -----------
            TOTAL            .10000E+03   .10000E+03   .10000E+03

MOLES                        100.0000     .63038E+00   .99370E+02
VOLUME (CUBIC CM)            100.0000     .91010E+00   .99090E+02

MOLECULAR WEIGHT             125.9850    230.1281    125.3243
DENSITY ( G/CUBIC CM)           .7428       .9398       .7410
Z = PV/RT                       .0263       .0379       .0262
GIBBS ENERGY (KJ/MOLE FEED)                -.5224      -.5224
VOLUME (CU CM/ MOLE)         169.6130    244.8740    169.1356


ITERATIONS TO CONVERGE        TEMP. OR PRESS.  1    TOTAL  10
```

APPENDIX II

Gas Oil Cracking Kinetics

Weekman-Nace Gas Oil Cracking Model

The following reaction scheme for gas oil cracking was proposed by Weekman and Nace (AIChE J, 16, 397 (1970)):

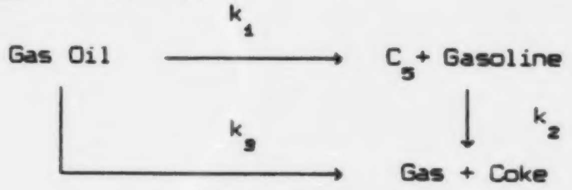

For gas oil cracking the rate is assumed to be second order

$$\frac{dy_1}{dt} = -(k_1 + k_3)^2 y_1 \phi \tag{1}$$

with y_1 the mole fraction of gas oil and ϕ the fractional catalyst activity. For debutanized gasoline, cracking is first order, leading to

$$\frac{dy_2}{dt} = k_1 y_1^2 \phi - k_2 y_2 \phi \tag{2}$$

for the rate of formation of debutanized gasoline, mole fraction y_2.
If the catalyst activity decays as a first order function then

$$\frac{d\phi}{dt} = -\alpha\phi \tag{3}$$

so that

$$\phi = e^{-\alpha t} \tag{4}$$

after time t, assuming $\phi = 1$ when $t = 0$.

For a reactor system of length L, the rate of change of composition, at some distance x along the reactor, with respect to the dimensionless coordinate z is given by

$$dy_1/dz = -(\varepsilon/S)\cdot(\rho_v\ /\rho_1)\cdot k_o y_1^{\,2}\ e^{-\alpha t} \tag{5}$$

$$dy_2/dz = (\varepsilon/S)\cdot(\rho_v\ /\rho_1)\cdot(k_1 y_1^{\,2} - k_2 y_2)\ e^{-\alpha t} \tag{6}$$

$$z = x/L \tag{7}$$

$$k_o = k_1 + k_3 \tag{8}$$

where S is the liquid volume hourly space velocity, ρ_v is the total vapour density at operating conditions and ρ_1 is the liquid density of the feed at ambient. For convenience, Weekman and Nace lumped the catalyst voidage space, ε, and the density ratio in with the rate constants i.e.

$$K_n = \varepsilon \cdot (\rho_v / \rho_1) \cdot k_n \qquad (9)$$

Equation 5 may solved for y_1 at the exit of the reactor giving

$$y_1 = \left[1 + (K_o/S) \cdot e^{-\alpha t}\right]^{-1} \qquad (10)$$

This equation is integrated from time zero to time t_c, the time-on-stream, to obtain the time averaged conversion $(1 - \bar{y}_1)$

$$(1 - \bar{y}_1) = \frac{1}{\alpha t_c} \log_e \left[\frac{1 + K_o/S}{1 + (K_o/S) \cdot \exp(-\alpha t_c)} \right] \qquad (11)$$

For equation 6 the solution for y_2 is

$$y_2 = r_1 r_2 e^{-r_2/y_1} \left[(e^{r_2})/r_2 - (y_1/r_2) \cdot e^{r_2/y_1} - E_i(r_2) + E_i(r_2/y_1) \right] \qquad (12)$$

with $r_1 = K_1/K_o$ and $r_2 = K_2/K_o$, and with y_1 from equation 10 to give y_2 at the reactor exit. In equation 12, $E_i(x)$ is the exponential integral of x defined as

$$E_i(x) = \int_{-\infty}^{x} \frac{e^x}{x}\, dx \qquad (13)$$

For a fixed bed reactor the time averaged value of $\bar{y}_2$ is obtained by calculating y_2 at time intervals $0.1t_c$ from zero to t_c and integrating the resulting values using Simpson's rule.

$$\bar{y}_2 = \int_0^{t_c} y_2\, dt \qquad (14)$$

The exponential integral is calculated from a series of polynomial equations used to fit tabulated values of the integral or related functions, such as $xe^{-x}E_i(x)$, over different ranges of x within the variable space $0 \le x \le 8$.

DETERMINATION OF THE RATE CONSTANTS

1. Nonlinear Regression Analysis

As detailed in Appendix I, the Weekman-Nace model gives equations for the time averaged conversion and debutanized gasoline yield in terms of the space velocity and time-on-stream (independent variables) plus four rate constant parameters i.e.

$$\text{Conversion} = f(S,\ t_c\ ;\ K_o,\ \alpha) \qquad (1)$$
$$\text{Gasoline} = f(S,\ t_c\ ;\ K_1,\ K_2) \qquad (2)$$

By fitting these functions to the measured conversions and gasoline yields from microactivity tests, the rate constant parameters may be determined. For the overall gas oil cracking rate constant, K_o, and the catalyst activity decay rate, α, the experimental data are regressed using equation 1 to calculate the response function - conversion. Similarly, the rate constants K_1 and K_2 are calculated by regression of function 2 with the time averaged gasoline yield as response function.

A propietary generalized multiple nonlinear regression program (MNLREG), based on Marquardt's algorithm (1) was used for the regression analysis. MNLREG calculates the response function and derivatives of the response function from user-supplied subroutines. Two separate subroutines, to calculate either the time averaged conversion, or the debutanized gasoline yield (along with the associated exponential integral function and quadrature with Simpson's rule), were written to obtain the Weekman-Nace rate constants.

The procedure used in MNLREG is to expand the nonlinear function in a Taylor series about trial estimates of the parameters, terminating the series after the first order derivative terms. This yields a set of approximate linearised equations in the parameter increments; one equation for each experimental observation. The linearised set is solved using convential linear least squares to obtain improved estimates of the parameters. The procedure is repeated with the updated parameter estimates, iterations continuing until the parameter estimates converge and the sum of squares of the residuals (calculated response - measured response) is minimized. In the Marquardt-Levenberg algorithm, the procedure is modified by placing constraints on the incremental change in the parameters from iteration to iteration in order to improve the convergence characteristics of the search.

Since MNLREG is a generalized procedure, the first order derivatives of the response functions are calculated numerically. Each of the parameters is varied in turn and the value of the response function, from the user-supplied subroutine, is recalculated.

2. Alternative Methods of Parameter Determination

Although the procedure of sequential least squares determination of the rate constant parameters described in the last section works satisfactorily, it is not statistically rigorous. The correct approach, statistically, requires simultaneous determination of all the parameters so as to minimize the determinant of the covariance matrix. This criterion for parameter determination from multi-response data was derived by Box and Draper (2).

In the early part of these studies an optimization algorithm was used with the multi-response data - conversion and gasoline yields - from MAT experiments to calculate rate constants satisfying the minimum determinant criterion. Comparison of the parameters with those from sequential least squares revealed no significant differences, possibly a reflection of the limited data available for the fitting process. Given this observation, plus the fact that the nonlinear regression procedure was faster and more robust than the optimization algorithm, and the result was abandonment of statistical rectitude in favour of computational efficiency with the adoption of sequential least squares for routine rate constant determination.

3. References

(a) D.W. Marquardt, 'An Algorithm for Least Squares Estimation of Nonlinear Parameters', J.Soc. Indust. Appl. Math., 11, 431 (1963).

(b) K. Levenberg, 'A Method for the Solution of Certain Nonlinear Problems in Least Squares', Quart. Appl. Math., 2, 164 (1944).

2. G.E.P. Box and N.R. Draper, 'The Bayesian Estimation of Common Parameters from Several Responses', Biometrika, 52, 355 (1965).

EXAMPLE CALCULATIONS

Two actual data files and computer outputs from MNLREG are given as examples. The first example is for fitting the conversion function, 1, to experimental space velocity and time-on-stream measurements. The input data is structured as follows:-

Line 1 Problem title

Line 2 Control integers, in order:-

• Number of parameters to be determined, (K_0, α)	2
• Number of independent variables (S, t_c)	2
• Number of experimental data sets	3
• Select Marquardt's option	1
• Select forward finite difference derivatives	2
• Select data echo check	1

Line 3 Starting estimates for K_0, 100 hr^{-1} and alpha, 50 hr^{-1}

Line 4 Percent increments in the parameters for calculating the numerical derivatives - 2% on K_0 and on alpha

Lines 5-7 3 sets of experimental space velocities (volumetric) and time-on-stream (hr)

Line 8 Fractional gas oil conversion (dependent variable) for each set of experimental conditions

Line 9 Weighting factors for experimental data - all equal

The MNLREG output starts with a check of the independent variable data input. A summary of the parameter values at the start of each iteration is given (program can output up to 10 parameters in two lines of five) together with the calculated sum of squares of residuals (SSR) and the value of lamda in Marquardt's method. The latter is set automatically by the program and shows how closely the method is approximating steepest descents (lamda large - far from solution) or Gauss-Newton (lamda small - close to solution).

In the example shown, the values of the two parameters K_0 and alpha are adjusted from 100 and 50 hr^{-1} over six iterations to 62.25 and 101.6 hr^{-1}, at which point the sum of squares of residuals has dropped to approximately 10^{-4} and is not changing, indicating convergence.

Calculated values of the dependent variable (conversion) are obtained at each experimental condition, using the converged parameters, for comparison with the observed values in the final output table. This also includes the percentage difference between the calculated and observed dependent variables.

The second example illustrates the fitting of debutanized gasoline function 2. Once again the number of parameters to be determined is 2 - K_1 and K_2. In this case, however, the number of independent variables is 4, S and t_c plus K_0 and alpha obtained from fitting the conversion data. The initial estimates for K_1 and K_2 are 50 and 20 hr^{-1}, on line 3. Lines 5 to 7 contain the same experimental data as in example 1 with the converged values of K_0 and alpha added as the third and fourth independent variables. The dependent variables on line 8 are the fractional debutanized gasoline yields.

After 6 iterations the sum of squares of residuals is reduced to 2.10^{-6} with converged values for K_1 and K_2 of 53.7 and 14.2 hr^{-1}. Agreement between the calculated and observed gasoline yields is better than 0.3% in all cases.

SAMPLE FROM PROGRAM MNLREG

Input Data File

```
C5+ Gasoline Model -- Demonstration Calculation
02       04       03       01       02       01
50.      20.
2.       2.
17.79    .02501   62.25    101.6
18.87    .01278   62.25    101.6
17.21    .00833   62.25    101.6
.3435    .4060    .4137
1.       1.       1.       1.       1.       1.       1.       1.
```

Sample Output

```
    DATA ECHO CHECK

    INDEPENDENT VARIABLE MATRIX

        17.790      .025    62.250   101.600
        18.870      .013    62.250   101.600
        17.210      .008    62.250   101.600




    C5+ Gasoline Model -- Demonstration Calculation


    DERIVATIVE TYPE:  2      % INCREMENTS      2.   2.


      ITERATION     LAMDA        SSR                          PARAMETERS
                                              1/6           2/7           3/8           4/9           5/10
          1                    .1331E-01   .5000E+02    .2000E+02
          2         .10E+01    .9223E-02   .5085E+02    .1913E+02
          3         .10E+00    .8468E-03   .5363E+02    .1629E+02
          4         .10E-01    .8270E-05   .5456E+02    .1504E+02
          5         .10E-02    .2741E-05   .5397E+02    .1446E+02
          6         .10E-03    .2237E-05   .5372E+02    .1423E+02


                 CONVERGED VALUES          .5371E+02    .1422E+02



                  YOBS           WT             YCALC          % DIFF

                  .3435          1.00            .3427          -.2327
                  .4060          1.00            .4072           .2874
                  .4137          1.00            .4132          -.1174
```

SAMPLE FROM PROGRAM MNLRES

Input Data File

```
---------------

Conversion   Model -- Demonstration Calculation
02        02        03        01        02        01
100.      50.
2.        2.
17.79     .02501
18.87     .01278
17.21     .00833
.4938     .6363     .6948
1.        1.        1.        1.        1.        1.        1.        1.
```

Sample Output

```
-------------

     DATA ECHO CHECK

     INDEPENDENT VARIABLE MATRIX

         17.790      .025
         18.870      .013
         17.210      .008




     Conversion   Model -- Demonstration Calculation


     DERIVATIVE TYPE:  2      % INCREMENTS      2.   2.


       ITERATION      LAMDA        SSR                                    PARAMETERS
                                              1/6           2/7           3/8            4/9            5/10
            1                   .1040E+00   .1000E+03     .5000E+02
            2          .10E+01  .7110E-01   .9057E+02     .5918E+02
            3          .10E+00  .3226E-02   .6383E+02     .8749E+02
            4          .10E-01  .1235E-03   .6052E+02     .9774E+02
            5          .10E-02  .9840E-04   .6204E+02     .1012E+03
            6          .10E-03  .9815E-04   .6225E+02     .1016E+03


                    CONVERGED VALUES          .6225E+02     .1016E+03



                      YOBS                WT                YCALC             % DIFF

                      .4938              1.00                .4961              .4624
                      .6363              1.00                .6287            -1.1980
                      .6948              1.00                .7007              .8493
```

APPENDIX III

Dilute Phase Riser FCC Model

Dilute Phase Riser FCC Model

The riser model is made up of four calculation sections: the feed-catalyst mixer, the dilute phase riser, the stripper-regenerator and the slide valve catalyst flow control. The calculations performed by each of these sections are detailed, by section, below.

1. Feed-Catalyst Mixer

A preheated feed stream plus a dispersion stream (either steam or N_2) are contacted by catalyst at regenerator temperature, the feed is vaporized and all three streams enter the base of the riser at a common temperature. The Feed-Catalyst Mixer subroutine calculates the riser entry temperature from the enthalpy balance around the mixer:

$$\text{Enthalpy In} = F \cdot H_F^{L}(T_F) + D \cdot H_D(T_D) + CCR \cdot s_C \cdot T_C$$

$$\text{Enthalpy Out} = F \cdot H_F^{V}(T_I) + D \cdot H_D(T_I) + CCR \cdot s_C \cdot T_I$$

where F,D and CCR are the mass flows of feed, dispersion medium and catalyst respectively, with temperatures T_F, T_D and T_C. H_F^L, H_F^V and H_D are the enthalpies of the liquid feed, the feed vapour and the dispersion medium at the indicated temperature, s_C is the catalyst specific heat. Equating the enthalpies in and out permits direct solution for the riser inlet temperature, T_I. However, as both the enthalpies of the vaporized feed and the dispersion medium are nonlinear functions of the riser inlet temperature, T_I is found iteratively using Newton's method to solve the balance equation in the form

$$\text{Enthalpy In} - \text{Enthalpy Out} = 0$$

2. Dilute Phase Riser

This is the most complex section of the model requiring description of the reactor material and heat balance differential equations, the rate equations for reactants and products plus the conditions for pneumatic flow in the riser.

2.1 Material Balance Equations

For a 1-dimensional steady state reactor the change in mass fraction of a component y along the length of the reactor is given by

$$\frac{dy}{dz} = \frac{L}{u}\cdot R(y)$$

z is the dimensionless distance along the reactor, x/L, where L is the total reactor length, R(y) is the rate of formation of the component, dy/dt, and u is the linear velocity through the reactor. The term (L/u) is the total residence time during which reaction can occur. In a catalytic reactor the reaction time is the vapour-catalyst contact time t_{vc}, rather than the total residence time so that

$$\frac{dy}{dz} = t_{vc}\cdot R(y)$$

2.2 Heat Balance Equation

The rate of change of temperature along the length of the reactor can be derived from a heat balance for the 2-phase system

$$(F\cdot s_v + CCR\cdot s_c)\cdot\frac{dT}{dz} = \frac{dy}{dz}\cdot F\cdot\Delta H - H_{loss}$$

The term on the left side is the heat capacity of the vapour and catalyst streams factored by the temperature gradient. The right side is the overall heat of reaction in the vapour phase ($F\cdot\Delta H$) factored by the reaction gradient dy/dz, minus any heat loss. The temperature gradient along the reactor is then

$$\frac{dT}{dz} = \left[\frac{dy}{dz}\cdot F\cdot\Delta H - H_{loss}\right] / \, (F\cdot s_v + CCR\cdot s_c)$$

F is the vapour (hydrocarbon and dispersion) mass flow rate, CCR the catalyst circulation rate. s_v and s_c are the specific heats of the vapour and catalyst streams and ΔH is the heat of reaction per unit mass of reactant. The heat loss term is due to conduction and can be calculated from the riser dimensions and the effective thermal conductivity Kw through the riser walls

$$H_{loss} = Kw\cdot\Pi(d+h)(T-Tw)/h$$

where d and h are the riser diameter and wall thickness and Tw is the external wall temperature. Alternatively, in the absence of conductivity or wall temperature data, the heat loss may be estimated on the basis of the feed rate and included with the $F \cdot \Delta H$ portion of the heat balance equation.

The differential equation for dT/dz can be solved once the term dy/dz has been defined.

2.3 Rate Equations

The Weekman Nace reaction scheme (AIChE J, 16, 397 (1970)) is assumed for the overall cracking of the gas oil and net formation of debutanized gasoline

$$\frac{dy_1}{dt} = -k_o y_1^2 \phi$$

$$\frac{dy_2}{dt} = k_1 y_1^2 \phi - k_2 y_2 \phi$$

y_1 and y_2 are the mass fractions of gas oil and debutanized gasoline, k_o is the overall cracking rate constant while k_1 and k_2 are the rate constants for the formation and cracking of gasoline. ϕ is the fractional catalyst activity which is assumed to decay as a first order function

$$\frac{d\phi}{dt} = -\alpha\phi$$

so that

$$\phi = e^{-\alpha t}$$

after the catalyst has been on stream (in contact with the vapour) for time t.

Combining these rate equations with the reactor equations for material and heat balance, the following equations describe the cracking of gas oil and formation of debutanized gasoline in the riser:

$$dy_1/dz = -t_{vc} k_o y_1^2 e^{-\alpha t}$$

$$dy_2/dz = t_{vc} (k_1 y_1^2 - k_2 y_2) e^{-\alpha t}$$

$$\frac{dT}{dz} = \left[\frac{dy_1}{dz} \cdot F \cdot \Delta H - H_{loss} \right] / (F \cdot s_v + CCR \cdot s_v)$$

To account for variations in temperature the different rate constants, including α, are all defined by pre-exponential factors and activation energies in the Arrhenius form

$$k = A \exp(-E/RT)$$

for use in the riser equations.

The three riser equations are solved simultaneously using a numerical differential solution method. An important practical requirement of the ordinary differential equation solver is for automatic step sizing since the step size range required for riser modelling is quite wide (0.0005 to 0.05, typically, from the bottom to the top of the riser). The explicit fourth order Runge-Kutta-Fehlberg technique with imbedded error estimation for automatic step control proved satisfactory for the non-stiff system of riser equations.

On each step of the solution the rate constants are recalculated at the prevailing temperature. The vapour-catalyst contact time, t_{vc}, and the catalyst on-stream time, t, are also calculated, as described in the next section.

2.4 Pneumatic Flow in the Dilute Phase Riser

An analysis of the flow conditions in the riser is required to define the vapour-catalyst contact time and the catalyst residence time, since these variables govern the extent of reaction at any point in the riser. In the riser there is two-phase flow with the volumetrically dilute catalyst phase being pneumatically conveyed by the principal vapour phase. Gravitational effects coupled with the relatively high density of the catalyst results in the velocity of the catalyst particles lagging that of the conveying vapour stream, u_v, by the free fall velocity of the particles, u_f. The ratio of the velocities of the conveying and conveyed phases is expressed as the slip factor, SF

$$SF = u_v / (u_v - u_f)$$

For a riser of length L, the vapour and catalyst residence times are

$$t_v = L/u_v \quad \text{and} \quad t_c = SF \cdot t_v = L / (u_v - u_f)$$

With the high dilution of catalyst that exists in the riser the vapour will only be in contact with the catalyst for a fraction of its total residence time in the riser: conversely, the catalyst particles are in contact with vapour for essentially the duration of their residence time. The vapour-catalyst contact depends on the volume of catalyst held up in the riser, V_c, and the vapor flow rate, F_v, so that

$$t_{vc} = V_c / F_v$$

with $V_c = t_c \cdot F_c$, and the catalyst flow rate, F_c, calculated from the catalyst circulation rate and the particle density, ρ_c

$$F_c = CCR / \rho_c$$

With the appropriate substitutions the vapour-catalyst contact time is

$$t_{vc} = \frac{L}{(u_v - u_f)} \cdot \frac{F_c}{F_v}$$

The vapour velocity is obtained from

$$u_v = F_v / (\theta \cdot A)$$

where A is the cross-sectional area of the riser and θ is the volume fraction of the vapour phase in the riser,

$$\theta = 1 - V_c / LA$$

Substituting for V_c then t_c in this equation it may be noted that θ itself is also a function of u_v

$$\theta = 1 - F_c / [A(u_v - u_f)]$$

Elimination of u_v gives the following quadratic in θ

$$-u_f A \theta^2 + (F_c + u_f A + F_v)\theta - F_v = 0$$

Solution for θ is followed by calculation of u_v thence the residence times t_v and t_c, and the vapour-catalyst contact time t_{vc}.

All of these calculations hinge on the vapour flow rate, F_v, which varies considerably along the length of the riser, given that each mole of gas oil cracked has a product yield of 3 to 4 moles. To properly account for such changes, and the fact that a portion of the gas oil product, in the form of coke, is removed from the vapour phase, F_v is determined from the moles present in the vapour. Using a correlation for the number of moles of vapour produced per unit mass of gas oil, n_p, in terms of the gas oil mass fraction and temperature, obtained from laboratory measurements,

$$n_p = f(y_1, T)$$

the total moles of vapour phase is then calculated as

$$N_v = F(n_p + y_1/M) + D/M_D$$

where F and D are the mass flows of gas oil and dispersion medium with molar mass M and M_D respectively. Finally,

$$F_v = N_v \cdot V$$

with V the vapour molar volume at the riser temperature and pressure.

2.5 Riser Exit Calculations

The previous sections have indicated the procedure for calculating the conversion and debutanized gasoline yield along the length of the riser. Individual gas products and coke yield are not included in the Weekman-Nace mechanism and were necessarily omitted from the differential equation set. Separate, non-kinetic, correlations are used in the model to calculate the coke, dry gas and C3C4 gas yields at the riser exit, pending development of suitable kinetic mechanisms and data.

The coke on catalyst is determined using Voorhies relation

$$m_e = A' \cdot t_c^{\,n}$$

where the parameters A′ and n are derived from laboratory data for each feed and the catalyst total residence time in the riser, t_c, is calculated during solution of the riser equations. The coke yield per unit mass of feed is

$$y_{coke} = m_e \cdot CCR/F$$

Two correlations are supplied for each feed expressing the dry gas and C3C4 yields as functions of conversion, temperature and Conradson carbon,

$$y = f[(1-y_1), T, \mathrm{Con\ C}]$$

The total gas yield is normalized for material balance at the riser exit so that

$$y_{DG} + y_{C3C4} = (1 - y_1 - y_2 - y_{coke})$$

3. Stripper-Regenerator

An enthalpy balance is made within an envelope drawn around the stripper and the regenerator catalyst bed. The initial temperature level is at the riser exit temperature, T_1; the final level is the regenerator temperature, T_c, which is to be calculated. Spent catalyst and coke from the riser exit are contacted first with stripping steam, then enter the regenerator and contact moist air at temperature T_{air}. The catalyst, coke and air are then raised to T_c, where a portion of the coke is burned off the catalyst yielding an overall combustion enthalpy $H_c$coke. The enthalpy balance for this system is

$$\Sigma H_j(i) + H_{SS}(P_{SS}) = H_c\text{coke} + H_{loss} + H_{SS}(T_1) + \Sigma H_j(f)$$

$$\Sigma H_j(i) = H_{coke}(T_1) + H_{cat}(T_1) + H_{air}(T_{air}) + H_{RS}(P_{RS})$$

$$\Sigma H_j(f) = H_{coke}(T_c) + H_{cat}(T_c) + H_{air}(T_c) + H_{RS}(T_c)$$

The individual enthalpy terms are identified by the subscripts. SS and RS refer to stripping steam and regenerator steam , calculated initially at their respective pressures P. The final condition for the stripping steam is the stripper temperature, assumed here to be the riser exit temperature. For convenience, the coke, catalyst, regenerator steam and moist air stream enthalpies are grouped together in summations at either the initial $H_j(i)$, or final $H_j(f)$ condition. Noting that

$$\Sigma H_j(f) = (\Sigma C_j)\cdot T_c$$

where C_j are the heat capacities of the various streams i.e. mass flow times specific heat, the heat balance may be rewritten to calculate T_c

$$T_c = \left[\Sigma H_j(i) - H_c\text{coke} - H_{SS}(T_1) - H_{SS}(P_{SS}) - H_{loss}\right] / (\Sigma C_j)$$

To solve this equation the terms in the initial enthalpy summation are calculated from the stream heat capacities, as is $H_{SS}(T_1)$. H_{loss} is input. The coke combustion enthalpy is determined from the heat of the reaction

$$CH_z + \left[\frac{2+\beta}{2(1+\beta)} + \frac{z}{4}\right] O_2 \longrightarrow \left[\frac{\beta}{1+\beta}\right] CO + \frac{1}{(1+\beta)}\ CO_2 + (z/2)\ H_2O$$

at T_I, calculated from the heats of formation, ΔH_f, of the various species,

$$\Delta H_c = \Sigma \nu_i \Delta H_f(i)$$

In these equations β is the molar ratio CO/CO_2 in the products and ν_i is the stoichiometric coefficient, positive for reaction products and negative for reactants. With this heat of combustion the coke combustion term is

$$H_c\text{coke} = (m_s - m_r)\cdot CCR\cdot \Delta H_c/100$$

m_s and m_r are the coke mass % on the spent and regenerated catalyst and CCR is the catalyst circulation rate. Terms in the equation for T_c which are dependent on T_c - air and steam heat capacities or the component heats of formation, for instance - are calculated using the regenerator bed temperature from the previous heat balance iteration.

4. Slide Valve - Catalyst Flow Control

In the slide valve mode the catalyst circulation rate is adjusted so that a specified riser exit temperature or feed conversion level can be met. Once the riser-stripper-regenerator are heat balanced at some initial condition, the catalyst circulation rate is adjusted by 10% in the direction required to move toward the specified target for the dependent variable (riser exit temperature or conversion). On subsequent iterations the catalyst circulation rate to match the dependent variable target is determined by the secant method

$$CCR^{k+1} = CCR^{k} + (y - y^{k})/(dy/dCCR)$$

where the gradient is calculated as

$$\frac{dy}{dCCR} = \frac{(Y^{k} - Y^{k-1})}{(CCR^{k} - CCR^{k-1})}$$

CCR is the catalyst circulation rate, Y the target value of the dependent variable and the superscript k denotes the iteration number. Iterations are continued until $100|Y - Y^{k}|/Y$ is less than 0.2%; this is usually accomplished within 5 iterations.

PROGRAM DEMONSTRATIONS

Two complete demonstration cases are provided. The first case represents a situation where there is no constraint on the regenerator operating temperature (IPL base case) while the second demonstration case includes the regenerator constraint (C3 DAO, 5). Each case actually consists of two separate runs on RISERD. The first run is with the slide value option operating and the required riser exit temperature specified. Estimates of the regenerator temperature and catalyst circulation rate are used by the model as starting values. First the regenerator temperature is calculated iteratively until the unit is heat balanced (regenerator temperature unchanged on successive iterations). Then the catalyst circulation rate is adjusted, and the unit heat balance recalculated, until the specified riser exit temperature is reached. The second run consists of a single pass through the riser at the converged heat balanced conditions calculated in the first run, with a printout of operating conditions at 10 equal intervals along the riser.

Demonstration Case

The input data file is unformatted, the first control integer on the second line determines the mode; 2 is the slide value option. Most of the contents of the data file are summarized in the first part of the program, the data are taken from Tables 8 and 9 in the main report. Some unit conversions are used for model consistency (cm rather than feet for instance) and some data are redundant - for example, the wall thickness and wall temperature which are only used for heat loss calculations when the riser thermal conductivity (KCOND) is non-zero.

The second part of the output summarizes the conditions at the riser exit and the calculated regenerator temperature after each pass through the riser. The first series of 6 heat balance iterations is made with the input catalyst circulation rate (equivalent to a catalyst/oil ratio of 7.7). The estimated regenerator temperature of 640°C results in a riser exit temperature of 497.1°C and a calculated regenerator temperature of 652.4°C. Taking this as the catalyst temperature, a second iteration through the riser yields an exit temperature of 505.9 and a regenerator temperature of 659.1. Iterations continue until the regenerator temperature is constant (within 1°C) and the unit is heat balanced.

Since the riser exit temperature at heat balance is 5°C above the target value of 510°C, the catalyst circulation rate is reduced and a further 5 iterations carried out to reach a new heat balance.

A final adjustment to the catalyst rate (catalyst/oil ratio 7.5) produces a heat-balanced unit with the regenerator at 662°C and with the riser temperature within 0.5°C of the target 510°C.

These conditions form the basis for the second run in mode 0 - once through the riser without adjusting the input variables. The catalyst circulation rate is set at 0.2687E+10 g/hr and the regenerator temperature at 662°C. All remaining data is the same as in the heat balance run. In this mode, conditions in the riser at 0.1 intervals are tabulated (0 height is the bottom of the riser, 1.0 is the riser exit), giving a riser profile of the conversion, gasoline yield, vapour volume fraction, cumulative catalyst volume and velocity data for the vapour and catalyst.

SAMPLES FROM PROGRAM RISERD

Input Data File

```
Demonstration Case -- Flow 50 ft/sec. - 510 C Riser Outlet Target
2 0 0 -1 10
510.
3353. 134.7 2.54 0.0
3.5707E08 2.7494E09 5.3560E06
24.2 12.0 0.0 1.431
410. 18.
.75 .260 .55
350. 640.0 500. 25. 50. 0.
61. 125.
5.44E08 12.3 12.63 -3.1 1.09E09 13.2 1.08E08 12.2
0.59 0.29
6.8082E-03 -0.0147939 2.1360E-03 12.449E-06
-36.0924 0.37099 0.0 0.04727
-7.82658 0.04978 0.0 0.012205
20. 800. 3.0E09 0.2 0.66
3.0E08 4.0E06 150.
0.0 40. 7.4985E06 50.
```

Sample Output

```
Demonstration Case -- Flow 50 ft/sec. - 510 C Riser Outlet Target


INPUT DATA

RISER        LENGTH     DIA    WALL    WALL   KCOND   PRESS
                 CM      CM      CM    TEMP    CAL/    PSIG
                                          C  CM.S.C

              3353.   134.7    2.54    500.    .000     25.

FEED           FLOW    TEMP     API       K   MOLAR    SPEC    DELH
               G/HR       C    GRAV    FACT    MASS    HEAT   CAL/G

            .36E+09    350.    24.2    12.0   410.0   .7500   125.0

CATALYST       CIRC    TEMP   POINT    FALL    SPEC CAT/OIL
               RATE   (EST)    DENS     VEL    HEAT
               G/HR       C  G/CM3    CM/S

            .27E+10    640.   1.431    61.0   .2600     7.7

STEAM          RATE   PRESS
               G/HR    PSIG

       DISP .54E+07    50.0
      STRIP .75E+07    50.0
      REGEN .00E+00    40.0

REGEN         PRESS     MAX     MAX     AIR     AIR    HEAT     CO/
               PSIG    TEMP     AIR     H2O    TEMP    LOSS     CO2
                          C    G/HR    G/HR       C  CAL/HR

               20.0    800. .30E+09 .40E+07    150. .30E+10    .660

RATE DATA       CRACKING          CAT DECAY          GASOLINE          C5+ CRACKING
                FREQ     ACT      FREQ     ACT      FREQ     ACT      FREQ     ACT
              FACTOR  ENERGY    FACTOR  ENERGY    FACTOR  ENERGY    FACTOR  ENERGY
                HR-1    KCAL      HR-1    KCAL      HR-1    KCAL      HR-1    KCAL

           .5440E+09  12.300 .1263E+02  -3.100 .1090E+10  13.200 .1080E+09  12.200

COKE EQN          A       N

              .5900   .2900
```

```
RISER EXIT AND REGENERATOR

ITER  RISER    REG    CONV    GAS    C3C4  C5+GAS    LCO      DO    COKE  SPENT    REG     DRY
       TEMP   TEMP     WT%    WT%     WT%     WT%    WT%     WT%     WT%   COKE   COKE     AIR
         C      C                                                          WT%    WT%    G/HR

   1  497.1  652.4    74.8    1.7    13.2    54.3   25.2      .0     5.7     .9     .2 .2419E+09
   2  505.9  659.1    75.4    1.8    13.7    54.2   24.6      .0     5.7     .9     .2 .2399E+09
   3  510.6  662.7    75.7    1.9    14.0    54.2   24.3      .0     5.6     .9     .2 .2388E+09
   4  513.2  664.7    75.8    1.9    14.1    54.1   24.2      .0     5.6     .9     .2 .2382E+09
   5  514.6  665.8    75.9    1.9    14.2    54.1   24.1      .0     5.6     .9     .2 .2379E+09
   6  515.3  666.4    76.0    1.9    14.3    54.1   24.0      .0     5.6     .9     .2 .2377E+09

CCR   .27494E+10 g/hr   Cat/Oil    7.7
----------------------------------------------------------------------------------------------------

   1  503.3  657.0    74.0    1.6    12.1    55.2   26.0      .0     5.1     .9     .2 .2174E+09
   2  497.3  652.4    73.6    1.5    11.8    55.1   26.4      .0     5.2     .9     .2 .2186E+09
   3  494.2  650.0    73.4    1.5    11.6    55.1   26.6      .0     5.2     .9     .2 .2193E+09
   4  492.6  648.8    73.3    1.5    11.5    55.1   26.7      .0     5.2     .9     .2 .2197E+09
   5  491.8  648.2    73.2    1.5    11.5    55.1   26.8      .0     5.2     .9     .2 .2199E+09

CCR   .24745E+10 g/hr   Cat/Oil    6.9
----------------------------------------------------------------------------------------------------

   1  500.9  655.2    74.8    1.7    13.1    54.5   25.2      .0     5.6     .9     .2 .2358E+09
   2  505.4  658.7    75.1    1.8    13.3    54.4   24.9      .0     5.5     .9     .2 .2348E+09
   3  507.8  660.5    75.2    1.8    13.5    54.4   24.8      .0     5.5     .9     .2 .2342E+09
   4  509.1  661.5    75.3    1.8    13.6    54.4   24.7      .0     5.5     .9     .2 .2340E+09
   5  509.8  662.1    75.4    1.8    13.6    54.4   24.6      .0     5.5     .9     .2 .2338E+09

CCR   .26873E+10 g/hr   Cat/Oil    7.5
----------------------------------------------------------------------------------------------------
```

```
Input Data File
---------------

Demonstration Case -- Flow 50 ft/sec. - Riser Profile at Heat Balance
0 0 0 -1 10
510.
3353. 134.7 2.54 0.0
3.5707E08 2.6873E09 5.3560E06
24.2 12.0 0.0 1.431
410. 18.
.75 .260 .55
350. 661.5 500. 25. 50. 0.
61. 125.
5.44E08 12.3 12.63 -3.1 1.09E09 13.2 1.08E08 12.2
0.59 0.29
6.8082E-03 -0.0147939 2.1360E-03 12.449E-06
-36.0924 0.37099 0.0 0.04727
-7.82658 0.04978 0.0 0.012205
20. 800. 3.0E09 0.2 0.66
3.0E08 4.0E06 150.
0.0 40. 7.4985E06 50.
```

Sample Output

```
Demonstration Case -- Flow 50 ft/sec. - Riser Profile at Heat Balance


INPUT DATA

RISER       LENGTH     DIA    WALL    WALL   KCOND   PRESS
                CM      CM      CM    TEMP    CAL/    PSIG
                                         C  CM.S.C

             3353.   134.7    2.54    500.    .000     25.

FEED          FLOW    TEMP     API       K   MOLAR    SPEC    DELH
              G/HR       C    GRAV    FACT    MASS    HEAT   CAL/G

           .36E+09    350.    24.2    12.0   410.0   .7500   125.0

CATALYST      CIRC    TEMP   POINT    FALL    SPEC CAT/OIL
              RATE   (EST)    DENS     VEL    HEAT
              G/HR       C   G/CM3    CM/S

           .27E+10    662.   1.431    61.0   .2600     7.5

STEAM         RATE   PRESS
              G/HR    PSIG

      DISP .54E+07    50.0
     STRIP .75E+07    50.0
     REGEN .00E+00    40.0

REGEN        PRESS     MAX     MAX     AIR     AIR    HEAT     CO/
              PSIG    TEMP     AIR     H2O    TEMP    LOSS     CO2
                         C    G/HR    G/HR       C  CAL/HR

              20.0    800. .30E+09 .40E+07    150. .30E+10    .660

RATE DATA         CRACKING           CAT DECAY          GASOLINE           C5+ CRACKING
                  FREQ     ACT       FREQ     ACT       FREQ     ACT       FREQ     ACT
                FACTOR  ENERGY     FACTOR  ENERGY     FACTOR  ENERGY     FACTOR  ENERGY
                 HR-1     KCAL      HR-1     KCAL      HR-1     KCAL      HR-1     KCAL

             .5440E+09  12.300  .1263E+02  -3.100  .1090E+10  13.200  .1080E+09  12.200

COKE EQN         A       N

             .5900   .2900
```

```
RISER PROFILE DATA

  HGT    TEMP    CONV  C5+GAS     VAP     CAT    SLIP     VAP     CAT    TVAP    TCAT CONTACT
            C     WT%     WT%     VOL     VOL  FACTOR     VEL     VEL     SEC     SEC    TIME
                                 FRAC       L          CM/SEC  CM/SEC                     SEC

  .00   537.7      .0      .0   .9509      0.   1.082   806.7   745.7     .00     .00   .0000
  .10   530.6    42.6    44.7   .9721    156.   1.046  1374.2  1313.2     .29     .30   .0082
  .20   523.8    53.3    52.6   .9751    280.   1.042  1530.6  1469.6     .52     .54   .0132
  .30   520.0    59.3    55.8   .9765    395.   1.039  1622.0  1561.0     .73     .76   .0175
  .40   517.3    63.5    57.1   .9775    504.   1.038  1685.3  1624.3     .93     .97   .0215
  .50   515.4    66.6    57.4   .9781    610.   1.036  1733.2  1672.2    1.13    1.17   .0252
  .60   513.8    69.0    57.3   .9786    713.   1.036  1771.2  1710.2    1.32    1.37   .0289
  .70   512.5    71.0    56.8   .9790    814.   1.035  1802.5  1741.5    1.51    1.56   .0324
  .80   511.5    72.7    56.1   .9793    913.   1.035  1828.9  1767.9    1.69    1.75   .0358
  .90   510.6    74.1    55.3   .9796   1011.   1.034  1851.5  1790.5    1.87    1.94   .0391
 1.00   509.8    75.4    54.4   .9798   1108.   1.034  1871.3  1810.3    2.05    2.12   .0424


RISER EXIT AND REGENERATOR

ITER  RISER     REG    CONV     GAS    C3C4  C5+GAS     LCO      DO    COKE   SPENT     REG       DRY
       TEMP    TEMP     WT%     WT%     WT%     WT%     WT%     WT%     WT%    COKE    COKE       AIR
          C       C                                                           WT%     WT%      G/HR

   1  509.8   662.1    75.4     1.8    13.6    54.4    24.6      .0     5.5      .9      .2 .2339E+09
```

Demonstration Case 2

As with case 1, the first run is to establish heat balanced conditions with a riser exit temperature of 510°C. Input data is taken from Tables 8 and 9 in the report. The initial estimate for the regenerator temperature is 650°C but maximum regenerator temperature is restricted to 662°C. On the first iteration the calculated regenerator temperature exceeds 662°C (as evidenced in the run reported in Table 13, with unrestricted regenerator operation). Consequently, excess heat is removed from the regenerator to maintain the temperature at 662°C and a second iteration is commenced with this catalyst temperature. As long as conditions in the riser are such that the calculated regenerator temperature exceeds 662°C, the model will automatically adjust the heat removal from the regenerator to maintain a heat balanced unit at 662°C. The only variable from this point on is the catalyst circulation rate, which is increased in two further steps to bring the riser exit temperature to within 0.4°C of the target. Both of these catalyst rate adjustments tend to give higher regenerator temperatures (i.e. above 662°C) so that heat balance at the restricted temperature level is achieved in 1 iteration on each step.

The second run, to produce the riser profile, is made at the heat balanced conditions of run 1 with the regenerator temperature set to 662°C and a catalyst circulation rate of 0.2489E+10 g/hr.

SAMPLES FROM PROGRAM RISERD

Input Data File

```
Demonstration Case 2 -- 510 C Riser Outlet Target, Regen 662 C Max
2 0 0 -1 10
510.0
3353. 134.7 2.54 0.0
3.3094E08 2.1842E09 4.9641E06
19.2 11.8 1.7 1.431
440. 18.
.75 .260 .55
350. 650. 500. 25. 50. 0.
61. 125.
6.48E08 12.3 14.25 -3.1 1.22E09 13.2 1.30E08 12.2
0.71 0.29
.0135 -.0135 0.0 0.0
-5.49461 0.30083 -0.39021 0.0
-3.10 0.1044 0.0882 0.0
20. 662. 3.0E09 0.2 0.66
3.0E08 4.0E06 150.
0.0 40. 5.9569E06 50.
```

Sample Output

```
Demonstration Case 2 -- 510 C Riser Outlet Target, Regen 662 C Max


INPUT DATA

RISER       LENGTH     DIA    WALL    WALL   KCOND   PRESS
                CM      CM      CM    TEMP    CAL/    PSIG
                                         C  CM.S.C

             3353.   134.7    2.54    500.    .000     25.

FEED          FLOW    TEMP     API       K   MOLAR    SPEC    DELH
              G/HR       C    GRAV    FACT    MASS    HEAT   CAL/G

            .33E+09    350.    19.2    11.8   440.0   .7500   125.0

CATALYST      CIRC    TEMP   POINT    FALL    SPEC CAT/OIL
              RATE   (EST)    DENS     VEL    HEAT
              G/HR       C   G/CM3    CM/S

            .22E+10    650.   1.431    61.0   .2600     6.6

STEAM         RATE   PRESS
              G/HR    PSIG

      DISP .50E+07    50.0
     STRIP .60E+07    50.0
     REGEN .00E+00    40.0

REGEN        PRESS     MAX     MAX     AIR     AIR    HEAT     CO/
              PSIG    TEMP     AIR     H2O    TEMP    LOSS     CO2
                         C    G/HR    G/HR       C  CAL/HR

              20.0    662. .30E+09 .40E+07    150. .30E+10    .660

RATE DATA        CRACKING           CAT DECAY           GASOLINE          C5+ CRACKING
               FREQ     ACT       FREQ     ACT       FREQ     ACT       FREQ     ACT
             FACTOR  ENERGY     FACTOR  ENERGY     FACTOR  ENERGY     FACTOR  ENERGY
               HR-1    KCAL       HR-1    KCAL       HR-1    KCAL       HR-1    KCAL

          .6480E+09  12.300  .1425E+02  -3.100  .1220E+10  13.200  .1300E+09  12.200

COKE EQN         A       N

             .7100   .2900
```

```
RISER EXIT AND REGENERATOR

ITER  RISER    REG    CONV     GAS    C3C4  C5+GAS     LCO      DO    COKE  SPENT     REG      DRY
       TEMP    TEMP    WT%     WT%     WT%     WT%     WT%     WT%     WT%   COKE    COKE      AIR
        C       C                                                             WT%     WT%     G/HR

   1  486.8   662.0   74.0     3.9    13.2    51.0    26.0      .0     6.0    1.1      .2  .2220E+09
   2  494.7   662.0   74.8     4.1    13.9    50.8    25.2      .0     5.9    1.1      .3  .2144E+09

CCR   .21842E+10 g/hr   Cat/Oil    6.6
------------------------------------------------------------------------------------------------------

   1  505.6   662.0   76.9     4.8    16.1    49.5    23.1      .0     6.5    1.2      .4  .2232E+09

CCR   .24026E+10 g/hr   Cat/Oil    7.3
------------------------------------------------------------------------------------------------------

   1  509.6   662.0   77.6     5.1    17.0    48.9    22.4      .0     6.7    1.3      .5  .2267E+09

CCR   .24891E+10 g/hr   Cat/Oil    7.5
------------------------------------------------------------------------------------------------------
```

Input Data File

```
Demonstration Case 2 -- 510 C Riser, Regen 662 C, Riser Profile
0 0 0 -1 10
510.0
3353. 134.7 2.54 0.0
3.3094E08 2.4891E09 4.9641E06
19.2 11.8 1.7 1.431
440. 18.
.75 .260 .55
350. 662. 500. 25. 50. 0.
61. 125.
6.48E08 12.3 14.25 -3.1 1.22E09 13.2 1.30E08 12.2
0.71 0.29
.0135 -.0135 0.0 0.0
-5.49461 0.30083 -0.39021 0.0
-3.10 0.1044 0.0882 0.0
20. 662. 3.0E09 0.2 0.66
3.0E08 4.0E06 150.
0.0 40. 5.9569E06 50.
```

Sample Output

```
 Demonstration Case 2 -- 510 C Riser, Regen 662 C, Riser Profile


 INPUT DATA

 RISER        LENGTH     DIA    WALL    WALL   KCOND   PRESS
                  CM      CM      CM    TEMP    CAL/    PSIG
                                           C  CM.S.C

               3353.   134.7    2.54    500.    .000     25.

 FEED           FLOW    TEMP     API       K   MOLAR    SPEC    DELH
                G/HR       C    GRAV    FACT    MASS    HEAT   CAL/G

             .33E+09    350.    19.2    11.8   440.0   .7500   125.0

 CATALYST       CIRC    TEMP   POINT    FALL    SPEC CAT/OIL
                RATE   (EST)    DENS     VEL    HEAT
                G/HR       C   G/CM3    CM/S

             .25E+10    662.   1.431    61.0   .2600     7.5

 STEAM          RATE   PRESS
                G/HR    PSIG

       DISP  .50E+07    50.0
      STRIP  .60E+07    50.0
      REGEN  .00E+00    40.0

 REGEN         PRESS     MAX     MAX     AIR     AIR    HEAT     CO/
                PSIG    TEMP     AIR     H2O    TEMP    LOSS     CO2
                           C    G/HR    G/HR       C  CAL/HR

                20.0    662. .30E+09 .40E+07    150. .30E+10    .660

 RATE DATA        CRACKING           CAT DECAY          GASOLINE            C5+ CRACKING
                  FREQ     ACT       FREQ     ACT       FREQ     ACT       FREQ     ACT
                FACTOR  ENERGY     FACTOR  ENERGY     FACTOR  ENERGY     FACTOR  ENERGY
                  HR-1    KCAL       HR-1    KCAL       HR-1    KCAL       HR-1    KCAL

             .6480E+09  12.300  .1425E+02  -3.100  .1220E+10  13.200  .1300E+09  12.200

 COKE EQN         A       N

              .7100   .2900
```

```
RISER PROFILE DATA

  HGT    TEMP     CONV  C5+GAS      VAP      CAT     SLIP      VAP      CAT     TVAP    TCAT CONTACT
            C      WT%     WT%      VOL      VOL   FACTOR      VEL      VEL      SEC     SEC    TIME
                                   FRAC        L            CM/SEC   CM/SEC                      SEC

  .00   559.0       .0      .0    .9299       0.    1.126    544.8    483.8      .00     .00   .0000
  .10   528.6     47.8    45.9    .9740     152.    1.047   1366.5   1305.5      .30     .31   .0080
  .20   522.5     57.4    51.5    .9768     267.    1.042   1525.0   1464.0      .53     .55   .0126
  .30   519.0     62.9    53.4    .9782     374.    1.039   1614.5   1553.5      .74     .77   .0166
  .40   516.6     66.7    53.9    .9790     476.    1.038   1675.5   1614.5      .95     .98   .0203
  .50   514.8     69.6    53.6    .9796     574.    1.037   1720.9   1659.9     1.15    1.19   .0239
  .60   513.3     71.8    53.0    .9800     670.    1.036   1756.6   1695.6     1.34    1.39   .0273
  .70   512.2     73.6    52.1    .9803     765.    1.035   1785.7   1724.7     1.53    1.58   .0307
  .80   511.2     75.2    51.1    .9806     858.    1.035   1810.1   1749.1     1.72    1.78   .0339
  .90   510.4     76.5    50.0    .9808     950.    1.034   1831.0   1770.0     1.90    1.97   .0371
 1.00   509.6     77.6    48.9    .9810    1041.    1.034   1849.0   1788.0     2.08    2.15   .0403


RISER EXIT AND REGENERATOR

ITER   RISER     REG    CONV      GAS    C3C4  C5+GAS      LCO       DO    COKE   SPENT      REG        DRY
        TEMP    TEMP     WT%      WT%     WT%     WT%      WT%      WT%     WT%    COKE     COKE        AIR
           C       C                                                               WT%      WT%       G/HR

   1   509.6   662.0    77.6      5.1    17.0    48.9     22.4       .0     6.7     1.1       .3  .2261E+09
```

APPENDIX IV

Pseudo-Ternary Diagrams

FIGURE 1A

Lloydminster - C3
75C 465 PSIA

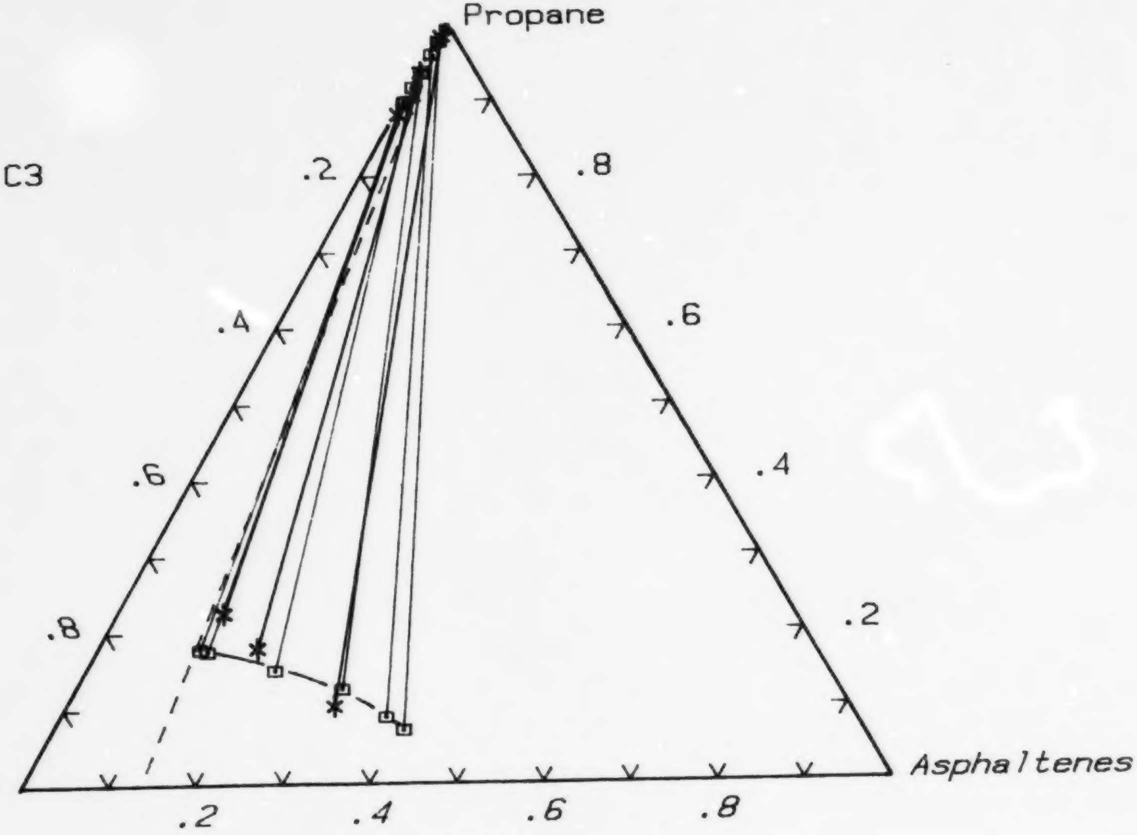

FIGURE 2A

Athabasca - C3
75C 465 PSIA

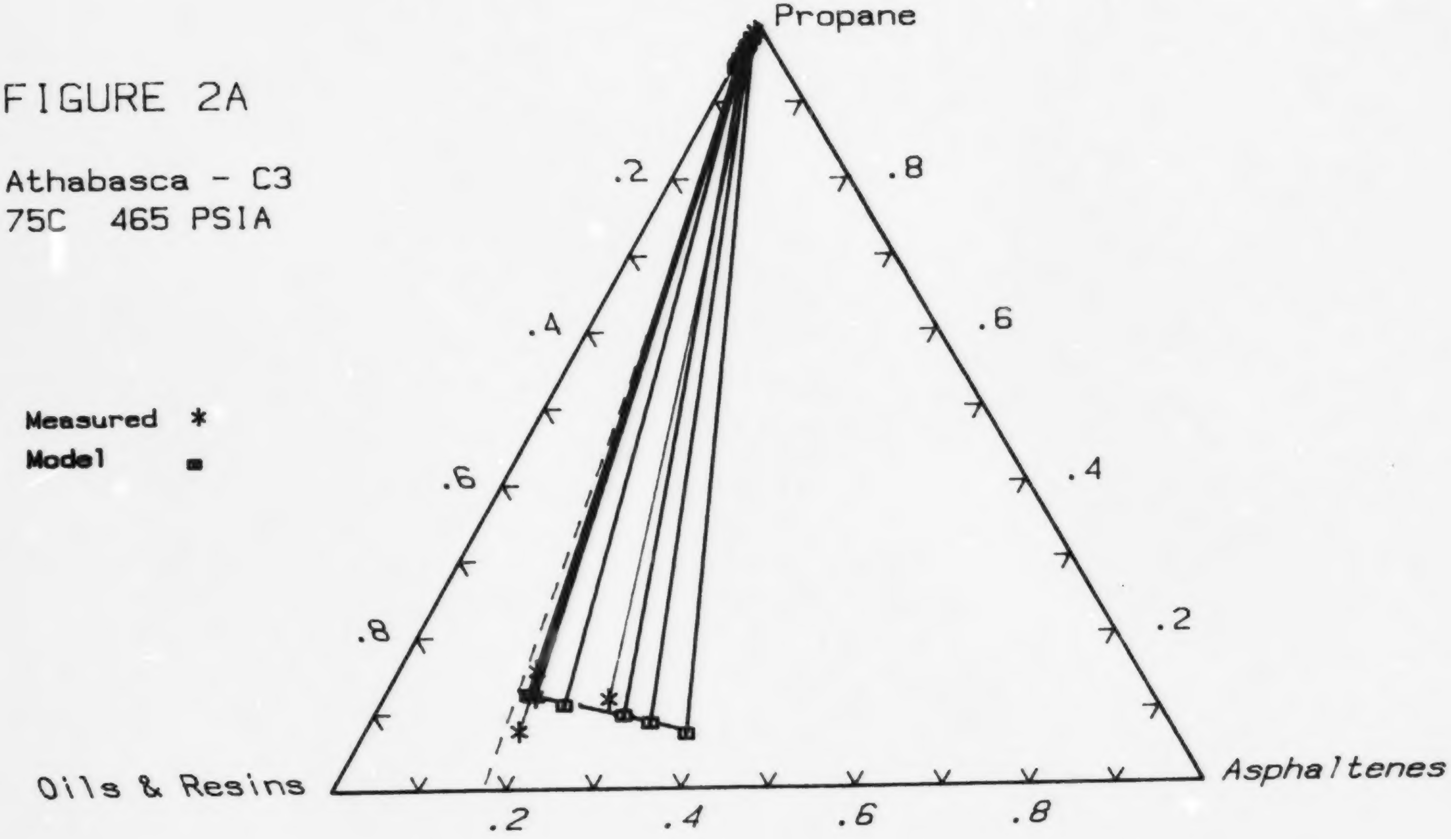

FIGURE 3A

Lloydminster - C4
120C 415 PSIA

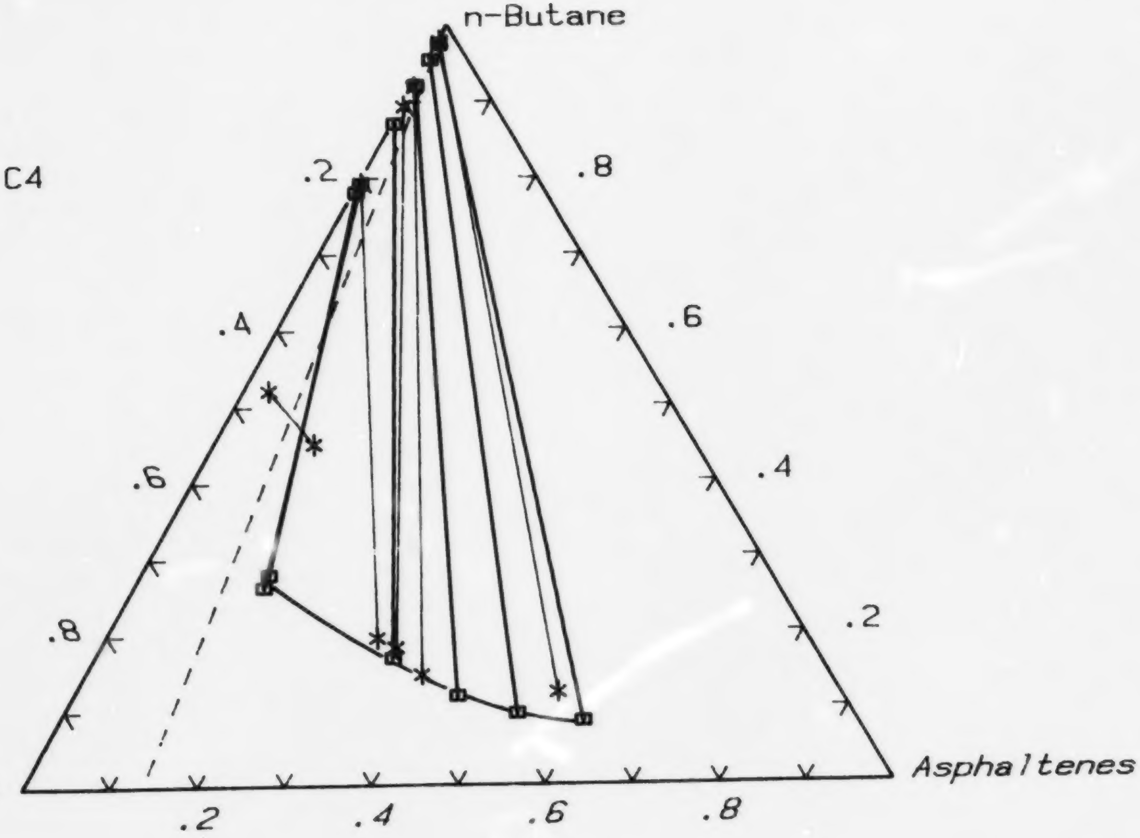

FIGURE 4A

Athabasca - C4
120C 415 PSIA

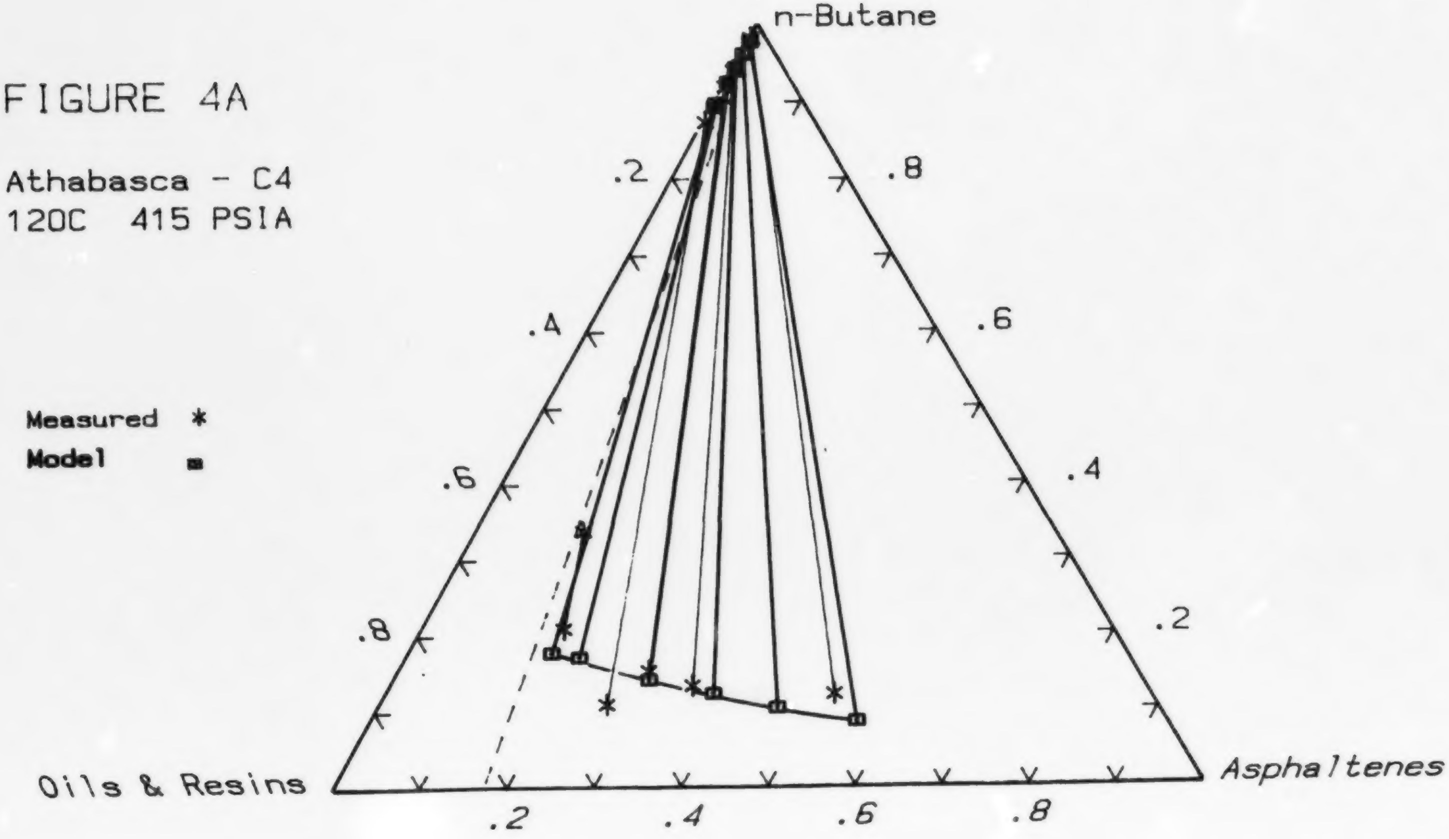

FIGURE 5A

Lloydminster - C5
160C 365 PSIA

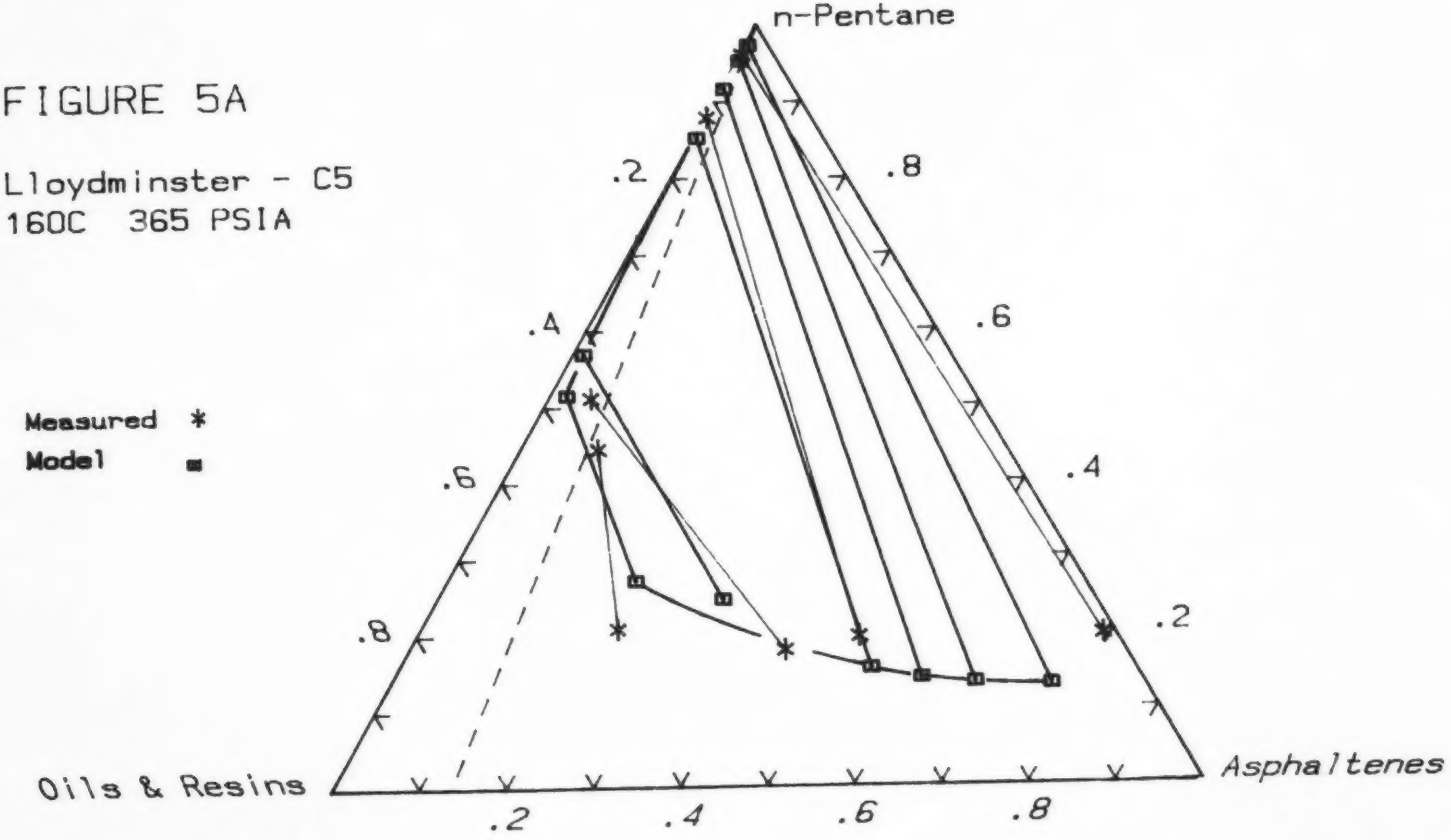

FIGURE 6A

Athabasca - C5
160C 365 PSIA

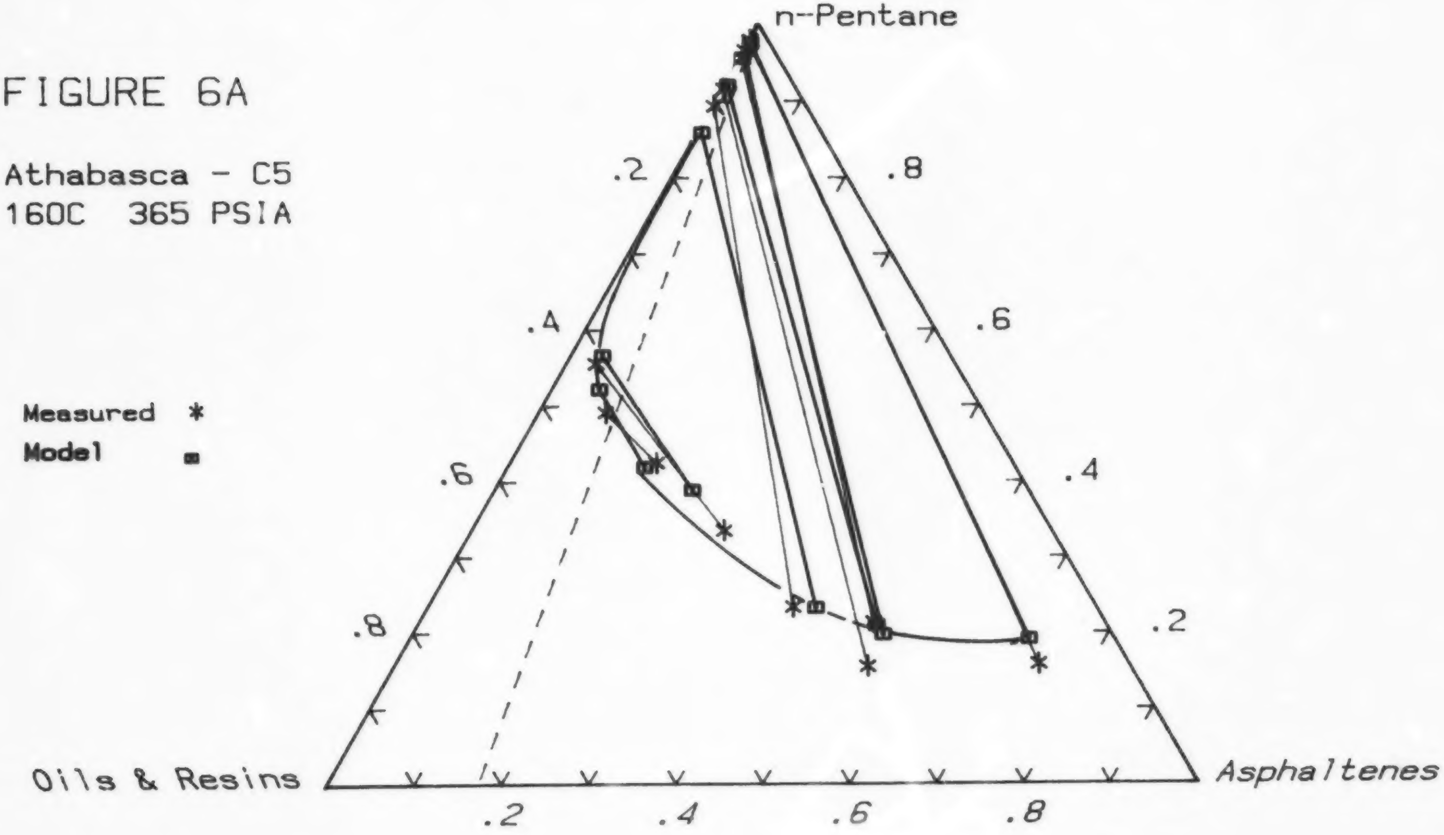

FIGURE 7A

Lloydminster - C7
75C 65 PSIA

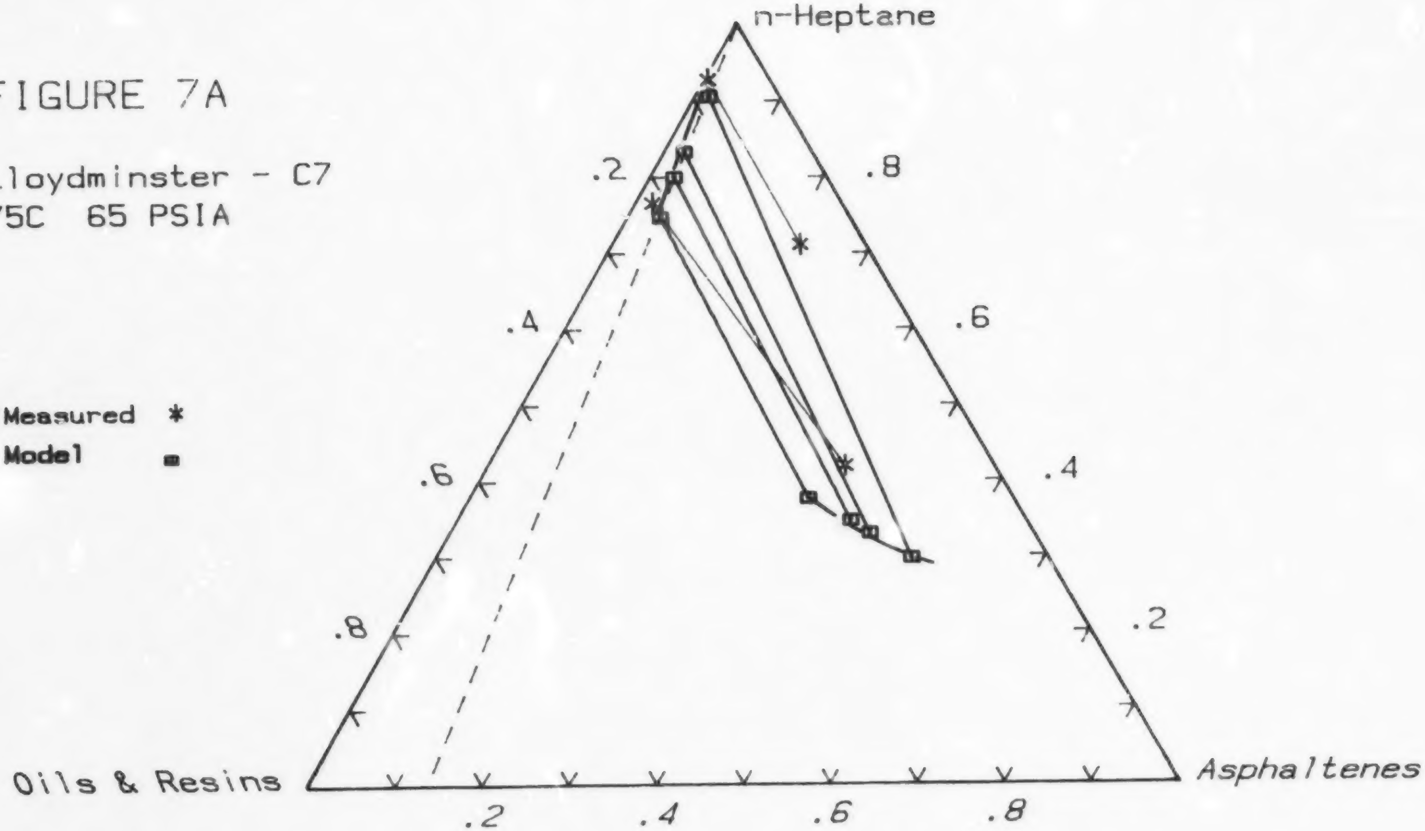

FIGURE 8A

Athabasca - C7
75C 65 PSIA